Functional organisation of the Hrd1 ubiquitin ligase complex and its role in ERAD

Jasmin Schulz

A thesis submitted in fulfilment of the requirements for the degree of

Doctor of Philosophy

Green Templeton College

Ludwig Institute for Cancer Research

Nuffield Department of Clinical Medicine

University of Oxford

Trinity 2013

Declaration

I declare that this thesis has never been submitted, either in the same or a different form, to this or another University for a degree or other qualification. All the work presented in this thesis is the result of my own work unless otherwise stated and does not constitute parts of any other thesis. The work herein described was carried out while I was a DPhil student at the Ludwig Institute for Cancer Research, under the supervision of Dr. John Christianson.

Functional organisation of the Hrd1 ubiquitin ligase complex and its role in ERAD

Jasmin Schulz, Green Templeton College, DPhil in Clinical Medicine, Trinity 2013

Abstract

Endoplasmic reticulum (ER)-associated degradation (ERAD) of misfolded proteins of the secretory pathway is crucial for ER homeostasis and the physiological importance of this mechanism is reflected by more than 60 diseases that have been linked to ERAD to date. The best characterised mammalian ERAD complex is centred on the ubiquitin ligase Hrd1, and for a complete understanding of the dynamics of the ERAD network it is important to thoroughly characterise the interactions within the Hrd1 complex and to decipher the functions of the individual accessory factors.

SEL1L is a well characterised interaction partner of Hrd1 and here we identify a highly hydrophobic region in the lumenal part of SEL1L as necessary, but not sufficient, to interact with Hrd1; as a consequence, the topology of SEL1L may need to be re-evaluated. Furthermore, we investigate the roles of the novel Hrd1 interaction partners AUP1 and FAM8A1 in ERAD. We establish here that AUP1 adds to the complexity of the ERAD network by making the cognate E2 of gp78, Ube2g2, accessible to Hrd1 and by regulating the access of polyubiquitinated proteins to the Hrd1 complex. Moreover, we demonstrate that Hrd1 is the regulator of FAM8A1 half-life and that the interaction between these two proteins is necessary for degradation of the lumenal ERAD model substrate TTR_{D18G}.

Acknowledgements

The past four years have been a very unique and intense experience. There were happy periods and moments of despair, but in the end I submitted my DPhil thesis and I feel like I am the happiest person on this planet. During this time, many people helped and supported me and I would like to acknowledge them in the following.

I am very grateful to my supervisor, Dr. John Christianson, for his invaluable guidance, criticism and support over the past four years. He has always been understanding, especially during the negative moments, and motivated me with inspiring ideas. I would like to thank all the past and present members of the Christianson group for their help, scientific discussion and friendship. My most special colleague will always be Stephanie Jones, we were “the lab” when we started our DPhils together four years ago (or as we would say: we are sitting in the same boat) and became friends immediately. I am thankful to Margarita Chibalina for her advice, Federica Lari for her positive energy, Rodrigo Ribeiro for his Brazilian charm, Norbert Volkmar for patiently enduring my complaints about getting older and Michael Liu for his Mikey miracles. Special thanks go to Jiexin Cao, a medical student at Oxford University who spent her laboratory internship in our group and who collaborated with me on my DPhil project. I am very grateful to Simon Hör, a former postdoc in our group, for invaluable help and support and who always found time to discuss any scientific question I had.

Beyond Dr. Christianson’s group, I would like to thank all the other members of the Ludwig Institute for Cancer Research (LICR) Oxford for their help, and I would especially like to acknowledge Rasmus Freter for technical advice, Anna

Grawenda for help with statistical analysis, Mark Shipman for help with images, Kimberley Bryon-Dodd for critical reading of my thesis and Alexandra Ward for help with administrative issues. A special thank you goes to my College Adviser Prof. John Lennox, who did not miss a single of our termly dinners during the past four years.

I am very thankful to my friends that stood by my side and motivated me. In particular my housemates Sofia Koch, Melania Zauri and Elisa Vergari, with whom I do not only share a house but as well deep friendships; how boring would life be in Oxford without you amazing girls around me! A special mention goes to Minhee Yeo, Eda Süer, Paola Falletta, Magdalena Jeznach, Bilge Daldeniz and José Hernández for their love, friendship and all the enjoyable moments we shared.

Most of all, I would like to thank my family. Ieva Navickiene, her husband Vaidas and my little godson Jonas are like my second family and have always been there for me. Although I don't have the time to visit them as often as I wish, I know that this bond will last for a lifetime. I am deeply grateful to my aunt Marlies Göhl, whose encouragement and support cannot be thanked enough; I would not be where I am without her. The most important person to me is my sister, Ines Schulz, who always loved me the way I am and who gave me strength when I was weak. She and her boyfriend Richard Bankwitz make me feel home wherever they live and I feel unbelievably privileged to have them in my life. My curiosity to learn, to question and to explore was inspired by my parents, who always believed in me and let me follow my interests and dreams; I wish we were still walking on the journey of life together.

Table of Contents

Chapter I: Introduction 9

1.1 Protein quality control in the endoplasmic reticulum (ER) - general introduction . 9

1.2 Early History of ERAD 10

1.3 Translation of secretory pathway proteins 11

1.3.1 Co-translational insertion 11

1.3.2 Post-translational insertion 14

1.4 Protein Maturation in the ER lumen 16

1.4.1 Chaperone-assisted folding 16

1.4.2 Oxidative folding in the ER 17

1.4.3 Prolyl Isomerisation 19

1.4.4 N-linked glycosylation 20

1.4.5 Glycan trimming 23

1.5 Protein misfolding in the ER 24

1.5.1 ERAD substrates 25

1.5.2 Terminally misfolded proteins 25

1.5.3 Unassembled subunits of protein complexes 27

1.5.4 Metabolically regulated proteins 28

1.5.5 Immune evasion 29

1.6 Substrate Recognition 30

1.7 Substrate Retrotranslocation/Dislocation 33

1.8 Substrate Ubiquitination 37

1.9 Ubiquitin ligase complexes involved in ERAD 41

1.10 Substrate Degradation 46

1.11 Unfolded protein response (UPR) 50

1.12 ERAD and diseases 52

1.13 Aim of the study 56

Chapter II: Materials and Methods 57

2.1 Materials 57
2.1.1 Reagents 57
2.1.2 Antibodies 61
2.1.3 Plasmids 62
2.1.4 Primers 65
2.2 Methods 66
2.2.1 Mammalian cell methods 66
2.2.3 Protein techniques 75
2.2.4 Protein Expression systems 79
2.2.5 Cell biology techniques 82
CHAPTER III: Characterisation of the Hrd1-FAM8A1 interaction and its role in ERAD 84
3.1 Introduction 84
3.2 Results 86
3.2.1 FAM8A1 interacts with Hrd1 independently of its ligase activity 86
3.2.2 Hrd1 and FAM8A1 interact through both TM and cytosolic domains 87
3.2.3 FAM8A1 and Hrd1 interact through multiple TMDs 89
3.2.4 Hrd1 500-540 mediates interaction with FAM8A1 and is functionally important for ERAD 91
3.2.5 Cytosolic Trp residues in FAM8A1 are important for Hrd1 binding 97
3.2.6 Disrupting the Hrd1-FAM8A1 interaction impairs ERAD 99
3.2.7 Hrd1 stabilises FAM8A1 in the ER membrane 100
3.3 Discussion 104
CHAPTER IV: Identification of a lumenal SEL1L determinant mediating the interaction with Hrd1 108
4.1 Introduction 108
4.2 Results 111
4.2.1 The first TMD of Hrd1 is involved in the interaction with SEL1L 111
4.2.2 A region proximal to the SEL1L TMD participates in Hrd1 binding 113
4.2.3 SEL1L may contain a second TMD 115
4.2.4 The putative TMD of SEL1L is not sufficient to co-precipitate Hrd1 122
4.2.5 $SEL1L_{short}$ localises to the ER but does not interact with Hrd1 125
4.3. Discussion 131

Chapter V: The Role of AUP1 in ERAD 136

5.1 Introduction 136

5.2 Results 139

5.2.1 AUP1 Localisation 139

5.2.2 AUP1 Membrane Topology 141

5.2.3 Ube2g2 binds to the C-terminus of AUP1 142

5.2.4 The C-terminal G2BR domain is essential for Ube2g2 binding 144

5.2.5 The CUE domain of AUP1 is monoubiquitinated 145

5.2.6 AUP1 binds polyubiquitinated proteins 147

5.2.7 The AUP1 CUE domain does not contain a conserved motif for efficient ubiquitin binding 149

5.3 Discussion 150

Chapter VI: Discussion 156

6.1 Degradation of misfolded proteins from the ER 156

6.2 The SEL1L HID is crucial for interaction with Hrd1 and potentially determines SEL1L topology 159

6.3 AUP1 bridges Ube2g2 with the Hrd1 complex 167

6.4 The stability of FAM8A1 is dependent on its cytosolic interaction with Hrd1 174

6.5 Conclusion 180

Bibliography 182

Chapter I: Introduction

1.1 Protein quality control in the endoplasmic reticulum (ER) - general introduction

The functionality of each cell is dependent upon the enzymatic and structural properties provided by correctly folded proteins. Proteins of the secretory pathway are co-translationally inserted into the lumen of the ER for maturation. Protein maturation comprises correct folding and addition of post-translational modifications, performed by molecular chaperones and enzymes present in the ER lumen. Upon achieving its final conformation, the polypeptide is transported through the secretory pathway to its final destination. But protein maturation in the crowded environment of the ER, where the protein concentration reaches approximately 300 mg/ml (Zimmerman and Trach, 1991), is an error-prone process and a sophisticated quality control machinery is in place to distinguish between folding intermediates and terminally misfolded proteins. The latter ones need to be efficiently degraded, as misfolded polypeptides are prone to aggregation and therefore potentially toxic to the cell.

As the ER does contain only limited protein degradation capacity, misfolded proteins need to be retro-translocated into the cytosol, where they are degraded by the proteasome. This pathway of degradation is referred to as ER-associated degradation (ERAD). ERAD is also responsible for controlling the levels of metabolically regulated proteins as well as unassembled subunits of multi-protein complexes. If this surveillance machinery fails or its capacity is exceeded, the increasing burden of unfolded proteins in the ER lumen activates the unfolded protein response (UPR), resulting in a general inhibition of protein

translation and upregulation of chaperones and ERAD genes. But in case that these backup systems fail to resolve protein stress, the cell triggers apoptosis.

1.2 Early History of ERAD

Until the late 1980s two different mechanisms had been proposed for degradation of misfolded or unneeded secretory proteins retained in the ER. One explanation was the existence of ER-resident proteases. Promising results supporting this hypothesis came from studies on human lysozyme mutants. Unlike the wild type enzyme, lysozyme mutants were retained in the ER (Omura et al., 1992) and their degradation impaired by treatment with cysteine protease inhibitors (Otsu et al., 1995). Furthermore, ER-60, an ER-resident protein exhibiting cysteine-protease activity (Urade et al., 1992), was identified as interaction partner of only the mutant lysozyme, not the wild type, and *in vitro* assays demonstrated the capability of ER-60 to degrade mutant lysozyme (Otsu et al., 1995). Despite these findings a broader role for ER-60 in ERAD could never be established and the protein was finally re-annotated as ERp57A, which is a calnexin-associated disulphide isomerase in the PDI family (Hirano et al., 1995).

A second hypothesis was the degradation of ER retained proteins by the lysosomal pathway. Lysosomes are Golgi-derived vesicles and resident proteins are delivered to the lysosome through the secretory pathway [reviewed in (Kornfeld and Mellman, 1989; Marzella and Glaumann, 1983)]. This view was challenged by studies on the degradation of the T cell receptor (TCR). TCR is expressed on the surface of T lymphocytes and responsible for recognition of antigens presented by major histocompatibility complexes (MHC). The TCR is a heteromeric complex composed of seven polypeptide chains: the α-β disulphide

bond linked heterodimer (antigen-binding site), the ζ-ζ homodimer and three non-covalent chains (CD3-γ, -δ and –ε) (Samelson et al., 1985). Only completely assembled complexes are transported to the plasma membrane (Sussman et al., 1988), while unassembled subunits are degraded (Minami et al., 1987). The finding that this degradation was lysosome-independent hinted towards a degradation mechanism in the early secretory pathway (Lippincott-Schwartz et al., 1988), referred to as pre-Golgi or ER degradation.

An important breakthrough in the understanding of ERAD was obtained from genetic studies in yeast (Sommer and Jentsch, 1993). It could be demonstrated that deletion of UBC6, which encodes a yeast ubiquitin conjugating (E2) enzyme, rescued a thermosensitive mutant of the ER-embedded translocation channel Sec61, indicating that cytoplasmic components are required for ER protein quality control. Subsequent studies confirmed that mutant versions of Sec61 (Biederer et al., 1996; Esnault et al., 1994) and another component of the same apparatus that catalyses protein translocation into the endoplasmic reticulum (ER), Sss1, were degraded in a ubiquitin and proteasome dependent manner. In the following years, this concept held true for a number of ER retained proteins (discussed below) and it was understood that ER proteins were removed from the ER and degraded in the cytosol.

1.3 Translation of secretory pathway proteins

1.3.1 Co-translational insertion

The translation of secretory and integral membrane proteins as well as resident proteins of the ER, Golgi, nuclear envelope and lysosomes is directed to the ER, comprising approximately 30% of a cell's total protein content

(Ghaemmaghami et al., 2003; Kanapin et al., 2003). The ER membrane of eukaryotic cells is contiguous with the nuclear envelope and composed of interconnected cisternae and tubules. For co-translational insertion, the re-location of the ribosome from the cytosol to the ER membrane is mediated by the signal sequence, a short (30-50 aa) and hydrophobic sequence at the N-terminus of secretory pathway proteins, that can be cleaved off by ER-resident Signal Peptidase (SP) (Paetzel et al., 1998; von Heijne, 1983). Additionally, the transmembrane domains (TMDs) of integral membrane proteins can serve as signal sequence when close to the N-terminus (Friedlander and Blobel, 1985) or inserted into a protein without a signal sequence (Mize et al., 1986).

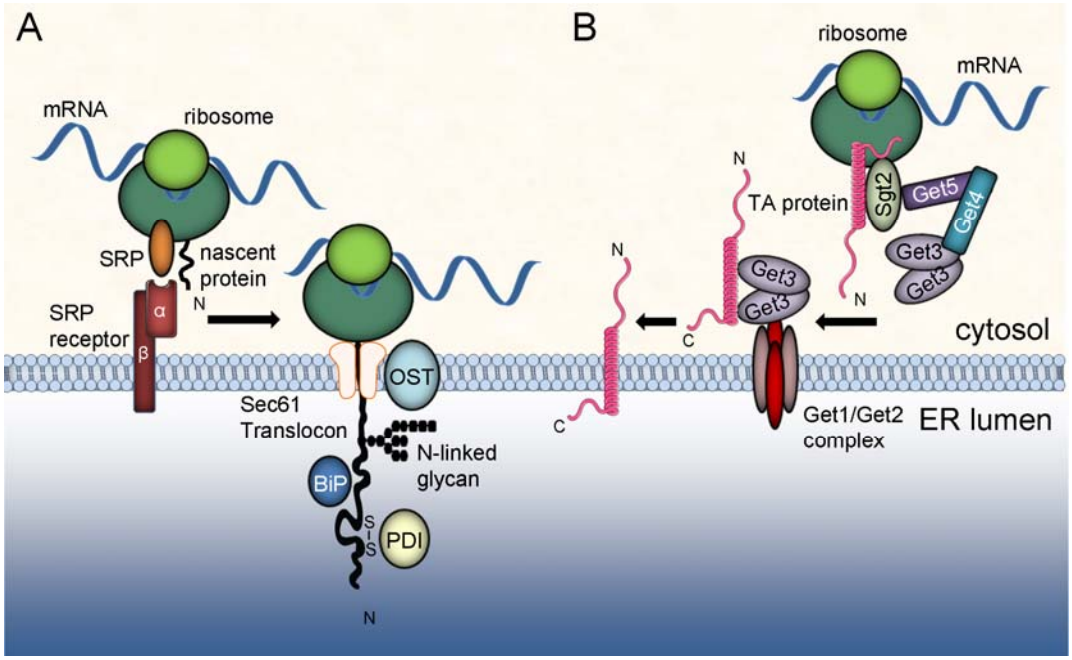


Fig. 1.1: Membrane translocation of secretory proteins. (A) The signal recognition particle (SRP) binds the signal sequence of nascent polypeptides emerging from the ribosomal exit tunnel and targets the ribosome to the ER through interaction with the SRP receptor. Polypeptides are translocated into the ER lumen via the Sec61 complex and immediately bound by the chaperone BiP. N-X-S/T sites are glycosylated by the Sec61-bound oligosaccharyl transferase complex (OST) and disulphide bonds formed through the action of protein disulfid isomerase (PDI) family members. **(B)** The transmembrane domain (TMD) of tail anchored (TA) proteins is bound by Sgt2 and targeted to Get3 through Get4/Get5. The TA protein-Get3 complex binds the ER membrane heterodimer Get1/Get2, mediating TA protein membrane insertion.

The signal sequence is recognised by the signal recognition particle (SRP) (Walter and Blobel, 1980), which selectively binds to ribosomes translating secretory pathway proteins (Walter et al., 1981) (Fig. 1.1A). The interaction between SRP and ribosome halts protein synthesis elongation (Walter and Blobel, 1981a) and targets the ribosome-nascent chain complex to the ER membrane (Walter and Blobel, 1981b). In mammalian cells, the SRP is composed of six protein subunits (SRP9, SRP14, SRP19, SRP54, SRP68, SRP72), the 7S RNA (Walter and Blobel, 1982) and exhibits GTPase activity. SRP54 is positioned near to the ribosomal exit tunnel (Halic et al., 2004) and binds the signal sequence as well as the 7S RNA through its methionine-rich domain (Zopf et al., 1990).

Soon after the discovery of SRP, the SRP-receptor in the ER membrane was identified (Gilmore et al., 1982a; Gilmore et al., 1982b). The receptor is a heterodimer formed by an α- and a β- subunit and is integrated into the ER membrane through the β-subunit (Lauffer et al., 1985). The interaction between the SRP and its receptor is regulated through a GTPase cycle (Connolly and Gilmore, 1986, 1989), performed by the α-subunit of the SRP receptor, SRP54 and the 7S RNA (Miller et al., 1993). GTP hydrolysis results in dissociation of SRP from the signal sequence (Connolly et al., 1991) and attachment of the ribosome-nascent chain complex to the translocation channel.

The translocation channel was first identified in yeast in a screen for gene products essential for protein translocation, namely SEC61, SEC62 and SEC63 (Deshaies and Schekman, 1987; Rothblatt et al., 1989), forming the SEC complex embedded in the ER membrane (Deshaies et al., 1991; Deshaies and Schekman, 1989; Feldheim et al., 1992). Mutation analysis gave further

evidence that Sec61 is the core component of the translocation channel (Stirling et al., 1992). Later studies in higher eukaryotes then demonstrated that the mammalian Sec61 complex (Sec61α, Sec61β and Sec61γ), in conjunction with the accessory factor translocating chain-association membrane (TRAM) protein, is mediating protein translocation across the ER membrane (Gorlich and Rapoport, 1993; Voigt et al., 1996). Mammalian Sec61α is homologous to yeast Sec61 and *E.coli* SecY *(Gorlich et al., 1992)*, demonstrating that protein translocation channels are conserved between eukaryotes and bacteria.

1.3.2 Post-translational insertion

A minority of proteins is not co-translationally, but post-translationally inserted into the ER membrane. These polypeptides contain a single TMD near their carboxyl terminus and are therefore named tail-anchored (TA) proteins. During translation, their TMD only emerges from the ribosomal exit tunnel after the stop codon has been reached; hence a different insertion mechanism has to be in place. TA proteins represent ~3-5 % of all membrane proteins (Beilharz et al., 2003; Kalbfleisch et al., 2007; Kriechbaumer et al., 2009) and play a role in many cellular pathways, like vesicle fusion and protein degradation. The factor recognising TA proteins and targeting them to the ER in an ATP-dependent manner was subsequently identified as TMD-recognition complex protein of 40 kDa (Trc40, Guided Entry for TA proteins 3 [Get3] in yeast) (Stefanovic and Hegde, 2007).

In yeast, the mediator of TA protein insertion is the Get complex (Get1, Get2, Get3) (Schuldiner et al., 2008) as well as its accessory factors Get4, Get5 and small Glu-rich tetratricopeptide repeat-containing 2 (Sgt2) (Copic et al., 2009; Costanzo et al., 2010; Jonikas et al., 2009) (Fig. 1.1B). Get3 forms a

homodimer and each subunit has ATPase activity as well as an α-helical domain, the latter mediating interaction with the TMD of TA proteins through hydrophobic interactions (Bozkurt et al., 2009; Hu et al., 2009; Mateja et al., 2009; Suloway et al., 2009; Yamagata et al., 2010). According to the current view, Get3 is not associated with the ribosome. Instead, Sgt2 binds the TMDs of TA proteins when they emerge from the ribosomal exit tunnel (Wang et al., 2010a). Loading of the TA protein onto Get3 is subsequently facilitated by the Get4-Get5 complex. This complex forms a scaffold to bring Sgt2 and Get3 in close proximity, whereby Get4 binds Get3, in an ATP-bound state, and Get5 binds Sgt2 (Chartron et al., 2010).

The receptor for the Get3 complex in the ER membrane is formed by Get1 and Get2. Get1 and Get2 are multi-spanning ER membrane proteins forming a heterodimeric complex through their TMDs and interact with Get3 through their cytosolic domains (Mariappan et al., 2011; Wang et al., 2011a). Both proteins have distinct functions: Get2 directs the complex to the ER membrane (Mariappan et al., 2011) whilst Get1 is responsible for substrate release (Mariappan et al., 2011; Stefer et al., 2011; Wang et al., 2011a). The moment of ATP hydrolysis remains elusive, but it must occur after substrate binding to Get3 (Chartron et al., 2010; Wang et al., 2011a) and before binding of the Get3 complex to Get1 (Mariappan et al., 2011; Wang et al., 2011a).

In mammals, the accessory complex for Trc40 is composed of Bag6, Trc35 (Get4 in yeast) and Ubl4A (Get5 in yeast) (Leznicki et al., 2010; Mariappan et al., 2010). The Bag6 complex binds SGTA (the mammalian homologue of Sgt2) (Winnefeld et al., 2006) and brings it in close proximity to Trc40 for substrate transfer. The Trc40 receptor in the ER membrane is composed of Trp-rich

protein (WRB) and calcium-modulating cyclophilin ligand CAML, whereby WRB mediates targeting to the ER membrane (Vilardi et al., 2011) and both proteins synergistically perform TA protein insertion (Yamamoto and Sakisaka, 2012).

1.4 Protein Maturation in the ER lumen

1.4.1 Chaperone-assisted folding

Although the native conformation of a polypeptide encoded within its primary amino acid sequence is often sufficient for protein folding *in vitro* (Anfinsen, 1973), folding conditions in the aqueous and crowded environment of the ER are more complex. Nascent polypeptides can aggregate through hydrophobic domains and are bound by molecular chaperones to maintain their solubility. BiP, an Hsp70 family member, is often the first chaperone to bind a nascent polypeptide emerging from the Sec61 translocon, preferentially to surfaces with alternating aromatic and hydrophobic amino acids (Blond-Elguindi et al., 1993). Apart from stabilisation, this interaction prevents the folding polypeptide from slipping back into the cytosol (Matlack et al., 1999). Like all Hsp70 family members, BiP interacts with substrates through its C-terminal substrate binding domain (SBD), which is tightly regulated by the N-terminal nucleotide binding domain (NBD).

A substrate is first encountered by a J-domain containing cofactor (Hsp40) that brings the substrate and BiP in close proximity. This event does not only result in substrate transfer onto BiP, binding of the J-domain containing cofactor promotes ATP hydrolysis, thereby stabilising Hsp70 interaction with the substrate (Liberek et al., 1991). In mammals, seven ER proteins with J-domains inside the ER lumen have been identified. ERdj1 is a transmembrane protein

whose cytosolic domain is interacting with translating ribosomes and inhibits translation if BiP is not bound to its lumenal J-domain, ensuring that BiP is present to interact with newly synthesised polypeptides of the secretory pathway (Dudek et al., 2005). ERdj3 directly interacts with folding substrate as well as with terminally misfolded proteins (Shen and Hendershot, 2005). Furthermore, ERdj3 was found in a complex with BiP and other folding enzymes (Meunier et al., 2002), suggesting that ERdj3 recruits BiP to substrates. ERdj5 contains four thioredoxin-like domains, contributing to its reductase activity (Cunnea et al., 2003; Hosoda et al., 2003). It plays a role in disulphide bond formation, which will be discussed later in this chapter. ERdj6 binds unfolded substrates and acts as BiP co-chaperone (Petrova et al., 2008; Rutkowski et al., 2007).

No distinct roles have been discovered so far for ERdj2, ERdj4 and Erdj7. The termination of the cycle, substrate release from BiP, is achieved through the action of a nucleotide exchange factor (NEF), exchanging ADP with ATP. The first NEF identified in the ER was BiP-associated protein (BAP) (Chung et al., 2002), involved in releasing BiP substrates (Awe et al., 2008).

1.4.2 Oxidative folding in the ER

The ER provides a unique cellular environment for oxidative folding. While the environment in the cytosol is highly reducing with a ratio of reduced (GSH) to oxidised (GSSG) glutathione of ~100:1 (Hwang et al., 1992), the oxidizing environment of the ER [GSH: GSSG ratio 3:1, (Hwang et al., 1992)] promotes disulphide bond formation by PDIs, and in addition, PDIs can reduce and isomerise disulphide bonds. Disulphide bonds are formed through the oxidation

of pairs of free thiols on cysteine residues and are believed to confer stability for proteins facing the extracellular milieu.

There are at least 15 PDI family members, which might reflect different substrate specificity or preference for either reduction or oxidation reactions (Hatahet and Ruddock, 2007; Jessop et al., 2007; Jessop et al., 2009; Schulman et al., 2010). Substrate specificity can be conducted by the interaction partners of a PDI family member. For example, ERp57 interacts preferentially with glycosylated substrates (Jessop et al., 2007). This is facilitated by the interaction of ERp57 with the ER lectins calnexin and calreticulin (Oliver et al., 1997). Furthermore, it has been demonstrated that P5 associates with BiP (Jessop et al., 2009) and ERdj5 with BiP and EDEM during protein degradation (Ushioda et al., 2008).

PDIs contain two thioredoxin-like catalytic domains, a and a', which are separated by two non-catalytic domains, b and b' (Kemmink et al., 1996, 1997); substrate binding is mediated by the b' subunit (Klappa et al., 1998). The two catalytic domains comprise the characteristic CXXC active-site motif (X=any amino acid), whereby the two amino acids between the two cysteine residues determine the redox potential of the enzyme and hence its function as disulphide reductase, oxidase or isomerase. To catalyse disulphide bond formation, the PDI family member has to be oxidised itself by an oxidase.

In yeast, a single protein named ER oxidase 1 (Ero1p) has been identified as necessary and sufficient to perform this reaction (Frand and Kaiser, 1998; Pollard et al., 1998). In mammals, two Ero1 homologues are present, Ero1α and Ero1β, which accomplish the same function as Ero1p but have a differential

expression pattern in tissues (Cabibbo et al., 2000; Pagani et al., 2000). In yeast and mammals, the primary enzyme oxidised by Ero1 is PDI, although other PDI family members might be substrates as well (Inaba et al., 2010). The source of the oxidising environment in the ER is flavin adenine dinucleotide (FAD) bound to Ero1p (Tu et al., 2000) and molecular oxygen serves as the terminal electron acceptor (Tu and Weissman, 2002).

Apart from Ero1, the mammalian system contains a number of peroxidases that use hydrogen peroxide as their terminal electron acceptor. The best characterised member is peroxiredoxin IV (Cao et al., 2011; Tavender et al., 2008; Tavender et al., 2010; Wang et al., 2012a; Zito et al., 2010). To date, PDI, ERp46 and P5 have been validated as peroxiredoxin IV substrates (Tavender et al., 2010). As PDI family members are able to reduce disulphide bonds, their active site must be in a reduced state. Therefore, as a consequence, there must be a pathway for PDI reduction, but no candidates have been identified so far.

1.4.3 Prolyl Isomerisation

The peptide bond linking two adjacent amino acid residues can adopt either a *cis* or a *trans* conformation, with the *trans* state being energetically favourable for all amino acids except Pro. For Pro, the energy difference between the *cis* and the *trans* conformation is much smaller with the *cis* conformer being found in 5-6 % of protein structures (Pal and Chakrabarti, 1999; Stewart et al., 1990). PPIs catalyse the intrinsically slow *cis-trans* isomerisation of peptide bonds N-terminal of Pro, a rate-limiting step in folding of a number of proteins, such as antibodies (Feige et al., 2009; Jager and Pluckthun, 1997) and ribonuclease A (Schmid and Baldwin, 1978). To date, four ER-resident PPIs have been

identified, namely cyclophilin B (Bose et al., 1994), FKBP13 (Gopalan et al., 2006), FKBP23 (Feng et al., 2011), and FKBP65 (Murphy et al., 2011).

1.4.4 N-linked glycosylation

The majority of proteins that enter the ER are covalently N-linked glycosylated as addition of sugar moieties increases both protein stability and solubility [reviewed in (Mitra et al., 2006)]. N-linked glycosylation occurs prior to BiP binding if the recognition site resides at the very N-terminus of the polypeptide (Molinari and Helenius, 2000). The glycan is partially assembled onto the lipid carrier dolichol pyrophosphate (Dol-PP) at the cytosolic face of the ER membrane. The precursor, Dol-$GlNac_2$-$Man_{5,}$ is then flipped to the lumenal side of the ER, putatively by Rtf1 (Helenius et al., 2002) and assembly is reassumed to finalise the glycan composed of $GlcNac_2$-Man_9-Glc_3 (GlcNAc: N-acetylglucosamine, Man: mannose and Glc: glucose).

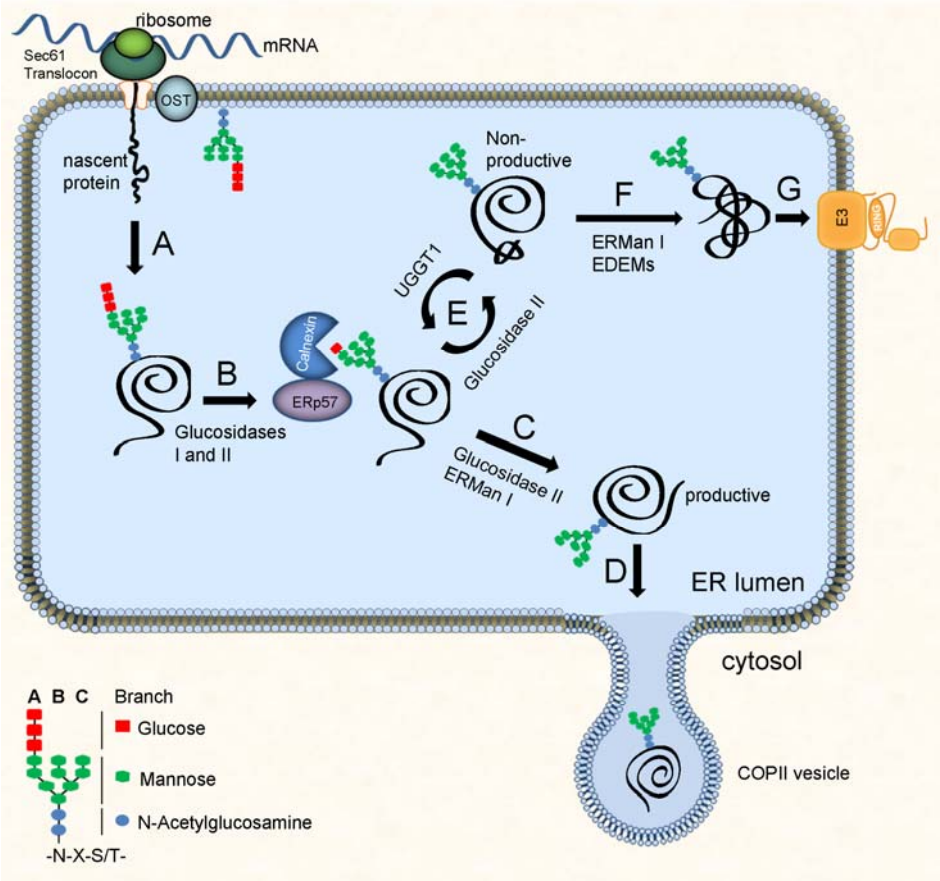


Fig. 1.2: Maturation of glycoproteins. (A) Nascent polypeptides are appended with a glycan composed of $GlcNac_2$-Man_9-Glc_3 by the OST complex. Shortly after addition of the glycan, glucosidases I and II remove the two distal Glc moeities and the resulting monoglucosylated peptide is subsequently bound by calnexin/calreticulun **(B)**. Glucosidase II removes the third Glc residue and ERMan I cleaves the outmost Man of the B branch from correctly folded proteins **(C)**, allowing their exit in COPII vesicles **(D)**. Misfolded polypeptides are re-glucosylated by UGGT1 and re-bound by calnexin to allow correct folding, in the process referred to as calnexin cycle **(E)**. However, if misfolding persists, slow-acting ERMan I and EDEMs remove further Man residues **(F)**, hence marking the polypeptide as substrate for ER quality control (ERQC) **(G)**.

The first seven sugar moieties added on the cytosolic face derive from nucleotide sugars (UDP-GlcNAc, GDP-Man), while those added in the ER lumen derive from lipid intermediates (Dol-PP-Man, Dol-PP-Glc) that were flipped across the membrane, like the growing glycan tree. The oligosaccharide composed of $GlcNAc_2$-Man_9-Glc_3 is then attached *en bloc* to asparagine residues with a consensus Asn-X-Ser/Thr motif in a co-translational reaction catalysed by the oligosaccharyl transferase complex (OST), which is attached

to membrane-bound ribosomes (Chavan et al., 2005; Harada et al., 2009; Shibatani et al., 2005) (Fig. 1.2). Site occupancy analysis revealed a preference for Asn-X-Thr over Asn-X-Ser sites and the exclusion of Pro at the second position as well as at position +3 relative to Asn (Bause, 1983; Chen et al., 2007; Gavel and von Heijne, 1990). Furthermore, putative glycosylation sites <12-14 amino acids away from a TMD are not glycosylated by OST (Nilsson and von Heijne, 1993).

The catalytic subunit of mammalian OST is primarily STT3A (Nilsson et al., 2003). The STT3B isoform glycosylates recognition sites skipped by STT3A and is responsible for post-translational glycosylation (Ruiz-Canada et al., 2009; Sato et al., 2012). The two catalytic isoforms form specific OST complexes with non-catalytical subunits mediating glycosylation of a different set of substrates (Kelleher et al., 2003; Roboti and High, 2012a), but they can functionally complement each other (Roboti and High, 2012b; Ruiz-Canada et al., 2009). Specific functions for most of the non-catalytic subunits have been identified. DAD1, OST48 and KCP2 are necessary for the assembly of functional OST complexes (Roboti and High, 2012b). Ribophorin I recruits a subset of membrane protein clients to the OST complex (Wilson and High, 2007; Wilson et al., 2005; Wilson et al., 2008) while ribophorin II increases the N-glycosylation of P-glycoprotein (Honma et al., 2008). OST4 promotes N-glycosylation by stabilising STT3A containing OST complexes (Dumax-Vorzet et al., 2013). For DC2, N33 and IAP no characteristic function has been determined yet.

1.4.5 Glycan trimming

Almost immediately after glycan attachment, ER-resident and membrane integrated Glucosidase I removes the terminal Glc residue, releasing the glycan from the OST complex (Hettkamp et al., 1984; Kalz-Fuller et al., 1995). This is followed by the removal of the second Glc residue by Glucosidase II (Brada and Dubach, 1984; Burns and Touster, 1982), resulting in a $GlcNAc_2$-Man_9-Glc_1 form recognised by the lectins calnexin and calreticulin (Fig. 1.2).

Membrane-bound calnexin and soluble calreticulin act as chaperones in proper folding and prevent nascent chains from aggregation [reviewed in (Caramelo and Parodi, 2008)]. Although the glycan-specificity is identical for these two chaperones (Kapoor et al., 2004; Patil et al., 2000; Schrag et al., 2001), they interact with different glycoproteins and calnexin seems to be more important as a folding assistant (Hebert et al., 1997; Molinari et al., 2004; Pieren et al., 2005). The protein disulphide isomerase ERp57 forms a complex with calnexin and accelerates protein folding, as is the case for RNAse B (Zapun et al., 1998) (discussed earlier in this chapter).

During folding of the polypeptide the remaining glucose is trimmed by glucosidase II, thus releasing the protein from calnexin/calreticulin. The cleavage of the terminal B-branch mannose by ER-mannosidase I allows a correctly folded glycoprotein to transit to its final destination in COPII-coated vesicles [reviewed in (Hebert et al., 2010)] (Fig. 1.2). Misfolded $GlcNAc_2$-Man_9 glycoproteins released from the calnexin cycle are recognised by UDP-glucose:glycoprotein-glucosyltransferase (UGGT1) and reglucosylated on the A branch. UGGT1 preferentially binds hydrophobic patches in nearly native polypeptides (Caramelo et al., 2003; Caramelo et al., 2004) and the presence

of both glycan and misfolded protein are required for this interaction (Sousa and Parodi, 1995; Sousa et al., 1992; Trombetta and Helenius, 2000). In more detail, the enzyme mainly recognises the core pentasaccharide $Man_3GlcNAc_2$ (Totani et al., 2009) and the innermost GlcNAc is indispensable for binding (Ritter et al., 2005). Reglucosylation allows a misfolded glycoprotein to rebind the calnexin/calreticulin complex and undergo additional folding cycles catalysed by ERp57 (Hebert et al., 1995) (Fig. 1.2).

1.5 Protein misfolding in the ER

The topological and structural complexity of glycoproteins, especially those that are polytopic, can often result in a high degree of protein misfolding and subsequent exposure of hydrophobic amino acid residues and/or reduced Cys residues. Genetic mutations, improper transcription or translation as well as cellular and environmental stresses can also disrupt protein folding. The outcome for each of these scenarios is an accumulation of terminally misfolded proteins in the ER, which are degraded by ERAD (Fig. 1.3). If the level of misfolded proteins exceeds the clearance capacity of ERAD, the unfolded protein response (UPR) is activated signalling a condition of ER stress. Activation of the UPR causes attenuation of protein translation and a transcriptional upregulation of chaperones and ERAD components to help clearing the excess protein load and restore ER function (discussed below).

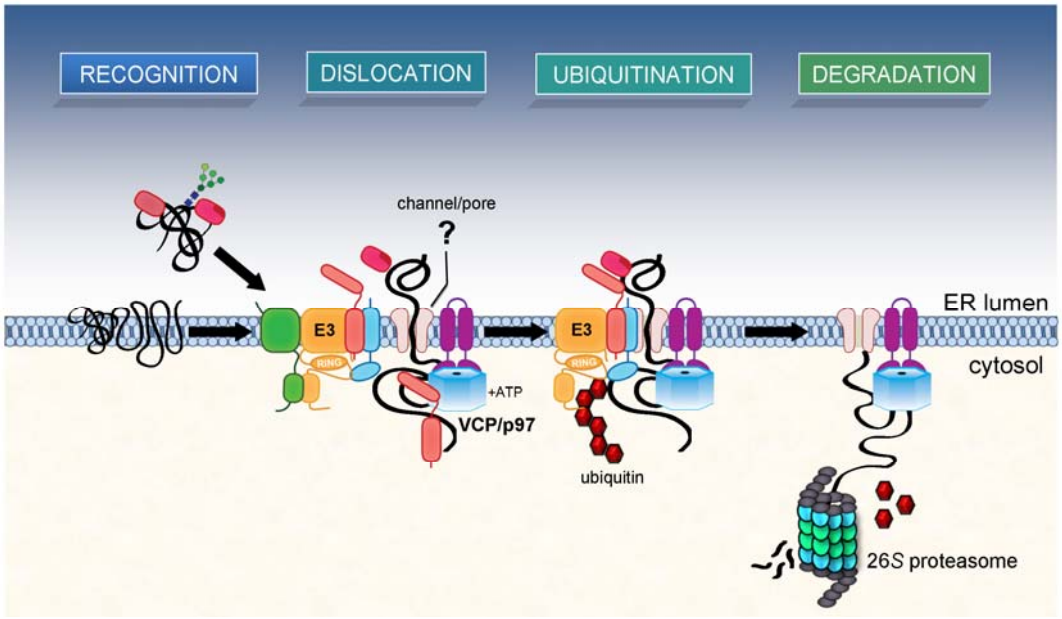


Fig. 1.3: Overview of ERAD. Misfolded proteins with lesions in their lumenal, membrane or cytosolic region are recognised in the ER lumen and subsequently targeted to ERAD complexes embedded in the ER membrane. Membrane proteins are dislocated and lumenal proteins retrotranslocated into the cytosol through a poorly defined mechanism and ubiquitinated by RING type, membrane embedded ubiquitin ligases upon emerging in the cytosol, which targets misfolded proteins for degradation by the 26S proteasome.

1.5.1 ERAD substrates

A robust ERAD machinery is in place to accommodate a wide range of potential substrates (Fig. 1.4). A large body of knowledge about this pathway has arisen from studies on model clients and examples will be discussed representing the four classes of ERAD substrates.

1.5.2 Terminally misfolded proteins

Cystic fibrosis (CF) is caused by dysfunction of the cystic fibrosis transmembrane conductance regulator (CFTR). CFTR is a member of the ATP-binding cassette (ABC) family of transporters and expressed in the apical membrane of epithelial cells. Loss of CFTR from the plasma membrane alters the transport of water, chloride and bicarbonate, leading to pancreatic

insufficiency, increased sweat chloride, severe constipation and chronic lung infection, leading to death due to respiratory failure. Although over 1,000 disease causing mutations have been reported in the CFTR gene, the most prominent one, in approximately 90 % of the cases, is the deletion of Phe 508 (ΔF508) (Riordan et al., 1989). This mutant is functionally active (Dalemans et al., 1991; Haws et al., 1996) but constitutively degraded from the ER, resulting in a loss of protein expression on the cell surface (Cheng et al., 1990). CFTR is comprised of two TMDs that form the pore and each TMD is followed by a cytosolic nucleotide-binding domain (NBD) that drives channel gating. ΔF508 interrupts the interaction between the first NBD and a cytosolic loop in the second TMD, preventing correct folding (Serohijos et al., 2008).

α-1 antitrypsin (AAT) is a serine protease inhibitor belonging to the serpin superfamily and is expressed primarily in hepatocytes. The protein is secreted into the blood stream where it inhibits neutrophil-derived proteases and elastase in the lung by acting as suicide inhibitor (Elliott et al., 1996; Huntington et al., 2000). Deficiency in AAT leads to uncontrolled breakdown of elastin, which contributes to elasticity of the lung, leading to pulmonary diseases and cirrhosis of the liver. Several disease-causing mutations have been identified for the AAT gene (DeMeo and Silverman, 2004) and the most common is termed Z-variant (E342K). Loss of an intramolecular salt bridge results in AAT-Z instability and self-aggregation in the ER of hepatocytes (Kass et al., 2012). Another mutant is the naturally occurring Null Hong Kong (NHK) variant, which has a premature stop-codon that prevents NHK from folding correctly (Sifers et al., 1988).

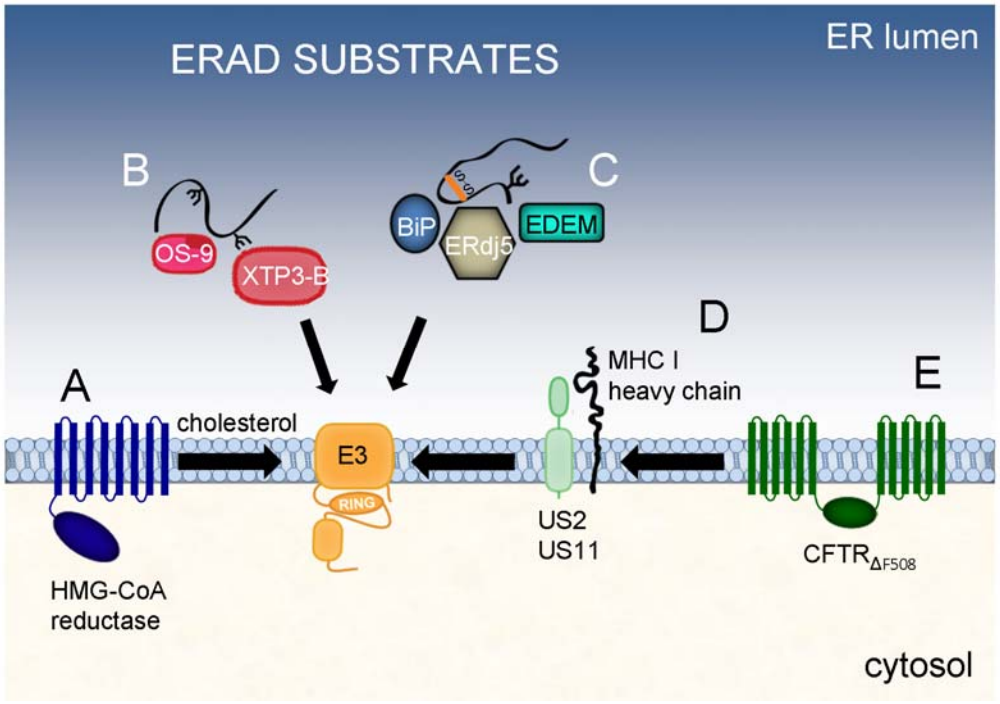


Fig. 1.4: Targeting of different ERAD substrate classes to ligase complexes. (A) High cholesterol levels induce degradation of HMG-CoA reductase. **(B)** Misfolded glycoproteins are recognised by two specific lectins, OS-9 and XTP3-B through their trimmed glycans as well as their polypeptide backbone. **(C)** ERdj5 interacts with misfolded proteins through BiP and EDEM and facilitates ERAD through reduction of disulphide bonds of substrate proteins **(D)**. The ERAD pathway is hijacked by viruses like the human cytomegalo virus (HCMV) proteins US2 and US11, which employ the ERAD machinery to degrade MHC class I heavy chains to avoid detection by the immune system. **(E)** Misfolded polytopic membrane proteins like CFTRΔF508 are recognised by ERAD complexes in the ER membrane.

1.5.3 Unassembled subunits of protein complexes

Subunits of multi-protein complexes are not synthesised in stoichiometric ratios and factors produced in excess are not stored in the ER for future complex assembly, but instead degraded by ERAD. The first substrate leading to the discovery and characterisation of ERAD was the TCR subunit TCRα (discussed earlier in this chapter). A second TCR subunit that is synthesised in surplus and has been extensively characterised as ERAD client is CD3δ (Bonifacino et al., 1989; Klausner et al., 1990; Yang et al., 1998).

The muscle-type acetylcholine receptor (AChR) in vertebrates is a heteromeric complex composed of five subunits (α1, β1, δ and γ/ε) whereby only 30% of α-subunits are assembled in functional AChRs (Merlie and Lindstrom, 1983). Maturation of AChR is dependent on the conserved ER membrane complex (EMC) in *Caenorhabditis elegans* (Richard et al., 2013) and unassembled subunits are degraded by ERAD (Christianson and Green, 2004).

During B-cell differentiation, an excess number of immunoglobulin (Ig) light chains is synthesised compared to Ig heavy chains. Most of these extra Ig light chains are still secreted (Stevens and Williamson, 1974), but some are degraded due to a destabilising sequence in the variable region (Davis et al., 2001; Dul et al., 1992). It could be demonstrated that Ig light chains were degraded in a non Ig heavy chain-expressing cell line as a result of the inability to assemble, not because of dysfunction (Arnold et al., 1988; Gardner et al., 1993).

1.5.4 Metabolically regulated proteins

Mammalian cells primarily obtain cholesterol from plasma lipoproteins. However, in case of reduced cholesterol availability or increased demand, cells upregulate the mevalonate pathway, in which sterols and non-sterol isoprenoids are produced. The rate-limiting step in this pathway is performed by 3-hydroxy 3-methylglutaryl coenzyme A (HMG-CoA) reductase, an integral membrane protein of the ER. HMG-CoA reductase stability is inversely regulated by metabolites of the mevalonate pathway (Edwards et al., 1983; Faust et al., 1982; Nakanishi et al., 1988). When cholesterol levels are low, HMG-CoA reductase is stable. But upon cholesterol saturation, the enzyme is rapidly

degraded (Ravid et al., 2000). Furthermore, Insig-1 and/or Insig-2 are involved in this regulated degradation by recruiting the E3 ubiquitin ligases gp78 and Trc8 to HMG-CoA reductase (Jo et al., 2011; Sever et al., 2003a; Sever et al., 2003b; Song et al., 2005b).

Another example is apolipoprotein B-100 (ApoB-100), the major protein component present in chylomicrons, very low density (VLDL) and low density lipoproteins (LDL) secreted from the liver and intestine. Lipids are co-translationally loaded onto ApoB-100 to form a primordial lipoprotein which matures along the secretory pathway (Fisher and Ginsberg, 2002; Hussain et al., 2003; Olofsson et al., 1999). When cholesterol or lipid levels are low, ApoB-100 is degraded by ERAD instead of being incorporated into lipoproteins (Benoist and Grand-Perret, 1997; Fisher et al., 1997; Yeung et al., 1996).

1.5.5 Immune evasion

The cell employs a number of defence mechanisms to survey and communicate viral infections. In order to evade detection, a number of viruses engage the ERAD pathway to downregulate components of the immune system, e.g. MHC class I, in order to prevent presentation of viral peptides on the plasma membrane. US2 and US11 are two proteins of the human cytomegalovirus (HMCV) expressed during infection that promote ERAD dependent degradation of MHC class I heavy chains (Wiertz et al., 1996a; Wiertz et al., 1996b). Despite the fact that US2 and US11 are similar, both are glycoproteins embedded in the ER membrane, they utilise different ERAD complexes for MHC class I dislocation. While US2 employs Signal Peptide Peptidase and the ubiquitin ligase Trc8 (Loureiro et al., 2006; Stagg et al., 2009), US11 mediated MHC class I heavy chain degradation depends on a

Der1-like protein (Derlin)-SEL1L complex (Lilley and Ploegh, 2004; Mueller et al., 2006; Ye et al., 2004).

On the other hand, there are examples demonstrating an active role of ERAD components in degradation of viral proteins. Infection with Hepatitis C virus (HCV), primarily affecting the liver, upregulates expression levels of the ERAD factors EDEM1 and EDEM3 (discussed in more detail below), which interact with glycosylated HCV envelope proteins and promote their ubiquitination (Saeed et al., 2011). In addition, downregulation of EDEM1 and EDEM3 or inhibition of mannosidases with kifunensine increases stability of viral proteins and virus particle production (Saeed et al., 2011). Similarly, infection with Hepatitis B virus (HBV) increases EDEM1, EDEM2 and EDEM3 levels, which are implicated in degradation of viral proteins (Lazar et al., 2012).

1.6 Substrate Recognition

The ERAD process can be divided into four steps, beginning with recognition of the misfolded protein. It is important that ER chaperones distinguish between folding competent and misfolded protein intermediates. Features of ERAD substrates can be exposure of hydrophobic domains that would normally be buried within the protein, unpaired Cys residues not participating in a disulphide bond or the specific trimming of the glycan moiety. In the event of persistent misfolding, slow-acting ER mannosidases (ERMan I and EDEMs) start to trim the oligosaccharide (Fig. 1.3).

ERMan I has a preference to trim an α1,2-linked mannose residue from the B Branch (Gonzalez et al., 1999; Tremblay and Herscovics, 1999). On the other hand, in case of a misfolded protein the specificity of the enzyme is less strict

and able to remove further mannose residues *in vivo* (Avezov et al., 2008; Frenkel et al., 2003; Gonzalez et al., 1999; Hosokawa et al., 2003; Wu et al., 2003) and *in vitro* (Aikawa et al., 2012; Herscovics et al., 2002). Three ER degradation enhancing alpha-mannosidase-like proteins (EDEMs) have been identified in mammals and thought to participate in mannose trimming of ERAD substrates. EDEM1 might be involved in extraction of ERAD substrates from the ER membrane through an as yet unknown mechanism (Molinari et al., 2003; Oda et al., 2003). A mannosidase activity could not be detected *in vitro* (Hosokawa et al., 2001) but overexpressed EDEM1 induces mannosidase activity *in vivo* (Hosokawa et al., 2010; Olivari et al., 2006). An enzymatic activity for EDEM2 could not be observed *in vivo* or *in vitro*, but the enzyme can associate with an ERAD substrate and overexpression results in accelerated ERAD of this substrate (Mast et al., 2005). However, overexpressed EDEM3 displays processing α1,2-mannosidase activity *in vivo* (Hirao et al., 2006).

A glycoprotein whose α1,2-linked mannose from the A branch has been removed cannot be recognised by UGGT1 for re-glucosylation anymore and is bound by the soluble ER resident lectins OS-9 and XTP3-B (Fig. 1.4). These lectins are homologues of yeast Yos9p and contain one or two mannose 6-phosphate receptor homology (MRH) domain(s), respectively, which bind glycan moieties. Osteosarcoma-9 (OS-9) is implicated in recognition of glycosylated (Christianson et al., 2008; Hosokawa et al., 2009b; Mikami et al., 2010; Satoh et al., 2010) as well as unglycosylated ERAD substrates (Christianson et al., 2008). Transactivated protein B/ Erlectin (XTP3-B) inhibits ERAD of NHK and its glycosylation-deficient mutant NHK-QQQ, indicating it is

a negative regulator of ERAD or protects nascent folding intermediates from degradation (Fujimori et al., 2013; Hosokawa et al., 2008).

OS-9 and XTP3-B are required for lumenal but not membrane substrates (Bernasconi et al., 2010) and mutations that disrupt their lectin domain results in impaired binding to SEL1L (Christianson et al., 2008). The OS-9 and XTP3-B MRH domain was therefore thought to mediate interaction with SEL1L but not with misfolded glycoproteins (Bernasconi et al., 2008; Christianson et al., 2008). In contrast, several groups demonstrated that the Yos9p/OS9/XTP3-B MRH domain is able to interact with a misfolded ERAD client by recognising the C branch α1,6-linked Man residue (Clerc et al., 2009; Hosokawa et al., 2009a; Mikami et al., 2010; Quan et al., 2008; Yamaguchi et al., 2010). Furthermore, the crystal structure of the OS-9 MRH domain has been resolved, revealing that two Trp residues mediate the specific interaction with the three α1,6-linked Man residues of the C-arm (Satoh et al., 2010). OS-9 binds as well the nonglycosylated mutant of AAT, NHK-QQQ, independent of these two Trp residues, indicating that OS-9 recognises as well features other than the glycan moiety on ERAD substrates (Satoh et al., 2010). Hence, the mode of interaction between OS9/XTP3-B and SEL1L remains controversial.

Non-glycosylated proteins must also be recognised and targeted for ERAD, but how this may occur is not very clear. In mammalian cells, BiP controls the degradation of some immunoglobulin light chain mutants in concert with Herp and Derlin-1 (Okuda-Shimizu and Hendershot, 2007). Co-expression of transthyretin (TTR) wild type (WT) or different TTR mutants with BiP in *Escherichia. coli* showed specific retention of the D18G TTR mutant by the chaperone (Sorgjerd et al., 2006). However, it needs to be noted that D18G

TTR contains a cryptic N-glycosylation site, which becomes exposed upon misfolding of the protein and glycosylated by STT3B, resulting in HMG-CoA reductase degradation 1 (Hrd1)-dependent ERAD (Sato et al., 2012). An artificial variant of AAT, NHK-QQQ, lacking its three N-glycosylation sites, is recognised by an ERAD complex comprised of Hrd1, suppressor enhancer lin12/Notch 1 like (SEL1L) and OS-9 (Iida et al., 2011).

A recent study added to the understanding of degradation of unglycosylated ERAD substrates (Shenkman et al., 2013). Calnexin, EDEM1 and Hrd1 are recruited to glycosylated as well as unglycosylated mutant of asialoglycoprotein receptor H2a, but only degradation of the glycosylated version requires cytosolic SCF^{Fbs2} E3 ubiquitin ligase. Unglycosylated BiP substrates NS-1κ light chains as well as truncated Igγ heavy chains interact with OS9, XTP3-B and EDEM1 (Shenkman et al., 2013).

1.7 Substrate Retrotranslocation/Dislocation

Due to the absence of a degradation machinery from the ER lumen, misfolded proteins must be retrotranslocated (soluble proteins) or dislocated (integral membrane proteins) to the cytosol in order to be degraded. The means by which this occurs is not well understood, but several candidate channels/pores have been proposed for this process. In general, it is reasonable that the translocon is in close proximity to ERAD complexes in order to allow degradation with high efficiency. While membrane substrates may be extracted from the ER membrane directly, soluble substrates require a channel or pore for entrance into the cytosol. This pore could be formed by homo- or heteromers of as yet to be identified proteins or known ERAD factors. As ER

proteins differ in size, ERAD substrates may need to be at least partially unfolded in order to pass a retrotranslocation pore.

The Sec61 translocon, traditionally responsible for the translocation of nascent polypeptides into the ER lumen, might perform a dual function, participating in the retrotranslocation of misfolded proteins back to the cytosol. This hypothesis could be proved for small peptides (Gillece et al., 2000), some lumenal substrates (Plemper et al., 1997; Willer et al., 2008) and several studies in yeast and mammals have suggested that Sec61p/Sec61α participates in ERAD of transmembrane proteins (Rubenstein et al., 2012; Scott and Schekman, 2008; Wiertz et al., 1996b). Furthermore, yeast Sec61p associates with the proteasome (Ng et al., 2007) and the Hrd1p ERAD ligase complex (Plemper et al., 1999; Schafer and Wolf, 2009). However, other ERAD studies were not able to demonstrate Sec61 dependency (Garza et al., 2009; Sato and Hampton, 2006; Wahlman et al., 2007) and the crystal structure of the bacterial translocon and Sec61 homologue SecYEG is reported to adopt an hourglass shape in the ER membrane (Van den Berg et al., 2004). The central hydrophilic passage has a diameter of 20Å and thus could theoretically only allow fully unfolded polypeptides to pass (Rapoport, 2007). While some substrates might need to be partially unfolded for retrotranslocation (Bhamidipati et al., 2005), it was shown that at least some ERAD substrates remain folded during this process (Tirosh et al., 2003).

The Derlin family of multispanning membrane proteins has been proposed as an alternative channel/pore based on the observation that Derlin-1 associates with different substrates while they pass through the ER membrane (Ye et al., 2004). Furthermore, Derlin-1 is required for US11 mediated MHC class I heavy

chain degradation (Lilley and Ploegh, 2004; Ye et al., 2004) and Derlin-2 and -3 are required for the turnover of the ERAD model substrate NHK mutant of AAT (Oda et al., 2006). A recent study revealed an essential role for Derlin-2 in retrotranslocation and degradation of the C-terminal fragment of sonic hedgehog (SHH) (Huang et al., 2013). However, neither Derlin orthologue in yeast (Der1p, Dfm1p) is essential for ERAD of membrane substrates (Garza et al., 2009; Sato and Hampton, 2006), arguing for an important but diverse role of Derlins in ERAD.

Another suggested mechanism is one where integral ER membrane ubiquitin ligases, responsible for ubiquitination of ERAD substrates, have been put forward as possible channels enabling proteins to pass through the membrane. The transmembrane segments of polytopic ubiquitin ligases contain polar and hydrophilic amino acid residues at conserved positions. Mutating selected residues of the yeast ubiquitin ligase Hrd1p to hydrophobic residues specifically impairs degradation of membrane-bound substrates (Sato et al., 2009). It has also been demonstrated that excess Hrd1p is able to carry out ERAD without the need of other Hrd1p complex components (Carvalho et al., 2010) and that its oligomerisation is required for degradation of lumenal ERAD substrates (Carvalho et al., 2010); it is possible for lumenal substrates to interact with Hrd1p during retrotranslocation. Usa1p connects Der1p with Hrd1 and mediates Hrd1p oligomerisation (Horn et al., 2009); these two accessory factors could assist in creating a pore of appropriate size.

An alternative mechanism to a proteinaceous channel/pore is one where misfolded proteins could be removed from the ER through the formation of lipid droplets (Ploegh, 2007). Lipid droplets are lipid storage devices and contain a

core of neutral lipids surrounded by a monolayer of phospholipids. Lipid droplets participate in the degradation of the secretory protein ApoB-100 (Fujimoto and Ohsaki, 2006; Ohsaki et al., 2006). However, this hypothesis has been called into question with the observation that lipid droplet formation is not essential for ERAD in yeast (Olzmann and Kopito, 2011). On the other hand, it has to be taken into account that mammalian lipid droplets are far more complex than their yeast counterpart (Yang et al., 2012) and mammalian HMG-CoA reductase was demonstrated to be associated with a lipid droplet-like compartment after extraction from the ER membrane (Hartman et al., 2010b).

A final and very recent hypothesis on ERAD substrate dislocation is the involvement of rhomboid and rhomboid-like proteases. Rhomboid proteases are involved in cleavage of membrane bound substrates at specific sites within the lipid bilayer [reviewed in (Urban and Dickey, 2011)]. Mammalian Derlin-1 shares homology with the rhomboid family but is catalytically inactive, therefore named rhomboid pseudoprotease. Nevertheless, a recent study concluded that Derlin-1's rhomboid-homologous domain is necessary for dislocation of mutant ERAD model substrate NHK (Greenblatt et al., 2011). Even more striking is that the evolutionary conserved rhomboid protease RHBDL4 performs cleavage of membrane proteins in an ERAD-dependent manner (Fleig et al., 2012).

In summary, a number of ERAD factors have so far been associated with ERAD substrate retrotranslocation and it is likely that a unique protein complex is not necessary for this step, but that instead distinct complexes form in response to different types of ERAD clients.

1.8 Substrate Ubiquitination

Attachment of polyubiquitin chains during or after retrotranslocation is the third step in ERAD, facilitating the targeting of misfolded proteins to the 26S proteasome for degradation. Ubiquitin conjugation requires the sequential activity of three enzymes [reviewed in (Pickart, 2001)]. The C-terminal glycine of ubiquitin is covalently attached, in an ATP-dependent manner, to the active site cysteine of a ubiquitin-activating enzyme (E1). The ubiquitin moiety is then transferred to a ubiquitin-conjugating enzyme (E2) through the formation of a thioester bond with the active site cysteine. The third enzyme is a ubiquitin ligase (E3) (Fig. 1.5). In some cases the action of a ubiquitin-chain elongation enzyme, E4, is needed (Koegl et al., 1999).

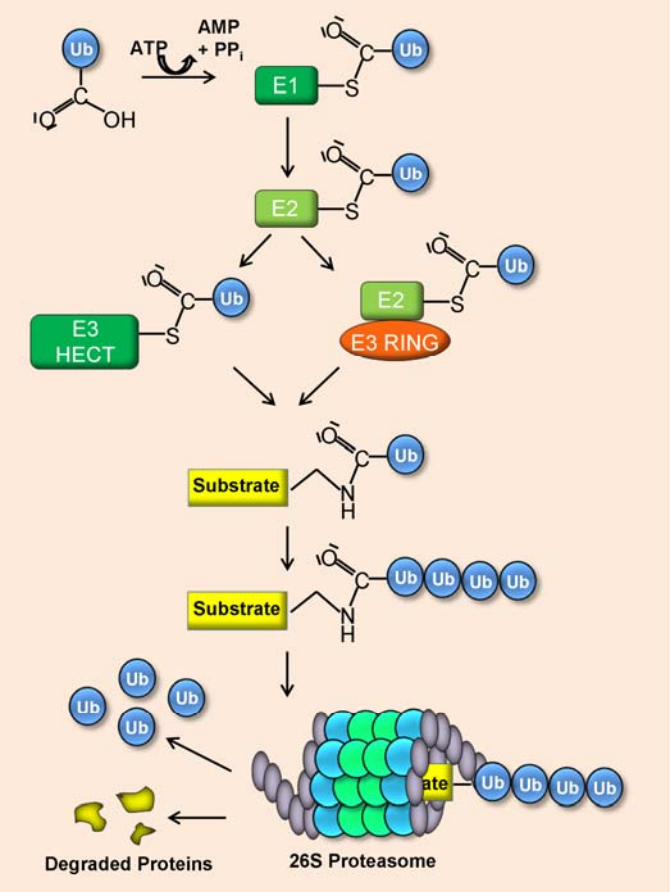


Figure 1.5: The ubiquitin-proteasome system. Ubiquitination of a target protein occurs in three steps. **1)** Ubiquitin is activated by conjugation to a ubiquitin-activating enzyme (E1) in an ATP-dependent manner. **2)** The ubiquitin moiety is transferred to a ubiquitin-conjugating enzyme (E2). **3)** Ubiquitin ligases (E3s) either bind directly to ubiquitin (HECT-domain E3s) before transfer to the target protein or function as a bridge between a ubiquitin-bound E2 and its target (RING-domain E3s). Ubiquitin is usually conjugated to the ε-amino group of lysine residues in proteins through an isopeptide bond. Polyubiquitin chains linked through Lys48 and a minimal chain length of 4 ubiquitin molecules target substrates to the 26S proteasome for degradation.

There are two main classes of ubiquitin ligases that are distinguishable not only by the structure of their catalytic domain but also by the mechanism through which they mediate ubiquitination (Wang and Schulman, 2009). One class of E3s are HECT domain (homologous to the E6AP carboxyl terminus) ligases which, like E1 and E2 enzymes, are directly conjugated to ubiquitin before transferring the ubiquitin molecule to the target protein (Fig. 1.5). On the

other hand, RING (Really Interesting New Gene) finger E3s are not directly conjugated to ubiquitin but mediate ubiquitin transfer to the substrate from E2-ubiquitin complexes (Fig. 1.5). Ubiquitin is generally linked to the ε-amino group of a lysine residue in the target protein via an isopeptide bond. However, studies show evidence for ubiquitin linkages to alternative amino acids including cysteine, serine and threonine residues (Ishikura et al., 2010; Shimizu et al., 2010) and the amino terminus (Breitschopf et al., 1998).

Ubiquitin cannot only be conjugated to substrates, but also to itself to form ubiquitin polymers. Linear polyubiquitin chains can be formed on all seven lysine residues in ubiquitin (K6, K11, K27, K29, K33, K48 and K63) (Adhikari and Chen, 2009). Proteasomal degradation is predominantly mediated by K48 linked polyubiquitin where a minimal chain length of four ubiquitin molecules is sufficient for targeting to the 26S proteasome (Chau et al., 1989; Thrower et al., 2000). Interestingly, a recent study in yeast showed enrichment of K11-linked polyubiquitin chains upon ER stress, suggesting a potential role for K11-linked polyubiquitin in ERAD (Xu et al., 2009). Monoubiquitination and K63-linked polyubiquitin chains on the other hand have mainly non-proteolytic functions in intracellular trafficking, DNA repair and signal transduction pathways [reviewed in (Grabbe and Dikic, 2009; Hicke et al., 2005)] although a recent report states that a monoubiquitin signal is sufficient to target short peptides for proteasomal degradation (Shabek et al., 2012).

While only about 30 HECT ubiquitin ligases have been identified in mammals, the vast majority of E3 ligases (> 600) are members of the RING and RING-related families like plant homology domain (PHD), leukemia associated protein (LAP) finger proteins and U-box domain E3s (Li et al., 2008). All 24

ubiquitin ligases so far associated with ERAD are RING finger ubiquitin ligases (Neutzner et al., 2011). The RING motif was identified in a number of proteins as a cysteine-rich sequence related to the zinc finger and named after the human gene RING1 (Freemont et al., 1991; Lovering et al., 1993). The canonical RING motif is Cys-X_2-Cys-$X_{(9-39)}$-Cys-$X_{(1-3)}$-His-$X_{(2-3)}$-Cys-X_2-Cys-$X_{(4-48)}$-Cys-X_2-Cys and the domain adopts a stable conformation by binding two zinc atoms, one through four cysteine residues and the second through the histidine and additional three cysteine residues. It was initially postulated that the RING finger mediates DNA binding (Freemont et al., 1991) but this assumption was challenged when it was demonstrated that the RING containing Rad 18 can promote histone ubiquitination (Bailly et al., 1997).

Two years later, a series of studies established that the RING domain binds E2s and promotes direct transfer of ubiquitin to substrates and that probably most of the RING domain family members possess this activity (Joazeiro et al., 1999; Kamura et al., 1999; Levkowitz et al., 1999; Lorick et al., 1999; Ohta et al., 1999; Seol et al., 1999; Skowyra et al., 1999; Tan et al., 1999; Yokouchi et al., 1999). RING E3s catalyse the transfer of ubiquitin to substrate with an apparent constant (k_{cat}) of one per second or faster (Petroski and Deshaies, 2005b; Saha and Deshaies, 2008) and the ubiquitin chain is built sequentially, although experimental evidence suggests that ubiquitin chains can as well be assembled on E2 or E3 and transferred *en bloc* (Bazirgan and Hampton, 2008; Li et al., 2007; Ravid and Hochstrasser, 2007; Wang and Pickart, 2005).

RING E3s can function as monomers, dimers or as part of multi-subunit complexes. Dimerisation often occurs through the RING domain or surrounding regions and can result in homodimers [e.g. cIAP (Mace et al., 2008), RNF4

(Liew et al., 2010), SIAH (Polekhina et al., 2002) or TRAF2 (Park et al., 1999)] or heterodimers [e.g. HDM2 and HDM4 (Linke et al., 2008; Sharp et al., 1999), BRCA1 and BARD1 (Brzovic et al., 2001; Simons et al., 2006; Wu et al., 1996), RNF2 and BMI1 (Buchwald et al., 2006; Satijn and Otte, 1999)]. An example of a multi-subunit E3 complex is the cullin-RING E3 [reviewed in (Hua and Vierstra, 2011; Petroski and Deshaies, 2005a)]. Little is known about the function of dimerisation of certain RING E3s but it can be essential for ligase activity (Liew et al., 2010; Mace et al., 2008; Plechanovova et al., 2011; Vander Kooi et al., 2006; Yin et al., 2009). Although the E2 binding surface on monomeric and dimeric RING E3s is similar and the binding domain of monomeric and dimeric RING E3s on the E2 is similar as well as (Dominguez et al., 2004; Mace et al., 2008; Shloush et al., 2011), it has been shown that RNF4 and cIAP dimers have a higher affinity for E2~ubiquitin conjugates than for E2 alone (Feltham et al., 2011; Plechanovova et al., 2011), indicating that RING E3 dimerisation is required for efficient ubiquitin transfer.

1.9 Ubiquitin ligase complexes involved in ERAD

In yeast, two ubiquitin ligases suffice to perform efficient ERAD. Hrd1p utilises the E2s Ubc7p as well as Ubc1p (Bays et al., 2001a) and degrades substrates with lesions in their membrane and ER lumenal domains while Doa10p, in conjunction with Ubc6p and Ubc7p (Chen et al., 1993), specialises in substrates with cytosolic lesions (Bordallo et al., 1998; Carvalho et al., 2006).

Mammals contain more than ten times as many ER ubiquitin ligases with less strict substrate specificities, reflecting the more elaborate quality control machinery in higher eukaryotes. Even three cytosolic ubiquitin ligases have an impact on ERAD. Parkin includes two RING fingers and has been identified as

ubiquitin ligase for Parkin-associated endothelin-like (Pael) receptor (Imai et al., 2001). Parkin is one of the most commonly mutated proteins in Parkinson's disease. CHIP is a U-box ubiquitin ligase and participates, for example, in the degradation of $CFTR_{\Delta F508}$ in concert with the ER E3 RMA1 (Younger et al., 2006). The Skp1-cullin-F-box (SCF) ligase complexes recognise and target some glycoproteins for degradation (Yoshida et al., 2005; Yoshida et al., 2003). The two mammalian ERAD E3s most research has been concentrated on so far are the homologues of Hrd1p: Hrd1 and gp78. These two enzymes will be discussed in detail in the following section.

The first mammalian ubiquitin ligase associated with ERAD was gp78/RNF45/AMFR (Fang et al., 2001). In addition to the RING domain, the C-terminus of gp78 contains a region homologous to yeast Cue1p. This region contains a CUE domain as well as a G2BR (Ube2g2 binding region) domain and both contribute to the ligase activity of the enzyme (Chen et al., 2006). CUE domains are ~40 aa long, fold as a three α-helix-bundle and bind ubiquitin (Kang et al., 2003; Prag et al., 2003). This domain might facilitate assembly of polyubiquitin chains by gp78. Gp78 binds the ubiquitin conjugating enzyme Ube2g2 via its G2BR, thereby recruiting this E2 to the gp78 complex (Chen et al., 2006).

Gp78 interacts with other components of the ERAD machinery, such as VCP/p97 (Zhong et al., 2004). This interaction is dispensable for ERAD (Chen et al., 2006) and it is anticipated that Ubxd2/Erasin recruits VCP/p97 to the complex through interaction with gp78 (Liang et al., 2006). The same study identified Derlin-1 as component of the gp78 complex (Liang et al., 2006). The E3 is recruited to the peripheral ER, the site of ERAD, by RING-palmitoylation

(Fairbank et al., 2012; St-Pierre et al., 2012). To date, a number of gp78-dependent ERAD substrates have been identified, including the T-cell receptor subunits TCR-α and CD3-δ, SOD1 and ataxin-3, $CFTR_{\Delta F508}$ as well as the Z-variant of AAT (Ballar et al., 2010; Chen et al., 2006; Shen et al., 2006; Ying et al., 2009). A very interesting finding is that gp78 is crucial for metastasis of an aggressive human sarcoma by degrading the transmembrane metastasis suppressor KIA1 (Tsai et al., 2007). Furthermore, gp78 ligase activity is required for sterol-regulated degradation of HMG-CoA reductase and Insig-1, indicating an important role in cholesterol metabolism (Lee et al., 2006; Song et al., 2005b).

Recently, a second ER-resident E3, Trc8, was implicated in HMG-CoA reductase degradation (Jo et al., 2011). While gp78 is recruited by Insig-1, Trc8 is bound by both Insig-1 and Insig-2 to induce sterol-dependent degradation of HMG-CoA reductase (Jo et al., 2011). Moreover, assembly of VLDL is regulated by ubiquitination of ApoB-100 through gp78 (Fisher et al., 2011). In agreement with these results, a subpopulation of gp78 localises to the smooth ER, the site of lipid and steroid biosynthesis (Benlimame et al., 1998; Benlimame et al., 1995; Wang et al., 1997).

There is also evidence of gp78 teaming up with other ubiquitin ligases to promote substrate degradation. Gp78 was found to work in concert with cytosolic E3 CHIP for degradation of cytochrome P450 of the 3A subfamily (CYP3A), the major family of liver enzymes clearing xenobiotics (Kim et al., 2010; Pabarcus et al., 2009; Peer et al., 2011; Wang et al., 2012b). Another example is the coordinated action of gp78 and Hrd1 in retrotranslocation of the cholera toxin catalytic subunit CTA1 from the ER (Bernardi et al., 2010). Gp78

levels appear to be controlled by Hrd1-mediated degradation (Shmueli et al., 2009).

The Hrd1 ligase complex is the so far best characterised ubiquitin ligase complex involved in ERAD (Fig. 1.6). Hrd1 and gp78 share 50 % homology in their TM region. Hrd1 does not contain a CUE or a G2BR domain and interacts with Ube2g2 through AUP1, which contains both of these domains (Klemm et al., 2011). In conjunction with another E2, Ube2j1, Hrd1 processes misfolded MHC class I heavy chains (Burr et al., 2011). In contrast to gp78 and Hrd1p, Hrd1 is not involved in sterol-mediated degradation of HMG-CoA reductase but in its basal regulation (Kikkert et al., 2004; Nadav et al., 2003). So far, the C-terminal fragment of hedgehog (Chen et al., 2011) and CD147 (Tyler et al., 2012) have been identified as constitutive Hrd1-dependent ERAD substrates.

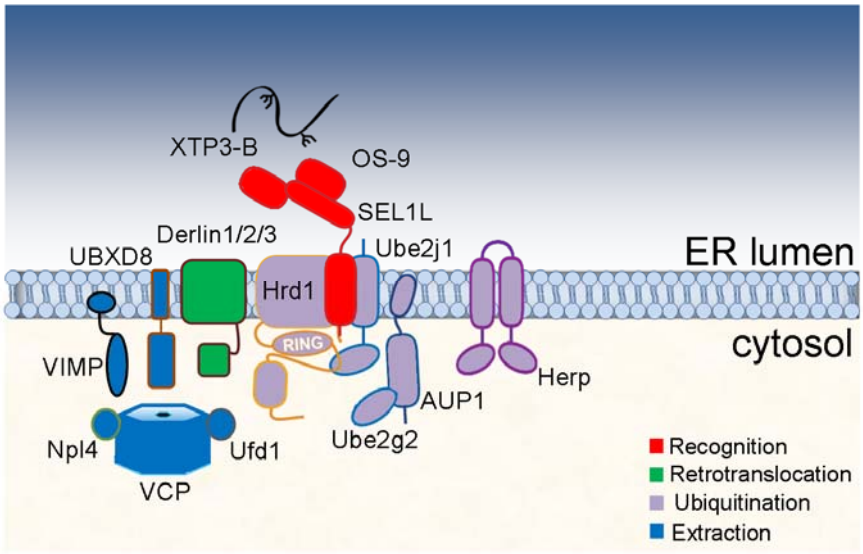


Fig. 1.6: The Hrd1 complex promotes degradation of misfolded proteins from the ER. Misfolded proteins can be recognised by the lectins OS-9 and XTP3-B, which target ERAD substrates to the Hrd1 complex through interaction with SEL1L. Retrotranslocation of ERAD clients may be mediated by the ubiquitin ligase Hrd1 and/or the Derlins. Hrd1 ubiquitinates dislocated/retrotranslocated proteins utilising the E2s Ube2j1 or Ube2g2, which is recruited to the complex by AUP1. Herp associates with Hrd1 under ER stress and facilitates substrate ubiquitination. ERAD substrates are extracted from the membrane by VCP/p97 and its co-factors Npl4 and Ufd1; VCP/p97 is recruited to the ER membrane through VIMP, UBXD8 and Derlin-1.

Glycosylated substrates are commonly targeted to the Hrd1 complex by OS-9 and XTP3-B (described previously) where these ER lectins bind the lumenal adaptor of Hrd1, SEL1L (Christianson et al., 2008; Hosokawa et al., 2008). Other substrates include Z variant of AAT, TCR-α and CD3-δ (Kikkert et al., 2004; Nadav et al., 2003; Wang et al., 2011b). These two subunits of the T cell receptor and this AAT mutant are as well degraded by gp78, as described before, and might represent promiscuous substrates that can be processed by different E3s. Hrd1 is furthermore implicated in the degradation of Pael receptor, like parkin; the accumulation of this receptor is associated with Parkinson's disease (Omura et al., 2006). Another neurodegenerative disease is Chorea Huntington and Hrd1 was shown to act on polyglutamin-expanded huntingtin (Yang et al., 2007).

Hrd1 is not only associated with neurodegenerative diseases but as well with rheumatoid arthritis (RA). RA includes chronic inflammation of joints linked to synovial cell overgrowth, resulting in cartilage and bone destruction (Aarvak and Natvig, 2001; Schett et al., 2001). These synovial cells overexpress Hrd1 and are resistant to ER-stress induced apoptosis *ex vivo* (Amano et al., 2003). Furthermore, Hrd1 overexpression in mice leads to RA with synovial hyperplasia (Amano et al., 2003) while siRNA mediated knockdown of Hrd1 sensitises rheumatoid synovial cells to ER-stress related cell death (Yamasaki et al., 2006).

Interestingly, a few studies identified cytosolic clients of Hrd1. A hydrophobic sequence targets cytosolic serum- and glucocorticoid-induced kinase (Sgk1) for Hrd1-dependent ERAD (Arteaga et al., 2006) and tumour suppressor p53 can as well be cleared through the action of this E3 (Yamasaki et al., 2007).

Recently, it was demonstrated that the transcription factor Nrf1, maintaining cellular homeostasis, is degraded from the cytosol under basal conditions in a Hrd1-dependent manner (Tsuchiya et al., 2011). Moreover, a quantitative proteomics approach identified a number of novel ERAD substrates, which need to be validated in further experiments (Lee et al., 2011).

1.10 Substrate Degradation

Polyubiquitinated substrates are extracted from the ER membrane by the cytosolic AAA (ATPase associated with various cellular activities) ATPase VCP/p97 (Jarosch et al., 2002; Rabinovich et al., 2002; Ye et al., 2001) as part of ERAD (Fig. 1.7). The enzyme contains two ATPase domains and the first of these assembles VCP/p97 into a barrel-like hexamer with a central pore (Wang et al., 2004). VCP/p97 associates with its cofactors Ufd1 and Npl4 (Meyer et al., 2000; Ye et al., 2001) and the correct recognition of polyubiquitin chains through the ubiquitin binding motif on Ufd1 is crucial for its dislocation function (Bays et al., 2001b; Flierman et al., 2003; Park et al., 2005; Ye et al., 2003).

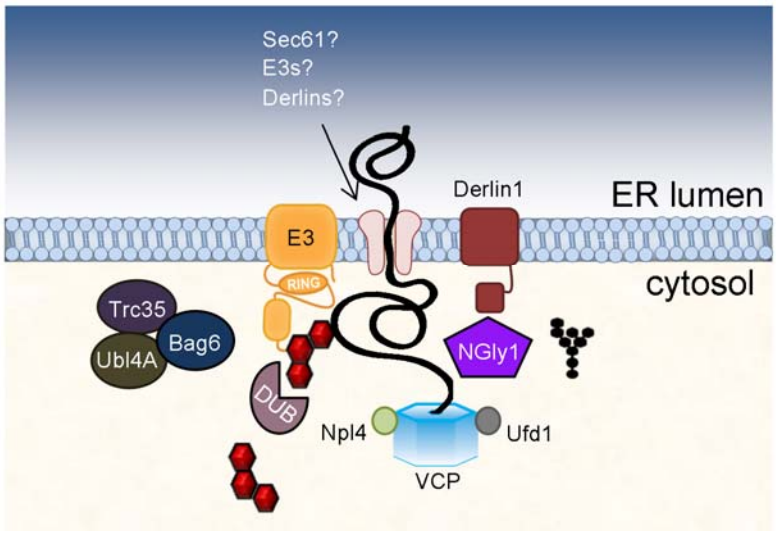


Fig. 1.7: Model for ERAD substrate extraction from the ER membrane. (A) During extraction through VCP/p97, polypeptides are de-glycosylated by NGly1, which binds to Derlin-1 and VCP/p97. DUBs play an increasingly important role in protein extraction and they likely act upstream of VCP/p97 to facilitate extraction from the ER membrane. The Bag6 complex is novel player in membrane extraction by acting as chaperone for ERAD substrates in the cytosol.

VCP/p97 is recruited to the ER through binding domains on the ER-resident proteins VIMP, UBXD8, Erasin and the SHP domain of Derlin-1 (Greenblatt et al., 2011; Liang et al., 2006; Lilley and Ploegh, 2005; Mueller et al., 2008; Ye et al., 2004). ATP-hydrolysis provides the energy to allow a change in VCP/p97 conformation (Rouiller et al., 2002; Zhang et al., 2000), resulting in the mechanic force to extract substrates from the membrane in an as yet undefined mechanism. Experimental evidence that substrates pass through the VCP/p97 central pore is missing; in contrast to this hypothesis, it was demonstrated that a VCP/p97 substrate can be released into the cytosol in a folded state (Fiebiger et al., 2002).

A recent study reports the importance of the deubiquitinating enzyme (DUB) YOD1 for membrane extraction (Ernst et al., 2009). YOD1 interacts with the VCP/p97-Ufd1-Npl4 complex and ERAD components. DUB activity of YOD1 is

independent of ATP hydrolysis by VCP/p97, indicating that YOD1 acts upstream of or in parallel to protein extraction. The authors therefore propose a model in which removal of some of the ubiquitin chains from degradation substrates facilitates the passage through the VCP/p97 pore. This model is challenged though by the lack of data proving substrate threading through the VCP/p97 pore.

A second DUB having an impact on ERAD is ataxin-3. Ataxin-3 interacts with HHR23a and HHR23b, two ubiquitin receptor proteins of the proteasome (Doss-Pepe et al., 2003; Wang et al., 2000) and VCP/p97 (Boeddrich et al., 2006; Doss-Pepe et al., 2003). In contrast to YOD1, ataxin-3 acts downstream of substrate extraction as the enzyme cannot mediate ubiquitin chain cleavage upon VCP/p97 inactivation (Wang et al., 2006, 2008; Wang et al., 2010b). Overexpression of ataxin-3 moderately inhibits ERAD but its knockdown has no significant effect on protein homeostasis (Wang et al., 2006; Zhong and Pittman, 2006). While Zhong et al. suggest a negative regulation of ataxin-3 on ERAD substrate flow to the proteasome, Wang et al. propose a positive but non-essential role of ataxin-3 in ERAD, facilitating substrate flow to the proteasome. Results from studies in *C. elegans* and mice support the second hypothesis (Hubener et al., 2011; Rodrigues et al., 2011).

Recent efforts identified at least four additional DUBs with a putative role in ERAD, namely USP13, USP50 and VCPIP1(Sowa et al., 2009) and USP19 (Hassink et al., 2009). Expression of a DUB catalytic domain derived from Epstein-Barr virus (EBV) resulted in accumulation of cytosolic and ER-extracted proteins that were not degraded by the proteasome, likely due to pre-emptive ubiquitin chain removal (Ernst et al., 2011). In addition, it was very recently

shown that DUBs act on ERAD substrates that dissociate rapidly from E3s, therefore discriminating between folding competent and misfolded proteins (Zhang et al., 2013) (Fig. 1.7).

Interestingly, the Bag6 complex, previously introduced as mediator of TA-protein insertion into the ER membrane, might act in concert with DUBs to facilitate proteasomal transport of dislocated ERAD substrate (Wang et al., 2011c). The three components of the Bag6 complex (Bag6, Trc35 and Ubl4A) interact with gp78 and might act as chaperones for dislocated ERAD substrates, maintaining them in a soluble state and therefore enhancing ERAD efficiency (Fig. 1.7). An additional prerequisite for ERAD substrate degradation is removal of the glycan upon dislocation into the cytosol by peptide:N-glycanase (NGly1), which recognises $GalNAc_2$ (Suzuki, 2007). NGly1 is recruited to the site of ERAD through interaction with Derlin-1 and the C-terminus of VCP/p97 (Katiyar et al., 2005; Li et al., 2006) (Fig. 1.7). Phosphorylation of the C-terminal Tyr residue of VCP/p97 abolishes interaction with NGly1, indicative of a further regulatory control step in ERAD (Zhao et al., 2007).

The final step of ERAD is delivery of the substrate to the 26S proteasome. The proteasome is composed of a catalytic 20S core and two 19S regulatory caps. The 20S core has a barrel-shaped form comprised of four stacked rings, each containing seven subunits. The active sites reside in the inner chamber of 20S and are sheltered from the external milieu. The subunits RNP10 and RNP13 of the proteasome recognise ubiquitin and thus the substrate (Deveraux et al., 1994; Husnjak et al., 2008). Access to the proteasome requires cleavage of the polyubiquitin chains by DUBs and protein unfolding by ATPases present

in the regulatory particles. Within the proteasome the protein is degraded by the proteolytic 20s core and peptide fragments of 8-10 aa are subsequently released into the cytosol.

1.11 Unfolded protein response (UPR)

The imbalance between protein synthesis and degradation in the ER can result in the accumulation of misfolded proteins, termed ER stress. The ER responds to this challenge by triggering the UPR, consisting of three branches to restore protein homeostasis. Each UPR branch possesses a specific effector protein in the ER membrane, IRE1, PERK and ATF6, and together their action results in general inhibition of translation, expression of ER chaperones and ERAD components, and an increase in ER membrane capacity. Under basal conditions these three stress sensors are bound by the ER chaperone BiP. Upon an increase of misfolded proteins in the ER lumen, BiP is titrated away from IRE1, PERK and ATF6 in order to keep the folding defective polypeptides soluble. This leads to the activation of the UPR mediators and their specific mode of action will be discussed in the following section.

The Inositol-requiring enzyme-1 (IRE1) pathway is the most conserved branch of the UPR. In mammals, there are two isoforms, IRE1α and IRE1β, executing different functions. While IRE1β promotes cleavage of 28S rRNA and translational attenuation, IRE1α mediates splicing of the X-box-binding protein 1 (XBP1) mRNA (Iwawaki et al., 2001; Tirasophon et al., 1998). Ribosome-bound XBP1 unspliced (XBP1u) mRNA is targeted to the ER membrane through a hydrophobic patch in the XBP1u nascent chain (Yanagitani et al., 2009). Spliced XBP1 translocates to the nucleus and induces transcription of genes involved in ER protein synthesis, folding, glycosylation, ERAD, redox

metabolism, autophagy, lipid metabolism and vesicular trafficking [reviewed in (Walter and Ron, 2011)].

ER stress further activates the JNK and NF-κB pathways through the IRE1α branch. Activation of JNK requires TRAF2, MAP3K, ASK1 and ASK1-interacting protein-1 (AIP1) (Luo et al., 2008; Nishitoh et al., 2002; Urano et al., 2000). This pathway can exhibit apoptotic (Yoneda et al., 2001) as well as survival functions during ER stress, the latter including activation of c-Jun (Fuest et al., 2012; Zhao et al., 2008) and upregulation of Hrd1 (Kaneko et al., 2007) as well as the ER chaperones BiP and GRP94 (Shinkai et al., 2010). Activation of NF-κB, which requires IRE1α and TRAF2 (Kaneko et al., 2003), regulates expression of manganese superoxide dismutase (MnSOD), an antioxidant enzyme of the mitochondrial matrix (Kaneko et al., 2004).

IRE1 levels are regulated in different manners. For one, IRE1α regulates its expression by cleaving its own mRNA (Tirasophon et al., 2000). After prolonged ER stress IRE1α activity is attenuated by complex disassembly, dephosphorylation and decreased endoribonuclease activity (Li et al., 2010).

Double-stranded RNA-activated protein kinase (PKR)-like ER kinase (PERK) is conserved across metazoan but not in yeast. The protein contains a PEK-like catalytic domain and phosphorylates the α-subunit of the eukaryotic translation initiation factor-2 (eIF2α), resulting in general translation attenuation (Shi et al., 1998). eIF2α-GTP associates with initiator Met-tRNA and participates in the ribosomal selection of the start codon. GTP is subsequently hydrolysed and eIF2α-GDP released from the ribosome. eIF2β is the nucleotide exchange factor of eIF2α, which is inhibited upon eIF2α phosphorylation and therefore

leading to a reduced translation rate [reviewed in (Dever, 2002)]. Protein translation is not entirely blocked though; the transcription factor ATF4 is specifically upregulated (Harding et al., 2000), inducing expression of the pro-apoptotic factor CHOP (Fawcett et al., 1999). PERK activity is negatively regulated by dephosphorylation through GADD34 (Novoa et al., 2001) and binding of P58 (IPK), a HSP40 family member (Yan et al., 2002).

The two isoforms of activating transcription factor 6 (ATF6), ATF6α and ATF6β, traffic to the Golgi under ER stress where they are cleaved by Site-1 and Site-2 proteases (Haze et al., 1999; Ye et al., 2000). The N-terminal fragments, p50ATF6α and p60ATF6β, translocate to the nucleus and p50ATF6α induces transcription of several genes, including SEL1L (Kaneko et al., 2007), BiP and GRP94 (Yamamoto et al., 2007; Yamamoto et al., 2004), XBP1 (Yoshida et al., 2001), Herp (Kokame et al., 2001), CHOP (Ma et al., 2002) and P58 (IPK) (van Huizen et al., 2003). p60ATF6β on the other hand is a transcriptional repressor of p50ATF6α, modulating the intensity of the response signal (Thuerauf et al., 2007; Thuerauf et al., 2004).

1.12 ERAD and diseases

The importance of understanding the molecular basics of ERAD is emphasised by the remarkable fact that more than 60 pathologies are associated with ERAD to date [reviewed in (Guerriero and Brodsky, 2012)]. Cystic fibrosis is undoubtedly caused by ERAD, as discussed earlier in this chapter, but the direct link to other diseases is currently less clear. Future work will hopefully elucidate the role of ERAD in those pathologies to design novel drugs and therapies. A number of diseases, largely affecting modern societies and associated with ERAD, will be presented in the following section.

Alzheimer's disease is currently affecting approximately 36 million people worldwide and is the cause of 70% of diagnosed dementia (http://www.alz.co.uk/research/WorldAlzheimerReport2011.pdf). The disease is marked by progressive cognitive decline due to neuronal degeneration and synaptic loss in hippocampus, amygdala and temporal neocortex (Serrano-Pozo et al., 2011). The major toxic cause for this neurodegeneration is the formation of extracellular plaques comprised of amyloid-β (Aβ) peptide (Dickson, 1997; Glenner and Wong, 1984; Masters et al., 1985). The Aβ peptides are generated by β- and γ-secretase-mediated cleavage of amyloid precursor protein (APP) in the trans-Golgi network and endosomes (Haass et al., 1995; Kaether et al., 2006; Kinoshita et al., 2003). APP is a type I membrane glycoprotein expressed on the plasma membrane and in the Golgi with unknown function. Recent work suggests a role for Hrd1 in Aβ formation, linking ERAD to Alzheimer's disease (Kaneko et al., 2010). Hrd1 protein levels were shown to be decreased in brains of Alzheimer's patients and the E3 co-localised with APP. Furthermore, Hrd1 mediated APP degradation, resulting in fewer Aβ peptides and knockdown of Hrd1 stabilises APP and promotes Aβ generation. These striking findings need to be evaluated with caution though as it is unknown whether the decrease of Hrd1 in patient brains is the cause of Aβ production or its consequence.

Diabetes mellitus is another disease associated with ERAD. Diabetes type I is mainly diagnosed in young people, the cause being destruction of the pancreatic β-cells by the immune system, resulting in decreased level of insulin production for glucose clearance. In type II diabetes, muscle, fat and liver cells lose the ability to respond to insulin cues which is combined with decreased

insulin expression, but the underlying mechanism remains unknown. In 2010, approximately 285 million people worldwide suffered from diabetes, with type II being the prevalent form in 90% of the cases (*Williams textbook of endocrinology* (12th ed.), Philadelphia: Elsevier/Saunders. pp. 1371–1435). It is estimated that the number will have doubled by 2030 (Wild et al., 2004). Under conditions of high demand, insulin comprises 50% of the total protein synthesis in pancreatic β-cells (Schuit et al., 1988), which can result in increased ER stress (Elouil et al., 2007; Harding et al., 2001). Unresolved ER stress terminates in apoptosis, which contributes largely to diabetes type I and II β-cell death (Butler et al., 2003; Fonseca et al., 2010). In some cases, point mutations in the insulin gene cause neonatal diabetes. One of these point mutations, C96Y, is found as well in the Akita diabetes mouse model (Allen et al., 2004; Araki et al., 2003). These mice display upregulated Hrd1 specifically in β-cells mediating ubiquitination and therefore degradation of the folding incompetent insulin mutant (Allen et al., 2004). Furthermore, downregulation of Hrd1 complex components or proteasomal inhibition aggravated β-cell apoptosis in a mouse model with inducible expression of the insulin mutant (Hartley et al., 2010).

The ERAD pathway is hijacked by several viruses which use it to evade recognition by the immune system, one being HIV (Human Immunodeficiency Virus). In 2010 34 million people were infected with HIV worldwide and men and women are equally affected (http://www.nichd.nih.gov/health/topics/hiv/conditioninfo/Pages/how-many.aspx). HIV infection is characterised by decreasing levels of CD4 positive T-helper lymphocytes and can progress into acquired immune deficiency

syndrome (AIDS) when less than 200 CD4 T-cells/mm^3 are detected (http://www.ncbi.nlm.nih.gov/pubmedhealth/PMH0001620/). Although CD4 is the main receptor for HIV to enter a host cell, this surface molecule is quickly degraded after infection (Klatzmann et al., 1984). Downregulation of CD4 is a defence mechanism from superinfection and enables correct virus assembly (Levesque et al., 2003). Two different viral proteins, Nef and Vpu, mediate degradation of the two pools of CD4, surface expressed and newly synthesised in the ER. Nef mediates interaction between cell surface CD4 and the clathrin-associated adaptor protein 2 (AP-2) complex (Aiken et al., 1994; Bresnahan et al., 1999; Chaudhuri et al., 2007; Chaudhuri et al., 2009; Craig et al., 2000; Greenberg et al., 1997; Lindwasser et al., 2008), resulting in CD4 internalisation by the clathrin pathway (Burtey et al., 2007; Chaudhuri et al., 2007; Jin et al., 2005; Rhee and Marsh, 1994) and lysosomal degradation (daSilva et al., 2009). Vpu, on the other hand, employs part of the ERAD machinery for degradation of newly synthesised CD4 (Binette et al., 2007; Magadan and Bonifacino, 2012; Magadan et al., 2010; Schubert et al., 1996; Willey et al., 1992). Vpu interacts with CD4 (Bour et al., 1995; Magadan and Bonifacino, 2012; Margottin et al., 1996) and the $SCF^{\beta\text{-}TrCP1/2}$ ubiquitin ligase complex subunit SCFβ-TrCP1/2 (Butticaz et al., 2007; Margottin et al., 1996), bringing CD4 and the E3 in close proximity. CD4 is subsequently extracted from the ER membrane by VCP/p97 (Binette et al., 2007; Magadan et al., 2010), ubiquitinated by $SCF^{\beta\text{-}TrCP1/2}$ on the cytosolic tail (Magadan et al., 2010) and degraded in a UPS-dependent manner (Schubert et al., 1998).

In summary, it becomes increasingly evident that ERAD plays a pivotal role in a large number of diseases, but its distinct contribution requires further

investigation. Especially in diseases affecting an increasing number of patients worldwide, like Alzheimer's disease, diabetes and HIV, which are under intense research. Hopefully the associated link to ERAD will help to develop future therapies in order to relieve patients' suffering.

1.13 Aim of the study

The amazing feature of ERAD is that a relatively small number of ubiquitin ligases account for the degradation of potentially thousands of misfolded or regulated polypeptides arising in the ER. The best so far characterised ERAD ubiquitin ligase complex is the Hrd1 complex, but although many interactors have been identified, a complete picture of the composition and organisation of the Hrd1 complex in human cells is still lacking. To gain a more detailed insight into this aspect of ERAD, this work aims to characterise the interactions between Hrd1 and its accessory factors SEL1L, AUP1 and FAM8A1.

The research originated from a proteomics study with a particular interest in identifying novel and metazoan specific components of the Hrd1 complex, reflecting necessary adaptation in higher eukaryotes (Christianson et al., 2012). Furthermore, the interaction between Hrd1 and its established lumenal adaptor SEL1L is re-evaluated. Hrd1 and SEL1L comprise the core of the Hrd1 complex and the finding that the TMD of SEL1L is dispensable for the interaction with Hrd1, which had long been the assumed binding modus, requires the investigation of the mode of interaction (Christianson et al., 2008).

Chapter II: Materials and Methods

2.1 Materials

2.1.1 Reagents

Unless stated otherwise, chemicals were obtained from Sigma or Fisher BioReagents®. All restriction enzymes and their buffers were purchased from New England BioLabs (NEB). All tissue culture dishes, pipettes and Falcon tubes (15ml and 50ml) were obtained from Corning Incorporated. 1.5 ml and 2ml reaction tubes were obtained from Eppendorf. PVDF membrane was purchased from GE Healthcare and Nitrocellulose membrane from Whatman. N-ethylmaleimide (NEM) was purchased from Fluka Analytical and phenylmethylsulfonyl fluoride (PMSF) from Boehringer Mannheim.

5 x Agarose sample buffer

50 % (w/v) sucrose

100 mM EDTA, pH 8.0

0.1 % (w/v) bromphenol blue

0.1 % (w/v) xylene cyanol FF

Ammonium persulphate (APS)

10 % (w/v) stock solution was prepared in ddH_2O and stored at 4°C.

Coomassie staining solution

10 % Acetic acid

20 % EtOH

0.02 % Coomassie Brilliant Blue

in ddH_2O, stored at room temperature (RT)

COmplete Mini protease inhibitor cocktail

One tablet is dissolved in 1 ml of ice cold ddH_2O. 50 µl aliquots were stored at -20 °C.

Destaining solution

10 % Acetic acid

20 % EtOH

In ddH_2O, stored at RT

Extraction buffer for bacterial cells

250 mM Tris HCl pH 8.5

500 mM NaCl

5 mM EDTA

Stored at 4 °C

Add fresh: cOmplete EDTA-free protease inhibitor cocktail (Roche) (1 tablet per 50 ml of extraction buffer), 1:500 PMSF, 1 mM DTT

Freezing medium

90 % FBS

10 % DMSO

Stored at -20 °C

2x HEPES

8 g NaCl

0.105 g Na_2HPO_4

6.5 g HEPES

ddH2O to 500 ml, pH 6.95 to 7.10

stored at RT

High salt buffer for membrane protein extraction

10 mM Tris HCl, pH 8.0

0.5 M NaCl

Stored at 4 °C

Hypotonic buffer for membrane protein extraction

10 mM KOAc

10 mM HEPES, pH 7.5

2.5 mM $Mg(OAc)_2$

Stored at 4 °C

Add fresh: 1 mM PMSF, 1x cOmplete Mini Protease inhibitor cocktail (Roche)

Mammalian cell lysis buffer

50 mM Tris pH 7.4

5 mM EDTA

150 mM NaCl

Stored at 4 °C

Add fresh: 1x cOmplete Mini protease inhibitor cocktail (Roche), 2 mM NEM

PBS-Tween (PBS-T)

0.02%Tween (final) was diluted in 1 x PBS and stored at RT.

Primers

Primers (table 2.1.4) used for this study were synthesised by MWG, Invitrogen and Integrated DNA Technologies (IDT). The lyophilised primers were diluted in ddH_2O to obtain a concentration of 100 mM.

Sodium dodecyl sulphate (SDS) solution

A 10% (w/v) solution of SDS is dissolved in ddH_2O and stored at RT.

2x Laemmli buffer

0.125 M Tris HCl pH 6.8Tris

4% SDS

20% glycerol

0.004% Bromphenol blue

20 mM DTT

Stored in 2 ml aliquots at – 20 °C.

10x Transfer buffer

288.4g glycine

60.6g Tris Base

For 2L, prepared in ddH_2O and stored at RT.

1x Transfer buffer

10% 10x transfer buffer

20% methanol

70% ddH_2O

Stored at 4 °C

20 x ubiquitination buffer

800 mM Tris HCl, pH 7.5

100 mM MgCl2

40 mM ATP

40 mM DTT

Water

Nanopure water (Type I) generated from MilliQ water system was used for all experiments.

2.1.2 Antibodies

2.1.2.1 Primary antibodies

Table 2.1: List of primary antibodies

antigen	host	source	application
α-tubulin	mouse mAb	Sigma-Aldrich	WB (1:10000)
AUP1	rabbit pAb	Atlas antibodies	WB (1: 5000)
Derlin-1	rabbit pAb	kind gift of Dr. Yihong Ye, NHI Bethesda, MD, USA	WB (1:1000)
Derlin-2	rabbit pAb	kind gift of Dr. Yihong Ye, NHI Bethesda, MD, USA	WB (1:1000)
FAM8A1	rabbit pAb	purified serum	WB (1:10,000)
GAPDH	rabbit pAb	Sigma	WB (1:2000)
GST	rabbit pAb	Santa Cruz Biotechnology	WB (1: 10,000)
Hrd1	rabbit pAb	Bethyl Laboratories, Inc	WB (1:2000)
KDEL		Enzo Life Sciences	WB (1:3000), IF (1:500)
mono- and	mouse mAb	Enzo life Sciences	WB (1:1000)

polyubiquitinated conjugates (FK2)			
myc (9E10)	mouse mAb	kind gift of Prof. Xin Lu, LICR Oxford, UK	WB (1:5000)
myc (9B11)	mouse mAb	NEB	WB (1:5000)
SEL1L	goat pAb	Santa Cruz Biotechnology	WB (1:2000)
S-tag	rabbit pAb	ascites	WB (1:5000)
S-tag	mouse mAb	Thermo Scientific	WB (1: 10,000)
VCP/p97	rabbit pAb	acsites	WB (1:2000)

Abbreviations: monoclonal antibody (mAb), polyclonal antibody (pAb), western blot (WB), Immunofluorescence (IF)

2.1.2.2 List of secondary antibodies

Table 2.1.2: List of secondary antibodies

Ab name	host	source	application
anti-rabbit Immunoglobulins/HRP	goat	Santa Cruz Biotechnology	WB (1:10,000)
anti-mouse Immunoglobulins/HRP	goat	Santa Cruz Biotechnology	WB (1:10,000
anti-goat Immunoglobulins/HRP	donkey	Santa Cruz Biotechnology	WB (1:10,000
Alexa Fluor® 488 Anti-rabbit IgG (H+L)	rabbit	Invitrogen	IF (1:400)
Alexa Fluor® 647 Anti-rabbit IgG (H+L)	mouse	Invitrogen	IF (1:400)

Abbreviations: antibody (Ab), horseradish peroxidase (HRP), western blot (WB), Immunofluorescence (IF)

2.1.3 Plasmids

Table 2.1.3: List of plasmids

name	vector	information	tag	source
control	pcDNA3.1 (+)	empty vector	/	lab stock
S-AUP1 1-410	pcDNA3.1 (+)	human AUP1	S-tag	lab stock
S-AUP1 1-290	pcDNA3.1 (+)	fragment (1-290) of human AUP1	S-tag	cloned for this study
S-AUP1 1-364	pcDNA3.1 (+)	fragment (1-364) of human AUP1	S-tag	cloned for this study
AUP1-S 1-410	pcDNA3.1 (-)	human AUP1	S-tag	lab stock
S-AUP1 MFP	pcDNA3.1 (+)	mutant (VLP-> MFP) of human AUP1	S-tag	cloned for this study
GST-AUP1 290-344	pCMV-GST	fragment (290-344) of human AUP1	GST	cloned for this study
GST-AUP1 364-410	pCMV-GST	fragment (364-410) of human AUP1	GST	cloned for this study

GST-AUP1 348-410	pCMV-GST	fragment (348-410) of human AUP1	GST	cloned for this study
GST-AUP1 290-344	pGEX4T-2	fragment (290-344) of human AUP1	GST	cloned for this study
GST-AUP1 290-344 MFP	pGEX4T-2	mutant (VLP-> MFP) of human $AUP1_{CUE}$	GST	cloned for this study
S-FAM8A1 1-413	pcDNA3.1 (+)	human FAM8A1	S-tag	lab stock
S-FAM8A1 1-229-DFP	pcDNA3.1 (+)	fragment (1-229) of human FAM8A1 C-terminally fused to DFP	S-tag	lab stock
S-FAM8A1 1-255	pcDNA3.1 (+)	fragment (1-255) of human FAM8A1	S-tag	cloned for this study
S-DFP-FAM8A1 230-413	pcDNA3.1 (+)	fragment (230-413) of human FAM8A1 N-terminally fused to DFP	S-tag	lab stock
S-DFP	pcDNA3.1 (+)	non-fluorescent mutant of GFP	S-tag	lab stock
S-FAM8A1 W120/122A	pcDNA3.1 (+)	mutant (W120/122A) of human FAM8A1	S-tag	cloned for this study
S-FAM8A1 W131A	pcDNA3.1 (+)	mutant (W131A) of human FAM8A1	S-tag	cloned for this study
S-FAM8A1 W131A	pcDNA3.1 (+)	mutant (W131A) of human FAM8A1	S-tag	cloned for this study
S-FAM8A1 100-140-DFP	pcDNA3.1 (+)	fragment (100-140) of human FAM8A1 C-terminally fused to DFP	S-tag	cloned for this study
S-FAM8A1 1-370	pcDNA3.1 (+)	fragment (1-370) of human FAMA81	S-tag	cloned for this study
S-FAM8A1 1-277	pcDNA3.1 (+)	fragment (1-277) of human FAM8A1	S-tag	cloned for this study
sfGFP	pcDNA3.1 (+)	superfolder GFP	/	lab stock
Hrd1-myc 1-251	pcDNA3.1 (-)	fragment (1-251) of human Hrd1	myc	lab stock
Hrd1-myc 1-365	pcDNA3.1 (-)	fragment (1-365) of human Hrd1	myc	lab stock
Hrd1-myc 1-499	pcDNA3.1 (-)	fragment (1-499) of human Hrd1	myc	lab stock
Hrd1-myc 1-540	pcDNA3.1 (-)	fragment (1-540) of human Hrd1	myc	cloned for this study
Hrd1-myc 1-600	pcDNA3.1 (-)	fragment (1-600) of human Hrd1	myc	cloned for this study
Hrd1-myc 1-617	pcDNA3.1 (-)	human Hrd1	myc	lab stock
Hrd1-myc 252-617	pcDNA3.1 (-)	fragment (262-617) of human Hrd1	myc	lab stock
Hrd1-myc Δ1-59	pcDNA3.1 (-)	fragment (60-617) of human Hrd1	myc	cloned for this study
Hrd1-myc Δ1-84	pcDNA3.1 (-)	fragment (85-617) of human Hrd1	myc	cloned for this study
Hrd1-myc Δ 41-124	pcDNA3.1 (-)	human Hrd1 lacking aa 41-14	myc	cloned for this study

Hrd1-myc Δ 71-253	pcDNA3.1 (-)	human Hrd1 lacking aa 71-253	myc	lab stock
Hrd1-myc Δ 165-253	pcDNA3.1 (-)	human Hrd1 lacking aa 165-253	myc	lab stock
Hrd1-myc C294A	pcDNA3.1 (-)	mutant (c294A) of human Hrd1	myc	lab stock
Hrd1-myc 252-617 C294A	pcDNA3.1 (-)	mutant (C294A) of fragment (252-617) of human Hrd1	myc	lab stock
Hrd1-S 1-365	pcDNA™5/FRT	fragment (1-365) of human Hrd1	S-tag	cloned for this study
Hrd1-S 1-499	pcDNA™5/FRT	fragment (1-499) of human Hrd1	S-tag	cloned for this study
Hrd1-S 1-540	pcDNA™5/FRT	fragment (1-540) of human Hrd1	S-tag	cloned for this study
Hrd1-S 1-617	pcDNA™5/FRT	human Hrd1	S-tag	cloned for this study
S-SEL1L 1-377	pcDNA3.1 (+)	fragment (1-377) of human SEL1L, C-terminal KDEL sequence	S-tag	lab stock
S-SEL1L 1-699	pcDNA3.1 (+)	fragment (1-699) of human SEL1L, C-terminal KDEL sequence	S-tag	lab stock
S-SEL1L 1-708	pcDNA3.1 (+)	fragment (1-708) of human SEL1L, C-terminal KDEL sequence	S-tag	lab stock
S-SEL1L 1-718	pcDNA3.1 (+)	fragment (1-718) of human SEL1L, C-terminal KDEL sequence	S-tag	lab stock
S-SEL1L 1-728	pcDNA3.1 (+)	fragment (1-728) of human SEL1L, C-terminal KDEL sequence	S-tag	lab stock
S-SEL1L 1-737	pcDNA3.1 (+)	fragment (1-737) of human SEL1L, C-terminal KDEL sequence	S-tag	lab stock
S-SEL1L 1-794	pcDNA3.1 (+)	human SEL1L	S-tag	lab stock
S-SEL1L L709/712G	pcDNA3.1 (+)	mutant (L709/712G) of human SEL1L	S-tag	cloned for this study
S-SEL1L K711L	pcDNA3.1 (+)	mutant (K711L) of human SEL1L	S-tag	cloned for this study
S-SEL1L P704L	pcDNA3.1 (+)	mutant (P704L) of human SEL1L	S-tag	cloned for this study
S-SEL1L 1-737 L709/712G	pcDNA3.1 (+)	mutant (L709/712G) of human SEL1L 1-737	S-tag	cloned for this study
S-SEL1L 1-737 L712G	pcDNA3.1 (+)	mutant (L712G) of human SEL1L 1-737	S-tag	cloned for this study
S-SEL1L 600-699	pcDNA3.1 (+)	fragment (600-699) of human SEL1L, C-terminal KDEL sequence	S-tag	cloned for this study
S-SEL1L 600-728K	pcDNA3.1 (+)	fragment (600-728) of human SEL1L, C-terminal KDEL sequence	S-tag	cloned for this study

S-SEL1L 600-794	pcDNA3.1 (+)	fragment (600-794) of human SEL1L KDEL sequence	S-tag	cloned for this study
S-sfGFP-SEL1L 700-723K	pcDNA3.1 (+)	fragment (700-723) of human SEL1L fused to superfolder GFP, C-terminal KDEL sequence	S-tag	cloned for this study
S-sfGFP-SEL1L 738-760K	pcDNA3.1 (+)	fragment (738-760) of human SEL1L fused to superfolder GFP, C-terminal KDEL sequence	S-tag	cloned for this study
S-sfGFP	pcDNA3.1 (+)	superfolder GFP, C-terminal KDEL sequence	S-tag	cloned for this study
shRNA 95	psuper	shRNA against human Hrd1	/	lab stock
myc-Ube2g2	pcDNA3.1 (+)	mouse Ube2g2	myc	lab stock

2.1.4 Primers

Table 2.1.4: List of primers

name	sequence
CMV Forward	CGCAAATGGGCGGTAGGCGTG
BGH Reverse	TAGAAGGCACAGTCGAGG
S-AUP1_290_R	GGTCTAGATTAACCAGGGGAGGGAGGGAAAGA
S-AUP1_364_R	CCGTCTAGATTAGCCAGAGCTGGGAAACTTGGA
H6 AUP1_290_F	CAGCCATATGGGTCCTTCTCCTGATGTGCAA
H6 AUP1_364_F	CAGCCATATGGGCCCGGTGACCCCTCAGCCAACA
H6 AUP1_427_R	TAACTCGAGTTAGTCAGCCTCCTGGGCTCGTC
H6 AUP1_348_F	CAGCCATATGGGAACTCAGTCCCTACCCACA
CUE_MUT_F	CAG AGA GTC AAG GAA ATG TTC CCC CAT GTG CCA TTG
CUE_MUT_REV	CAATGGCACATGGGGGAACATTTCCTTGACTCTCTG
AUP1 (L393S)_F	CAGGAGCGCAAGCAAGCATCATATGAATACGCAAG
AUP1 (L393S)_R	CTTGCGTATTCATATGATGCTTGCTTGCGCTCCTG
FAM8A1 255 stop_R	CCTCTAGATTACACCATCTCTGCCATAAATCTG
FAM8A1 delta 107-139_F	AAGCTCTTCTGCTTACTGCAGCCCCCAGCCC
FAM8A1 delta 107-139_R	AAGCTCTTCTAGCTGGTCTCTCTCGTGGCGCC
FAM8A1_W120A/W122A_F	CGGCAAGTGCACGAGGCGCTGGCGCAGTCCTACTGCGG
FAM8A1_W120A/W122A_R	CCGCAGTAGGACTGCGCCAGCGCCTCGTGCACTTGCCG
FAM8A1_W131A_F	CGGCTACCTCACCGCGCACAGCGGCCTG
FAM8A1_W131A_R	CAGGCCGCTGTGCGCGGTGAGGTAGCCG
FAM8A1 100_F	ATAACCGGTCCACGAGAGAGACCAGCTCGG
FAM8A1 140 rev XhoI	TAACTCGAGGTAGGCTGGGAAGGCGGCCAG
FAM8A1 140 rev EcoRI	TAAGAATTCGTAGGCTGGGAAGGCGGCCAG
FAM8A1 370_R	CCGTCTAGAAGCTCGGATAGTGGACGTTGT
FAM8A1 277_R	CCGTCTAGACTTTATCCCACTGAGGTGC
FAM8A1_2F qRT-PCR	AAAATGATGGTTGTGGCACTTA
FAM8A1_2R qRT-PCR	TGTATCACATGTCACAACTCGAA
GAPDH_F qRT PCR	ACCCACTCCTCCACCTTTGA
GAPDH_R qRT PCR	CATACCAGGAAATGAGCTTGACAA
Hrd1 540_R	ATAGGTACCGACTGAAGTGGCAGGCCG

Hrd1 600_R	ATAGGTACCTGCATCGGGCTCTCCATC
Hrd1 delta 1-84_F	TATCTAGAGCCACCATGGTCACAGAGACTT
Hrd1 delta 1-59_F	TATCTAGAGCCACCATGGGCAAGGTGTTCTTTGGGCAACT
Hrd1 delta 41-124_F	AAGCTCTTCTAGCCGCATTGTCTCTCTTATGTTCCTC
Hrd1 delta 41-124_R	AAGCTCTTCTGCTGGACTTGGTCAGGTACACCAC
Hrd1_1F qRT-PCR	TCTTCCTCAAATGTTTCCACTG
Hrd1_1R qRT PCR	TCGTCATCAGGATGGCATAA
SEL1L L709G/L172G_F	AGTTCCAGTCTTCCTAGCCGGCTGCAAAGGGGGCGTCGTC TATTTCTTG
SEL1L L709G/L172G_R	CAAGAAATAGACGACGCCCCCTTTGCAGCCGGCTAGGAAG ACTGGAACT
SEL1L K711L_F	GTCTTCCTAGCCCTCTGCTTATTGGGCGTCGTCTATTT
SEL1L K711L_R	AAATAGACGACGCCCAATAAGCAGAGGGCTAGGAAGAC
SEL1L P704L_F	CCAGATGCACAAGTTCTAGTCTTCCTAGCCCTC
SEL1L P704L_R	GAGGGCTAGGAAGACTAGAACTTGTGCATCTGG
SEL1L 600 FOR	TATACCGGTAGAGAAGCAAGCATTGTAGGTGAG
SEL1L R727T_F	GCAGTACATACGGGAAACAAACATTACGGATATGTTCACCC AACTTGATATG
SEL1L R727T REV	CCATATCAAGTTGGGTGAACATATCCGTAATGTTTGTTTCC CGTATGTACTGC
SEL1L_701-722_F	CGCACAAGTTCCAGTCTTCCTAGCCCTCTGCAAATTGGGC GTCGTCTATTTCTTGCAGTACATACGGGAAGGATCCAGTAC
SEL1L 701-722_R	TGGATCCTTCCCGTATGTACTGCAAGAAATAGACGACGCC CAATTTGCAGAGGGCTAGGAAGACTGGAACTTGTGCGGTA C
SEL1L 738-760_F	CCTTTTGGGACCTGAGTGGGACCTTTACCTCATGACCATCA TTGCGCTGCTGTTGGGAACAGTCATAGCTGGATCCAGTAC
SEL1L 738-760_R	TGGATCCAGCTATGACTGTTCCCAACAGCAGCGCAATGAT GGTCATGAGGTAAAGGTCCCACTCAGGTCCCAAAAGGGTA C

2.2 Methods

2.2.1 Mammalian cell methods

Mammalian cell Lines

The cell lines used in this study were obtained from long term lab stocks. Human Embryonic Kidney (HEK293) cells as well as Flp-In™ TREx™ 293 cells were cultured in Dulbecco's modified eagle medium (DMEM) (Lonza) supplemented with 10% FBS (Biosera), 100 U/ml penicillin & 100 µg/ml

streptomycin (Gibco® by Life Technologies) and 2 mM L-Glutamine (Gibco® by Life Technologies) in a Heraeus incubator at 37 ºC, 5% v/v CO_2.

Maintaining mammalian cell lines

Monolayer cell cultures were grown in 10 cm dishes (Nunc) in 10 ml medium until confluency (2 days in average). Cells were washed with 4 ml of 1x PBS prior to incubation with 1.5 ml of pre-warmed trypsin-EDTA (Gibco® by Life Technologies) until detached from the dish. Trypsin was inhibited by addition of the appropriate amount of fresh medium and seeded at the desired density.

Long term storage of cells

For long term storage, cells were grown in a 15 cm dish to 80% confluency and collected by trypsinisation (as described above). The cell pellet was resuspended in 6 ml of freezing medium and aliquoted into 4 cryo vials (Nunc). The vials were cooled at a rate of 1 ºC per minute in a Mr Frosty freezing container (Thermo Scientific Nalgene) in a -80 ºC freezer (New Brunswick Scientific) for 24 hours before being transferred to liquid nitrogen for long term storage.

To thaw cells from liquid nitrogen stocks, cryovials were placed in a 37 ºC water bath until cell pellet had thawed and plated in a 10 cm dish containing 10 ml of fresh growth medium.

Introduction of DNA into mammalian cells

Three methods were used to transfect mammalian cells transiently with DNA:

1) Cells were transiently transfected using the calcium phosphate method. 1x 10^6 cells were seeded the day prior to transfection in a 6 cm dish. 4 µg of

DNA (the DNA concentration was normalised with empty vector of the same backbone, each sample was co-transfected with 0.5 µg of sfGFP to monitor transfection efficiency) were mixed to 250 µl with 215.5 µl of ddH_2O and 30.5 µl of 2M $CaCl_2$. In a second tube, 250 µl of 2x HEPES was gassed using a glass Pasteur pipette while the DNA mixture is added dropwise. The solution is incubated at (RT) for 15 minutes and added dropwise to the cells. The medium is changed after 6 hours and cells harvested 48 hours later. Where indicated, cells were treated with proteasomal inhibitor MG-132 (Calbiochem) for 6 hours prior to collection.

2) Cells were transiently transfected using the lipid-based FuGENE 6 transfection reagent (Promega). 10^5 cells were seeded in a 24 well plate and grown until 50-70% confluency. On the day of transfection 1.2 µl of FuGENE transfection reagent is diluted in 20 µl of OptiMEM and incubated for 5 minutes at RT. The mixture is added to 400 ng of DNA (250 ng pcDNA3.1+/- vector containing the gene of interest, 80 ng pStar vector containing CD4, 70 ng empty pcDNA3.1+/- vector to normalise DNA concentration) and incubated for 15 minutes at RT before added to the cells. Cells were transferred to 12 well plates 24 hours after transfection and harvested 24 hours later. Where indicated cells were treated with 10 µg/ml proteasome inhibitor MG-132 (Calbiochem) for 6 hours prior to collection.

3) Cells were transiently reverse transfected with DharmaFECT (Dharmacon). In one tube 2.5 µl of DharmaFECT 1 was diluted in 197.5 µl DMEM (without antibiotics). In a second tube 4 µl of pooled Dharmacon siRNA (corresponding to 40 nM) were diluted in 196 µl of DMEM (without antibiotics). Both were incubated at RT for 10 minutes prior to mixing. The solution was incubated for 20 minutes at RT and added to a 6 well plate. 200,000 cells were taken up in 1600 µl of complete medium, added to the transfection mix and harvested 72 hours later.

Generation of stable cell lines

The following cell lines and methods were applied for establishing stable cell lines:

1) A 6 cm dish of 70% confluent HEK293 and Flp-In™ TREx™ 293 cells was transfected with the Hrd1 shRNA (in psuper vector) using the calcium phosphate method. 24 hours after transfection 50 % of the cells were transferred to a 10 cm dish. Selection with 2 µg/ml puromycin was induced after another 24 hours and maintained until clone formation. Single clones were taken up using a pipette tip and grown under selection until the amount of cells was sufficient for western blot analysis.

2) Flp-In™ T-Rex™ 293 cells contain a single stably integrated flippase (Flp) recognition target (FRT) site at a transcriptionally active genomic locus resulting in a homogenous expression of the gene of interest. 3 µg pcDNA™5/FRT containing the gene of interest and 1 µg FlpE Recombinase (in pOG44) were transfected into Flp-In™ T-Rex™ 293 cells using the calcium phosphate method. Upon integration, cells became resistant to hygromycin, which was

used at a concentration of 100 µg/ml at the beginning of selection and later increased to 200 µg/ml. The integrated gene is under a hybrid CMV/TetO2 promoter and gene expression was induced with 1 µg/ml doxycycline and tested by western blot.

Sodium dodecyl sulphate (SDS) treatment

Transfected HEK293 cells were lysed in 1% TritonX-100. SDS at a final concentration of 1% is added and samples incubated for 1 hour at RT to allow protein degradation. SDS was subsequently diluted 10 fold with 4% TritonX-100 solution for 30 minutes at RT. Samples were subjected to affinity purification and subsequently analysed by western blotting.

Cycloheximide chase

Cells grown to confluency were treated with 100 µg/ml of cycloheximide for the indicated period of time. Cells were harvested, lysed and 50 µg of protein sample subjected Western blotting.

2.2.2 DNA and RNA techniques

Bacterial strains and culture

Chemically competent *E. coli* strain MC1061 (araD139 Δ(araA-leu)7697 ΔlacX74 galK16 galE15(GalS) λ^- e14$^-$ mcrA0 relA1 rpsL150(strR) spoT1 mcrB1 hsdR2) was used as host for general cloning of recombinant plasmids (obtained from long term lab stocks). The *E. coli* strain Rosetta (F^- *ompT* *hsdS*$_B$(r_B^- m_B^-) *gal dcm* pRARE2 (Cam^R)) cells was used for protein expression (kindly provided by Dr. Opher Gileadi. SGC Oxford, UK). The Rosetta strain is a BL21 strain derivative and supplies tRNAs for 7 codons rarely used in *E .coli* (AGA,

AGG, AUA, CUA, GGA, CCC, and CGG) on a chloramphenicol resistant plasmid.

Bacteria were cultured in Lennox L broth base (LB) media (1% w/v SELECT peptone, 0.5% w/v SELECT yeast extract, 0.5% w/v NaCl) (Invitrogen) containing the required antibiotic (100 µg/ml ampicillin, 50 µg/ml kanamycin or 20 µg/ml chloramphenicol) at 37 °C in an orbital rotary shaker at 250 rpm. To grow single bacterial colonies on solid substrate, LB-agar medium (LB broth containing 1.5% bacto-agar) was melted and allowed to cool to 50 °C prior to addition of the selection antibiotic and pouring into Petri dishes (Sterilin). Plates were stored at 4 °C and air-dried before use.

Glycerol stocks of bacteria containing a specific plasmid contained a glycerol:bacterial culture ratio of 1:1.5 and were stored in cryovials (Nunc) at -80 °C.

Agarose gel electrophoresis

Agarose (at the appropriate concentration) was heated in 1x TAE buffer until completely resolved. Ethidium bromide (Severn Biotech Ltd) was added to a final concentration of 20 µg/ml. DNA samples containing 1x loading buffer were loaded into gels submerged with 1xTAE buffer and run next to a DNA ladder (1 kb ladder, Invitrogen) at 135 V. Bands were visualised in a UV-imaging system (UVP Bio Imaging Systems).

DNA purification from agarose gels

DNA fragments separated on agarose gels were visualised under UV light and cut out using a clean scalpel. DNA is extracted from the gel slice using the QIAquick gel extraction kit according to the manufacturer's instructions. The

method is based on dissolving the agarose in the provided buffer under high temperature and applying the DNA solution onto a silica membrane. DNA binds to this membrane under high-salt conditions present in the buffer. Impurities are washed away and DNA eluted in an appropriate amount of water (30-50 µl).

Annealing of complementary oligonucleotides

A solution of complementary oligonucleotides in an equal molar ratio was heated to 95 °C for 5 minutes to denature all secondary structures and then cooled down at RT to allow annealing.

Polymerase chain reaction (PCR)

For cyclical amplification of a target DNA sequence *Phusion® Hot Start II* DNA Polymerase (NEB), 50 ng of template plasmid DNA and 0.5 µM of each primer were used according to the manufacturer's instructions for reaction mix and cycling parameters.

Site-directed mutagenesis

To introduce a single amino acid change into a protein of interest the nucleotide sequence of the corresponding codon was altered using the QuikChange site-directed mutagenesis (Stratagene) according to the manufacturer's protocol. The method is based on a PCR using a complementary primer pair containing the desired nucleotide change in the middle of the sequence. The reaction is carried out with *PfuUltra*™ polymerase (Stratagene) to ensure amplification of the entire plasmid with high fidelity and without primer displacement. The 5' primer overhangs are ligated by the endogenous ligases of the *E. coli* strain used. Following the PCR, the parental methylated plasmid DNA is digested with the restriction enzyme *DpnI* and the

mutated plasmid DNA is transformed into competent bacteria and plated on agar plates containing the appropriate antibiotics for selection.

Restriction endonuclease digest

For digesting a PCR product, 1 µl of the restriction enzyme and the required amount of buffer were added to the whole reaction mix and incubated for 1 hour at 37 °C. For digesting plasmid DNA, 1 µg of DNA was incubated with a 3-5 fold unit excess of enzyme in a total volume of 20 µl at 37 °C for 1 hour. Following digest, the sample was run out on an agarose gel to verify successful DNA fragmentation and, if required, the band of interest was cut out of the gel and purified.

Determination of DNA concentration

The concentration and purity of a nucleic acid containing solution was determined by measuring the absorbance at 260 nm and 280 nm with a Nanodrop spectrophotometer (Thermo Scientific).

Ligation of DNA fragments

Digested vector DNA was treated with Alkaline Phosphatase (Invitrogen) for 30 minutes at 37 °C to catalyse the hydrolysis of the 5' phosphate in order to avoid re-ligation. Vector and insert DNA were used at a 1: 3 ratio. The ligation reaction was performed in a total volume of 20 µl containing T4 DNA ligase H.C. (Invitrogen) for 1 hour at RT.

Transformation

Competent cells were thawed on ice. 5.5 µl of the ligation mix were diluted in 50 µl of bacteria and incubated on ice for 15 minutes. The bacteria suffered a heat shock at 42 °C for 1 minute and were then placed on ice for 2 minutes.

300 µl of pre-warmed SOC (super optimal broth containing glucose) medium (Invitrogen) were added and bacterial cells incubated for 10 minutes at 37°C under agitation. The solution was spun down at 6000 rpm for 1 minute and 200 µl of medium discarded. The bacteria were re-suspended in the remaining 150 µl of medium and plated on agar plates containing the appropriate antibiotic. Plates were incubated for 16 hours at 37 °C to allow colony formation.

Colony screening

Colonies grown on agar plates were screened for positive clones with a 10 µl PCR reaction containing 5 µl 2x MyTaq^{TM} Red Mix (Bioline), 0.08 µl each forward and reverse primer, 4 µl ddH_2O and 1 µl of bacterial colony (previously diluted in 50 µl ddH_2O). Cycling parameters were as follows: initial denaturation at 95 °C for 2 minutes, 30 cycles of denaturation at 94 °C for 10 s, annealing at the primer specific temperature for 10 s, elongation at 72 °C for 30 s; final elongation step for 5 minutes at 72 °C.

Small scale preparation of plasmid DNA (QIAprep® Spin Miniprep Kit)

5 ml of antibiotic-containing LB medium were inoculated with a single bacterial colony and incubated at 37 °C under agitation for 16 hours. Bacteria were collected from 4 ml of culture by centrifugation at 14 000 rpm for 1 minute. DNA was extracted using the QIAGEN Miniprep kit following the manufacturer's instructions. The method is based on alkaline lysis followed by binding of plasmid DNA to anion-exchange resin under low salt and pH controlled conditions. Impurities are removed with medium salt washes. Plasmid DNA is finally eluted in 50 µl of elution buffer.

Large scale preparation of plasmid DNA (QIAfilter® Plasmid Midi and Maxi kit)

5 ml of antibiotic containing LB medium were inoculated with a single bacterial colony and incubated at 37 °C under agitation for 8 hours. 100 ml (Midi kit) or 300 ml (Maxi kit) of antibiotic containing LB medium were inoculated with 1 ml of the pre-culture and incubated at 37°C under agitation for 16 hours. The plasmid DNA was isolated according to the manufacturer's protocol using the appropriate QIAGEN kit.

RNA extraction and reverse transcription

RNA was extracted from a confluent 10 cm tissue culture dish using the QIAgen RNeasy mini kit according to the instructions. 0.5 µg of RNA were used for transcription into cDNA using the QuantiTect® Reverse Transcription Kit (QIAGEN) according to the manufacturer's protocol but scaling down the total volume by half.

Real-time quantitative PCR (qRT-PCR)

cDNA obtained from reverse transcription was diluted 1:100 and used as template for qRT-PCR. Reactions were carried out with the SensiFAST™ SYBR Hi-ROX Kit (Bioline) according to the manufacturer's protocol but scaling down the total reaction volume by half.

2.2.3 Protein techniques

Preparation of cell extracts

Cells growing in tissue culture dishes were first washed and then taken up in cold 1x PBS. Cells were scraped with a sterile disposable cell scraper (Greiner), transferred to a 1.5 ml tube and centrifuged for 1 minute at 6000 rpm.

The cells were resuspended in lysis buffer, vortexed and incubated on ice for 1 hour or at 4 °C overnight. The cell lysate was centrifuged at 14 000 rpm for 20 min and the supernatant transferred to a new tube containing 100 µl slurry of sepharose® CL-4B beads (Pharmacia) and incubated for pre-clear at 4 °C under rotation for 2 hours or overnight. The pre-cleared lysate was then used for protein quantification.

Protein concentration determination

The protein concentration of cell lysates was determined with Bradford reagent (BioRad). In a 1.5 ml microcuvette (VWR) 1 µl of lysate is diluted in 1 ml of Bradford solution (Bradford reagent diluted 1:5 in ddH_2O) and incubated for 5 minutes at RT. To establish a standard curve, known concentrations of bovine serum albumin (BSA) were diluted in the same way. The samples were read in a spectrophotometer (Thermo Scientific) at 595 nm and the concentration of the cell lysate was determined by extrapolating the BSA standard curve.

Affinity purification

Affinity purification was carried out using pre-cleared cell lysate. From each sample, 50 µg of protein were collected as input sample and 1.5 mg for affinity purification. Depending on the protein tag, the following capture resins were used: S-protein agarose (Novagen) for S-tagged proteins or glutathione superflow resin (Fisher Scientific) for GST-tagged proteins. The appropriate amount of lysate was incubated with 60 µl of bead slurry and the volume adjusted to 500 µl with lysis buffer. Purification was performed for 2 hours at 4 °C under rotation. Beads were washed three times with lysis buffer, taken up in

100 µl of 2x Laemmli buffer and heated to 56 °C for 10 minutes. Samples were stored at -20 °C until subjected to further analysis.

Immunoprecipitation

Immunoprecipitation is performed in the same way as affinity purification but using 1 µl of antibody per 500 µg of lysate and 30 µl slurry of protein G beads (Roche).

SDS-polyacrylamide gel electrophoresis (PAGE)

Protein samples heated in 2x Laemmli buffer were separated on a two phase acrylamide:bis-acrylamide gel (29:1). The bottom phase consisted of a 7%-15% resolving gel and the top phase consisted of a 4% stacking gel (table 2.2.1). The electrophoresis running buffer was purchased as 10x stock from National Diagnostics. Electrophoresis was performed in a BioRad gel apparatus for 15 minutes at 100 V and subsequently at 40 mA (per gel) for 45 minutes. All blue Pre-stained protein ladder (BioRad) marker was used as size standard.

Gels that were not subjected to western blotting were stained with Coomassie solution for 30 minutes and destained in destaining solution for 3x 20 minutes. Gels were kept in ddH_2O overnight and scanned the following day.

Table 2.2.1: Composition of polyacrylamide gels

	Resolving Gels				Stacking
	7.5 %	10 %	12 %	15 %	4 %
1.5 M Tris HCl pH 8.8	4.25ml	4.25ml	4.25ml	4.25ml	/
0.5 M Tris HCl pH 6.8	/	/	/	/	2.52ml
Acryl/Bis	3.19ml	4.25ml	5.10ml	6.38ml	1ml
10 % SDS	0.17ml	0.17ml	0.17ml	0.17ml	0.1ml
TEMED	0.01ml	0.01ml	0.01ml	0.01ml	0.01ml
10 % APS	0.09ml	0.09ml	0.09ml	0.09ml	0.05ml
ddH_2O	9.22ml	8.16ml	7.31ml	6.04ml	6.36ml
Total volume	17 ml	17 ml	17 ml	17 ml	10 ml

Abbreviations: Ammonium persulphate (APS), N,N,N',N'-tetramethyl-ethylenediamine (TEMED), Tris (Tris(hydroxymethyl) aminomethane), sodium dodecylsulphate (SDS)

Western blotting

After SDS-PAGE, gels were placed against either a Hybond P PVDF membrane (activated for 2 minutes in methanol) or a Hybond C nitrocellulose membrane, assembled into the blotting apparatus and submerged in 1x transfer buffer. Transfer of proteins onto the membrane was carried out at 110 V for 73 minutes at 4 °C.

After transfer, membranes were washed in 1x PBS-T for 5 minutes prior to blocking in either 5% milk or 2% BSA in 1x PBS-T for 40 minutes. The primary antibody was diluted in either 1.3% milk in 1x PBS-T or 2% BSA in 1x PBS-T according to the recommended dilution. Membranes were incubated in primary antibody solution overnight at 4 °C and subsequently washed 3 x for 5 minutes in 1x PBS-T. The secondary antibody tagged to horseradish peroxidase was diluted 1:10 000 in either 1.3% milk in 1 x PBS-T or 2% BSA in 1x PBS-T and membranes were incubated for 30 minutes in secondary antibody solution. Membranes were subsequently washed in 1x PBS 3 x for 10 minutes. Protein bands were visualised using the Super Signal® West Pico Chemiluminescent

substrate (Thermo scientific) according to the manufactorer's protocol. In this system, horseradish peroxidase and hydrogen peroxide were used to oxidise luminol, which decayed to a ground state emitting light. This reaction was performed in the presence of phenols which extended the time of reaction and the intensity of light emission. The emitted light was detected on X-ray films (Fujifilm).

Membrane stripping

The membrane was incubated in 2 ml stripping buffer (Thermo Scientific) for 20 minutes at RT and then washed in 1 x PBS for 1 hour (buffer is exchanged every 5 minutes for the first 20 minutes and then every 10 minutes).

2.2.4 Protein Expression systems

2.2.4.1 Bacterial expression systems

pGEX4T2 vector

pGEX vectors were designed to express proteins in *E .coli* as fusions to the C-terminus of Glutathion-S-Transferase (GST). GST is a 30 kDa protein and the fusion protein usually remains soluble in bacteria and can be purified from bacterial cell lysates based on the affinity of GST for glutathione which is immobilised on agarose or sepharose beads. The fusion ORF is under the control of the IPTG-inducible *lac* promoter. The vector expresses as well the *lac* repressor, the product of the *lac I* gene, to repress the expression of the GST-fusion protein. The fusion protein is produced upon induction with IPTG and can be purified from bacterial cell lysate. The immobilised fusion protein can be eluted from the capture resin with free reduced glutathione at reduced pH.

Recombinant protein purification from a bacterial culture

Chemically competent *E. coli* Rosetta cells were transformed with a pGEX vector containing the gene of interest. 20 ml of LB medium containing 100 µg/ml ampicillin and 20 µg/ml chloramphenicol were inoculated with a pool of five clones and incubated at 37 °C for 16 hours under agitation. 1L of LB medium containing 100 µg/ml ampicillin was inoculated with the overnight culture and grown at 37 °C under agitation until the OD_{600} had reached 0.5. Protein expression was induced with 1 mM IPTG and carried out for 3 hours at 30 °C under agitation. Cells were pelleted by centrifugation at 5, 000 x g for 15 minutes at 4 °C and stored at -80 °C or directly resuspended in 50 ml of extraction buffer. After an incubation of 60 minutes on ice sarcosyl was added to a final concentration of 1% and the suspension was mixed by inversion. Cells were broken up by sonication with multiple pulses of 15 seconds until the solution became fluid and clear. TritonX-100 was added to a final concentration of 1% and the solution mixed by inversion. The supernatant was cleared through a spin at 15,000x g for 15 minutes at 4 °C and separated into two 50 ml tubes each containing 0.5 ml of glutathione superflow resin (Fisher Scientific) After an incubation of 60 minutes at 4 °C under rotation the beads were washed twice in extraction buffer for 15 minutes. The beads bound to the fusion protein were used as affinity purification resin.

2.2.4.2 Mammalian expression vectors

pcDNA3.1 +/- vectors

pcDNA3.1 vector was designed for high-level and constitutive expression in many mammalian cell lines. The multiple cloning site is either in forward (+) or reverse (-) orientation and expression is driven from the promoter region of the

human cytomegalovirus (CMV). The pcDNA3.1 vector used in this study was modified with an S- or a myc-tag as either an N-terminal (in pcDNA3.1^{+}) or C-terminal fusion (in pcDNA3.1^{-}). N-terminal fusion protein used in this study will be referred to as S-/myc-construct name and C-terminal fusions as construct name-S/-myc. The vector was obtained from long term lab stocks.

pcDNA™5/FRT vector

pcDNA™5/FRT was designed for usage in the Flp-In™ system. The vector contains the CMV promoter for high-level expression in mammalian cells and the FLP Recombination Target (FRT) site for Flp recombinase-mediated integration of the vector into the Flp-In™ host cell line. Selection of successfully integrated DNA is achieved through resistance to hygromycin. The vector was obtained from long term lab stocks.

pCMV-GST vector

pCMV-GST is a derivative of pCIS designed for high-level expression of GST-fusion proteins in mammalian cells . Upstream of the GST coding region the vector has a region comprising of a thrombin cleavage and a PKA phosphorylation site. The promoter region of human CMV drives transcription of the recombinant protein. The vector was a kind gift of Colin Goding, Ludwig Insitute for Cancer Research Oxford, UK.

pSUPER vector

pSUPER vector was used to mediate shRNA mediated knockdown of a specific gene in mammalian cell lines. Expression is driven by the polymerase III H1-RNA gene promoter and positive clones are selected with puromycin. The vector was obtained from long term lab stocks.

2.2.5 Cell biology techniques

Preparation of samples for flow cytometry associated cell sorting (FACS) analysis

HEK293 cells stably expressing a GFP-tagged ERAD substrate co-transfected with the gene of interest and CD4 were transferred from 24-well plates to 12-well plates 24 hours after transfection. After additional 24 hours, cells grown in 12-well plates were washed once in PBS-EDTA (3 mM), taken up by pipetting into 1 ml of PBS-EDTA and transferred to FACS tubes (BD Falcon). The cells are washed by addition of 10 ml of PBS-EDTA and collected through centrifugation at 1000 rpm for 3 minutes at 4 °C. The supernatant was poured off and 1 µl of CD4-APC conjugated antibody was added. Cells were resuspended in the residual volume and mixed with the antibody by running the tube over a rack. Staining was carried out for 30 minutes on ice, cells were subsequently washed with 10 ml of PBS-EDTA and collected through centrifugation at 1000 rpm for 3 minutes at 4 °C. The supernatant was poured off and cells resuspended in 250 µl of PBS-EDTA. FACS analysis was carried out immediately and the change in GFP- fluorescence in APC-positive cells was determined. As a positive control for impaired substrate degradation, and therefore accumulation of GFP- fluorescence, one well of cells was treated with 10 µg/ml proteasomal inhibitor MG-132 (Calbiochem) for 6 hours. Statistical analysis for this experiment was conducted using three independent experiments, each with three technical replicates. As some populations were not normally (Gaussian) distributed, a non-parametric test was performed using Graphpad InStat.

Deubiquitination assay

Affinity purified complexes bound to beads were incubated with deubiquitinating enzyme Usp2cc (5 µl of enzyme, 45 µl lysis buffer stock) for 30 minutes at 37 °C. Beads were washed thrice in lysis buffer, resuspended in 100 µl 2 x Laemmli buffer, heated up to 56 °C for 10 minutes and subjected to western blotting.

Immunofluorescence

COS1 cells growing on coverslips were transfected with the plasmid of interest and fixed 24 hours later in 4% paraformaldehyde (PFA) for 30 minutes. Cells were extensively washed with 1x PBS and permeabilised in 0.1% TritonX-100/ digitonin in 1x PBS for 4 minutes followed by blocking in 1x PBS + 1% BSA in 1x PBS. Primary antibodies were diluted in blocking solution and incubated with coverslips for 1 hour. Coverslips were washed with 1x PBS and incubated with the fluorescent secondary antibody for 45-60 minutes. After washing with 1x PBS, coverslips were mounted in ProLong® Gold Antifade Reagent (Invitrogen for confocal microscopy.

De-glycosylation assay

Affinity-purified complexes coupled to beads and heated in 2x Laemmli buffer were treated with 1 µl of EndoH (NEB) for 1 hour at 37 °C. Samples were subsequently analysed by Western blotting.

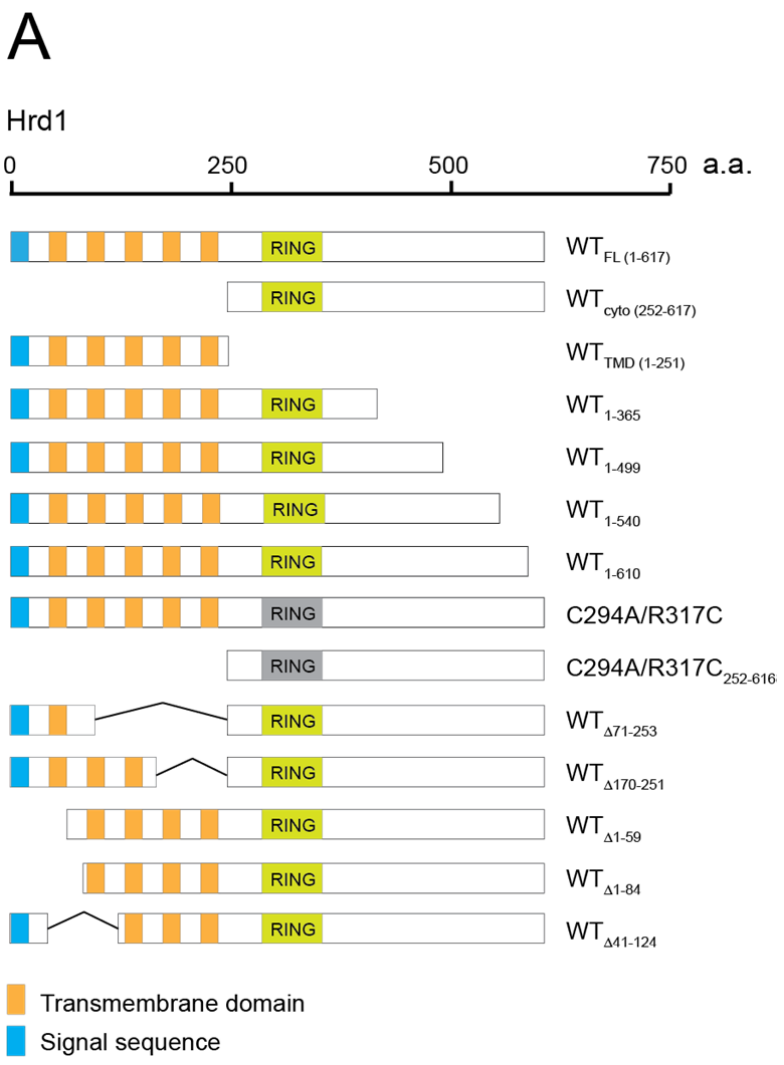
CHAPTER III: Characterisation of the Hrd1-FAM8A1 interaction and its role in ERAD

3.1 Introduction

Many components that participate in ERAD have already been identified as cofactors of ER resident ubiquitin ligases, but what remains to be established is whether these factors regulate a ligase's ability to engage and degrade topologically disparate substrates (e.g. lumenal, membrane or cytosolic). To shed light on how the mammalian ERAD system is functionally organised, previous work from the Christianson lab employed a strategy of integrating proteomic, functional genomic and gene expression data sets to establish a more comprehensive view of the ERAD network (Christianson et al., 2012). Among its many findings, this study established that while the RING type ubiquitin ligase HMG-CoA reductase degradation 1 (Hrd1) was required for a wide range of substrates, associated interactors demonstrated selectivity for distinct ERAD substrates. One of those factors was a novel interaction partner of Hrd1, a poorly characterised protein known as FAM8A1 (Family with Sequence Similarity 8 Member A1). The FAM8A1 gene is localised on chromosome 6p23 and is thought to have propagated during primate evolution by an endogenous retrovirus (Jamain et al., 2001). FAM8A1 is present only in metazoans and absent from fungi, perhaps suggesting an evolutionary adaptation may have occurred in the complex mammalian ER stress response pathway.

FAM8A1 is considered to be an essential component of the Hrd1 ubiquitin ligase complex (Christianson et al., 2012). Along with Hrd1, FAM8A1

is transcriptionally upregulated in response to ER stress. It is an ER-resident integral membrane protein with three highly conserved transmembrane domains (TMDs) at the C-terminus and a cytosolic (cyto) N-terminus. As Hrd1 appears to be the unique binding partner of FAM8A1 within the ERAD network (Christianson et al., 2012), it suggests that FAM8A1 may selectively impact ERAD through this ligase alone. The experiments described below test the hypothesis that the interaction between FAM8A1 and Hrd1 is essential for optimally functioning ERAD.



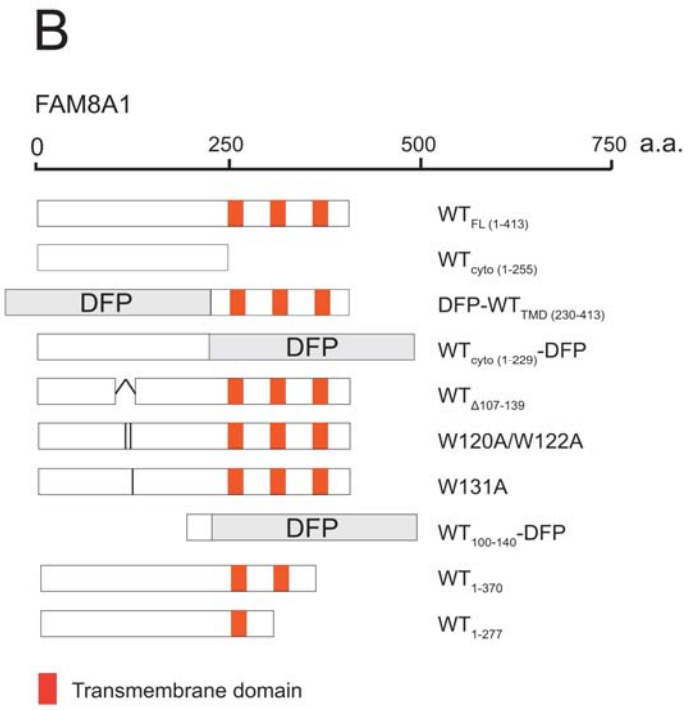


Figure 3.2.1: Schematic representation of Hrd1 and FAM8A1. Hrd1 **(A)** and FAM8A1 **(B)** mutants, truncation and deletion constructs used in this study. WT= wild type, FL= full length, DFP= non-fluorescent variant of GFP

3.2 Results

3.2.1 FAM8A1 interacts with Hrd1 independently of its ligase activity

The ubiquitin ligase Hrd1 occupies the central position in an oligomeric complex responsible for ubiquitinating a wide variety of dis-/retro-translocated ERAD substrates. The RING domains of E3 ligases are essential to recruit E2 conjugating enzymes (E2s) for subsequent Ub transfer and conjugation. To determine whether FAM8A1 required intact ligase activity for interaction with Hrd1, we asked whether Hrd1 containing a non-functional RING domain (C294A, Fig. 3.2.1) could still be co-precipitated by FAM8A1. HEK293 cells stably knocked down for Hrd1 ($HEK293_{Hrd1\text{-}KD}$, Fig. 3.2.2A and B) were employed in these assays to mitigate the potential for exogenously expressed

constructs to oligomerise with endogenous Hrd1 (Horn et al., 2009; Schulze et al., 2005), which could complicate interpretation of any observed FAM8A1 interactions.

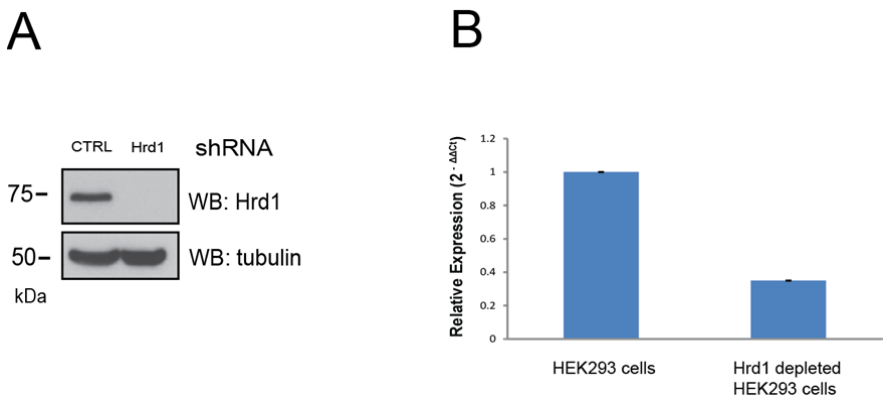


Fig. 3.2.2: Efficient knockdown of Hrd1 in HEK293 cells. Transfection experiments in this study were performed in HEK293 cells stably down-regulated for endogenous Hrd1 on protein **(A)** and mRNA **(B)** level by shRNA. Analysis is based on the ΔΔCt method using GAPDH as internal control. Error bars represent standard error from n=3 biological replicates with n=3 technical replicates each.

When a cytosolic fragment of FAM8A1 (S-FAM8A1$_{cyto}$) was transiently co-expressed with full length wild type (Hrd1$_{WT-FL}$-myc) and RING mutant Hrd1 (Hrd1$_{C294A-FL}$-myc) no difference in their co-precipitation profiles could be observed (Fig. 3.2.3A). Similar results were obtained when just the cyto domains were used (Hrd1$_{WT-cyto}$ and Hrd1$_{C294A-cyto}$), indicating that active ubiquitin conjugation capacity was not required for the Hrd1-FAM8A1 interaction (Fig. 3.2.3A).

3.2.2 Hrd1 and FAM8A1 interact through both TM and cytosolic domains

Both Hrd1 and FAM8A1 have extensive presence in the ER lipid bilayer as well as in the cytoplasm. To determine the domains/regions that are

responsible for their interaction, we designed truncations of both FAM8A1 and Hrd1 that contained only the TMD or the cyto domain (Fig 3.2.1).

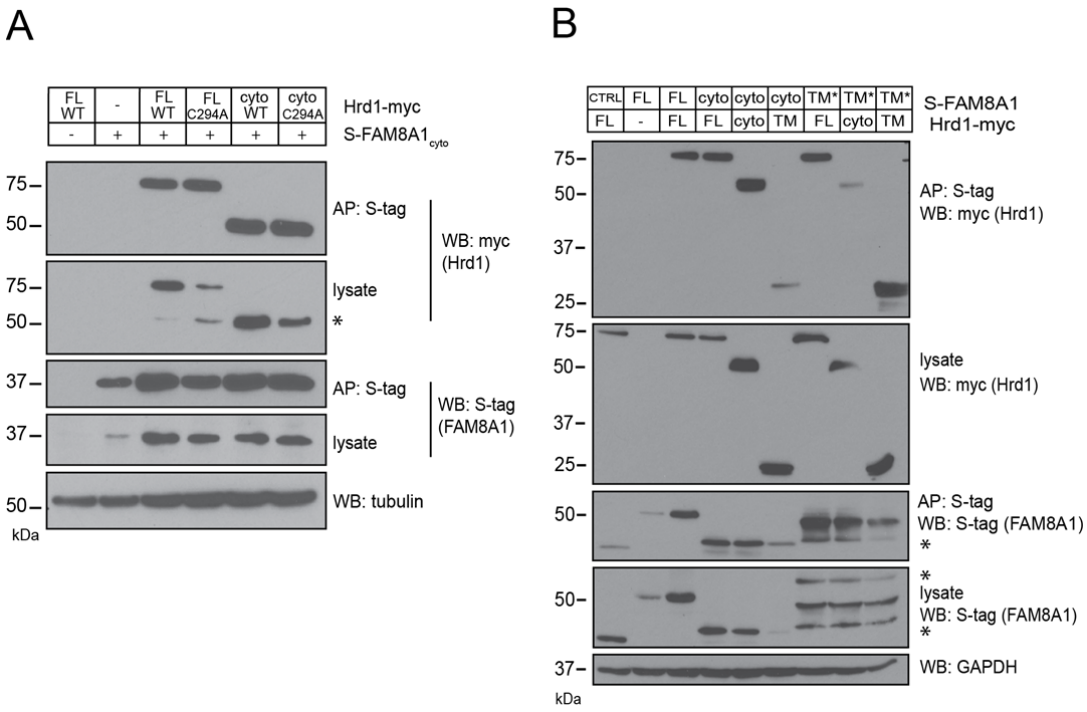


Figure 3.2.3: Hrd1 and FAM8A1 interact through both their TMD and cyto domain. (A) Hrd1 ligase activity is not essential for interaction with FAM8A1: S-tagged $FAM8A1_{cyto}$ was co-expressed with Hrd1-myc RING mutants, cell lysates affinity purified and analysed by western blot. **(B)** Hrd1 and FAM8A1 TMD and cyto regions interact independently with each other: Co-expression of S-FAM8A1 and Hrd1-myc truncations was analysed by western blot. * Additional S-tag reactive band, CTRL=S-DFP.

Initially, the TM region of FAM8A1 (aa 256-413) could not be detected by western blot, which was presumed to be due to intrinsic instability of the truncation (data not shown). By fusing this region to DFP, a non-fluorescent variant of GFP, we could stabilise the construct and allow the protein to be detected. FAM8A1 and Hrd1 constructs encoding the full length (FL), cyto domain and TMD were co-expressed in $HEK293_{Hrd1\text{-}KD}$ cells, affinity purified through the S-tag on FAM8A1 and the interaction with Hrd1 probed by western

blot (anti-myc). We observed FAM8A1 interaction with $Hrd1_{WT-FL}$ as well as with $Hrd1_{WT-cyto}$ and $Hrd1_{WT-TM}$ truncations (Fig. 3.2.3B). From these data, we conclude that FAM8A1 and Hrd1 are interacting through contact made independently via cyto domain and TMD.

3.2.3 FAM8A1 and Hrd1 interact through multiple TMDs

Since Hrd1 and FAM8A1 are able to interact solely through the regions encompassing their TMDs, we aimed to define which Hrd1 TM segment/s were necessary to mediate FAM8A1 interaction and designed a series of deletion constructs removing selected TMDs (Fig. 3.2.4A). Hrd1 deletion constructs co-expressed with $FAM8A1_{TM}$ were lysed in 1% digitonin to preserve membrane complexes, affinity purified and their interaction evaluated by western blot. A Hrd1 construct containing only TM1 and the cyto region ($Hrd1_{\Delta 71-253}$) was sufficient to co-precipitate FAM8A1 (Fig. 3.2.4B), but when either TM1 alone ($Hrd1_{\Delta 1-83}$) or TM1-TM2 ($Hrd1_{\Delta 41-124}$) were deleted, the Hrd1 interaction with FAM8A1 persisted (Fig. 3.2.4B). This suggests that while TM1 participates in binding, other Hrd1 TMs are also able to make contact with FAM8A1.

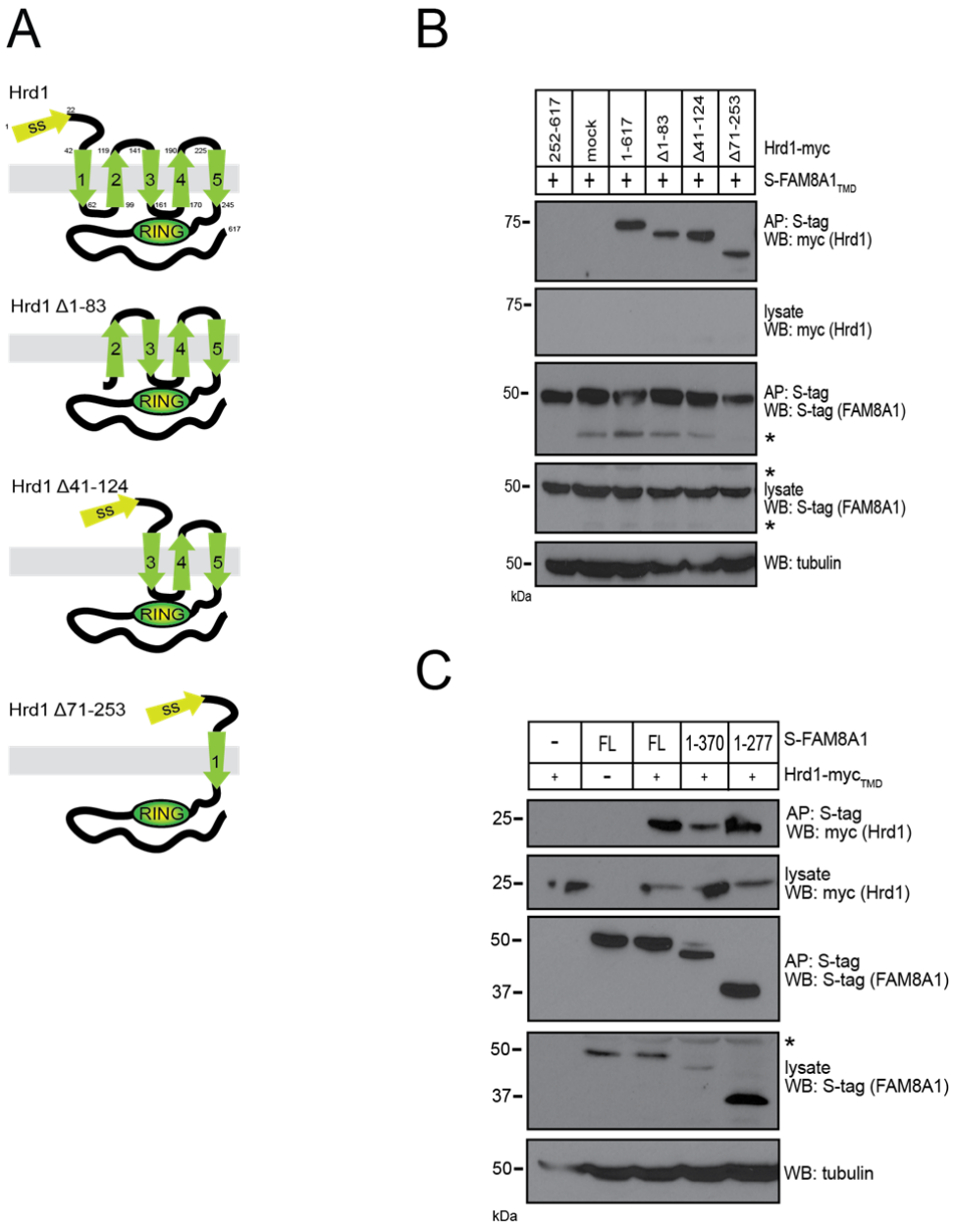


Figure 3.2.4: The interaction between the TMDs of Hrd1 and FAM8A1 is mediated by multiple interaction sites. (A) Topology of Hrd1 TMD deletion constructs. **(B)** Independent contact points in the $Hrd1_{TMD}$ interact with $FAM8A1_{TMD}$: S-$FAM8A1_{TMD}$ was co-expressed with Hrd1-myc TMD deletions and cells lysed in 1% digitonin. Samples were affinity purified and analysed by western blot. **(C)** The first TMD of FAM8A1 is sufficient to bind $Hrd1_{TMD}$: S-FAM8A1 TMD deletions were co-expressed with $Hrd1_{TMD}$-myc, cells lysed in 1% digitonin and analysed by western blot. * Additional S-tag reactive band.

A reciprocal experimental setup was used to identify the FAM8A1 TMD(s) required to bind Hrd1. $Hrd1_{WT\text{-}TM}$ interaction with $FAM8A1_{TM}$ remained even when TM3 ($FAM8A1_{1\text{-}370}$) or TM2 and TM3 ($FAM8A1_{1\text{-}277}$) were deleted, suggesting that $FAM8A1_{TM1}$ was sufficient for binding to Hrd1 (Fig. 3.2.4C). Future experiments will use a FAM8A1 construct lacking the TM1 ($FAM8A1_{\Delta TM1}$) to determine whether that domain is also sufficient for interaction with Hrd1.

3.2.4 Hrd1 500-540 mediates interaction with FAM8A1 and is functionally important for ERAD

The above analyses of TM deletions suggest a model where multiple points of contact mediate Hrd1-FAM8A1 interaction. Subsequently, we switched our attention to the FAM8A1-Hrd1 interaction through their cytosolic regions, as it was this interaction that was resistant to more stringent solubilisation conditions [1% TritonX-100, (Christianson et al., 2012)]. To address this interaction, $FAM8A1_{cyto}$ was co-expressed with a series of Hrd1 constructs serially truncating the C-terminus (Fig. 3.2.5). Within this series, $FAM8A1_{cyto}$ was only able to co-precipitate $Hrd1_{WT\text{-}FL}$ and $Hrd1_{cyto}$ efficiently, with shorter truncations failing to interact or interacting weakly, as in the case of $Hrd1_{1\text{-}499}$ (Fig. 3.2.5). Interestingly, although $Hrd1_{1\text{-}499}$ was not co-precipitated at levels comparable to $Hrd1_{FL}$, the steady-state level of $FAM8A1_{cyto}$ was elevated. $FAM8A1_{cyto}$ steady-state expression levels were lower when transfected alone in $HEK293_{Hrd1\text{-}KD}$ cells (Fig. 3.2.5, lane 1) or when co-transfected with Hrd1 truncations unable to interact (Fig. 3.2.5, lanes 3-4). This suggests that Hrd1 interacts with $FAM8A1_{cyto}$ through a region that may extend slightly beyond aa 499 as binding to $Hrd1_{1\text{-}499}$ was not stable under the conditions of affinity purification.

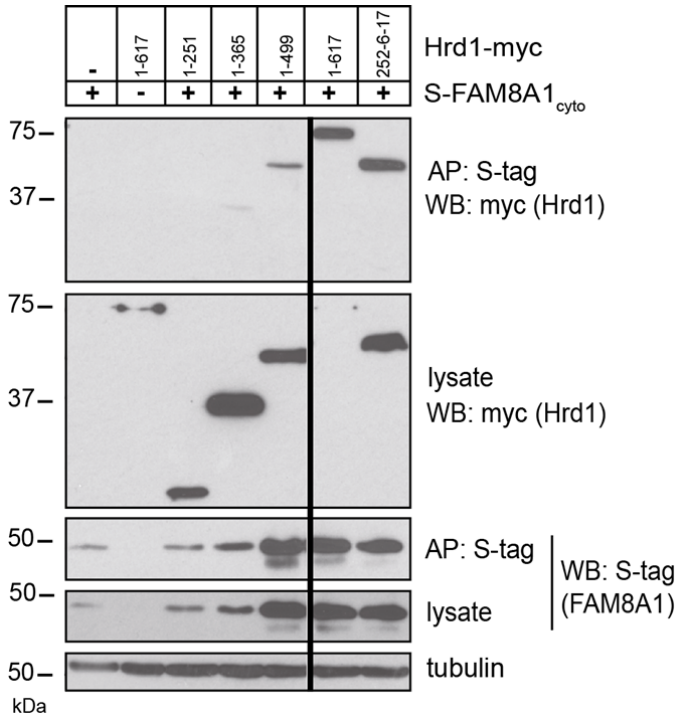


Figure 3.2.5: A small region close to the Hrd1 C-terminus is necessary for interaction with FAM8A1. (A) The cytosolic binding region for FAM8A1 resides at the Hrd1 C-terminus: Hrd1-myc truncations were co-expressed with $FAM8A1_{cyto}$, cells lysed after harvest and subjected to western blot analysis.

An algorithm identifying secondary structure (PsiPred) predicts two α-helices (aa 485-528 and aa 600-610) within the Hrd1 C-terminus that were covered by additional truncations (Fig. 3.2.6A). Ectopic expression showed that $Hrd1_{500-540}$ is important for binding to FAM8A1 (Fig. 3.2.6B). Together, these data support a model where Hrd1 binds to FAM8A1 using all or part of the helical domain stretching from 485-528.

A


Conf:
Pred:
Pred: CCCCCCCCCCCCCCCCCCCCCCCCCCCCCCCCCCCCCCC
AA: PLLPQPPNFPQGLLPPFPPGMFPLWPPMGPFPPVPPPPSS
370 380 390 400
Conf:
Pred:
Pred: CCCCCCCCCCCCCCCCCCCCCCCCCCCCCCCCCCCCCCC
AA: GEAVAPPSTSAAALSRPSGAATTTAAGTSATAASATASGP
410 420 430 440
Conf:
Pred:
Pred: CCCCCCCCCCCCCCCCCCCCCCCCCCCCCCCCCCCCCCC
AA: GSGSAPEAGPAPGFPFPPPWMGMPLPPPFAFPPMPVPPAG
450 460 470 480
Conf:
Pred:
Pred: CCCCCHHHHHHHHHHHHHHHHHHHHHHHHHHHHHHHHH
AA: FAGLTPEELRALEGHERQHLEARLQSLRNIHTLLDAAMLQ
490 500 510 520
Conf:
Pred:
Pred: HHHHHHHHCCCCCCCCCCCCCCCCCCCCCCCCCCCCCC
AA: INQYLTVLASLGPPRPATSVNSTEETATTVVAAASSTSIP
530 540 550 560
Conf:
Pred:
Pred: CCCCCCCCCCCCCCCCCCCCCCCCCCCCCCCCCCCCCC
AA: SSEATTPTPGASPPAPEMERPPAPESVGTEEMPEDGEPDA
570 580 590 600
Conf:
Pred:
Pred: HHHHHHHHHCCCCCCCC
AA: AELRRRRLQKLESPVAH
610
Legend:
= helix
= strand
= coil
Conf: - + = confidence of prediction
Pred: predicted secondary structure
AA: target sequence

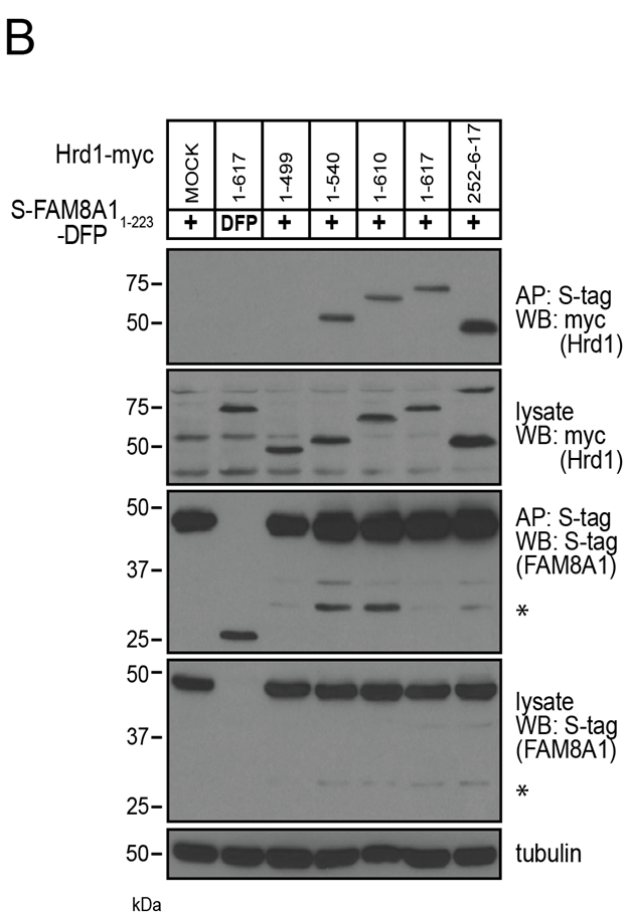


Figure 3.2.6: $Hrd1_{500-540}$ is necessary for interaction with FAM8A1. (A) Secondary structure prediction of the Hrd1 C-terminus (PsiPred). **(B)** $Hrd1_{500-540}$ is necessary to co-precipitate FAM8A1: The indicated Hrd1-myc truncations were co-transfected with $FAM8A1_{cyto}$ and samples analysed by western blot. * Additional S-tag reactive band.

Knockdown of either FAM8A1 or Hrd1 impaired ERAD of a soluble, post-translationally glycosylated mutant of transthyretin (TTR_{D18G}) (Christianson et al., 2012). Transthyretin is a transport protein for thyroxine and holo-retinol binding protein present in blood and brain. The D18G mutant is highly unstable with an unfolding half-time of 140 msec in 6M urea compared to 20 hours for WT TTR (Hammarstrom et al., 2002), causing amyloidosis in the CNS of Hungarian individuals (Hammarstrom et al., 2003). Interaction with BiP prevents TTR_{D18G} from aggregating and the mutant is efficiently degraded by ERAD

(Kabashima et al., 2006; Sorgjerd et al., 2006). More relevant to our interest, it serves as a useful model substrate to identify and investigate factors influencing ERAD. To determine whether Hrd1 interaction with FAM8A1 was necessary for ERAD, we screened Hrd1 truncations in our TTR_{D18G}-GFP reporter cell line assay described previously (Christianson et al., 2012) and asked whether they impaired substrate degradation. To identify the transfected population, Hrd1 constructs were transiently co-expressed with human CD4 lacking its intracellular signalling domain ($CD4_{\Delta TAIL}$), a Type I cell surface glycoprotein absent from HEK293 cells. By staining harvested reporter cells with anti-CD4 conjugated to APC (allophycocyanin), the population of transfected reporter cells could be differentiated from those that were not. By determining the geometric mean of GFP fluorescence (of the reporter) in the $CD4^+$ population, the impact of each transfected construct on ERAD could be evaluated. Relative impairment or enhancement of TTR_{D18G} degradation was determined by normalising obtained values to those expressing $CD4_{\Delta TAIL}$ alone.

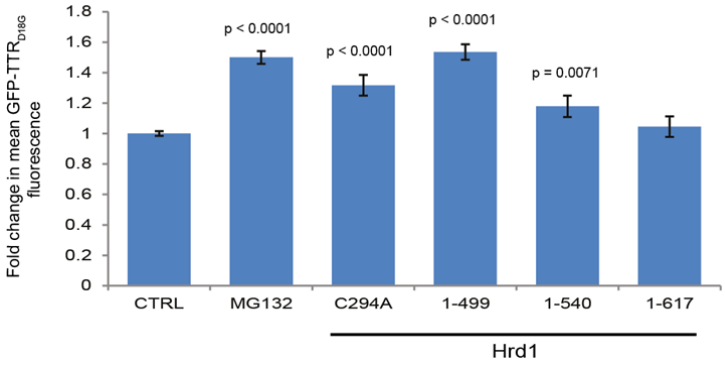


Figure 3.2.7: The Hrd1-FAM8A1 interaction is important for ERAD of a lumenal substrate. Ectopic expression of Hrd1 truncations impairs degradation of GFP-TTR$_{D18G}$: The indicated Hrd1 constructs were transfected into a reporter cell line stably expressing the lumenal ERAD substrate GFP-TTR$_{D18G}$ and impact on substrate degradation was determined by FACS analysis. Error bars represent standard error from n=3 biological replicates with n=3 technical replicates each.

Reporter cells treated with the proteasome inhibitor MG-132 for 6 hours served as the positive control for maximal ERAD impairment. MG-132 treatment increased TTR$_{D18G}$ levels by 50% compared to the control (Fig. 3.2.7) while the RING mutant (C294A) had a similar effect, confirming the requirement for Hrd1 ligase activity in substrate degradation (Fig. 3.2.7). When Hrd1 truncations were ectopically expressed, we observed that Hrd1$_{1-499}$, a construct unable to interact efficiently with FAM8A1 through the cytosolic region, markedly impaired the degradation of TTR$_{D18G}$ when compared to Hrd1$_{WT-FL}$ and was comparable to that of MG-132 treatment (Fig. 3.2.7). Hrd1$_{1-540}$, which was able to interact with FAM8A1, had a more modest effect on TTR$_{D18G}$ turnover (Fig. 3.2.7) which may indicate that proteins other than FAM8A1 are binding to the distal C-terminus of Hrd1 and contributing to TTR$_{D18G}$ degradation.

3.2.5 Cytosolic Trp residues in FAM8A1 are important for Hrd1 binding

After identifying the cytosolic region in Hrd1 necessary for interaction with FAM8A1, we set out to decipher the complementary cytosolic region in FAM8A1. Bioinformatic analyses of FAM8A1's cytosolic region indicated that this region, in contrast to the TMDs, is poorly conserved across metazoans (ProPhyler) and appears highly disordered (DisoPred) (Fig. 3.2.8).

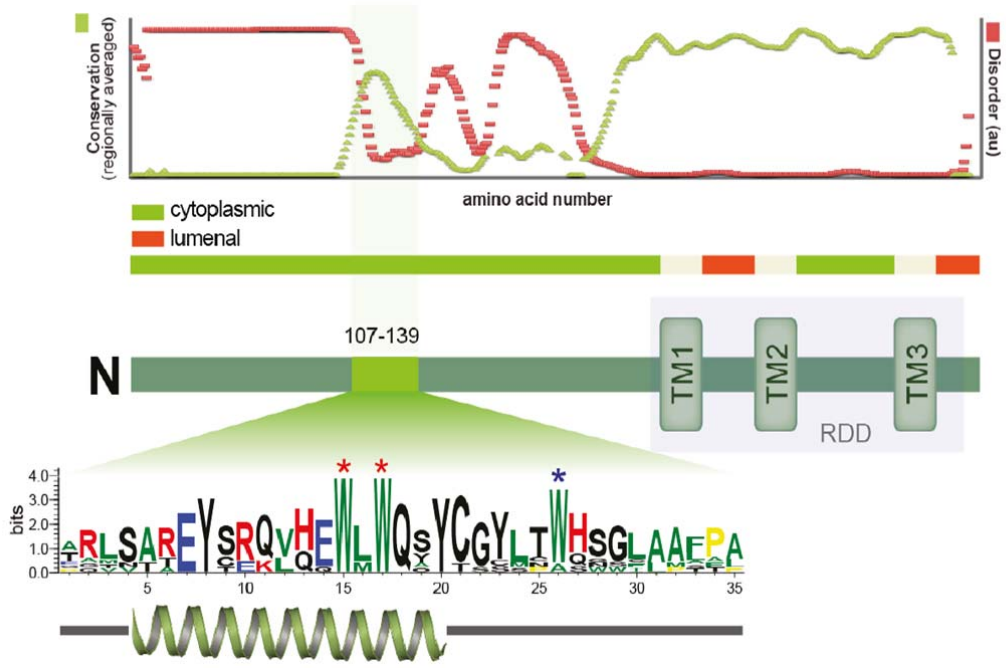


Figure 3.2.8: Prediction of conservation and disorder of the FAM8A1 protein. The cytosolic N-terminus contains a conserved domain with highly conserved Trp residues (ProPhyler, DisoPred).

Within the cytosolic N-terminus of FAM8A1, however, a small region (aa 100-140) was observed to be conserved with less intrinsic disorder (Fig. 3.2.8). Moreover, an α-helical segment mapping to this region (aa 110-125, PsiPred) contains two conserved Trp residues (W120, W122), with a third conserved Trp nearby (W131). As conservation is generally associated with an important function, we speculated that this region contributed to the interaction with Hrd1

and that these conserved Trp residues were necessary for binding. FAM8A1 mutants ($FAM8A1_{W120/122A}$, $FAM8A1_{W131A}$) were generated by site-directed mutagenesis (Fig. 3.2.1B) and secondary structure prediction (PsiPred) did not predict disruption of the α-helical stretch (not shown). Whilst $FAM8A1_{W131A}$ was able to co-precipitate $Hrd1_{WT-FL}$ at levels comparable to wild type FAM8A1 (Fig. 3.2.9A), this interaction was abolished with the W120/W122 mutant or with a construct lacking the entire conserved region ($FAM8A1_{\Delta 107-139}$) (Fig. 3.2.9A). This indicated that the region and specifically the two Trp residues were important to maintain the FAM8A1-Hrd1 interaction.

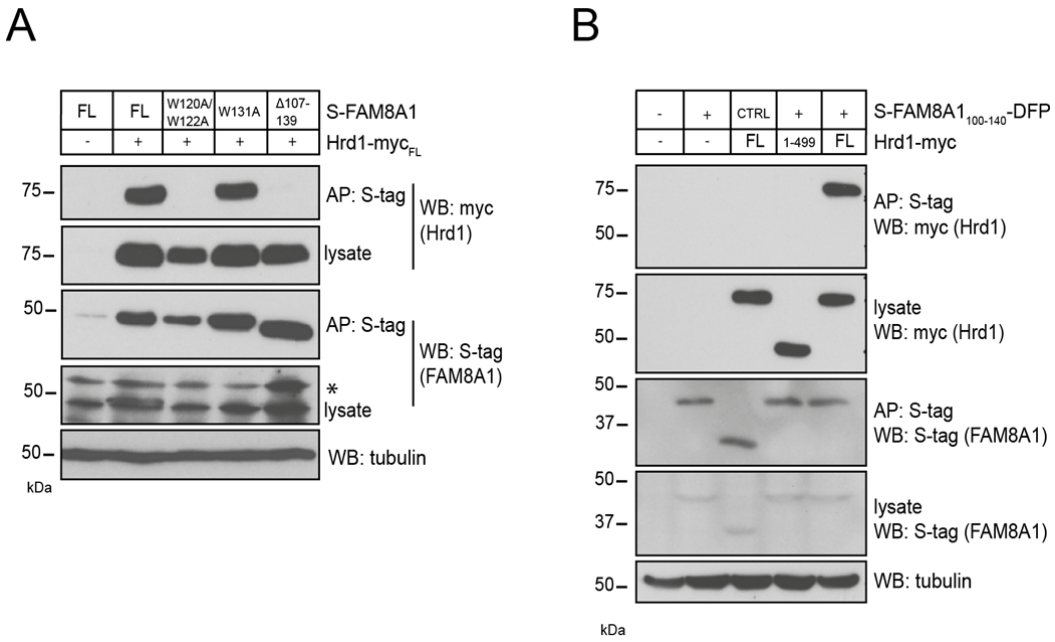


Figure 3.2.9: A conserved FAM8A1 N-terminal region is necessary and sufficient to bind Hrd1. (A) Two conserved FAM8A1 Trp residues are necessary for co-precipitation of Hrd1: The indicated S-FAM8A1 mutants were co-transfected with $Hrd1_{cyto}$-myc and samples analysed by western blot. **(B)** A conserved FAM8A1 region (aa 100-140) is sufficient to interact with Hrd1: S-$FAM8A1_{100-140}$-DFP fusion protein was co-transfected with the indicated Hrd1-myc truncations and samples analysed by western blot after affinity purification. * Additional S-tag reactive band.

In order to determine whether this cytosolic region of FAM8A1 was sufficient for interaction with Hrd1, we fused $FAM8A1_{100\text{-}140}$ to the N-terminus of DFP (Fig. 3.2.1B). The $FAM8A1_{100\text{-}140}$-DFP fusion protein co-precipitated $Hrd1_{WT\text{-}FL}$ at levels comparable to $FAM8A1_{cyto}$ (Fig. 3.2.9B). Hrd1 was not co-precipitated by DFP alone and $FAM8A1_{100\text{-}140}$ did not bind $Hrd1_{1\text{-}499}$, a truncation that did not interact with FAM8A1 (Fig. 3.2.9B). Taken together, these data demonstrate that $FAM8A1_{107\text{-}139}$ is indeed sufficient to interact with Hrd1.

3.2.6 Disrupting the Hrd1-FAM8A1 interaction impairs ERAD

Above we demonstrated that aa 500-540 of Hrd1 were important for degradation of the ERAD substrate TTR_{D18G}. To confirm that this was due to the loss of the Hrd1-FAM8A1 interaction, we used the TTR_{D18G} reporter cell line described previously and expressed FAM8A1 mutants to look for dominant negative effects. We observed that $FAM8A1_{W120/W122A}$ impaired TTR_{D18G} degradation ($p>0.0001$, Fig. 3.2.10), while the effects of $FAM8A1_{WT}$ and $FAM8A1_{W131A}$ were not statistically significant (Fig. 3.2.10).

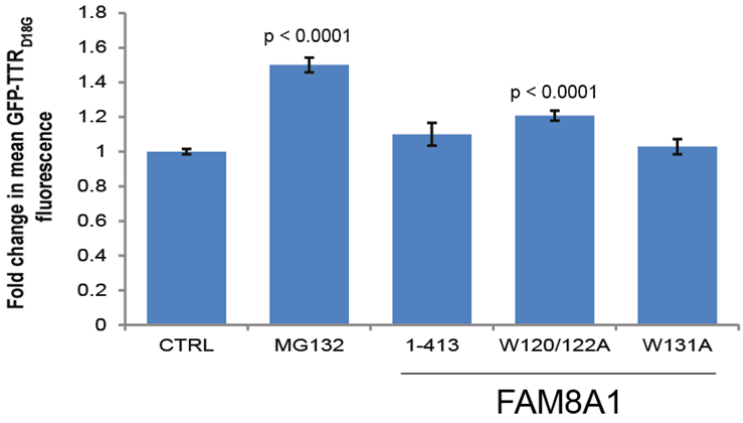


Figure 3.2.10: FAM8A1 needs to interact with Hrd1 to promote TTR$_{D18G}$ degradation. Expression of FAM8A1 mutants abrogating the cytosolic Hrd1 interaction have a dominant negative effect on degradation of a lumenal ERAD model substrate: The indicated FAM8A1 mutants were ectopically expressed in the ERAD reporter cell line stably expressing the lumenal ERAD substrate GFP-TTR$_{D18G}$. The impact on substrate degradation was assessed by FACS. Error bars represent standard error from n=3 biological replicates with n=3 technical replicates each.

These data show that FAM8A1$_{W120/122A}$, binding to Hrd1 through the TMDs but not the cytosolic region, acts as a dominant-negative and support the hypothesis that the cytosolic interaction between FAM8A1 and Hrd1 is essential for ERAD of a lumenal substrate.

3.2.7 Hrd1 stabilises FAM8A1 in the ER membrane

During the course of this study we made the observation that despite transfecting comparable amounts of FAM8A1 with each Hrd1 construct, the FAM8A1 steady-state expression levels varied greatly. Co-expression with Hrd1 constructs that did not interact with FAM8A1 (e.g. Hrd1$_{1-365}$) resulted in lower steady-state levels of FAM8A1 compared to those that did (e.g. Hrd1$_{1-540}$). This observation prompted us to suspect that Hrd1 may be influencing FAM8A1 stability. To begin to query this observation, the impact of Hrd1 knockdown on FAM8A1 transcription and translation levels was assessed. Using RNA isolated from HEK293 and HEK293$_{Hrd1-KD}$ cells, we measured the

levels of FAM8A1 mRNA by qRT-PCR (Fig. 3.2.11A). No difference in FAM8A1 mRNA was observed between HEK293 and HEK293$_{Hrd1\text{-}KD}$ cells, implying that FAM8A1 mRNA expression levels were not regulated through a transcriptional feedback-loop activated by loss of Hrd1. Next, we performed cycloheximide chase experiments with HEK293 and HEK293$_{Hrd1\text{-}KD}$ cells (Fig. 3.2.11B). While FAM8A1 was stable in HEK293s, its half-life was markedly decreased in HEK293$_{Hrd1\text{-}KD}$ cells, suggesting that the Hrd1 interaction had a positive effect on FAM8A1 stability. FAM8A1 levels were rescued by treating with MG-132, indicating that FAM8A1 is still synthesised in the absence of Hrd1, but is rapidly degraded by the UPS (Fig. 3.2.11B). Interestingly, suppressor enhancer lin12/Notch 1 like (SEL1L) appeared to be stabilised in the absence of Hrd1, which is in contrast to a recently published study (Iida et al., 2011). This inconsistency may be the result of different experimental conditions, but our results seem to suggest that SEL1L accumulation reflects the necessity of Hrd1 for its degradation.

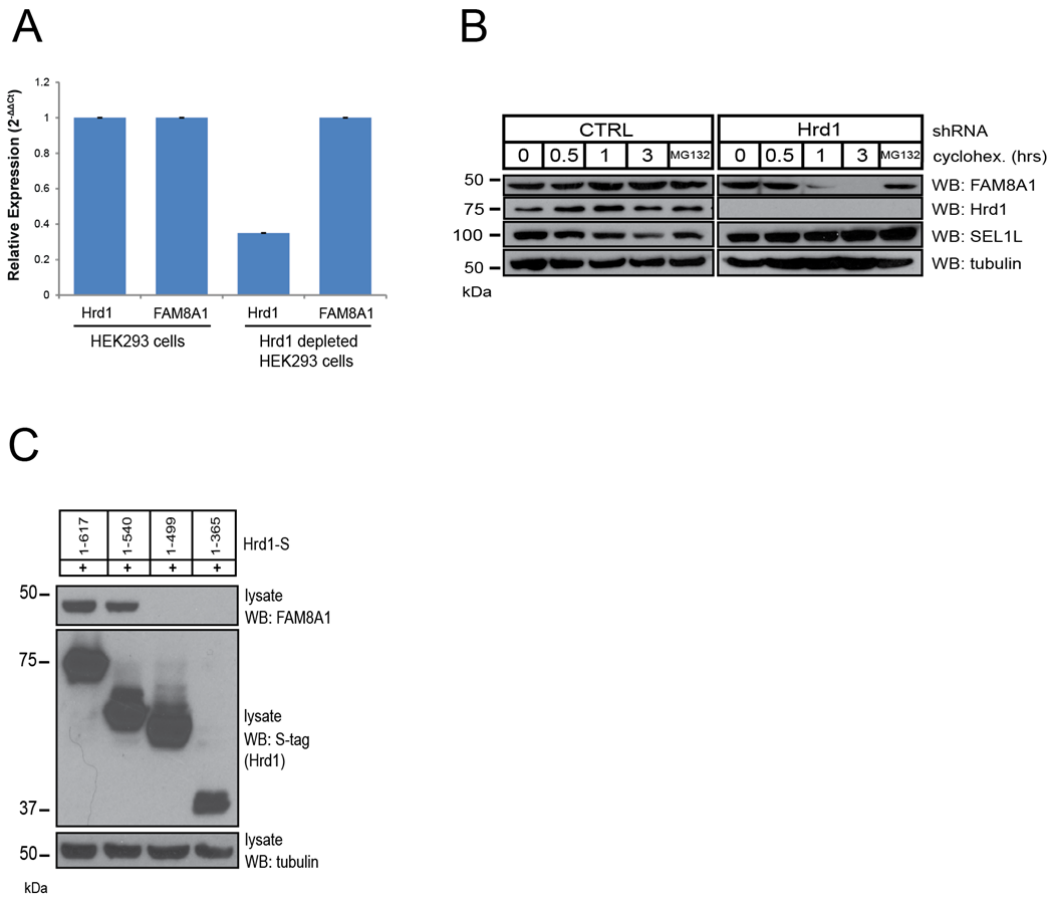


Figure 3.2.11: Hrd1 prevents degradation of FAM8A1. (A) Knockdown of Hrd1 does not alter FAM8A1 mRNA levels: FAM8A1 mRNA expression levels from HEK293 cells and HEK293$_{Hrd1\text{-}KD}$ are determined by qRT-PCR. Analysis was based on the ΔΔCt method using GAPDH as internal control. Error bars represent standard error from n=3 biological replicates with n=3 technical replicates each. **(B)** Knockdown of Hrd1 decreases half-life of FAM8A1: control and Hrd1 depleted HEK293 cells were subjected to cycloheximide chase for the indicated time points. Hrd1, FAM8A1 and SEL1L levels were detected by western blot. **(C)** Restoration of FAM8A1 protein levels by re-introduction of Hrd1: Flp-In™ T-REX™ 293 cells depleted for endogenous Hrd1 stably integrated the indicated Hrd1-S constructs. Gene expression was induced with 1µg/ml of doxycycline, cells lysed 24 hours post induction and Hrd1 and FAM8A1 levels analysed by western blot.

Above we have shown that FAM8A1 stability within the ER is dependent upon interaction with Hrd1. To confirm this observation and verify the essential region, we asked which Hrd1 variants would be able to restore FAM8A1 stability. To accomplish this, we used the Flp-In™ T-REx™ 293 cell line to express a series of Hrd1 variants. This cell line allows Flp-recombinase

mediated recombination of a gene of interest with a genomic locus via specific FRT sites in order to obtain single integration into the genome. The integrated gene is under the regulation of a hybrid CMV/TetO2 promoter and induced with doxycycline. As before, we stably depleted endogenous Hrd1 through shRNA mediated knockdown and re-introduced C-terminally S-tagged truncations of Hrd1 in this cell line. After induction with doxycycline, cells were lysed and relative expression determined by western blot. All Hrd1 truncations could be expressed at detectable levels (Fig. 3.2.11C), but only expression of the truncation $Hrd1_{1\text{-}540}$ and the FL protein conferred stability to FAM8A1 (Fig. 3.2.11C). These data are in agreement with our interaction study, confirming that $Hrd1_{500\text{-}540}$ is an essential interaction domain for FAM8A1 that is important for maintaining its stability in the ER.

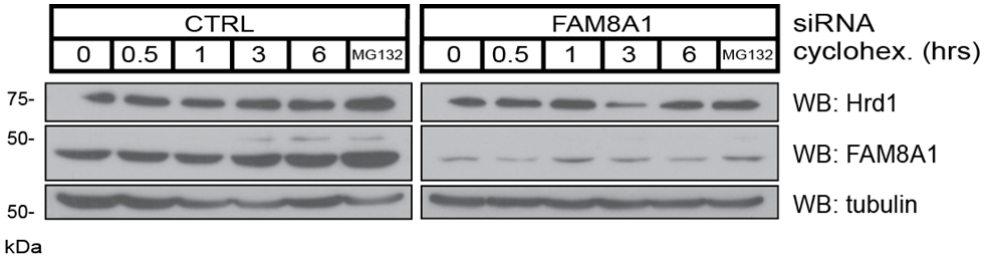


Figure 3.2.12: FAM8A1 does not regulate the half-life of Hrd1. Down-regulation of FAM8A1 has no impact on Hrd1 half-life: HEK293 cells were transiently knocked down for FAM8A1 using siRNA. Hrd1 and FAM8A1 levels are compared to control cells by western blot following cycloheximide chase.

Given the apparent dependence of Hrd1 for FAM8A1 stability, we questioned whether the absence of FAM8A1 had an equally striking effect on Hrd1 half-life. FAM8A1 was transiently knocked down with siRNA and cycloheximide chase experiments carried out as described above. Western blot analysis showed that

despite the loss of FAM8A1, the half-life of Hrd1 remained unaffected (Fig. 3.2.12). This indicates that the function of FAM8A1 appears not to be the regulation of Hrd1 stability.

3.3 Discussion

The Hrd1 ubiquitin ligase complex plays a central role in the ERAD mechanism of eukaryotes. This study aimed to determine the role of the novel Hrd1 interaction partner FAM8A1, a metazoan protein whose role in ERAD remains poorly defined. Here, we provide evidence that the interaction between Hrd1 and FAM8A1 occurs through independent contacts between their respective TM and cyto regions. These interactions occurred independently of ubiquitin ligase activity within Hrd1 (Fig. 3.2.3A). Similar findings were reported in yeast, where the Hrd1 RING domain is not necessary for complex assembly, but for interaction with Cdc48 (Gauss et al., 2006; Horn et al., 2009). In the mammalian system however, VCP/p97 recruitment to ubiquitin ligases does not necessitate a functional RING domain (Ye et al., 2005).

Our attempts to isolate and identify the Hrd1 and FAM8A1 TMDs mediating contact were not conclusive. While a Hrd1 construct containing only TM1 was sufficient to co-precipitate FAM8A1 (Fig. 3.2.4B), it could not be shown to be necessary, as $Hrd1_{\Delta TM1}$ still bound FAM8A1. This implies that in addition to TM1, other independent contact points contribute to the Hrd1-FAM8A1. The TMDs of both Hrd1 and FAM8A1 contain charged residues with a majority of positively charged aa and it is a possibility that charge-pairing mediates interaction between the two proteins. Co-expression of Hrd1 and FAM8A1 deletion constructs containing only positively charged residues as well as site-directed mutagenesis will be performed to investigate this hypothesis. For

FAMA81, it can so far only be concluded that TM1 is sufficient to bind Hrd1 (Fig. 3.2.4C), but additional FAM8A1 deletions are needed to confirm its necessity for Hrd1 binding.

In addition to interaction through TM regions, Hrd1 and FAM8A1 exhibited contact through their respective cytosolic domains. Analyses of FAM8A1 co-precipitation patterns with Hrd1 truncations revealed that aa 500-540 were required for interaction (Fig. 3.2.6B). Secondary structure analyses of the Hrd1 C-terminus predict an α-helical structure in this region, spanning aa 485-528, which could represent a suitable surface for FAM8A1 binding. Although not completed in this work, future studies will determine whether this fragment alone is sufficient for FAM8A1 cyto interactions. In general, α-helices are the most common secondary structure motif and are often involved in protein interactions (Guharoy and Chakrabarti, 2007; Jones and Thornton, 1995); it has been described, for example, that the tumor suppressor p53 binds its regulating E3, hDM2, through an α-helical stretch (Edwards and Wilson, 2011) and that HIF1α binds CBP through three separate α-helices (Dames et al., 2002).

The cyto N-terminus of FAM8A1 (aa 1-256) contains a region within it that is evolutionarily conserved and exhibits less protein disorder (aa 107-139), compared to regions on either side (Fig. 3.2.8). We were able to show that this region, and in particular two highly conserved Trp residues (W120A/W122A), were necessary for Hrd1 interaction (Fig. 3.2.9A). Trp, as well as Tyr and Arg residues are considered as “hot spots” of protein-protein interaction, contributing the largest amount of the required binding energy (Bogan and Thorn, 1998). Furthermore, transient expression of FAM8A1 mutants that did not bind the cytosolic region of Hrd1 (W120A/W122A) and Hrd1 truncations that

did not interact with the cytosolic region of FAM8A1 (1-499), acted as dominant-negative in an ERAD reporter assay (Fig. 3.2.7 and Fig. 3.2.10). Together, these data argue that the Hrd1-FAM8A1 interaction is functionally important for the degradation of lumenal ERAD substrates.

During our study we observed that FAM8A1 levels were elevated when Hrd1 forms containing aa 500-540 were present and lower when this region was absent. We hypothesised that interaction with Hrd1 may be influencing FAM8A1 half-life within the ER and indeed could show that FAM8A1 was rapidly degraded in cells lacking Hrd1 ($HEK293_{Hrd1\text{-}KD}$) (Fig. 3.2.11B). We could restore FAM8A1 levels by inhibiting degradation by the proteasome or by introducing Hrd1 truncations that supported FAM8A1 interaction (Fig. 3.2.11C). SEL1L, an integral component of the Hrd1 complex has recently been reported to be destabilised upon Hrd1 silencing (Iida et al., 2011). This finding could not be recapitulated in our experimental paradigm, which indicates that SEL1L accumulates because Hrd1 is required for its degradation. The source of this discrepancy is not known but may be explained by a different experimental setup. While Iida et al. analysed cells after 48 hours of Hrd1 knockdown, the cells used in our assay were stably silenced for Hrd1 and long-term adaption may have resulted in SEL1L translation.

Intriguingly, this finding also indicates that FAM8A1 can be degraded by an ER-resident ubiquitin ligase other than Hrd1. Studies demonstrated degradation of ERAD factors by ERAD ubiquitin ligases; Hrd1 is competent for gp78 degradation (Shmueli et al., 2009) and RNF5 mediates turnover of JNK-associated membrane protein (JAMP), a factor facilitating ERAD through recruitment of the proteasome and ERAD factors (Tcherpakov et al., 2009).

When we performed this experiment in the reciprocal manner, Hrd1 degradation rates remained unchanged upon transient depletion of FAM8A1 (Fig. 3.2.12). We therefore conclude that whilst Hrd1 must be present in order for FAM8A1 to stably remain in the ER, FAM8A1 is not one of the factors that control the stability of Hrd1. Moreover, this implies that all FAM8A1 within the cell is likely to be found in a complex with Hrd1 and not unassembled in the ER membrane.

In summary, we have determined that both TM and cytosolic contact points mediate the interaction between Hrd1 and FAM8A1. Deleting or mutating these regions resulted in impaired degradation of a model lumenal ERAD substrate (TTR_{D18G}), and illustrated the necessity of the Hrd1-FAM8A1 interaction through the cyto domains. We also identified Hrd1 as regulator of FAM8A1 stability. Still outstanding is a clear picture of how interaction with FAM8A1 modulates or tailors Hrd1 activity towards substrates. Currently, we cannot differentiate between a direct action on substrates by FAM8A1 or an indirect effect through modulation of Hrd1 ubiquitination reactions, oligomerisation or substrate engagement. Future experiments will address these questions in an effort to gain a more comprehensive understanding of how this ERAD E3 complex functions.

CHAPTER IV: Identification of a lumenal SEL1L determinant mediating the interaction with Hrd1

4.1 Introduction

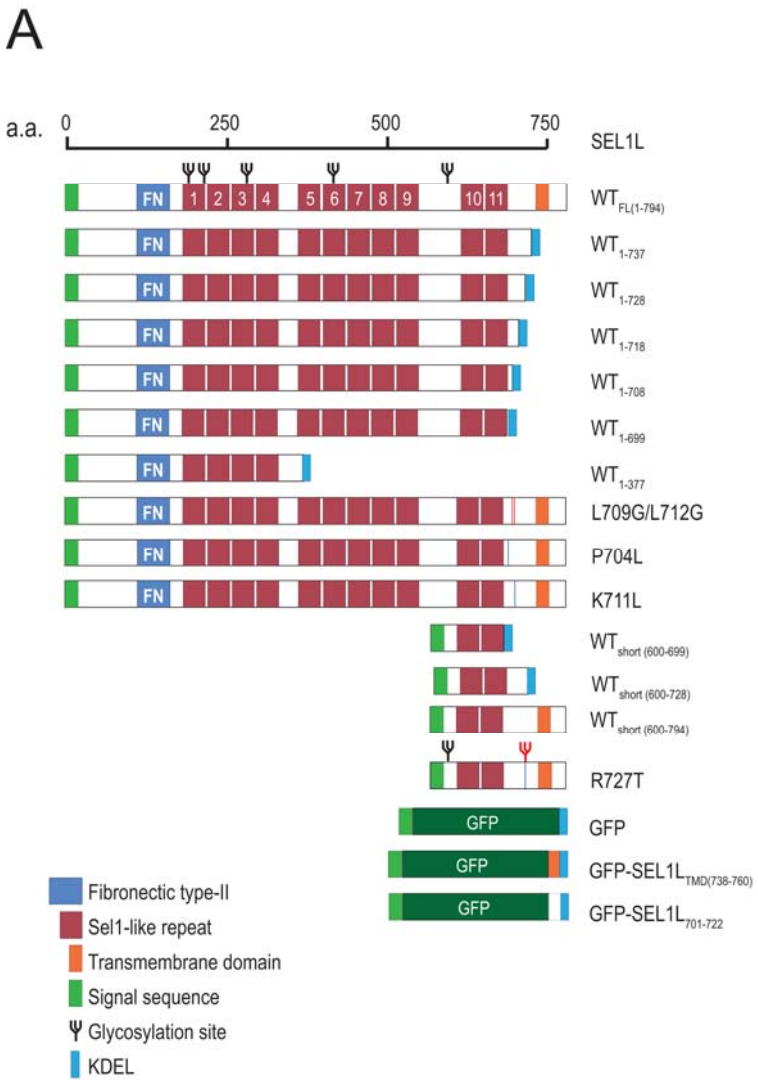
Membrane-embedded ubiquitin ligases occupy a central position within the ERAD mechanism, with the complexes forming around them responsible for substrate recognition, dislocation and ubiquitination. Much of the work to date has focused on the HMG-CoA reductase degradation 1 (Hrd1) ubiquitin ligase and its cofactor suppressor enhancer lin12/Notch 1 like (SEL1L) (Hrd3p in yeast), which together form the core of an evolutionarily conserved complex implicated in degradation of a wide range of substrates from the ER. Originally identified in yeast through mutagenesis screens for factors regulating stability of HMG-CoA reductase (Hampton et al., 1996) and degradation of misfolded carboxypeptidase Y (CPY*) (Bordallo et al., 1998; Knop et al., 1996), both Hrd1p and Hrd3p have played pivotal roles in defining the pathway that would come to be known as ERAD (Brodsky and McCracken, 1999). More recently, their mammalian orthologues Hrd1 and SEL1L have been shown to function as part of a similar but more extensive complex (Christianson et al., 2012; Christianson et al., 2008; Lilley and Ploegh, 2005; Mueller et al., 2008).

At the centre of this complex lies the direct interaction between the ligase (Hrd1/Hrd1p) and its cofactor (SEL1L/Hrd3p), an interaction conserved in yeast (Gardner et al., 2000) and human (Christianson et al., 2008; Mueller et al., 2008; Mueller et al., 2006). Hrd1 and Hrd3p/SEL1L form an interaction essential for ERAD of lumenal but not necessarily integral membrane substrates (Bernasconi et al., 2010; Christianson et al., 2012). Hrd3p/SEL1L

scaffolds factors involved in substrate recognition including OS-9 (Christianson et al., 2008), XTP3-B (Hosokawa et al., 2008), EDEM1 (Hosokawa et al., 2001) and ERFAD (Riemer et al., 2009) and may itself participate in recognising substrates (Mueller et al., 2006). Hrd1 and Hrd3p/SEL1L also co-stabilise each other; the deletion of Hrd3p from yeast results in the loss of Hrd1p and a defect in ERAD (Gardner et al., 2000; Plemper et al., 1999). For the mammalian complex, recent evidence suggests that the regulation may be reversed, whereby destabilisation of SEL1L results upon down-regulation (or deletion) of Hrd1 (Iida et al., 2011). Mice deficient for SEL1L die *in utero* and display brain abnormalities, a dilated liver ER and increased apoptosis (Francisco et al., 2010). Isolated SEL1L-/- mouse embryonic fibroblasts (MEFs) are more susceptible to ER stress and grow slower compared to WT due to increased apoptosis (Francisco et al., 2010).

Hrd1 and SEL1L exhibit very different topologies, which has complicated understanding how their interaction is mediated. The polytopic Hrd1 contains 5 putative transmembrane domains (TMDs) and a significant cytosolic (cyto) region while SEL1L has an extended ER lumenal domain with 11 Sel1 repeats, 5 putative glycosylation sites and a single predicted TM domain near the C-terminus. Thus, it is reasonable to suspect that their interaction occurs through their respective TMDs. But while Hrd1p TMD region is sufficient for interaction with Hrd3p (Gardner et al., 2000), the single TMD of Hrd3p or SEL1L is dispensable for interaction (Christianson et al., 2008; Gardner et al., 2000). This raises questions of how the presumably lumenal domain of Hrd3p/SEL1L is able to interact with the TMD region of Hrd1 which has minimal exposure to the ER lumen. Although this observation was made in very early work on Hrd3p, to

date no comprehensive study has attempted to decipher this conundrum. We therefore decided to investigate the mode/s of interaction between Hrd1 and its established cofactor SEL1L.



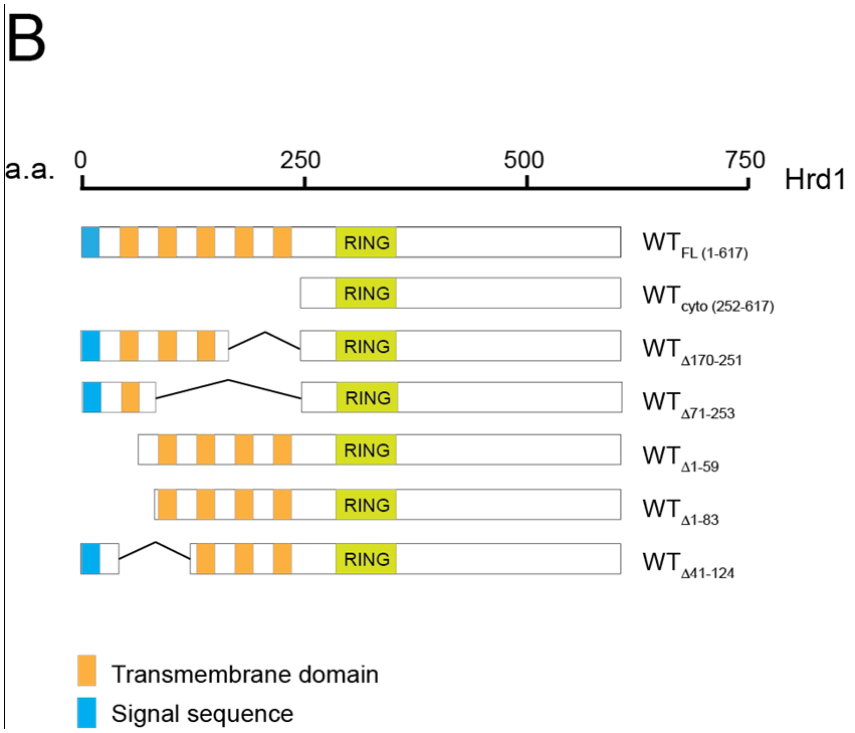


Figure 4.2.1: Schematic representation of SEL1L and Hrd1. S-SEL1L **(A)** and Hrd1-myc **(B)** constructs used in this study. WT= wild type, FL= full length, DFP= non-fluorescent variant of GFP

4.2 Results

4.2.1 The first TMD of Hrd1 is involved in the interaction with SEL1L

The TMDs of Hrd1p have been shown to be sufficient to co-precipitate Hrd3p (Gardner et al., 2000) and so we aimed to identify which Hrd1 TMD was responsible for SEL1L interaction. We co-expressed a series of Hrd1-myc constructs lacking different TMDs (Fig. 4.2.1) along with the presumably lumenal S-SEL1L$_{1\text{-}737}$ in HEK293$_{Hrd1\text{-}KD}$ cells (Fig. 4.2.2A). In the previous chapter it was shown that S-DFP-FAM8A1$_{TMD}$ co-precipitated these deletions, although some of them were expressed weakly. FAM8A1$_{TMD}$ was therefore used as positive control to demonstrate that loss of interaction with SEI1L$_{1\text{-}737}$ was not an effect of weak expression of a Hrd1 deletion. In contrast to Hrd1p-

Hrd3p, the Hrd1-SEL1L complex is notably unstable in common non-ionic detergents [e.g. TritonX-100, (Christianson et al., 2012; Christianson et al., 2008)] and so to preserve interactions between integral membrane segments, cells were lysed in 1% digitonin. We found that $SEL1L_{1-737}$ was able to interact with $Hrd1_{WT-FL}$ as previously published (Christianson et al., 2008) but not just its cytoplasmic region ($Hrd1_{WT-cyto}$, Fig. 4.2.2A, lane 14). Hrd1 excised of its N-terminus including TM1 ($Hrd1_{\Delta 1-83}$ Fig. 4.2.2A, lane 11,) or TM1 and TM2 ($Hrd1_{\Delta 41-124,}$ lane 12) failed to bind $SEL1L_{1-737}$, suggesting that it is the first Hrd1 TMD that binds to SEL1L. However, a Hrd1 deletion lacking TM1 but retaining the cytoplasmic loop between TM1-TM2 ($Hrd1_{\Delta 1-59}$) was able to support $SEL1L_{1-737}$ interaction. This observation suggests that either a segment of $SEL1L_{1-737}$ was able to access the cytosol or that $Hrd1_{\Delta 1-59}$ adopted a non-native topology that placed that domain in the ER lumen. It is noteworthy that co-precipitated $Hrd1_{\Delta 1-59}$ was less when compared to either $Hrd1_{WT-FL}$ or $Hrd1_{\Delta 71-253}$ (TM1 only + cytoplasmic region), which supports our hypothesis that Hrd1 TM1 has an important role in maintaining an interaction with SEL1L.

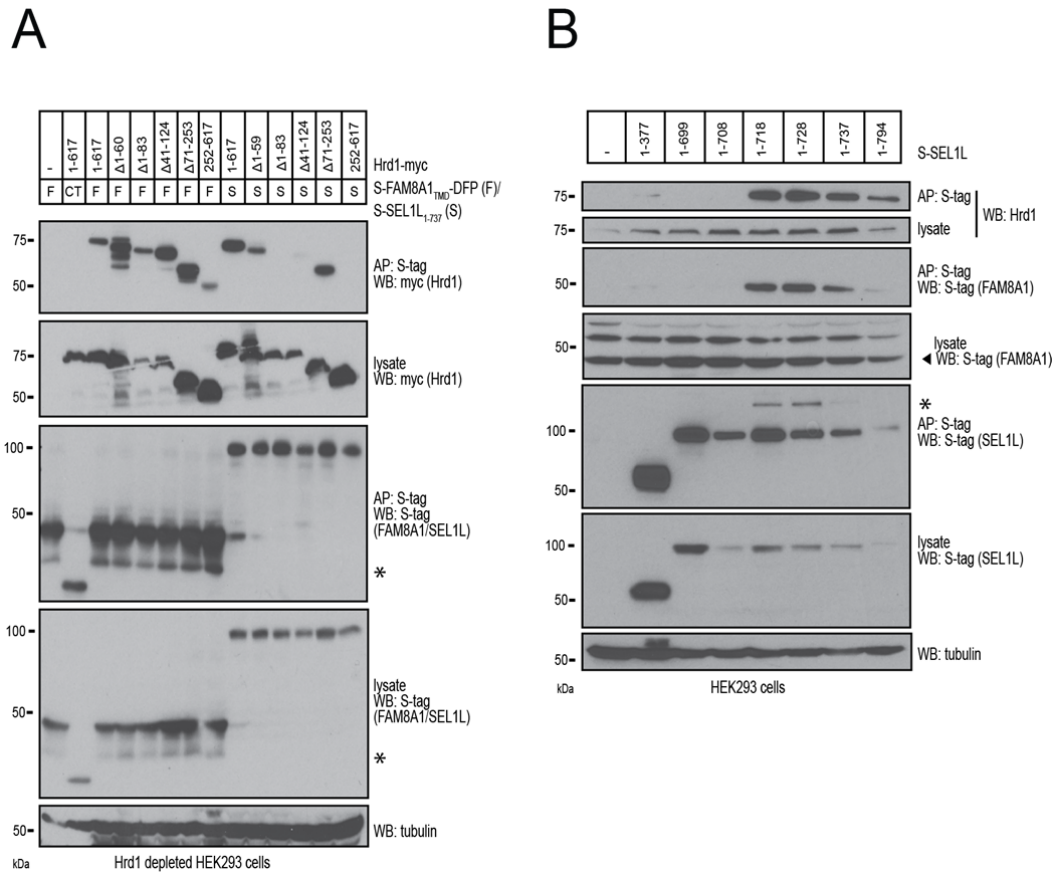


Figure 4.2.2: Interaction with Hrd1 does not depend on SEL1L TMD. (A) The first Hrd1 TMD is necessary to bind SEL1L: $HEK293_{Hrd1\text{-}KD}$ cells ectopically expressed $SEL1L_{1\text{-}737}$ and the indicated Hrd1-myc TMD deletions. S-DFP-$FAM8A1_{TMD}$ was expressed with Hrd1 TMD deletions as control. Co-precipitation analysis was carried out by western blot. **(B)** $SEL1L_{708\text{-}718}$ is essential for interaction with Hrd1: HEK293 cells were transiently transfected with the indicated SEL1L truncations and interaction with endogenous Hrd1 and FAM8A1 assessed by western blot. * Additional S-tag reactive band.

4.2.2 A region proximal to the SEL1L TMD participates in Hrd1 binding

Above we have shown that a putative ER lumenal SEL1L fragment is able to interact with the TM and/or cytoplasmic regions of Hrd1. To define the reciprocal SEL1L region required for Hrd1 binding, a panel of SEL1L truncations were ectopically expressed in HEK293 cells (Fig. 4.2.2B). Because aberrant secretion was a possibility, a KDEL sequence was fused to the C-terminus to ensure retention of these truncations in the ER. When cells were lysed in digitonin, Hrd1 was co-precipitated by $SEL1L_{FL}$, $SEL1L_{1\text{-}737}$, $SEL1L_{1\text{-}728}$

and $SEL1L_{1-718}$ at comparable levels (Fig. 4.2.2B). $SEL1L_{1-708}$ failed to interact with Hrd1, indicating that the SEL1L region between aa 708-718 is essential to bind Hrd1 (Fig. 4.2.2B). Co-precipitation of FAM8A1 with SEL1L fragments exhibited a pattern resembling that of Hrd1, consistent with previous data showing that FAM8A1 and SEL1L do not bind directly but rather through Hrd1 (Christianson et al., 2012). In lanes where Hrd1-SEL1L interactions were observed, a higher molecular weight band for SEL1L was detected. Given its approximate size, we suspect that Hrd1-interacting SEL1L forms oligomers that remain stable under denaturing and reducing conditions. SEL1L ubiquitination may also cause such a band to appear but its uniformity argues against modifications such as multiple mono- or polyubiquitination. For the time being, the nature of its identity remains undetermined.

We then asked whether the SEL1L truncations that fail to bind Hrd1 would impair degradation of a model ERAD substrate. It has been shown previously that SEL1L knockdown impairs degradation of lumenal substrates including the transthyretin mutant TTR_{D18G} (Christianson et al., 2012). Using the ERAD reporter assay described previously, we could demonstrate that ectopic expression of $SEL1L_{FL}$, $SEL1L_{1-718}$ and $SEL1L_{1-708}$ impaired TTR_{D18G} degradation while $SEL1L_{1-737}$ had only a modest effect (Fig. 4.2.3). This may mean that SEL1L interacts in a stoichiometric ratio with proteins of the Hrd1 complex; as the amount of ectopically expressed SEL1L is higher than the abundance of endogenous binding partners, the SEL1L truncations may become ERAD substrates and occupy the ERAD machinery. However, this does not explain why $SEL1L_{1-737}$ only had a modest effect on TTR_{D18G}

degradation. Additional experiments are required in order to verify this preliminary observation.

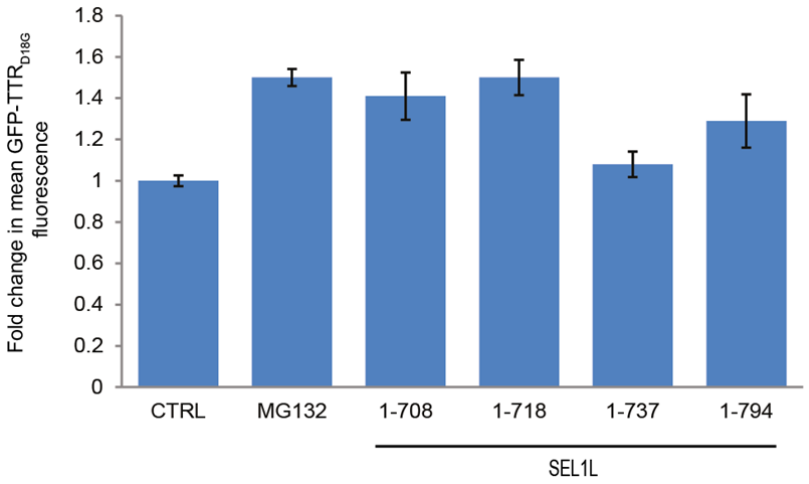


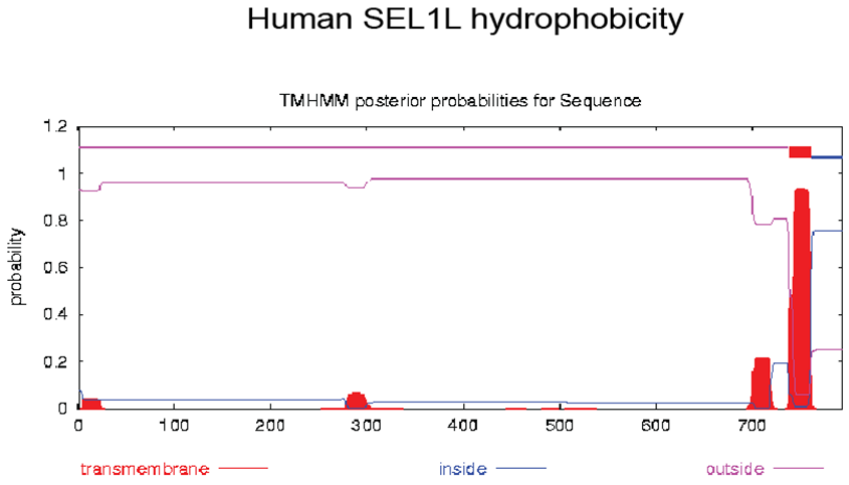
Figure 4.2.3: Ectopic SEL1L truncations impair TTR$_{D18G}$ degradation. Loss of Hrd1-SEL1L interaction decreases TTR$_{D18G}$ degradation: The indicated SEL1L truncations were ectopically expressed in the TTR$_{D18G}$ reporter cell line and substrate degradation measured by FACS. Error bars represent standard error from at least n=2 biological replicates, n=3 technical replicates each.

4.2.3 SEL1L may contain a second TMD

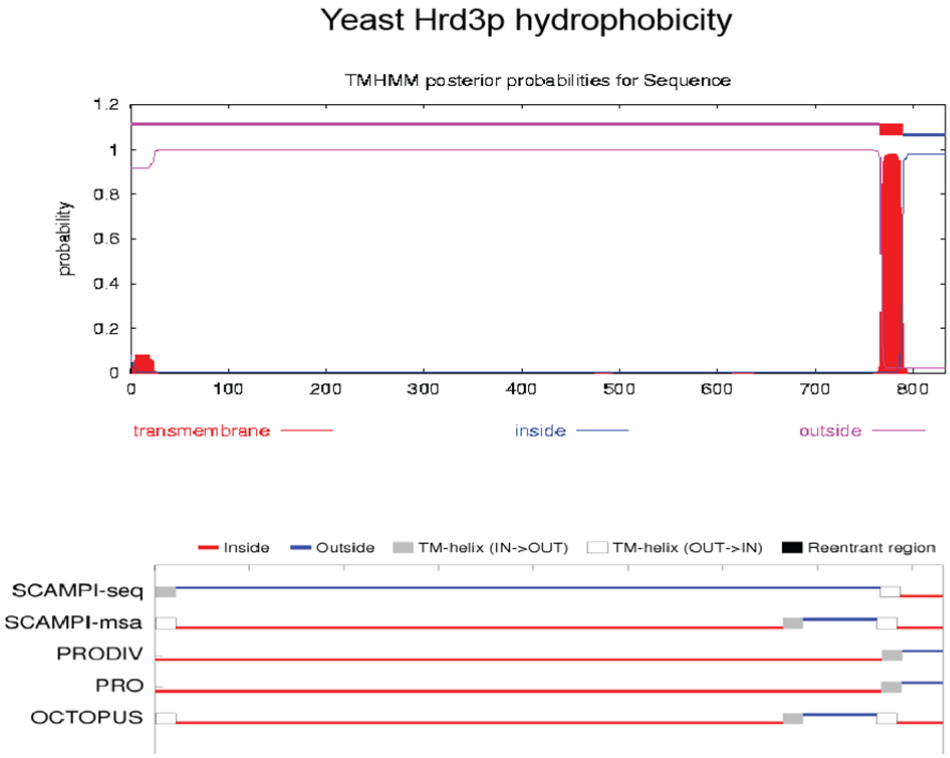
As mentioned earlier in this chapter, the notion of the ER lumenal portion of SEL1L interacting with the TMD of Hrd1 presents a topological challenge in the form of the ER lipid bilayer. We therefore asked whether the region of SEL1L important for interaction with Hrd1 displayed any notable features in its primary or secondary structure. Comparative sequence analysis of SEL1L (ProPhyler) revealed that aa 701-721 are highly conserved across metazoans (Fig. 4.2.4F) and to some degree with unicellular fungi. Moreover, multiple bioinformatic algorithms designed to predict TMDs (TMHMM, TOPCONS) revealed that the ~20 aa stretch corresponding to the Hrd1-interacting region of SEL1L (701-721) is distinctly hydrophobic (Fig. 4.2.4A) and in some models, predicted to be a TMD. Although not previously annotated as a TMD, the aa composition and

appropriate length suggest that this segment may be membrane-associated or even a bona fide TMD. The corresponding region in Hrd3p (aa 664-685) has fewer hydrophobic aa (Fig. 4.2.4B, upper panel), but a consensus prediction (TOPCONS) also identified this segment as a second TMD (Fig. 4.2.4B, bottom panel). These analyses support a model where this newly characterised, hydrophobic segment of SEL1L ($SEL1L_{701-721}$) is responsible for forming the complex with Hrd1 through an interaction/s that may occur near or within the ER membrane. We have designated aa 701-721 of SEL1L as the Hrd1-interacting domain, or HID.

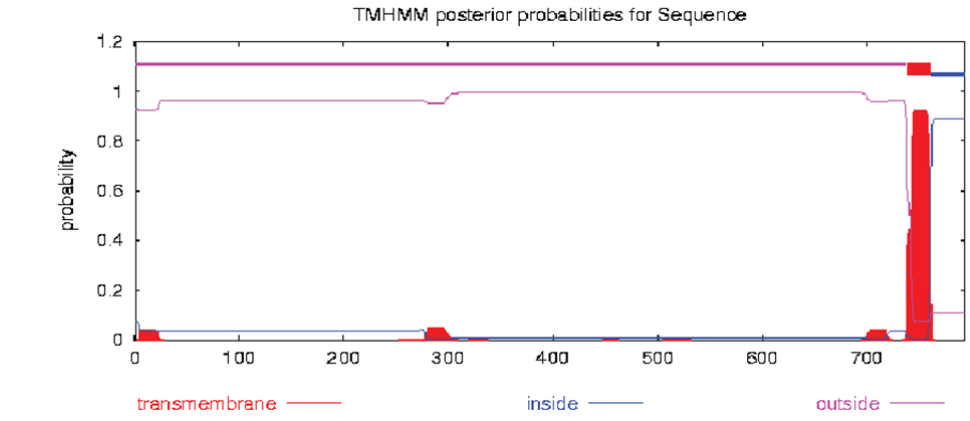
A



B

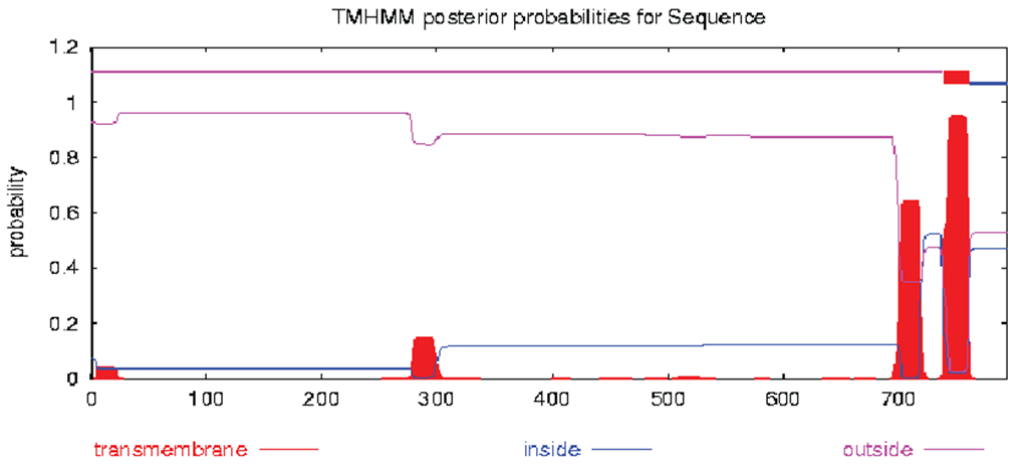

Yeast Hrd3p hydrophobicity
TMHMM posterior probabilities for Sequence
probability
1.2
1
0.8
0.6
0.4
0.2
0
0
100
200
300
400
500
600
700
800
transmembrane
inside
outside
Inside
Outside
TM-helix (IN->OUT)
TM-helix (OUT->IN)
Reentrant region
SCAMPI-seq
SCAMPI-msa
PRODIV
PRO
OCTOPUS

C


Human SEL1L (L709/712G) hydrophobicity
TMHMM posterior probabilities for Sequence
probability
1.2
1
0.8
0.6
0.4
0.2
0
0
100
200
300
400
500
600
700
transmembrane
inside
outside

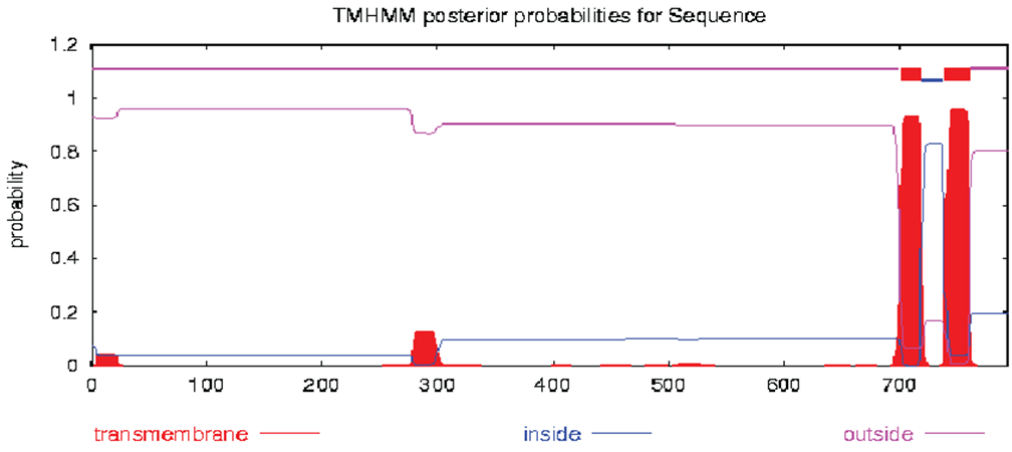
D

Human SEL1L (P704L) hydrophobicity



E

Human SEL1L (K711L) hydrophobicity



F



Figure 4.2.4: SEL1L contains a putative second TMD. Hydrophobicity prediction for human SEL1L **(A)** and its yeast homologue Hrd3p **(B)** shows that SEL1L contains a second putative TMD (TMHMM server, TOPCONS). Hydrophobicity of this putative TMD is decreased by the L709/712G mutation **(C)** and increased upon mutation of P704L **(D)** or K711L **(E)**. **(F)** Sequence conservation of the putative second SEL1L TMD (aa 701-721).

With the hypothesis that HID may represent a previously unrecognised TMD, we next asked the question whether the overall hydrophobicity within this segment influenced interaction with Hrd1. Site-directed mutagenesis of conserved residues was employed to generate SEL1L mutants with a HID that had reduced hydrophobicity (L709G/L712G, Fig. 4.2.4C), increased hydrophobicity (P704L, Fig. 4.2.4D) and where a charged residue was removed (K711L, Fig. 4.2.4E). These S-tagged SEL1L mutants were co-expressed with Hrd1-myc in HEK293$_{Hrd1\text{-}KD}$ cells and interactions evaluated under 1% digitonin lysis conditions. Hrd1-myc was co-precipitated by SEL1L$_{K711L}$ at levels comparable to SEL1L$_{FL}$, while interaction with SEL1L$_{P704L}$ mutant was markedly impaired (Fig. 4.2.5A, lanes 4 and 5). As Pro are known helix-breaking residues, this result suggests that P704 is necessary to maintain the native conformation of SEL1L$_{701\text{-}721}$ and it appears that the HID requires flexible secondary structure rather than just increased hydrophobicity in order to bind. Overall hydrophobicity of the HID was still important because when

L709G/L712G mutants were made to either $SEL1L_{FL}$ or $SEL1L_{1-737}$, interaction with Hrd1 was abolished (Fig. 4.2.5A, lanes 6 and 8). A single mutation at L712G was also sufficient to disrupt the Hrd1-SEL1L interaction (Fig. 4.2.5A, lane 9). It should be noted that L→G mutations not only decrease overall hydrophobicity but may disrupt secondary structure as well. These results indicate that both hydrophobicity and secondary structure of the HID are crucial for its interaction with Hrd1.

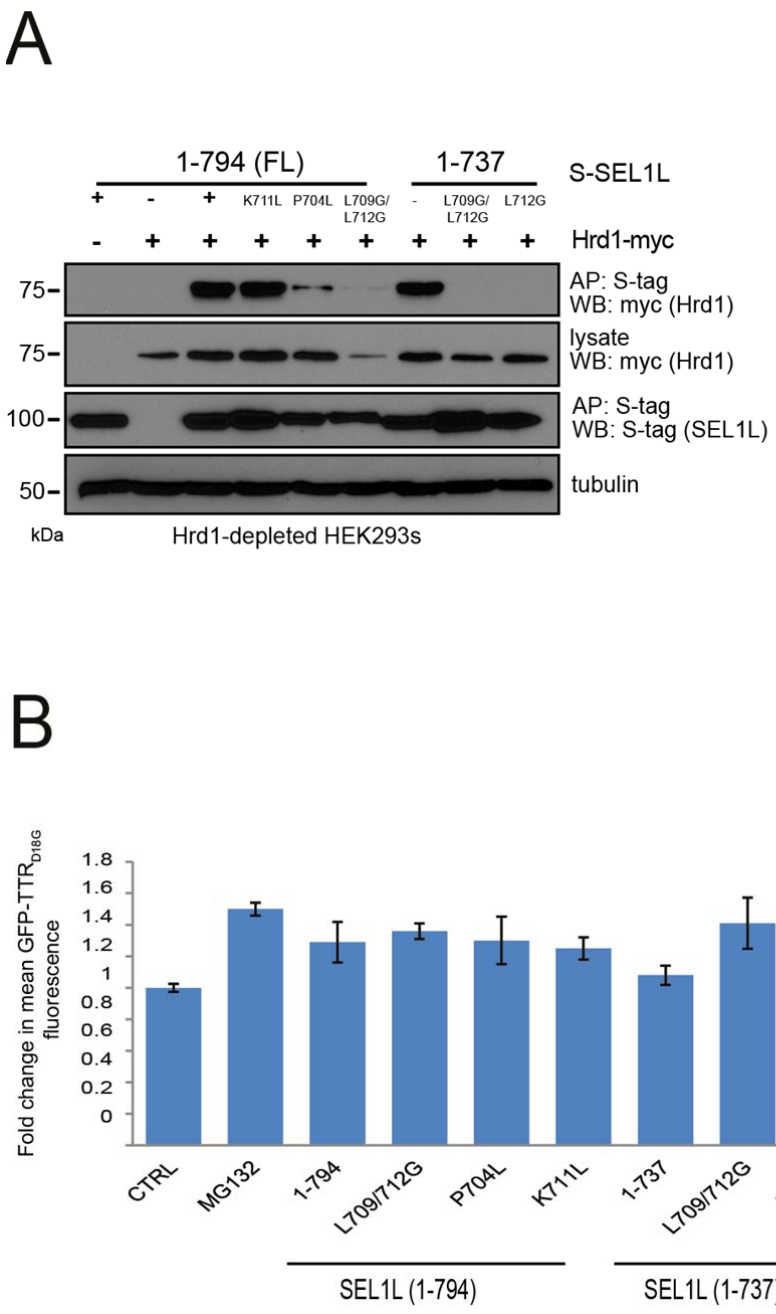


Figure 4.2.5: Decreased hydrophobicity of the putative SEL1L TMD impairs binding to Hrd1. (A) SEL1L mutants decreasing or increasing the hydrophobicity of SEL1L were co-expressed with Hrd1-myc and co-precipitation analysed by western blot. **(B)** Altering SEL1L hydrophobicity impairs degradation of a lumenal ERAD model substrate: The indicated SEL1L mutants were ectopically expressed in the TTR_{D18G} ERAD reporter cell line and substrate degradation measured by FACS. Error bars represent standard error from at least n=2 biological replicates, n=3 technical replicates each.

When SEL1L mutants were expressed in a functional ERAD reporter cell line, we observed accumulation of TTR_{D18G} (Fig. 4.2.5B). This result was anticipated for mutants that lost interaction with Hrd1 (e.g. P704L, L712G), but not for the K711L, in which binding to Hrd1 was unaffected. One possible explanation may be that increasing the hydrophobicity in the HID of SEL1L increased binding affinity to Hrd1. For efficient ERAD processing of substrates, a more labile interaction between Hrd1 and SEL1L might be essential, with the flexibility of $SEL1L_{701-722}$ allowing rapid changes between a membrane-bound/associated and lumenal state.

4.2.4 The putative TMD of SEL1L is not sufficient to co-precipitate Hrd1

Above we identified $SEL1L_{701-721}$ as necessary for interaction with Hrd1. To extend this analysis, we wished to determine whether this region alone was sufficient for Hrd1 binding. We fused the annotated TMD (TM1, aa 738-760) and the HID (aa 701-721) of SEL1L to the C-terminus of S-GFP. Each construct also contained an N-terminal signal sequence and a C-terminal KDEL sequence to ensure delivery to and retention in the ER. Constructs were expressed alone in HEK293 cells or co-expressed with Hrd1-myc in $HEK293_{Hrd1-KD}$ cells (Fig. 4.2.6).

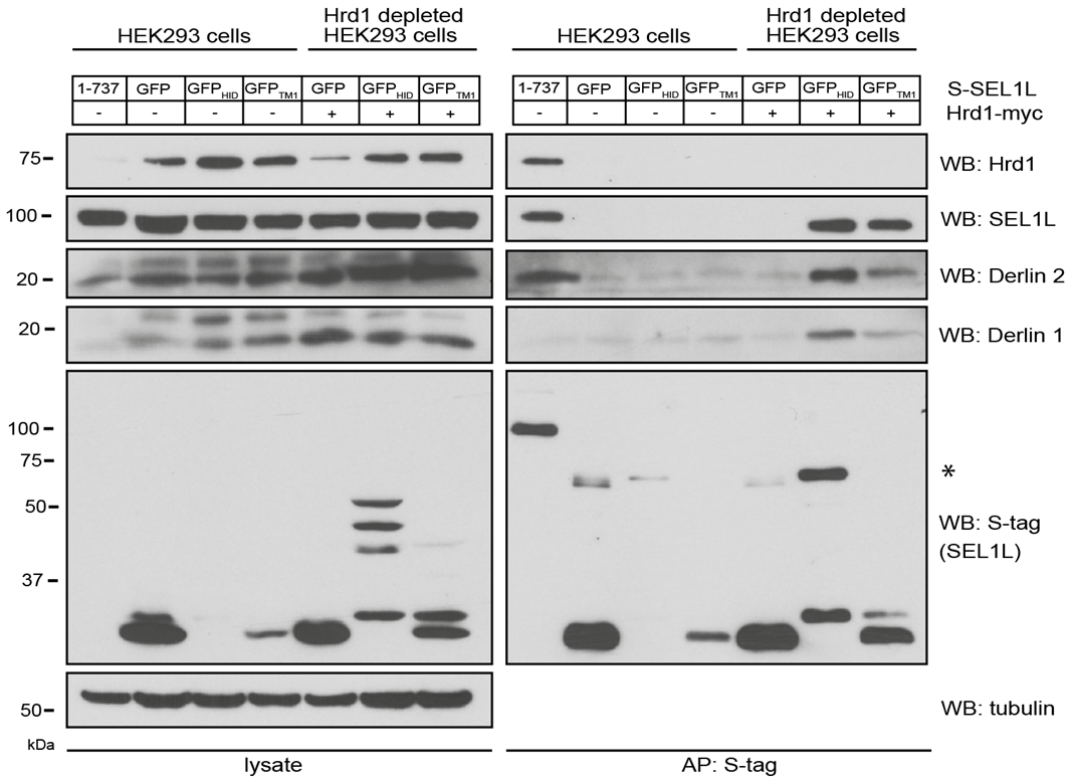


Figure 4.2.6: $SEL1L_{HID}$ is not sufficient to bind Hrd1. The annotated (TM1) and putative (HID) SEL1L TMDs are not sufficient to interact with Hrd1: GFP fusion proteins $SEL1L_{TM1}$ and $SEL1L_{HID}$, containing a signal sequence and a KDEL ER retention signal, were either expressed in HEK293 cells or co-transfected with Hrd1-myc in $HEK293_{Hrd1\text{-}KD}$ cells. Cells were lysed in 1% digitonin and interaction with Hrd1 complex components analysed by western blot. * Additional S-tag reactive band. HID= $SEL1L_{701\text{-}721,}$ TM1= $SEL1L_{738\text{-}760}$

Analysis by western blot revealed that the S-GFP-SEL1L fusion proteins alone expressed poorly in HEK293 cells compared to the negative control S-GFP alone. However, when co-expressed with Hrd1-myc, both SEL1L constructs could be detected (Fig. 4.2.6, lanes 6 and 7). This may indicate that the presence of Hrd1 created an environment that enabled the SEL1L domains to remain stable, yet neither TM1 nor the HID were sufficient to co-precipitate Hrd1, in contrast to $SEL1L_{1\text{-}737}$ (Fig. 4.2.6). Of note were the three distinct bands between 37-50 kDa observed in the lysate fraction of GFP-$SEL1L_{HID}$. The origin of these bands is not entirely clear but this region does contain a

single conserved cysteine (C710). Although SDS-PAGE assays were performed under reducing and denaturing conditions (10mM DTT, 1% SDS), it remains possible that detergent-resistant homo- or hetero-oligomers formed disulphide linkages through this cysteine. Unfortunately, time limitations prevented us from following up on this observation. No Hrd1 interaction was observed for SEL1L TM1 (Fig. 4.2.6), which was not unexpected, as previous work has shown that SEL1L truncations lacking TM1 remain able to co-precipitate Hrd1 (Christianson et al., 2008). For reasons that are not understood, two bands were detected for GFP-SEL1L$_{TM1}$, with the slower migrating band having the same molecular weight as GFP-only. This may indicate that a large proportion of the fusion protein was cleaved or prematurely truncated, which may mean that insufficient levels of GFP-SEL1L$_{TM1}$ were available to co-precipitated Hrd1.

Failure of SEL1L fusion proteins to bind Hrd1 might also have been the result of their mis-localisation, in spite of the signal sequence and KDEL sequence. We began by testing GFP-SEL1L$_{TM1}$ and GFP-SEL1L$_{HID}$ interactions with other validated components in the Hrd1 complex. To determine whether SEL1L might be forming homo-oligomers through the HID or TM1, co-precipitation of endogenous SEL1L was assessed. Both GFP-SEL1L$_{HID}$ and GFP-SEL1L$_{TM1}$ were able to pull down endogenous SEL1L, indicating that either of these two regions was sufficient for homo-oligomerisation (Fig. 4.2.6). An alternative explanation could be that GFP-SEL1L fusions interact with endogenous SEL1L as substrates, but due to time limitations experiments to delineate these possibilities were unable to be performed.

Der1-like protein-1 (Derlin-1) and Derlin-2 are both members of the rhomboid-like superfamily of intramembrane proteases (Greenblatt et al., 2011). More importantly, they are both polytopic ERAD components that have been described previously as interaction partners of SEL1L (Lilley and Ploegh, 2005) and part of the larger Hrd1-SEL1L complex (Christianson et al., 2012). Derlin-2, but not Derlin-1, was observed to interact with $SEL1L_{1\text{-}737}$, which is consistent with previous reports (Lilley and Ploegh, 2005). The Derlin family, like Hrd1, are ER-resident polytopic proteins with their C-terminus in the cytosol. This is noteworthy, as Derlin-2 interaction with SEL1L was also independent of SEL1L's validated TMD. Moreover, $SEL1L_{HID}$ co-precipitated Derlin-2 at levels comparable to $SEL1L_{1\text{-}737}$ while $SEL1L_{TM1}$ bound less. $SEL1L_{HID}$ also co-precipitated Derlin-1, but as no interaction was observed when $SEL1L_{1\text{-}737}$ was ectopically expressed, we cannot rule out the possibility that the GFP-fusion protein interacts with Derlin-1 as a substrate rather than as an associated ERAD component. Taken together, these results provided evidence that SEL1L may form oligomers and that the HID of SEL1L thought to bind Hrd1 does so through interactions with other membrane-bound Hrd1 complex components, including Derlin-2 and possibly Derlin-1.

4.2.5 $SEL1L_{short}$ localises to the ER but does not interact with Hrd1

Our previous analyses suggested that the HID of SEL1L (aa 701-721) had a particularly hydrophobic composition and given this, we wished to establish the topology of the SEL1L C-terminus and determine whether the presence of Hrd1 would alter its potential insertion in (or association with) the membrane. By mapping $SEL1L_{HID}$ onto a helical wheel (Fig. 4.2.7A), it was clear that the positively charged residue (K711) and the Pro (P704) were residing on the

same face, suggesting that $SEL1L_{HID}$ may be an amphipathic helix and membrane-associated through the opposing surface.

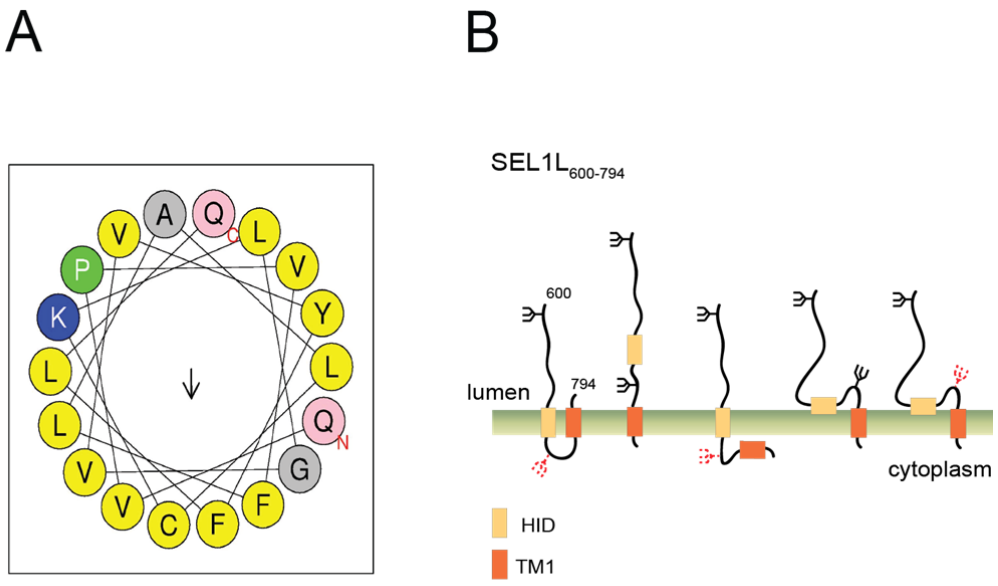


Figure 4.2.7: Potential topologies of the SEL1L C-terminus. (A) Helix wheel prediction of the putative SEL1L TMD, charged residue in blue (HeliQuest). **(B)** Schematic diagram of the putative topologies of $SEL1L_{600-794}$, additional glycosylation site in red.

To investigate this, we generated a short version of SEL1L ($SEL1L_{600-794}$) that removed all but the last two Sel1 domains (10 and 11) and all but one N-linked glycosylation site (N608). This short form was constructed because the observed molecular weight of SEL1L (~100kDa) by SDS-PAGE makes distinguishing small changes in mass (e.g. glycosylation) problematic to resolve consistently. Therefore, three SEL1L short constructs were generated: 600-699 (neither HID nor TM1), 600-728 (only HID) and 600-794 (both HID and TM1). Each contained an N-terminal signal sequence and the KDEL sequence at the C-terminus. In addition, a consensus N-linked glycosylation site (NX-S/T) was introduced into the region between the HID and TM1 (N725) by site-directed

mutagenesis (R727T, Fig. 4.2.1A, red). If exposed to the ER lumen, this second site will be glycosylated and its electrophoretic mobility will be retarded. Endoglycosidase H (EndoH) is a highly specific endoglycosidase which cleaves asparagine-linked mannose-rich oligosaccharides (a marker for proteins of the ER), but not highly processed complex oligosaccharides (a marker for proteins of the Golgi) from glycoproteins. If $SEL1L_{600\text{-}796/R727T}$ is EndoH sensitive, it will confirm that aa 722-737 of SEL1L are exposed to the ER lumen. Putative topologies for $SEL1L_{short}$ are shown in Fig. 4.2.7B.

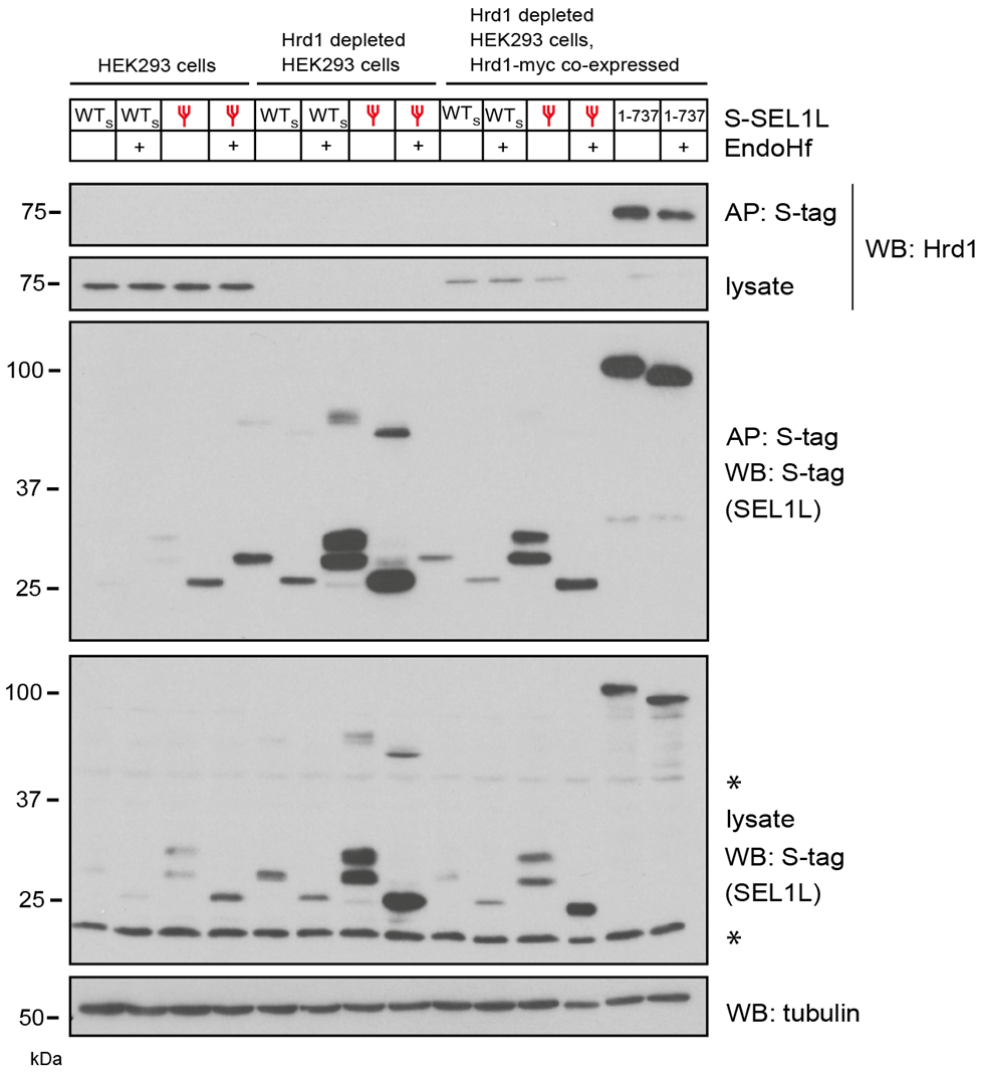


Figure 4.2.8: SEL1L$_{600\text{-}794}$ localises to the ER but does not interact with Hrd1. S-SEL1L$_{600\text{-}794}$ WT and SEL1L$_{600\text{-}794}$ R727T (Ψ) were expressed in HEK293 WT and HEK293$_{Hrd1\text{-}KD}$ cells as well as co-expressed with Hrd1-myc in HEK293$_{Hrd1\text{-}KD}$ cells. Cells were lysed in 1% digitonin and lysates as well as affinity purified complexes were treated with EndoH prior to analysis by western blot. * Additional S-tag reactive band.

To establish that S-SEL1L$_{short}$ and S-SEL1L$_{short/R727T}$ were expressed in the ER, each was transiently transfected in HEK293 cells. As with the GFP-SEL1L fusions, S-SEL1L$_{short}$ and S-SEl1L$_{short/R727T}$ expressed poorly (Fig. 4.2.8). However, when expressed in HEK293$_{Hrd1\text{-}KD}$ cells or co-transfected with Hrd1-myc in HEK293$_{Hrd1\text{-}KD}$ cells, each of the SEL1L short forms could be detected

(Fig. 4.2.8). Sensitivity to EndoH confirmed an ER-localisation for the two SEL1L constructs as well as glycosylation at the novel site (N725, Fig. 4.2.8). Modification of N725 only occurred at a frequency of ~50%, perhaps reflective of two different topologies that SEL1L might have adopted. However, this ratio was independent of the presence of Hrd1, which does not support our model where interaction with Hrd1 affects insertion and stabilisation of SEL1L through the HID. Efficient N-linked glycosylation requires a distance of 12-14 aa from a TMD (Nilsson and von Heijne, 1993). R727T is four aa beyond the Hrd1-binding region and eleven aa before the annotated TM1, which could be another explanation why N725 is inefficiently glycosylated.

Neither $SEL1L_{short}$ nor $SEL1L_{short/R727T}$ was able to co-precipitate Hrd1. This indicates that $SEL1L_{HID}$ likely requires a contribution from the lumenal domain preceding aa 600 in order to bind Hrd1. It may as well be that substrate recruitment by SEL1L is a prerequisite for the Hrd1 interaction and since $SEL1L_{short}$ has lost most of its lumenal domain, its substrate recognition capacity is likely to be diminished. $SEL1L_{short/R727T}$ appeared to express better than $SEL1L_{short}$, suggesting that the second glycosylation site may increase stability of the protein. In summary, $SEL1L_{short}$ constructs are localised to the ER and can expose aa 722-737 to the ER lumen, indicating that the HID was at least sometimes present in the ER lumen. This does not rule out the possibility that the region is cytosolically localised at some frequency and leaves open the idea of multiple topologies for SEL1L (Fig. 4.2.7B). However, as $SEL1L_{short}$ failed to co-precipitate Hrd1, in the end these constructs are not as suitable as anticipated for the assays to determine SEL1L topology. It will still be interesting

to test whether $SEL1L_{short}$ is able to bind SEL1L and the Derlin-1/-2, like the GFP-SEL1L fusions.

Despite their lack of ability to bind Hrd1, we were still interested in whether $SEL1L_{600-699}$, $SEL1L_{600-728}$ and the two $SEL1L_{short}$ constructs would affect ERAD. Using the previously described ERAD reporter cell line, we found that only transient expression of $SEL1L_{600-794}$ impaired TTR_{D18G} degradation (Fig. 4.2.9). $SEL1L_{600-699}$ and $SEL1L_{600-728}$ both lack TM1 and most part of the lumenal portion of SEL1L. This prevents interactions with a number of Hrd1 complex components like OS-9 and XTP3-B and possibly the correct insertion into ERAD complexes. Why $SEL1L_{600-794}$ had an impact may be due to its ability to integrate in the ER membrane where it could be interacting with other factors (i.e. Derlin-2) but disrupting function, since most of its lumenal portion has been truncated. Hence, $SEL1L_{short}$ may be acting as dominant negative. In principle, SEL1L truncations were designed to elucidate the molecular underpinnings of the Hrd1-SEL1L interaction. However, their failure to recapitulate the basic interaction has made their utility in these studies less than optimal. The complexity of the Hrd1-SEL1L interaction clearly requires an alternative strategy to elucidate its nature.

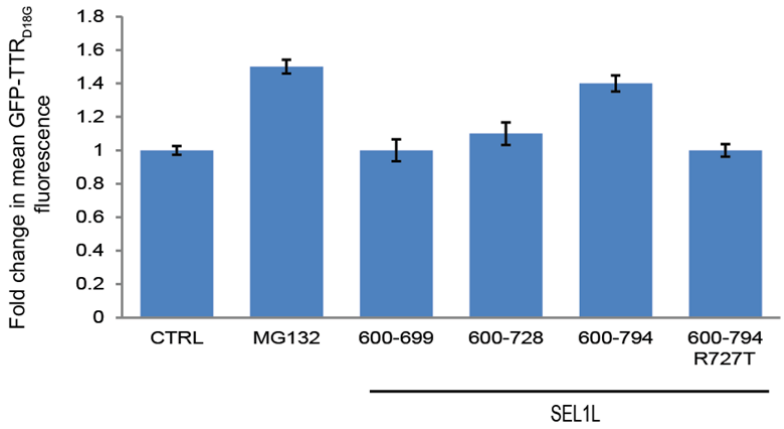


Figure 4.2.9: A SEL1L short construct containing the annotated TMD inhibits TTR$_{D18G}$ degradation. SEL1L short constructs containing either both TM1 and HID (600-794), only HID (701-721) or no TMD (600-699) were ectopically expressed in the GFP-TTR$_{D18G}$ reporter cell line. The effect on ERAD substrate degradation was measured by FACS. Error bars represent standard error from n=3 technical replicates.

4.3. Discussion

This chapter focused on the investigation of the binding modus between the ER-resident ubiquitin ligase Hrd1 and its cofactor SEL1L. Our aim was to resolve the intriguing observation from both yeast (Gardner et al., 2000) and mammals (Christianson et al., 2008) that the lumenal region of Hrd3p/SEL1L was sufficient to interact with Hrd1p/Hrd1. As it could be demonstrated in yeast that the TM region of Hrd1p is sufficient to bind SEL1L (Gardner et al., 2000), our first step was to identify the specific Hrd1 TMD mediating interaction with SEL1L. We found that Hrd1 TM1 was necessary for interaction with SEL1L, but not sufficient since Hrd1 forms lacking just TM1 but retaining the loop between TM1-TM2 still bound SEL1L (Fig. 4.2.2A). So while participating, clearly TM1 is not the only mode of interaction with SEL1L.

Next we turned our attention to mapping the lumenal region of SEL1L necessary and sufficient to interact with Hrd1. In yeast, it has so far been established that Hrd1p interacts with a region between aa 665-769 of Hrd3p

(Gauss et al., 2006) and in mammals the interacting domain is contained within aa 372-737 of SEL1L (Christianson et al., 2008). As SEL1L truncations are partially secreted, the retention sequence KDEL was fused to the C-terminus of the truncation constructs (Christianson et al., 2008). Based initially on sequence conservation, we empirically established a small region ($SEL1L_{701-721}$) between the last Sel1 domain (Sel1-11) and the TMD as necessary for co-precipitation of Hrd1 (Fig. 4.2.2B). The effect of SEL1L truncations on degradation of the lumenal and SEL1L dependent ERAD substrate TTR_{D18G} (Christianson et al., 2012) was assessed with the functional reporter cell line assay described in the previous chapter. We found that overexpression of full length SEL1L had a dominant negative effect on TTR_{D18G} degradation (Fig. 4.2.3), which is consistent with previous studies where the ectopic expression of ERAD factors impaired substrate degradation.

In mammals, a slight stabilisation of TCRα and $CFTR_{\Delta F508}$ was observed upon expression of Ube2j1 and Hrd1 (Kikkert et al., 2004; Lenk et al., 2002). In yeast, overexpression of Hrd3p and Usa1p stabilised the lumenal substrate carboxypeptidase mutant CPY* (Carvalho et al., 2010). Overexpression of Der1p, on the other hand, did not affect CPY* degradation and ectopic Hrd1p even accelerated ERAD of CPY*. This suggests that overexpression of certain ERAD factors interferes with the normal function of ERAD and this may be caused by limited abundance of certain interaction partners. In mammals, ectopic expression of SEL1L had no effect on degradation of α-1 antitrypsin mutant NHK, but accelerated turnover of NHK-QQQ, a mutant lacking its three glycosylation sites (Iida et al., 2011), indicating that distinct ERAD complexes are in place to degrade different classes of substrates.

Our data further demonstrates that expression of SEL1L with a truncated cytoplasmic tail and TMD ($SEL1L_{1-737}$) has no significant effect on TTR_{D18G} degradation (Fig. 4.2.3). In yeast, equivalent truncations in Hrd3p suffice to perform degradation of CPY* and Hmg2p, indicating that cytoplasmic and membrane regions of Hrd3p/SEL1L are dispensable for ERAD (Gardner et al., 2000; Gauss et al., 2006). However, shorter SEL1L truncations interacting with Hrd1 (1-718) or not (1-708) decrease degradation of TTR_{D18G}, like the full length protein, and in order to confirm this result, this experiment needs to be repeated to determine the statistical significance of this observation.

The HID of SEL1L (aa 701-721) is highly conserved across eukaryotes and contains a high concentration of hydrophobic residues (Fig. 4.2.4A and F). Although this region is not annotated as TMD, the segment length and its hydrophobic nature led to the hypothesis that the HID may be a cryptic TMD or perhaps membrane-associated in a way where SEL1L could access TM1 of Hrd1 to facilitate interaction. Mutations that decreased overall hydrophobicity (L709G/L712G, L712G) or presumably altered the conformation (P704L) abolished binding to Hrd1, while the K711L mutation that eliminated a charged residue and increased overall hydrophobicity of the segment had no effect on Hrd1 co-precipitation (Fig. 4.2.5A). This suggests that the Hrd1-SEL1L interaction is not mediated by charge-pairing, but that hydrophobicity is crucial. All mutants impaired ERAD of TTR_{D18G} (Fig. 4.2.5B). The L709/712L and P704L mutant likely impair TTR_{D18G} degradation due to loss of interaction with Hrd1. In yeast, Hrd3p truncations unable to co-precipitate Hrd1p exert stabilisation of CPY* and Hmg2p, indicating that interaction with Hrd1 is necessary for normal substrate degradation (Gardner et al., 2000; Gauss et al., 2006). Although

$SEL1L_{K711L}$ binds Hrd1, the mutant decreases ERAD of TTR_{D18G} (Fig. 4.2.5B); it may be that this mutation, by increasing hydrophobicity of $SEL1L_{701-721}$, increases the binding affinity to Hrd1, which is not favourable for a dynamic ERAD complex.

Our next aim was to assess whether $SEL1L_{HID}$ was sufficient to bind Hrd1. But rather than co-precipitating Hrd1, the isolated HID of SEL1L bound instead to other membrane-bound components of the Hrd1 complex, including homo-oligomerisation with SEL1L, Derlin-1 and Derlin-2 (Fig. 4.2.6). Interaction between Hrd3p molecules has previously been shown in yeast, confirming our results in the mammalian system (Horn et al., 2009). The Derlins are candidates for the ERAD retrotranslocation channel (Ye et al., 2004) and Derlin-1 as well as Derlin-2 are interaction partners of SEL1L (Lilley and Ploegh, 2005). Like Hrd1, Derlin-1 and -2 are polytopic, integral membrane proteins with an extended cyto region at the C-terminus. Where within Derlin-1 or -2 this SEL1L region interacts is not known and future experiments will address in more detail the nature of these interactions. These finding indicate that Hrd1 TM1 may not be the only means by which the SEL1L HID is contacting the Hrd1 complex and points to addition contact made through associated factors such as the Derlins.

As co-translational association seems to be a common feature of protein interaction (Duncan and Mata, 2011), a possibility is that Hrd1 influences SEL1L topology upon assembly. Because we had hypothesised that SEL1L HID was in contact with, or integrated into, the ER membrane and the topology affected by the presence of Hrd1, we designed a series of N-terminal truncations of SEL1L so as to simplify the readout for the planned protease

protection, glycosylation and subcellular fractionation assays (Fig. 4.2.7B). But while $SEL1L_{600\text{-}794}$ was expressed, localised to the ER (Fig. 4.2.8) and impaired degradation of TTR_{D18G} in our ERAD reporter assay (Fig. 4.2.9), it failed to co-precipitate Hrd1 and therefore made this approach unsuitable (Fig. 4.2.8). Moreover, the glycosylation mutant $SEL1L_{short/R727T}$ did exhibit glycosylation of N725, indicative of ER lumenal exposure, but only at ~50% efficiency and independent on the presence of Hrd1 (Fig. 4.2.8). Unfortunately, we were unable to differentiate between, 1) incomplete glycosylation due to constraints on accessibility of the consensus sequence and 2) multiple topologies of SEL1L. Therefore, further experiments are needed to distinguish these two possibilities.

In summary, we have identified a region of SEL1L that is necessary, but not sufficient, for Hrd1 binding. The HID of SEL1L has a high density of hydrophobic residues and likely associates with the ER membrane. It is also sufficient to interact with a number of Hrd1 complex components such as Derlin-1 and Derlin-2, suggesting an important role for this domain in determining the interactions of the Hrd1-SEL1L ubiquitin ligase complex and its functional role in ERAD.

Chapter V: The Role of AUP1 in ERAD

5.1 Introduction

Every class of protein entering the ER has the potential to misfold and so it is surprising that only a limited number of ubiquitin ligases (E3s) have been implicated in ERAD. Recruitment of adaptor proteins to these E3 complexes represents a means by which a wider range of substrates may be targeted to this small number of ligases. Along with FAM8A1 (discussed in Chapter III), AUP1 (Fig. 5.1.1) also represents a potential candidate for such an adaptor protein.

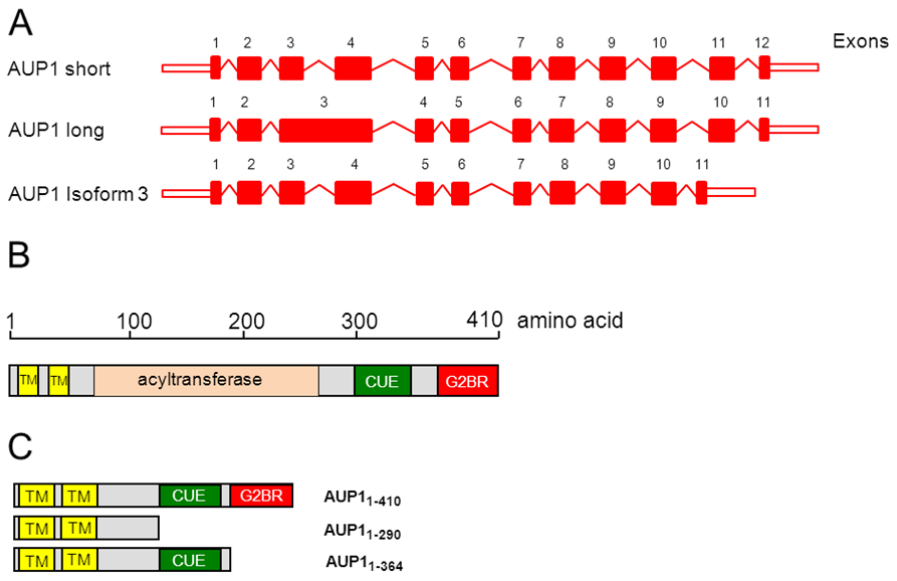


Figure 5.1.1: Schematic representation of AUP1. (A) Organisation of the AUP1 gene. **(B)** AUP1 domain structure. **(C)** AUP1 WT and AUP1 truncations, lacking conserved domains.

The AUP1 protein is highly conserved across metazoans (Fig. 5.1.2), but based solely on sequence homology it has no obvious equivalent in yeast (Jang

et al., 1996; Mueller et al., 2008). There does appear to be a functional equivalent, Cue1p, which is discussed in more detail below. Early studies identified AUP1 as a cytosolic protein with a role in integrin signalling (Kato et al., 2002; Kato and Oshimi, 2009). But more recent investigations have shown that AUP1 was in fact localised to the ER membrane (Mueller et al., 2008) as well as to lipid droplets (Spandl et al., 2009). This dual localisation makes AUP1 an intriguing candidate for a link between ER quality control and lipid droplet biogenesis. At the ER, AUP1 interacts with the Hrd1-SEL1L ubiquitin ligase complex (Christianson et al., 2012; Klemm et al., 2011; Mueller et al., 2008) and the ERAD-related E2 Ube2g2 (Klemm et al., 2011; Spandl et al., 2010). Ectopic expression of a putative AUP1 dominant-negative (AUP1-GFP) impaired degradation of both tail-anchored UBC6e [Ube2j1, (Claessen et al., 2010)] and MHC class I heavy chain (Mueller et al., 2008) indicative of an active functional role for AUP1 in ERAD.

The AUP1 gene is predicted to generate three transcript variants ($AUP1_{long}$, $AUP1_{short}$ and $AUP1_3$, Fig. 5.1.1A), but only $AUP1_{short}$ (hereafter AUP1) gives rise to a protein product (410 aa). AUP1 has two putative transmembrane domains (TMDs) (aa 20-40 and aa 40-60) (Fig. 5.1.1B) and the presence of a conserved acyltransferase domain (aa 90-193) suggests that AUP1 might have a role in phospholipid biosynthesis. AUP1 also contains a CUE (coupling of ubiquitin conjugation to ER degradation) domain (aa 290-344) (Fig. 5.1.1B). CUE domains are 42-43 aa sequences that were identified *in silico* by similarity to a region of the yeast Cue1p protein (Ponting, 2000). CUE domains have been shown to bind monoubiquitin and promote intramolecular

monoubiquitination (Shih et al., 2003). Moreover, the CUE domain of Vps9p is also capable of binding polyubiquitin chains *in vitro* (Shih et al., 2003).

```
sp|Q9Y679-2|AUP1_HUMAN      MELPSGPGP--------ERLFDSHRLPGDCFLLLVLLLYAPVGFCLLVLR 42
sp|P70295|AUP1_MOUSE        MEPPPAPGP--------ERLFDSHRLPSDGFLLLALLLYAPVGLCLLVLR 42
sp|P34426|AUP1_CAEEL        MASPEASSSGNTEDLRIEDLFHQKRN-EDTIAKIFSIIYAPVGLIILLIR 49
                            *  * ....        * **..:*   * :  :  ::*****: :*::*

sp|Q9Y679-2|AUP1_HUMAN      LFLGIHVFLVSCALP-DSVLRRFVVRTMCAVLGLVARQEDSGLRDHSVRV 91
sp|P70295|AUP1_MOUSE        LFLGLHVFLVSCALP-DSVLRRFVVRTMCAVLGLVARQEDSGLRDHRVRV 91
sp|P34426|AUP1_CAEEL        VFLGFHTFIVACLLRKSAALRMHTLRIMCSILGIVVEK--SGHRDESARV 97
                            :***:*.*:*:* *  .:.** ..:* **::**:*..:  ** **. .**

sp|Q9Y679-2|AUP1_HUMAN      LISNHVTPFDHNIVNLLTTCSTPLLNSPPSFVCWSRGFMEMNGRGELVES 141
sp|P70295|AUP1_MOUSE        LISNHVTPFDHNIVNLLTTCSTPLLNSPPSFVCWSRGFMEMDRRVELVES 141
sp|P34426|AUP1_CAEEL        LCANHVSILDHLAVDILTPCLLPSVWDIPSIIRWCFGYVDLGATRGRDQL 147
                            * :***: :**  *::**.*  * : . **:: *. *::::.      :

sp|Q9Y679-2|AUP1_HUMAN      LKRFCASTRLPPTPLLLFPEEEATNGREGLLRFSSWPFSIQDVVQPLTLQ 191
sp|P70295|AUP1_MOUSE        LKKFCASTRLPPTPLLLFPEEEATNGREGLLRFSSWPFSIQDVVQPLTLQ 191
sp|P34426|AUP1_CAEEL        VSRAKQLLTREQMPLLAFPEGIITSGEKALIKFNTWCFEVSSVVQPVSVR 197
                            :.:          *** ***   *.*.:.*::*.:* *.:..****::::

sp|Q9Y679-2|AUP1_HUMAN      VQRP---LVSVTVSDASWVSELLWSLFVPFTVYQVRWLRPVHRQLGEANE 238
sp|P70295|AUP1_MOUSE        VQRP---LVSVTVSDASWVSELLWSLFVPFTVYQVRWLHPIRRQLGEESE 238
sp|P34426|AUP1_CAEEL        VWRPYPWKVSVSVLGSSWWTDLFYFFALPFTVITVEYLPKMERRENESLE 247
                            * **    ***:* .:** ::*:: : :****  *.:*  :.*: .*  *

sp|Q9Y679-2|AUP1_HUMAN      EFALRVQQLVAKELGQTGTRLTPADKAEHMKRQRHPRLRPQSAQSSFPPS 288
sp|P70295|AUP1_MOUSE        EFALRVQQLVAKELGQIGTRLTPADKAEHMKRQRHPRLRPQSVQSSFPSP 288
sp|P34426|AUP1_CAEEL        EFTARVAETLAGNLKIAVSKFGISDATEAAKRLRTDRERAKKVVVREKTS 297
                            **: ** : :* :*    :::  :* :*  ** *  * *.:..     ..

sp|Q9Y679-2|AUP1_HUMAN      PGPSPDVQLATLAQRVKEVLPHVPLGVIQRDLAKTGCVDLTITNLLEGAV 338
sp|P70295|AUP1_MOUSE        PSPSSDVQLTTLAHRVKEVLPHVPLNVIQRDLARTGCVDLTITNLLEGAV 338
sp|P34426|AUP1_CAEEL        PRLADPRQMDECAMRIKQSFPSFHLSAIRRDLEKTRSQTTTVNNLKAGKI 347
                            *  :   *:   * *:*: :* . *..*:*** :* .   *:.**  * :

sp|Q9Y679-2|AUP1_HUMAN      AFMPEDITKGTQSLPTASASKFPSSGPVTPQPTALTFAKSSWARQESLQE 388
sp|P70295|AUP1_MOUSE        AFMPEDVTEGSQSPPAPSAPKFPSSGLATPQPTALTFAKSSWARQESLQE 388
sp|P34426|AUP1_CAEEL        SSSASDGQTG----------------------KVTLDAGTWRG--VFDN 372
                            :  ..*   *                      :*:  .:*    :::

sp|Q9Y679-2|AUP1_HUMAN      RKQALYEYARRRFTERRAQEAD 410
sp|P70295|AUP1_MOUSE        RKQALYEYARRRFRERQAQEAE 410
sp|P34426|AUP1_CAEEL        RKWQMIEVNRQKYMNRDS---- 390
                            **  : *  *::: :* :
```

Figure 5.1.2: Conservation of the AUP1 protein. Human, mouse and *C. elegans* AUP1 sequences were aligned using CLUSTALW. Asterisks: amino acid identity between all three species; dots: conservative substitutions.

Our current understanding of AUP1 implicates it as a functionally essential component within ERAD through its interactions with the Hrd1-SEL1L complex. The goal of this project is to further define the role of AUP1 in ERAD by determining the molecular aspects that support its interactions with ERAD components.

5.2 Results

5.2.1 AUP1 Localisation

Early experiments reported that AUP1 resided cytoplasmically (Kato et al., 2002) but a more detailed immunofluorescence analysis revised its localisation to the ER membrane as well as to lipid droplets (Mueller et al., 2008; Spandl et al., 2010). In an effort to resolve the apparent difference in AUP1 localisation from previous reports, we transiently expressed S-tagged AUP1 in COS1 cells and performed immunofluorescence microscopy using antibodies against the S-tag and the ER marker KDEL (Fig. 5.2.1). The KDEL sequence is present at the C-terminus of multiple ER-resident proteins (e.g. BiP, Grp94) and thus can be used as a marker for ER localisation. S-AUP1 co-localised with the ER marker (Fig. 5.2.1A), confirming that AUP1 is present in or associated with this compartment. A fraction of S-AUP1 was not co-localised with the ER marker but formed a punctate pattern surrounding the ER (Fig. 5.2.1B). As AUP1 has been suggested previously to localise to lipid droplets (Spandl et al., 2010), these structures may represent lipid droplets.

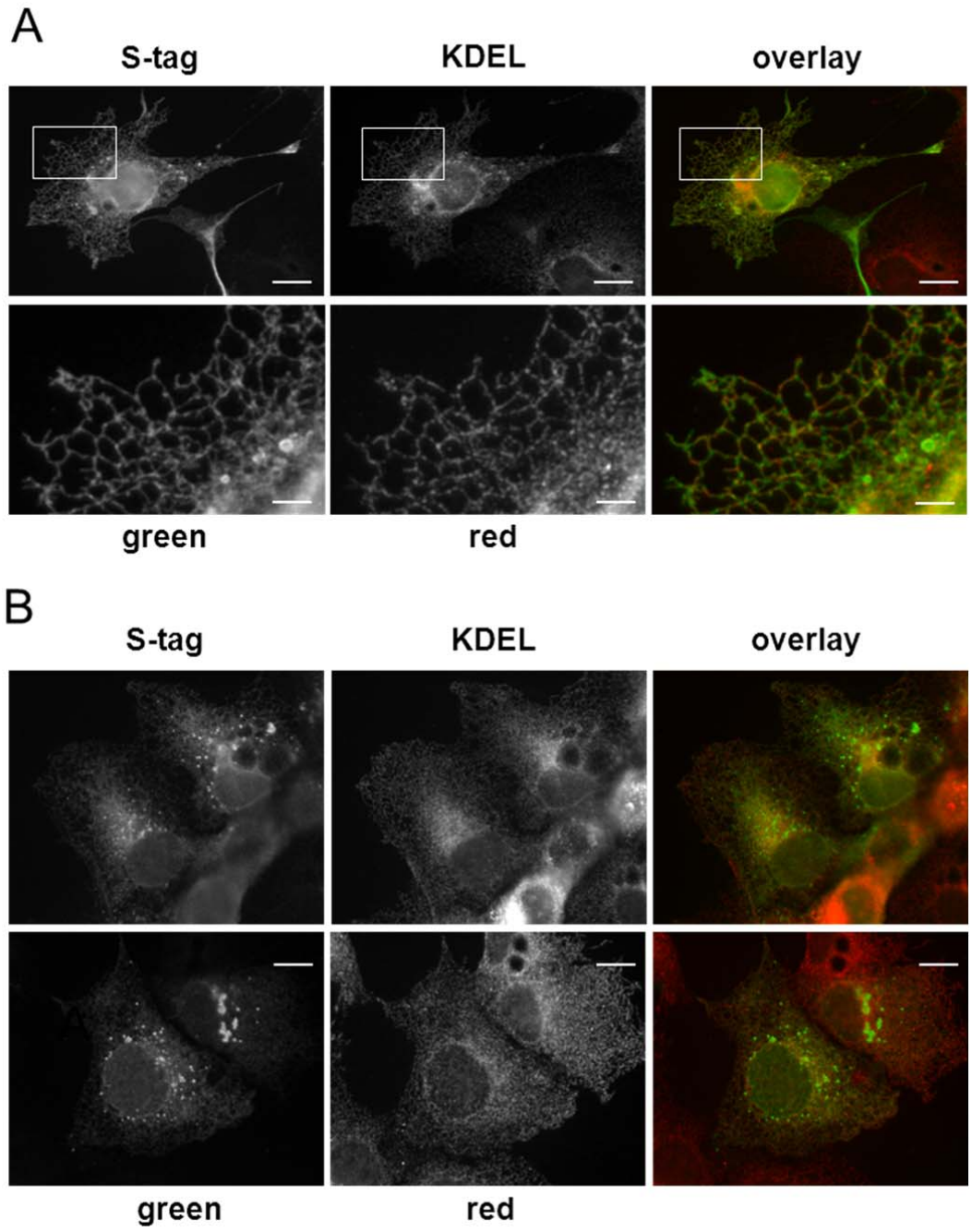


Figure 5.2.1: AUP1 Localisation in COS1 cells. AUP1 is expressed in the ER **(A)** and a second subcellular compartment **(B)**. COS1 cells were transfected with S-protein tagged AUP1, fixed, lysed in 1% TritonX-100 and incubated with anti-KDEL and anti-S-tag antibodies for immunofluorescence analysis. Scale bar = 10µm

5.2.2 AUP1 Membrane Topology

The components that make up the Hrd1-SEL1L complex are exposed simultaneously to the lumen, membrane and cytoplasm. To determine the orientation of AUP1 within the ER membrane and how it might interact with Hrd1 and/or SEL1L, COS1 cells were transfected with AUP1 appended with an S-tag either at the N- or the C-terminus (S-AUP1, AUP1-S). Limited exposure to digitonin is able to permeabilise plasma membranes while leaving intracellular membranes intact (Plutner et al., 1992). Under these conditions, only epitope tags that are exposed to the cytosolic environment can be recognised when cells are subjected to immunostaining (anti-S-tag). Positive immunostaining of both N- and C-terminal S-tagged AUP1 indicates that both termini face the cytosol (Fig. 5.2.2A). This result supports a model where AUP1 likely adopts a hairpin-like topology in the ER membrane (Fig. 5.2.2B) and possibly in the lipid droplet bilayer. AUP1 is predicted to contain two TMDs near the N-terminus (aa 20-40, 40-60), but the spacing between them is short enough to call into question whether they are able to entirely span the lipid bilayer. These data are consistent with an AUP1 topology consisting of either two TMDs or a re-entrant loop (Fig. 5.2.2C), but whether this domain (aa 20-40, 40-60) is sufficient to support interaction with either Hrd1 or SEL1L through interactions in the membrane is not yet clear.

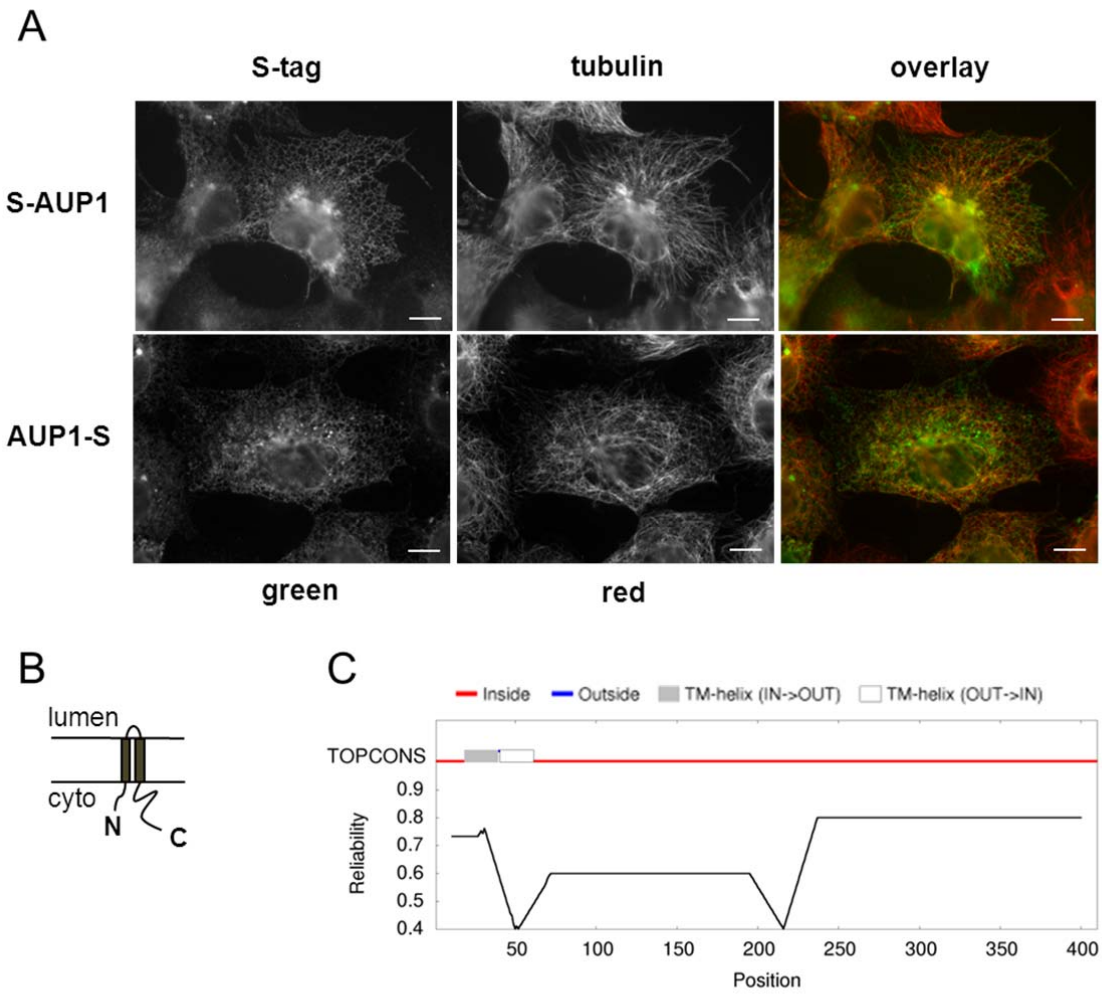


Figure 5.2.2: AUP1 is a membrane-anchored protein. (A) AUP1 C- and N-termini face the cytosol. COS1 cells were transfected with S-protein tagged AUP1, fixed, lysed in 1% digitonin and incubated with anti-KDEL and anti-S-tag antibodies for immunofluorescence analysis. Scale bar = 10µm **(B)** Model of AUP1 membrane topology. **(C)** AUP1 membrane domain prediction using TOPCONS.

5.2.3 Ube2g2 binds to the C-terminus of AUP1

The identification of AUP1 as part of the Hrd1-SEL1L ubiquitin ligase complex prompted us to identify and characterise additional AUP1 interacting proteins. Previous work from our lab using AP-LC-MS/MS (affinity purification-mass spectrometry) identified Ube2g2 as a putative interaction partner (Christianson et al., 2012). Ube2g2 is a cytosolic ubiquitin conjugating enzyme

(E2) whose yeast orthologue, Ubc7p is recruited to Hrd1p-Hrd3p complexes through the accessory factor Cue1p (Biederer et al., 1997). To validate the AUP1-Ube2g2 interaction, we co-expressed S-AUP1 and Ube2g2-myc in HEK293 cells and affinity purified complexes with S-protein agarose. Both N- and C-terminal S-tagged AUP1 bound Ube2g2 (Fig. 5.2.3A), indicating that placement of the tag had no influence on AUP1 expression or interaction with Ube2g2 (Fig. 5.2.3A). As no difference could be observed, all subsequent experiments were carried out using S-AUP1. To identify the region of AUP1 that binds Ube2g2 we designed a series of deletion constructs that removed conserved regions from the C-terminus (Fig. 5.1.1C). Full length and truncated versions of AUP1 (1-290, 1-364, 1-410) were co-expressed with Ube2g2-myc in HEK293 cells and subsequently affinity purified by S-protein agarose. Western blot analysis revealed that Ube2g2-myc bound full length AUP1 but not truncated forms of AUP1 (Fig. 5.2.3B), indicating that the C-terminus of AUP1 (364-410) was necessary for Ube2g2 binding, reminiscent of the yeast Cue1p-Ubc7p interaction.

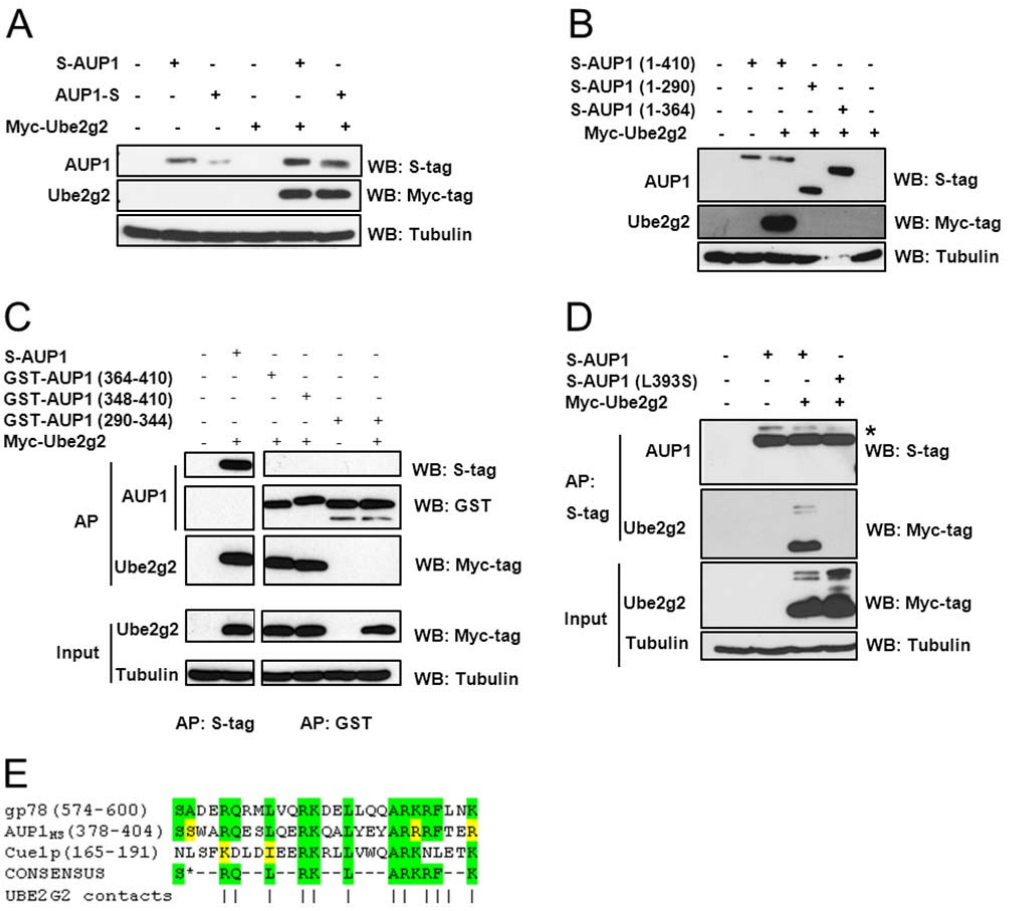


Figure 5.2.3: AUP1 binds Ube2g2 through its C-terminal G2BR domain. (A) Co-expression of S-tagged AUP1 and Ube2g2-myc in HEK293 cells. Affinity purified cell lysates were analysed by western blot, probed for AUP1 (anti S-tag) and binding to Ube2g2 (anti-myc). **(B)** The C-terminal region in AUP1 mediates Ube2g2-binding. Ube2g2 and AUP1 constructs (1-290 and 1-364) were co-transfected and cell lysates were analysed by western blotting. **(C)** Co-transfection of Ube2g2 with AUP1 constructs spanning the C-terminus (348-410 or 364-410) or amino acids 290-344 and interaction is assayed by western blot. **(D)** Co-transfection of S-AUP1 L393S and Ube2g2-myc in HEK293 cells is analysed by western blot. * Additional S-tag reactive band. **(E)** Alignment of the G2BR in gp78 and the AUP1 C-terminus.

5.2.4 The C-terminal G2BR domain is essential for Ube2g2 binding

Above we have identified a region within the C-terminus of AUP1 as necessary to bind Ube2g2. To further characterise the AUP1-Ube2g2 interaction, GST-fusions with C-terminal AUP1 fragments were co-expressed with Ube2g2-myc and demonstrated that AUP1 aa 364-410 were sufficient to

bind Ube2g2 (Fig. 5.2.3C). Sequence alignment of this region exhibited high homology to a region in the mammalian ubiquitin ligase gp78 (aa 574-600, Fig. 5.2.3E). Ube2g2 is the cognate E2 for gp78 and binds directly to it via a C-terminal domain referred to as the G2BR (Ube2g2 binding region) (Das et al., 2009). Comparing the G2BR in gp78 with AUP1 indicated that residues essential for binding to Ube2g2 are conserved in AUP1 (Fig. 5.2.3E). This strongly suggests that similar G2BR-domains in the C-terminus of AUP1 and gp78 bind to Ube2g2 by comparable means. Mutating two key Leu residues in the gp78 G2BR abolished binding to Ube2g2 (Das et al., 2009) and as expected, similar mutations in the G2BR of AUP1 (L393S) had the same effect (Fig. 5.2.3D). Similar findings have been reported recently by another group (Spandl et al., 2010).

5.2.5 The CUE domain of AUP1 is monoubiquitinated

During the course of our study, we observed an additional AUP1 immunoreactive band by western blot (Fig. 5.2.3D, asterisk). This band was detected only when NEM (N-ethylmaleimide) was present in the cell-lysis buffer (Fig. 5.2.4A). NEM is an alkene that forms thioester bonds with cysteine residues and is commonly used to prevent intermolecular disulphide bond formation and inhibit cysteine proteases (e.g. DUBs) during cell lysis. The additional band migrated more slowly and was less intense when compared to unmodified AUP1. The AUP1 form was detected after transient expression of S-AUP1 in HEK293 cells either with or without co-expression of Ube2g2-myc (Fig. 5.2.3D), but could not be distinguished from the primary AUP1 band in HEK293 cell lysate (Fig. 5.2.4B).

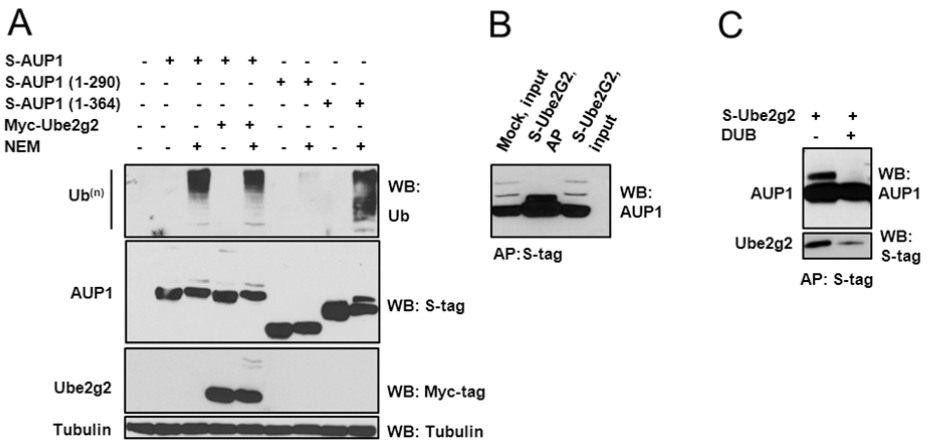


Figure 5.2.4: AUP1 is directly monoubiquitinated. (A) HEK293 cells were co-transfected with full length AUP1 or AUP1 truncations and Ube2g2-myc in HEK293 cells, lysed in 1% TritonX-100 buffer containing +/- NEM and samples were analysed by western blot. **(B)** Ube2g2 binds unmodified and modified AUP1. HEK293 cells were transfected with S-Ube2g2 and interaction with endogenous AUP1 was determined by western blot. **(C)** S-Ube2g2 pull down sample was treated with the DUB Usp2cc after affinity purification.

To determine if Ube2g2 is able to interact with both forms of AUP1, S-Ube2g2 was transiently expressed in HEK293 cells, affinity purified and western blot probed for endogenous AUP1. Bands corresponding to both modified and unmodified AUP1 were detected indicating that the appearance of the modified AUP1 form was not an artefact of transient expression (Fig. 5.2.4B). Given that the size difference between the two AUP1 bands was ~ 5-10 kDa, we suspected AUP1 may be monoubiquitinated, as this difference corresponds roughly to the molecular mass of a single ubiquitin molecule (7 kDa). To test this, S-tagged Ube2g2 was transiently expressed in HEK293 cells and complexes were affinity purified by S-protein agarose. Half of the bead-bound complexes were treated with the de-ubiquitinating (DUB) enzyme Usp2cc following affinity purification. The disappearance of the upper, AUP1 immunoreactive band with Usp2cc treatment confirms our hypothesis that

AUP1 also exists in a monoubiquitinated form (Fig. 5.2.4C), albeit in a small fraction of the total AUP1 population.

To determine the site of AUP1 monoubiquitination, we designed truncation constructs lacking the G2BR domain and/or the CUE domain (Fig. 5.1.1C). The CUE domain of AUP1 is a good candidate as these domains are often associated with monoubiquitin binding and intramolecular monoubiquitination (Shih et al., 2003). Only AUP1 lacking the CUE domain migrated as a single band, indicating that monoubiquitination occurs in the region between aa 290-364 (Fig. 5.2.5A). There are ten Lys in AUP1 but only four within this region (K305, K322, K347, K359). A peptide containing K359 of AUP1 was detected in an unbiased, affinity capture-mass spectrometry assay designed to isolate ubiquitin isopeptides (Kim et al., 2011). While unable to differentiate between a mono- or polyubiquitin modification, this analysis implicates K359 as a strong contender for the modified lysine.

5.2.6 AUP1 binds polyubiquitinated proteins

Western blots of full length AUP1 pull-downs probed for ubiquitin exhibited high molecular weight smears, a hallmark of polyubiquitination (Fig. 5.2.5A). To distinguish whether AUP1 itself is polyubiquitinated or rather binds polyubiquitinated proteins, HEK293 cells transfected with AUP1 were solubilised initially in 1% TritonX-100. Lysates were subsequently denatured by addition of SDS to a final concentration of 1%, SDS was subsequently diluted out with 4% TritonX-100, affinity purified and probed for ubiquitin as before. SDS-treated lysates lost their polyubiquitin immunoreactivity compared to the non-SDS treated controls, indicating that AUP1 itself is not covalently

polyubiquitinated but rather binds polyubiquitinated proteins (Fig. 5.2.5B). Without the CUE domain the polyubiquitin signal is lost (Fig. 5.2.5A), indicating that AUP1 requires this domain to bind polyubiquitinated proteins. Whether direct monoubiquitination of AUP1 controls the ability to bind polyubiquitin is not clear, but mutagenesis of AUP1's acceptor Lys residues may shed some light on that question.

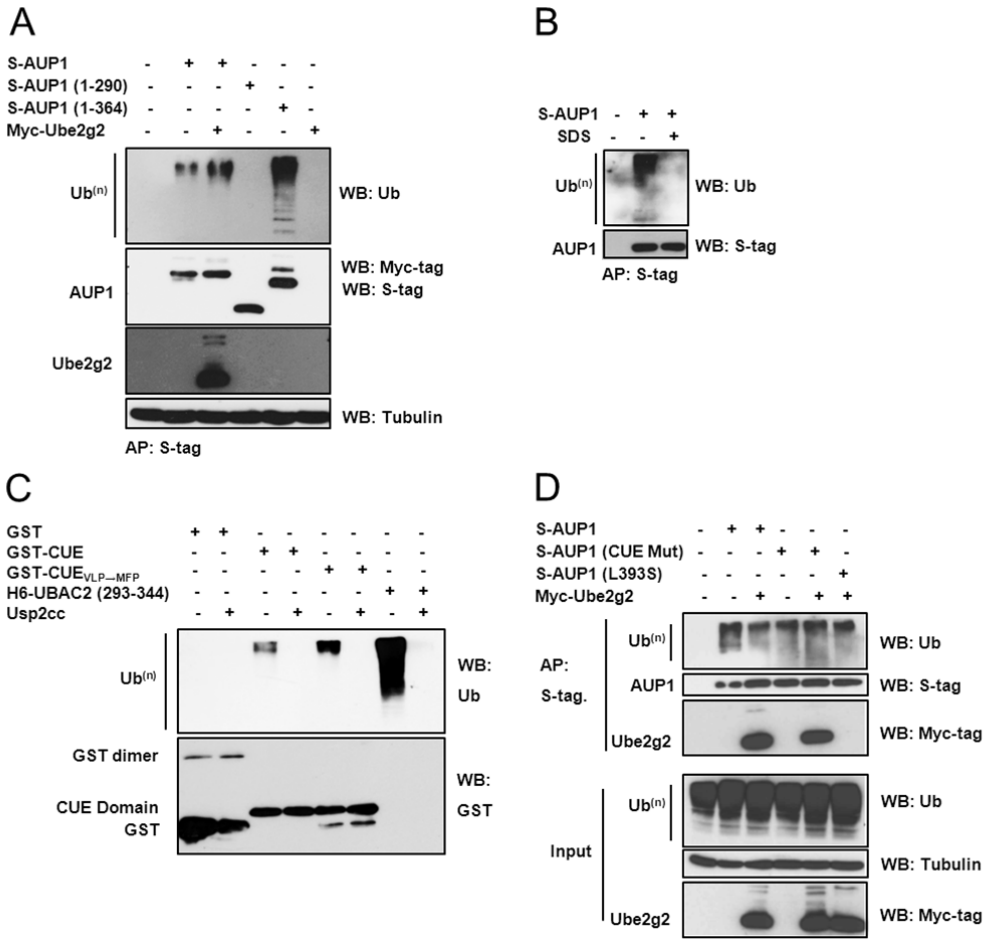


Figure 5.2.5: AUP1 mono- and polyubiquitination require presence of the CUE domain. (A) HEK293 cells transfected with either full length AUP1, $AUP1_{1-290}$ or $AUP1_{1-364}$ were analysed by western blot for ubiquitin. **(B)** HEK293 cell lysate containing S-AUP1 were treated with 1% SDS in lysis buffer. Polyubiquitin is detected by western blot analysis. **(C)** Recombinant GST-$AUP1_{WT}$ and GST-$AUP1_{VLP→MFP}$ were incubated with HEK293 cell lysate and western blots probed with anti-ubiquitin. The UBA domain from Ubac2 (His_6-UBAC2 (293-344)) is used as a positive control for ubiquitin binding. The ubiquitin signal is validated by treatment with the DUB Usp2cc. **(D)** WT AUP1 as well as the CUE domain and G2BR domain mutants are transfected in HEK293 cells. Lysates were affinity purified and tested for ubiquitin by western blot.

Interestingly, we observed a stronger polyubiquitin signal for the $AUP1_{\Delta G2BR}$ (Fig. 5.2.5A), suggesting that either the G2BR impairs binding of polyubiquitinated substrates or Ube2g2 binding facilitates release/transfer of polyubiquitinated proteins. If Ube2g2 recruitment was essential for polyubiquitin binding, the $AUP1_{L393S}$ mutant, deficient in Ube2g2 binding, should behave similarly. However, the polyubiquitin smear for the L393S mutant was comparable to that of WT AUP1 (Fig. 5.2.5D), suggesting that the G2BR domain itself is reducing interactions with polyubiquitinated substrates.

5.2.7 The AUP1 CUE domain does not contain a conserved motif for efficient ubiquitin binding

CUE domains of different yeast proteins bind ubiquitin with varying affinity (Shih et al., 2003). It is the tripeptide MFP at the end of the first α-helix of the CUE domain that determines the affinity (Kang et al., 2003). This motif is highly conserved across CUE domains of different species (Kang et al., 2003), but not in AUP1, which contains the tripeptide VLP instead of MFP. If weak binding of polyubiquitin by AUP1 was important for ERAD processing, we reasoned that increasing the CUE domain's affinity for ubiquitin by mutating VLP to MFP might act as dominant negative. Specifically, by increasing the dwell time of ubiquitinated substrates with AUP1, the ERAD process may be slowed, leading to an overall increase in steady-state substrate levels. To obtain a putative dominant negative AUP1 for functional studies, we first evaluated CUE domain mutations on the AUP1-ubiquitin interaction. We evaluated the ability of CUE_{VLP} and CUE_{MFP} to bind polyubiquitin *in vitro* (Fig. 5.2.5C). Recombinantly expressed GST-fusion proteins of each domain were purified on glutathione beads and then incubated with HEK293 cell lysate treated with MG-132.

Qualitatively, the amount of polyubiquitin brought down by CUE_{MFP} was greater than that of the WT (CUE_{VLP}) domain (Fig. 5.2.5C). Treatment with Usp2cc abolished ubiquitin immunoreactivity, confirming that the smears were polyubiquitin chains and not aggregated proteins. However, expression of either full length $AUP1_{WT}$ or $AUP1_{CUE\text{-}MFP}$ *in vivo* did not produce a marked difference in the intensity of polyubiquitin smears (Fig. 5.2.5D). Although not quantitative, these preliminary results suggest that either structural differences between the isolated domain and full length protein alter ubiquitin binding, or that ERAD-related DUB-activity present *in vivo* may be working counterproductively to limit ubiquitin chain formation recognised by AUP1. Alternatively, recruitment to the Hrd1-SEL1L complex may sterically hinder AUP1's ability to bind ubiquitin. Clearly further studies are needed to resolve the importance of ubiquitin binding by the CUE domain for AUP1 function.

5.3 Discussion

Proteins inserted into the ER for maturation are degraded by ERAD if they fail to achieve a correct conformation. Membrane-embedded ubiquitin ligase complexes like Hrd1-SEL1L play a central role in this process by ubiquitinating misfolded substrates during their retrotranslocation into the cytosol thus targeting them for degradation. Work from our lab and others identified AUP1 as an interactor of both Hrd1 and SEL1L (Christianson et al., 2012; Mueller et al., 2008). Our data suggest that AUP1 adopts a hairpin-like topology in the ER membrane. This finding was confirmed by the work of another group during the course of this study (Spandl et al., 2010). Moreover, it has recently been established that a PVG motif within the N-terminal hydrophobic stretch determines AUP1's hairpin-like topology and is sufficient to confer its

localisation to the ER and to lipid droplets (Stevanovic and Thiele, 2013). The role of AUP1 in lipid droplets has recently been further defined, suggesting that AUP1 may promote lipid droplet formation and clustering, the latter dependent on monoubiquitinated AUP1 (Klemm et al., 2011; Lohmann et al., 2013) .

Given the hairpin-like topology of AUP1, it is not clear how or with what stoichiometry AUP1 fits in the Hrd1-SEL1L complex. SEL1L is a type I transmembrane protein with a large lumenal domain. As the majority of AUP1 is facing the cytosol, our model speculates that interaction with SEL1L occurs between the TMDs of the two proteins. Hrd1 has five TMDs and a C-terminal cytosolic (cyto) RING domain, making interaction with AUP1 likely mediated through the TM or cyto domain of AUP1. AUP1 remained associated to Hrd1 with SEL1L knockdown and vice versa (Christianson et al., 2012), which may reflect simultaneous contact to both components. Alternatively, binding could occur through the aid of another ERAD-related protein (e.g. Derlin-1, Ube2j1) or an as yet unidentified protein. Future studies will determine whether this is the case.

Although AUP1 is highly conserved across species and ubiquitously expressed in tissues, its function in cells remains undetermined. To elucidate the role of AUP1 in ERAD, tandem LC-mass spectrometry experiments were carried out. Ube2g2, a cognate E2 of the gp78 ubiquitin ligase complex, was identified as an interaction partner of AUP1 (Christianson et al., 2012). This finding suggests that Ube2g2 is able to function with multiple E3s in the ERAD pathway (i.e. gp78, Hrd1-SEL1L). Furthermore, it provides an explanation of how the cytosolic Ube2g2 can be recruited to the ER membrane-embedded Hrd1-SEL1L complex. This interaction could be recapitulated by transient co-

expression of S-AUP1 and Ube2g2-myc. The C-terminus of AUP1 mediates binding to Ube2g2 via a domain with high homology to the G2BR domain of gp78. Similar results were published by two other groups during the course of this study, confirming our data (Klemm et al., 2011; Spandl et al., 2010). Disrupting key residues in this domain (L393S) abolished Ube2g2 binding and suggested that $AUP1_{L393S}$ may impair ERAD in functional assays.

Ube2g2 binds selectively to a domain within the ERAD E3 gp78 (Chen et al., 2006; Fang et al., 2001) known as the G2BR (Ube2g2 binding region) and can also function with Hrd1 *in vitro* (Kikkert et al., 2004). As Hrd1 is lacking a G2BR, Ube2g2 binding to AUP1 represents a promising means to recruit this E2 to the Hrd1 complex. In yeast, the Hrd1 and gp78 homologue Hrd1p interacts with Ubc7p (the Ube2g2 orthologue) via the membrane-associated adaptor protein Cue1p, which recruits Ubc7p to the ER membrane (Biederer et al., 1997). Cue1p can also stimulate Ubc7p activity *in vitro* and *in vivo*. When Ubc7 levels exceed that of Cue1p, Ubc7p is degraded (Ravid and Hochstrasser, 2007). Cue1p-bound Ubc7p exhibits enhanced *in vitro* ubiquitination activity and degradation of the ERAD substrate Hmg2p-GFP (Bazirgan and Hampton, 2008). Whilst the CUE domain and TMD of Cue1p are dispensable for ERAD, the C-terminal U7BR domain, mediating interaction with Ubc7p, is both necessary and sufficient for *in vitro* polyubiquitination and *in vivo* ERAD (Kostova et al., 2009). A very recent study resolved the crystal structure of Ubc7p-bound U7BR (Metzger et al., 2013). U7BR binds on the site of Ubc7p opposite of its catalytically active site and ubiquitin-binding region (Metzger et al., 2013). Mutations in U7BR disrupting interaction with Ubc7p stabilised ERAD substrates, indicating that the Ubc7p-Cue1p interaction is crucial for their

degradation. Furthermore, binding of U7BR activates Ubc7 by increasing its affinity for RING domains and ubiquitin. Although AUP1 shares little sequence homology with Cue1p and the structures of U7BR and G2BR are disparate, they appear to function similarly to recruit cytosolic proteins to the ER membrane.

Covalent modification by ubiquitin can alter the localisation, function or interactions of the protein to which it is attached. In *Saccharomyces cerevisiae* many plasma membrane proteins require monoubiquitination of their cytosolic domain to be internalised into the endocytic pathway [reviewed in (Hicke, 1999; Rotin et al., 2000)]. We demonstrated that AUP1 is monoubiquitinated and as AUP1 was reported to be associated with the membranes of the ER and lipid droplets, monoubiquitination may play a role in the control of AUP1 partitioning. Monoubiquitination can also alter protein activity. Monoubiquitinated histone H2B is important for meiosis in *S. cerevisiae* as yeast with a mutant H2B that lacks its ubiquitination site do not sporulate (Hicke, 2001).

Similar to our data, a report was published during the course of this study demonstrating a dependence of the CUE domain on AUP1 monoubiquitination and binding of polyubiquitinated substrates, which was impaired by the G2BR (Klemm et al., 2011). Furthermore, this work reported a dependence of the AUP1 interaction with components of the Hrd1 complex and ERAD substrates on its CUE domain, which may suggest that AUP1 is only incorporated into the Hrd1 complex upon substrate binding. It has recently been established that none of the ten Lys residues in AUP1 is solely mediating monoubiquitination, but that replacing them altogether abolished AUP1 modification; this suggests

that AUP1 is monoubiquitinated independently on different Lys residues (Lohmann et al., 2013).

Future experiments will address whether the loss of monoubiquitination abolishes AUP1's ability to bind polyubiquitinated proteins. If this is not the case, this may indicate that monoubiquitination is not required for binding to polyubiquitinated proteins but that the CUE domain provides an appropriate surface for such an interaction. If monoubiquitination is a prerequisite for AUP1 function, this modification may be affected by ER stress. ER stress activates the UPR leading to upregulated expression of both chaperone and ERAD genes. By treating HEK293 cells with ER stress-inducing agents such as tunicamycin and thapsigargin, we can assess whether monoubiquitination of AUP1 is enhanced/diminished compared to untreated cells.

Most CUE domains that bind ubiquitin with high affinity contain an MFP tripeptide motif at the end of the first α-helix, but this motif is absent in AUP1 and its functional homologue Cue1p. High affinity binding to ubiquitin may not necessarily be desirable for ERAD, as efficient degradation requires rapid ubiquitin transfer to substrates, and rapid substrate transfer from the ER environment to VCP/p97 and then to the proteasome. By generating a mutant AUP1 with a high affinity motif ($AUP1_{VLP \rightarrow MFP}$), we had hoped to create a gain of function AUP1 mutant for biochemical and functional studies. $AUP1_{VLP \rightarrow MFP}$ did exhibit a slight increase in co-precipitated polyubiquitinated proteins *in vitro*, a finding that could not be repeated with full length AUP1 expressed in mammalian cells. Unfortunately, these preliminary studies have not determined quantitatively whether $AUP1_{VLP \rightarrow MFP}$ has increased ubiquitin-binding affinity. Despite the absence of the MFP motif in yeast Cue1p, it has recently been

shown that the Cue1p CUE domain efficiently promotes formation of K48-linked ubiquitin chains, which increases activity of Hrd1p and Doa10p, emphasising the importance of the CUE domain in ubiquitin-mediated processes (Bagola et al., 2013).

A future aim of our research is to identify ERAD substrates that are dependent on AUP1. Our previous work identified a subset of ERAD model substrates that require AUP1 for degradation, including the integral membrane proteins GluR1 (a subunit of the AMPA-type glutamate receptor) and CFTRΔF508 (Christianson et al., 2012). Conversely, degradation of a soluble non-glycosylated model ERAD substrate (i.e. the transthyretin mutant, TTR_{D18G}) was not impaired. If AUP1 participates in a complex that preferentially facilitates degradation of integral membrane proteins, this may indicate that AUP1 may be discriminating between the topologies of substrates being processed by the Hrd1-SEL1L complex.

Chapter VI: Discussion

The aim of the work presented in this thesis is to characterise functional interactions in the HMG-CoA reductase degradation 1 (Hrd1) ubiquitin ligase complex involved in ERAD and is based on the recent discovery of novel Hrd1 interaction partners (Christianson et al., 2012). This study provides evidence that: 1) the stability of FAM8A1 is regulated by Hrd1 through interaction of specific domains and that this interaction is crucial for degradation of a lumenal ERAD model substrate (chapter III), 2) lumenal suppressor enhancer lin12/Notch 1 like (SEL1L) interacts with Hrd1 through a hydrophobic segment that may represent a putative transmembrane domain (TMD) (chapter IV), and that 3) AUP1 recruits the E2 Ube2g2 to the Hrd1 ligase complex through its G2BR domain and interacts with polyubiquitinated proteins in a CUE domain dependent manner (chapter V). I will discuss below how the results of this work fit in with our current understanding of the ERAD mechanism.

6.1 Degradation of misfolded proteins from the ER

Protein biosynthesis is a process essential for sustaining viability of all cells within an organism. For eukaryotes, maturation of proteins within the secretory pathway is a particular error-prone process because aspects associated with nascent chain biosynthesis such as targeting to the ER, insertion of TM domains in the lipid bilayer, post-translational modifications (e.g. disulphide bond formation, N-linked glycosylation) and assembly into oligomeric complexes, are difficult to coordinate with absolute fidelity and can easily lead to misfolding and potentially aggregation. To prevent aggregation-prone, terminally misfolded secretory pathway proteins from accumulating, the ERAD

surveillance mechanism has evolved to ensure degradation of these potentially cytotoxic intermediates. In principle, a misfolded protein, a candidate for ERAD, has a lesion that is recognised by factors either in the ER lumen, within the bilayer or possibly in the cytoplasm (for integral membrane proteins). Subsequently, removal of that substrate from the ER environment occurs via a dislocation (membrane protein) or retrotranslocation (lumenal protein) event, permitting exposure to the cytosol, ubiquitination by proximal RING domain ubiquitin ligases (embedded in the ER membrane) and ultimately degradation through the 26S proteasome.

The most widely studied ubiquitin ligase involved in ERAD is Hrd1, which promotes substrate degradation by recruiting accessory factors mediating the consecutive steps of this pathway. Many studies in both yeast and mammals have provided insight into the function of single ERAD factors, yet whether distinct Hrd1 complexes form in response to a specific type of substrate or rather factors mediating turnover of lumenal and membrane proteins centre around Hrd1 simultaneously, remains poorly understood. This work therefore aims at adding to the knowledge about functional interactions within the Hrd1 complex with the long term objective of understanding the dynamics of the ERAD network.

The ERAD mechanism operates as a series of interlinked activities that work to deliver misfolded proteins from the ER lumen (or membrane) to cytosolic proteasomes for degradation. Misfolded proteins are detected by the tandem actions of ER lectins (e.g. OS-9, XTP3-B) and chaperones (e.g. BiP, Grp94), which engage and target the client protein to the ER membrane through interaction with Hrd3p/SEL1L. Hrd3p/SEL1L is part of a complex that includes

the membrane embedded ubiquitin ligase Hrd1, mediating the subsequent retro-/dislocation and ubiquitination of misfolded proteins, resulting in proteasomal degradation [reviewed in (Vembar and Brodsky, 2008)]. The bulk of the SEL1L protein resides in the ER lumen and has been presumed to be tethered to the ER membrane through a single TMD near its C-terminus. The region spanned by the multiple Sel1 repeats within SEL1L is believed to act as a scaffold for substrate recognition factors such as: EDEM1 (Cormier et al., 2009; Marin et al., 2012), EDEM2 (Mast et al., 2005; Olivari et al., 2005), EDEM3 (Hirao et al., 2006; Sato et al., 2012), the ERFAD-ERp90/TXD16 complex (Riemer et al., 2009) as well as the ER-resident lectins OS-9 and XTP3-B (Bernasconi et al., 2010; Christianson et al., 2008; Hosokawa et al., 2009a; Hosokawa et al., 2008).

$SEL1L_{1-372}$ is dispensable for interaction with OS-9 but there is some disagreement as to the necessity of the SEL1L glycans for this binding (Christianson et al., 2008; Hosokawa et al., 2009a). The interaction between XTP3-B and SEL1L is glycan dependent, as mutations in the XTP3-B MRH domains abrogate binding to SEL1L (Christianson et al., 2008). These factors engage lumenal substrates and bring them in closer proximity to membrane-embedded components of the Hrd1 complex for ERAD. SEL1L also appears to be required for degradation of some glycosylated membrane proteins (Horimoto et al., 2013; Tyler et al., 2012) but not all (Christianson et al., 2012), indicating that both glycosylation state and topology are considerations for involving SEL1L in ERAD.

6.2 The SEL1L HID is crucial for interaction with Hrd1 and potentially determines SEL1L topology

The common presence of TMDs in both Hrd1p/Hrd1 and Hrd3p/SEL1L suggests that their interaction occurs though contact points within the lipid bilayer. The Hrd1-SEL1L interaction in mammals appears extremely labile upon solubilisation in non-ionic detergents (e.g. TritonX-100) (Christianson et al., 2012; Christianson et al., 2008), indicating that intact membranes are necessary to support their interaction. This observation is unique to the mammalian Hrd1-SEL1L interaction, as yeast Hrd1p-Hrd3p remains stable under similar conditions (Gardner et al., 2000). But while the Hrd1p/Hrd1 TMDs are sufficient to co-precipitate Hrd3p in yeast (Gardner et al., 2000), the predicted TMD of both Hrd3p and SEL1L (Bernasconi et al., 2012; Christianson et al., 2008; Gardner et al., 2000) are dispensable for their respective interactions with Hrd1p/Hrd1. Fusing the last 372 aa of SEL1L to a single-chain antibody or ligand was able to target the interaction protein for degradation (Vecchi et al., 2012), indicating that this SEL1L region contains all necessary domains to promote ERAD, most likely through a Hrd1-dependent process.

We have presented data demonstrating that $SEL1L_{701-721}$, rather than the expected TMD ($SEL1L_{738-759}$), is actually the region responsible for tethering SEL1L to Hrd1 (Fig. 4.2.2B) and have designated this segment as the HID (Hrd1-interaction domain). TMD algorithms (e.g. THMMM, TOPCONS) fail to predict this segment as a TMD but closer inspection revealed that this segment is highly conserved across species, contains a high density of hydrophobic residues and has the appropriate length for a potential TMD (Fig. 4.2.4). The possibility of a second TMD then raises issues of how SEL1L topology may be

affected and how that may impact interactions and functionality. These aspects are discussed below.

Truncated versions of SEL1L (1-737) retaining the HID but lacking the predicted TMD remain capable of interacting with Hrd1. Mutating the highly conserved charged residue K711L within the HID did not abrogate Hrd1 co-precipitation (Fig. 4.2.5A), indicating that a stable interaction was not likely to be dependent upon pairing with a negatively charged residue within Hrd1. Charged residues within hydrophobic domains have been identified as degradation signals or “degrons” in ERAD. Two basic residues in the TMD of unassembled TCRα (R154, K159) are necessary for degradation of this TCR subunit (Bonifacino et al., 1991; Bonifacino et al., 1990), and are able to act as a degron when fused to the stable type I TM protein haemagglutinin (Fayadat and Kopito, 2003) or the polytopic membrane protein opsin (Ray-Sinha et al., 2009). However, a recent report suggests that these two basic residues promote ERAD by maintaining a monomeric state of the TCR subunit (Soetandyo et al., 2010), rather than by acting as a degradation signal. Furthermore, the negatively charged Glu17 in the TM domain of the viral protein VP2 is an important mediator of simian virus (SV) 40 infection, where Glu17 represents a degradation signal to promote dislocation into the cytosol by ERAD factors, potentially through charge-pairing with BAP31 (Geiger et al., 2011). It is therefore a possibility that K711 of SEL1L acts as internal degradation signal, or alternatively, is necessary for interaction with a protein other than Hrd1.

Conversely, the P704L mutation within the HID abolished binding to Hrd1 (Fig. 4.2.5A). As Pro residues often serve as helix-breakers, this mutation may have altered a kinked conformation within the HID necessary for Hrd1

interaction. Similarly, mutating two highly conserved Leu residues (L709G/L712G, Fig. 4.2.4C) disrupted Hrd1 co-precipitation (Fig. 4.2.5A) and suggested that the overall hydrophobicity of the HID may be important for maintaining contact with Hrd1.

Even though the K711L mutant was able to bind Hrd1, its ectopic expression impaired degradation of the SEL1L dependent, lumenal ERAD substrate transthyretin mutant TTR_{D18G} (Fig. 4.2.5B). Similar results were observed for L709G/L712G and P704L. The reasons for this are not yet clear, but one possible explanation may be that substrate processing relies on a specific but transient interaction of SEL1L with Hrd1 within the membrane. Under this hypothesis, the weak hydrophobicity of the SEL1L HID may allow it to exist either in the lumen or transiently integrated in the lipid bilayer. By altering hydrophobicity within the SEL1L HID, the transient interaction with Hrd1 is made more stable, which in turn impedes efficient processing of ERAD. Alternatively, the positive charge associated with K711 may be contacting another protein in the complex necessary for ERAD, such as Derlin-1 or Derlin-2. Many other components are present in the Hrd1 complex but the additional studies required to characterise the nature of the SEL1L HID interaction are beyond the scope of this work.

To determine whether the SEL1L HID alone was sufficient for the Hrd1 interaction, we constructed and ectopically expressed a GFP-HID fusion in HEK293 cells. But rather than co-precipitating Hrd1, the HID bound instead to SEL1L, Derlin-2 and, to a lesser extent, Derlin-1 (Fig. 4.2.6). So while necessary, the HID clearly requires additional contributions from a portion of SEL1L between the N-terminus and the HID as $SEL1L_{1-718}$ binds Hrd1 at levels

comparable to $SEL1L_{WT}$ (Fig. 4.2.2B). Contrary to the current organisational model, this could also indicate that SEL1L does not interact with Hrd1 directly but rather makes contact with Derlin-2 (or Derlin-1) instead. Since digitonin preserves these complexes, this possibility cannot be ruled out without experiments knocking down either of these two factors. However, data published so far does not support this hypothesis, as silencing of neither Der1p nor Derlin-2 abrogates the interaction between Hrd1 and Hrd3p/SEL1L (Gauss et al., 2006; Horn et al., 2009; Huang et al., 2013). Our data also indicate that the HID is sufficient to support SEL1L homo-oligomerisation, similar to the observation made for the TMD of Hrd3p (Horn et al., 2009). One caveat to this interpretation would be if the GFP-HID fusion was an ERAD substrate and did not integrate into the Hrd1 complex as a bona fide component. Assaying degradation kinetics of each construct would need to be performed in order for this to be ascertained, but this has yet to be completed.

Members of the Derlin family of rhomboid-like proteins are candidates for the still elusive retrotranslocation channel (Lilley and Ploegh, 2004, 2005; Ye et al., 2004). Derlin-1 and -2 are established interaction partners of SEL1L (Lilley and Ploegh, 2005) and, like Hrd1, they are polytopic membrane proteins with an extended C-terminal region in the cytosol. We observed that higher levels of Derlin-2 were co-precipitated by the HID compared to Derlin-1, an observation also seen for $SEL1L_{FL}$ (Lilley and Ploegh, 2005). It must be noted though that Derlin-2 levels in the lysate were higher compared to Derlin-1 levels. Derlin-2 interacts with many components in the Hrd1 complex including; Hrd1, Ube2j1, OS-9, VIMP, VCP/p97 and Derlin-1 (Iida et al., 2011; Lilley and Ploegh, 2005; Oda et al., 2006). Derlin-2 plays a key role in degradation of substrates such as

NHK (Oda et al., 2006) and is necessary for efficient infection with murine polyomavirus, likely through retrotranslocation of virus particle from the ER into the cytosol (Lilley et al., 2006). Our evidence that Derlin-2 and Hrd1 are both able to interact with SEL1L through the HID could reflect a situation where Derlin-2 bound SEL1L adopts a conformation that promotes a transfer and subsequent binding to Hrd1. Clearly, further experiments that explore the stoichiometry of multimeric complexes that form between the factors are required to determine whether this is the case.

The Hrd3p/SEL1L-Hrd1 interaction occurs in a 1:1 stoichiometric ratio (Gardner et al., 2000; Lilley and Ploegh, 2005), but the amount of SEL1L in cells is in average 5-7 fold higher than the levels of Hrd1 (Kislinger et al., 2006). Why this imbalance exists is not clear but could be due to SEL1L moonlighting in functions unrelated to ERAD or more likely, it could be the consequence of an intricate adaptation to build on-demand degradation capacity into the ER (Bernasconi et al., 2012). It had been noted that OS-9 and EDEM1, ERAD factors involved in identification and processing of glycosylated ERAD substrates, have a shorter half-life compared to other ERAD components and are constitutively degraded by trafficking to the lysosome in LC3-I-coated vesicles (EDEMosomes) (Bernasconi et al., 2012; Cali et al., 2008; Le Fourn et al., 2009; Reggiori et al., 2010; Zuber et al., 2007).

An emerging concept to explain this observation is termed ERAD tuning, where ERAD factors are rapidly degraded under basal conditions because when folding-competent proteins are in abundance, these factors are superfluous. Upon accumulation of misfolded proteins however, these surplus factors are now engaged and become functionally incorporated into ERAD

complexes, allowing for a fast ER response without the need for transcriptional upregulation via the UPR [reviewed in (Bernasconi and Molinari, 2010)]. The cytosolic tail of SEL1L has been identified as a receptor for LC3-I, promoting the degradation of SEL1L-EDEM1 under basal conditions (Bernasconi et al., 2012). With expression of the lumenal ERAD substrate NHK, the levels of SEL1L-EDEM1 complexes are decreased, whilst the levels of SEL1L-Hrd1 complexes formed are increased. This suggests a model where EDEM1 and OS-9 dissociate from SEL1L to engage ERAD substrates, thereby promoting the interaction between SEL1L and Hrd1, which is absent from EDEMosomes. Consequently, fewer EDEMosomes are formed when misfolded proteins are expressed (Bernasconi et al., 2012). An explanation of how LC3-I distinguishes between EDEM- and Hrd1-bound SEL1L or under which conditions SEL1L is accessible to LC3-I may be mediated by different SEL1L topologies through the HID (Fig. 6.1). Interaction with EDEM1 and OS-9 may confer a lumenal locale for the HID, making the protein accessible for recognition by LC3-I. Interaction with Hrd1 may implement a conformational change and membrane-association or even integration of the HID. In this case, the protein conformation of the C-terminus of SEL1L would be altered and its interaction with LC3-I prevented.

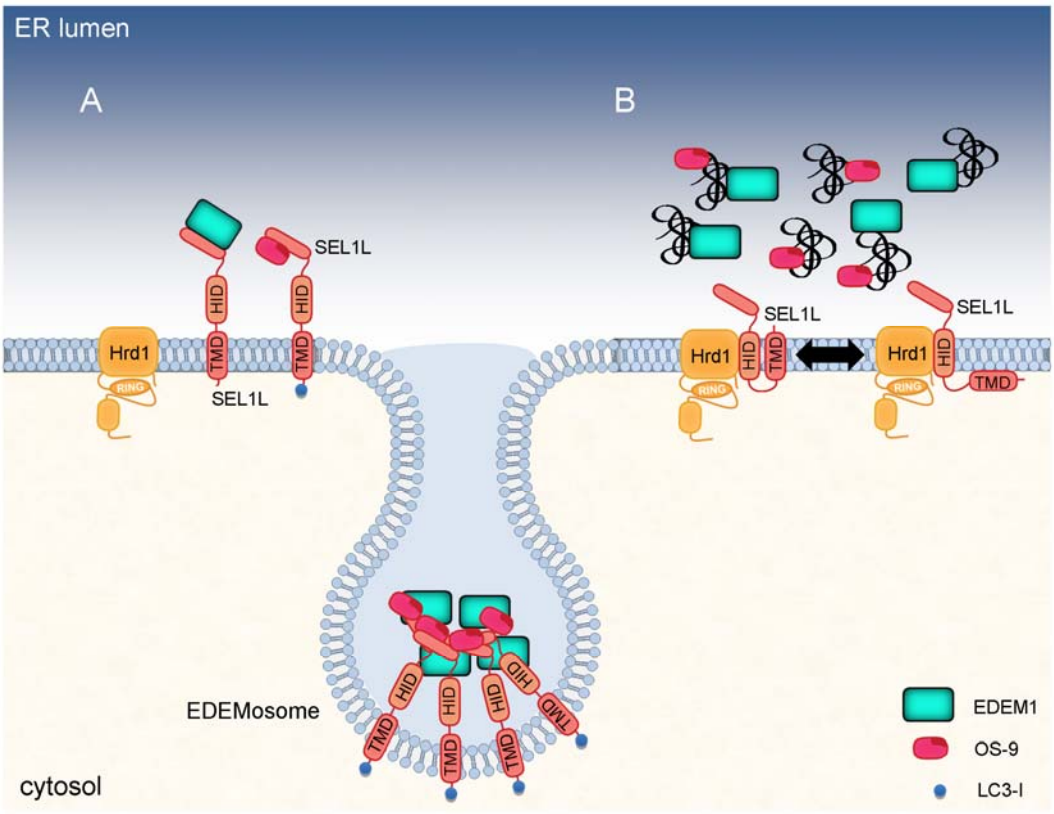


Fig. 6.1: Model of SEL1L topology. (A) Under basal conditions, the ERAD substrate recognition factors EDEM1 and OS-9 bind to SEL1L, which is inserted into the ER membrane through its TMD while the Hrd1 interacting domain (HID) resides in the ER lumen. This topology enables LC3-I to bind the C-terminus of SEL1L, followed by degradation of SEL1L, OS-9 and EDEM1 in EDEMosomes. **(B)** Upon accumulation of misfolded proteins, EDEM1 and OS-9 dissociate from SEL1L, which promotes interaction between Hrd1 and SEL1L in functional ERAD complexes. The Hrd1-SEL1L interaction occurs through the HID, resulting in a change of SEL1L topology; the TMD may be associated with the cytosolic site of or re-inserted into the ER membrane, making the SEL1L C-terminus inaccessible for LC3-I.

These data and our own results on the HID prompted a re-examination of the topology of SEL1L, specifically with respect to the C-terminus. $SEL1L_{short}$ constructs were designed to facilitate the readout of protease protection, glycosylation and membrane extraction assays. $SEL1L_{short}$ contains the terminal two Sel1-repeats (10 and 11) as well as one glycosylation site (N608). Like the GFP-HID fusion, $SEL1L_{short}$ failed to interact with Hrd1, even though glycosylation confirmed it was localised to the ER (Fig. 4.2.8). This argues that

a region of SEL1L before aa 600 also contributes to the binding of Hrd1. As mentioned earlier, the “degradins” contain the last 372 aa of the SEL1L C-terminus and are able to induce degradation of lumenal as well as membrane targets (Vecchi et al., 2012), indicating that a domain in $SEL1L_{422\text{-}600}$ may work in concert with HID for Hrd1 interaction and ERAD substrate degradation. The secondary structure provided by the multiple Sel1 domains may contribute to orientation of the HID or may simply be affecting stability of the protein. Indeed, steady-state expression levels of $SEL1L_{short}$ were weak and unaffected by the presence of Hrd1, suggesting that it may in fact become an ERAD substrate. However, when tested in the functional reporter assay, $SEL1L_{short}$ was able to impair TTR_{D18G} degradation (Fig. 4.2.9). This could mean that $SEL1L_{short}$ competes with TTR_{D18G} for ERAD components, saturates the capacity of the basal ERAD mechanism and retards degradation kinetics of TTR_{D18G}. Alternatively, $SEL1L_{short}$ may integrate into the ER membrane through its TMD and interact with ERAD factors other than Hrd1, resulting in competing these factors away from the ligase complex and therefore acting as a dominant negative.

By adding a glycosylation site at N725 of SEL1L we hoped to use oligosaccharide addition as an indicator of exposure to the ER lumen. $SEL1L_{short/R727T}$ could be glycosylated on both N608 and N725 only with about ~50% efficiency, independent of the presence of Hrd1 (Fig. 4.2.8). As glycosylation was not complete, this could indicate that 1) either SEL1L adopts different topologies (Fig. 4.2.7B) or simply that 2) the position of the second glycosylation site was not efficiently presented to the OST complex (Nilsson and von Heijne, 1993). Unfortunately, we could not differentiate whether singly

glycosylated forms of $SEL1L_{short/R727T}$ were modified only at N608 or N725. Although not interacting with Hrd1, $SEL1L_{short/R727T}$ had higher steady-state levels than $SEL1L_{short}$ (Fig. 4.2.8), indicating that this SEL1L mutant may not be recognised as a substrate by the ERAD machinery. Given that $SEL1L_{short}$ and $SEL1L_{short/R727T}$ do not share the Hrd1 binding exhibited by other SEL1L forms, the utility of these truncations to determine topology unfortunately is diminished. Preliminary data from membrane extraction assays under treatment with Na_2CO_3 or TritonX-100 using $SEL1L_{1-699}$ (containing neither HID not TMD), $SEL1L_{1-737}$ (containing HID) and $SEL1L_{FL}$ (containing both HID and TMD) indicate that SEL1L is at least membrane-associated (data not shown). If correct, it would point to a model where the position/orientation of the HID with respect to the membrane determines whether SEL1L is degraded in an LC3-dependent manner as part of an ER tuning mechanism (Bernasconi and Molinari, 2010) or whether SEL1L becomes integrated into functional ERAD complexes with Hrd1 (Fig. 6.1). Given the important position that SEL1L plays in ERAD, further characterisation of its orientation and integration into the Hrd1 complex is clearly warranted.

6.3 AUP1 bridges Ube2g2 with the Hrd1 complex

Once an ERAD substrate emerges at the cytosolic face of the ER, it is ubiquitinated by the consecutive action of three enzymes. In the first step, ubiquitin is activated through covalent linkage to a ubiquitin activating enzyme (E1), which subsequently transfers the ubiquitin moiety to a ubiquitin conjugating enzyme (E2). RING ubiquitin ligases, (E3s), bind ubiquitin-conjugated E2s and substrates, hence promoting substrate ubiquitination through bridging E2 and substrate [reviewed in (Pickart, 2001)]. The cognate

E2 of mammalian Hrd1 is Ube2j1 (Ubc6e), an orthologue of yeast Ubc6p (Arteaga et al., 2006; Burr et al., 2011; Lenk et al., 2002), while in yeast Hrd1p is less dependent on Ubc6p and commonly employs another E2, Ubc7p (Bays et al., 2001a). Ube2j1 plays a role in degradation of TCRα and $CFTR_{\Delta 508}$ (Lenk et al., 2002). In conjunction with Hrd1, Ube2j1 participates in turnover of cytosolic serum- and glucocorticoid-induced kinase 1 (Sgk1) (Arteaga et al., 2006), MHC class I heavy chains (Burr et al., 2011), GluR1 and TTR_{D18G} (Christianson et al., 2012). However, Ube2j1 does not appear to be the only E2 at work within the Hrd1 complex as our data revealed that Ube2g2 could also be associated through AUP1.

AUP1 is a conserved, metazoan protein whose role in ERAD came about when it was identified as interaction partner of both Hrd1 and SEL1L (Christianson et al., 2012; Mueller et al., 2008). Affinity purification-mass spectrometry analyses to identify interaction networks in ERAD resulted in the discovery that AUP1 bound Ube2g2 (Christianson et al., 2012), which was confirmed by overexpression studies [Fig. 5.2.3A, (Klemm et al., 2011; Spandl et al., 2010)]. AUP1 is predominantly associated with ERAD of membrane proteins: Ube2j1 (Claessen et al., 2010), MHC class I heavy chains (Klemm et al., 2011; Mueller et al., 2008), HMG-CoA reductase (Jo et al., 2011), $CFTR_{\Delta F508}$ and GluR1 (Christianson et al., 2012). While one study demonstrates AUP1-independent degradation of the lumenal ERAD substrates TTR_{D18G}, α-1 antitrypsin mutants NHK and NHK-QQQ (Christianson et al., 2012), another group reports stabilisation of NHK as well as a ribophorin I fragment (RI_{332}) after AUP1 silencing (Klemm et al., 2011). These contradictory results may be due to a different experimental setup; while one group

transiently expressed the indicated ERAD substrates (Klemm et al., 2011), the second group performed assays using cell lines stably expressing ERAD substrates (Christianson et al., 2012). Constitutive burden with certain substrates may promote formation of ERAD complexes that are distinct from those required for immediate clearance. In summary, these data point to a specialised role of AUP1 towards degradation of ERAD-M substrates.

Ube2g2 serves as the cognate E2 of the ERAD ubiquitin ligase gp78 by binding through a region designated as the G2BR (Das et al., 2009). While Hrd1 itself does not contain such a domain, a segment within the C-terminus of AUP1 exhibits a high degree of conservation with the G2BR of gp78 (Fig. 5.2.3E) and we could demonstrate that this C-terminal region of AUP1 is both necessary (Fig. 5.2.3B) and sufficient (Fig. 5.2.3C) for Ube2g2 interaction. Furthermore, mutating a conserved residue (L393S) that is crucial for the gp78-Ube2g2 interaction similarly abolished binding of Ube2g2 to AUP1 [Fig. 5.2.3D, (Jo et al., 2013)]. These data lead to a model where AUP1 functions to recruit Ube2g2 in a G2BR-dependent manner to the Hrd1 complex, reinforcing the notion that ERAD E2s do not act exclusively but are engaged by different ubiquitin ligases (Fig. 6.2).

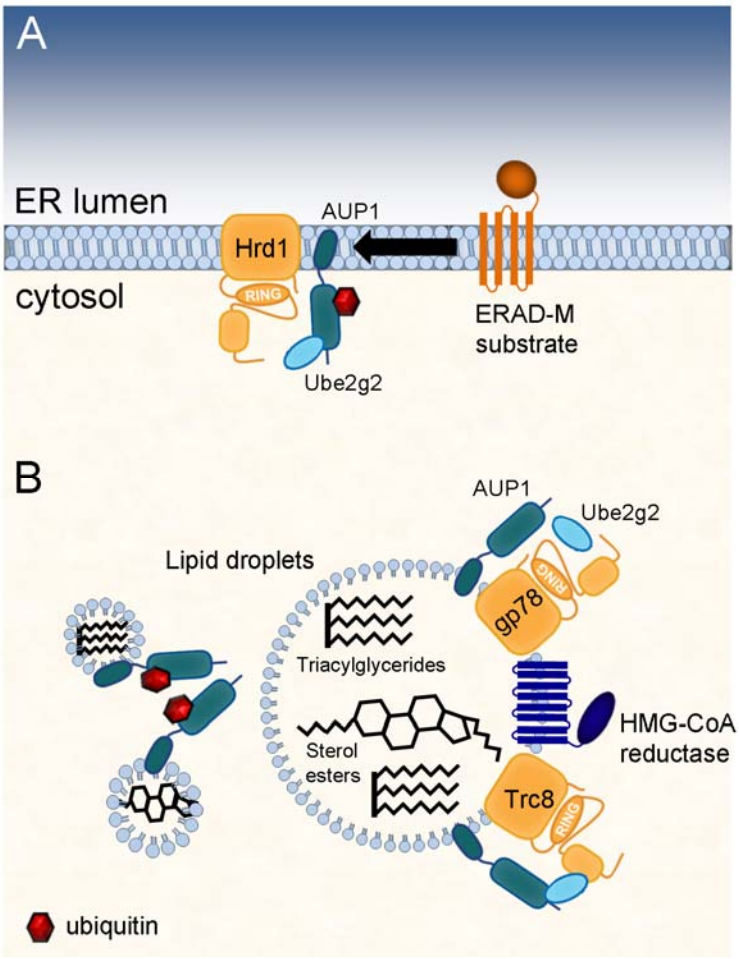


Fig. 6.2: AUP1 partakes in ERAD at the ER membrane and lipid droplets. (A) AUP1 interacts with Hrd1 in the ER membrane and targets the ubiquitin conjugating enzyme (E2) Ube2g2 to the Hrd1 complex, promoting degradation of ERAD-M substrates. **(B)** In addition, mono-ubiquitinated AUP1 promotes clustering of lipid droplets and AUP1 facilitates interaction between gp78 andTrc8 with Ube2g2 to degrade HMG-CoA in lipid droplets.

It remains to be determined though if Hrd1 interacts with both E2s simultaneously or if distinct complexes containing either Ube2j1 or Ube2g2 are formed. The RING ubiquitin ligase RNF8, involved in DNA damage response, assembles K48-linked chains through UBCH8 and K63-linked chains utilising UBC13. RNF8 interacts with its cognate E2s through different contact points, which would allow binding of both E2s at the same time (Lok et al., 2012). As Ube2g2 and Ube2j1 are recruited to the Hrd1 complex differently (via AUP1

and direct integration into the ER membrane, respectively), it is a possibility that Hrd1 forms a complex containing both E2s. Recruitment of different E2s may indicate that each of them mediates degradation of a distinct set of ERAD substrates. So far, when the effect of both Ube2g2 and Ube2j1 has been assessed on a certain substrate, functional redundancy has often been observed. Loss of either Ube2g2 or Ube2j1 results in impaired degradation of Sgk1 (Arteaga et al., 2006), Human Type 2 Iodothyronine Deiodinase (D2) (Kim et al., 2003) and TTR_{D18G} (Sato et al., 2012). Studies with contrary results have been published on the involvement of Ube2j1 in degradation of TCRα (Lenk et al., 2002; Tiwari and Weissman, 2001), indicating that some substrates may interact with a distinct E2 while others are promiscuous.

In addition to the G2BR, AUP1 contains a CUE domain (Fig. 5.1.1B). CUE domains are associated with high affinity binding of ubiquitin, which requires a conserved MFP motif (Kang et al., 2003; Shih et al., 2003). However, this motif is only absent from $AUP1_{CUE}$ and yeast Cue1p, the eponym of the CUE domain. Although they share very little sequence homology, AUP1 appears to be the functional homologue of Cue1p, which recruits the yeast homologue of Ube2g2, Ubc7p, to the Hrd1p/Hrd3p complex (Biederer et al., 1997). Despite the absence of the MFP motif, it has recently been demonstrated that the CUE domain of Cue1p can bind and stabilise K48-linked ubiquitin chains in order to assure efficient ERAD (Bagola et al., 2013).

Our data suggest that the CUE domain of AUP1 also binds polyubiquitinated proteins and at the same time, is itself monoubiquitinated (Fig. 5.2.4). Both modifications are CUE-domain dependent (Fig. 5.2.5A) and this domain has as well been described as necessary for encounter of AUP1 with ERAD factors

and substrates (Klemm et al., 2011). While mutating the CUE domain (VLP → MFP) did not lead to an increase in co-precipitated polyubiquitinated proteins that would reflect a higher affinity for ubiquitin (Fig. 5.2.5D), AUP1 truncations lacking the G2BR appeared to bind more polyubiquitinated proteins [Fig. 5.2.5A, (Klemm et al., 2011)], indicating that binding of Ube2g2 negatively regulates the interaction with polyubiquitinated proteins. However, the L393S mutant of AUP1 that is unable to bind Ube2g2, does not co-precipitate substantially more polyubiquitinated proteins when compared to $AUP1_{WT}$, thus indicating that it is the G2BR that impaired interactions between AUP1 and polyubiquitinated proteins (Fig. 5.2.5D). The G2BR induces a conformational change in Ube2g2, which increases the affinity for the RING domain (Das et al., 2013). Similarly, the G2BR may alter the conformation of $AUP1_{CUE}$ to destabilise the interaction with polyubiquitinated proteins, in order to allow rapid flux through the ERAD pathway.

Lipid droplets are the main storage organelle for triacylglycerides and cholesterol esters of the cell [reviewed in (Walther and Farese, 2012)]. Monoubiquitination appears to be required for AUP1-mediated clustering of lipid droplets (Lohmann et al., 2013), but whether this modification is a prerequisite for interaction with polyubiquitinated proteins has yet to be determined. AUP1 is predicted to be ubiquitinated on five Lys residues (K143, K250, K269, K359 and K377) [GG Base, (Kim et al., 2011)], however, monoubiquitination occurs on all ten Lys residues of AUP1 and only the lysineless AUP1 mutant is devoid of ubiquitin modifications (Lohmann et al., 2013). The roles of AUP1 in lipid droplets and in ERAD have been investigated concomitantly, as AUP1 is observed in both compartments (Spandl et al., 2010).

An N-terminal PVG motif is responsible for AUP1 targeting to the ER and lipid droplets (Stevanovic and Thiele, 2013). However, the stimuli that trigger AUP1 compartmentalisation are not yet understood. AUP1 overexpression increases the number of lipid droplets in the cell while its silencing reduces their levels (Klemm et al., 2011), indicating that AUP1 is necessary but not sufficient for lipid droplet formation. Monoubiquitinated AUP1 localised to lipid droplets appears to promote lipid droplet clustering, but the function of this clustering remains to be determined (Lohmann et al., 2013). Lipid droplet clusters have been so far observed under conditions such as; 1) overexpression of the lipid droplet associated protein FSP27 (Jambunathan et al., 2011) and 2) ectopic expression of perilipin, the master regulator of lipid storage and hydrolysis in adipocytes (Brasaemle et al., 2000; Marcinkiewicz et al., 2006). Induction of lipolysis leads to dispersion of the clusters (Marcinkiewicz et al., 2006). Thus, formation and dispersion of lipid droplet clusters correlates with the lipid status of the cell, preventing the cell from accumulation of free triacylglycerides and cholesterol esters and the ubiquitination state of AUP1 appears to be involved in this regulation (Fig. 6.2).

A control mechanism for regulating cellular cholesterol levels is the sterol-mediated degradation of HMG-CoA reductase, the key enzyme in the mevalonate pathway (Brown and Goldstein, 1980). Work on regulation of the yeast homologue Hmg2p led to key discoveries in ERAD, among them the requirement of the Hrd1p RING domain for substrate degradation (Bays et al., 2001a), the role of Hrd3p in Hrd1p regulation and substrate degradation (Gardner et al., 2001; Gardner et al., 2000) as well as the identification of Ubc7p as the cognate E2 of Hrd1p (Bays et al., 2001a). High levels of sterols

induce binding of HMG-CoA reductase to the ER membrane proteins Insig-1 and -2 (Sever et al., 2003b; Song et al., 2005a), which interact with the ubiquitin ligases gp78 and Trc8 (Jo et al., 2011; Sever et al., 2003a; Song et al., 2005b). This interaction brings HMG-CoA reductase and the E3s in close proximity and is followed by degradation of the enzyme by ERAD, which requires the translocation of HMG-CoA to lipid droplets prior to dislocation into the cytosol (Hartman et al., 2010a). Recent work has identified AUP1 as novel interaction partner of both gp78 and Trc8, facilitating the interaction of gp78 and Trc8 with Ube2g2 (Jo et al., 2013). Furthermore, it was found that AUP1 is necessary for sterol-dependent degradation of HMG-CoA from lipid droplets (Jo et al., 2013).

In conclusion, these data indicate that AUP1 is acting together with several ER-resident ubiquitin ligases to carry out multiple activities. AUP1 can recruit Ube2g2 to the Hrd1-SEL1L complex where it appears to regulate access of polyubiquitinated membrane proteins to the ligase complex for ERAD. Additionally, AUP1 may represent a putative regulator of cholesterol homeostasis (Fig. 6.2). High levels of sterols may induce AUP1 monoubiquitination, leading to the formation and clustering of lipid droplets, which are the site of gp78 and Trc8 mediated ERAD of HMG-CoA in an AUP1-dependent manner.

6.4 The stability of FAM8A1 is dependent on its cytosolic interaction with Hrd1

The Hrd1 complex contains a number of components whose functions remain insufficiently characterised. One such protein is the metazoan FAM8A1, a highly conserved Hrd1 interacting protein identified by AP-MS/MS (Christianson et al., 2012). FAM8A1 is notably absent from unicellular

eukaryotes, which suggests it has co-evolved to support a metazoan-specific functionality associated with the Hrd1 complex. Like other members of the Hrd1 complex, transcription of the FAM8A1 gene is upregulated in response to ER stress (Christianson et al., 2012), although it is not known whether this occurs via the Ire1-Xbp1 or ATF6 branch of the UPR. Beyond Hrd1, FAM8A1 does not make any additional connections to components in the Hrd1 complex (Christianson et al., 2012). This interaction occurs regardless of whether ligase activity of Hrd1 is intact (Fig. 3.2.3A), an aspect common with other Hrd1-interacting proteins in both yeast and mammals (Gauss et al., 2006; Horn et al., 2009; Ye et al., 2005).

Both FAM8A1 and Hrd1 are extensively exposed to both membrane and cytosolic environments and we could demonstrate that their interaction occurs independently through contact points in both regions (Fig. 3.2.3B). While multiple sites in their respective TMDs appeared necessary for co-precipitation (Fig. 3.2.4B and C), the domains with the cytosolic regions of both FAM8A1 and Hrd1 essential for interaction were determined. In contrast to the TMDs of the C-terminus (aa 257-413), the cytosolic N-terminus (aa 1-256) of FAM8A1 is not evolutionarily conserved and is predicted to have a high degree of structural disorder (Fig. 3.2.8). Within the FAM8A1 N-terminus though, a short segment (aa 107-139) was conserved and exhibited reduced levels of disorder (Fig. 3.2.8). Within this conserved segment, an algorithm that predicts secondary structure (PsiPred) identified a potential α-helical domain (aa 110-124). We could demonstrate that this segment was both necessary and sufficient for Hrd1 interaction. Furthermore, two conserved Trp residues (W120 and W122) within the putative α-helix were essential (Fig. 3.2.9A and B). For Hrd1, we identified a

complementary interacting domain that putatively forms an extended α-helix spanning aa 485-528 necessary to bind FAM8A1 (Fig. 3.2.6A and 6B). The cytosolic interaction between Hrd1 and FAM8A1 is essential for ERAD of lumenal substrates, as demonstrated by the impairment of ERAD when FAM8A1 mutants (W120A/W122A) and Hrd1 truncations ($Hrd1_{1-499}$) were introduced into TTR_{D18G}-expressing reporter cell lines (Fig. 3.2.7 and Fig. 3.2.10). How the cytosolic FAM8A1-Hrd1 interaction enables efficient ERAD is not yet clear. Aspects such as Hrd1 stability, ligase activity, or oligomerisation state are all possible modes of impact and further studies will be necessary to delineate what role it is playing in ERAD.

During the course of these studies, it was observed that FAM8A1 steady-state levels were lower than expected when expressed in $HEK293_{Hrd1\text{-}KD}$ cells or co-expressed with Hrd1 truncations unable to bind FAM8A1 (e.g. $Hrd1_{1-499}$). This strongly suggests that the interaction with Hrd1 actively stabilises FAM8A1 in the ER. Cycloheximide chase experiments in HEK293 and $HEK293_{Hrd1\text{-}KD}$ cells confirmed that in the absence of Hrd1, FAM8A1 was destabilised and degraded rapidly (Fig. 3.2.11B). FAM8A1 was degraded in a UPS-dependent manner as addition of MG-132 could mitigate its clearance. Re-introducing Hrd1 to these cells restored FAM8A1 stability, but only when Hrd1 contained the FAM8A1 binding region (aa 500-540, Fig. 3.2.11C). This suggests that FAM8A1 may only exist in complex with Hrd1 and any excess is likely to be rapidly degraded, potentially by an ER-resident E3 that is not Hrd1. As FAM8A1 only known interaction partner is Hrd1, one hypothesis is that FAM8A1 and Hrd1 actively co-stabilise each other to regulate their respective levels, similar to the regulation of Hrd1p by Hrd3p in yeast (Gardner et al., 2000; Plemper et

al., 1999). This turns out not to be the case however, as cycloheximide chase experiments demonstrate that Hrd1 levels were unaffected in FAM8A1 knockdowns (Figure 3.2.12). Collectively, this points toward a function for FAM8A1 beyond simply co-stabilising Hrd1. What that function is will require additional lines of inquiry beyond the scope of this work. Some of those ideas are discussed below.

Given the exposure of FAMA81 to the cytosolic face of the ER, one possible function may be as a chaperone for retrotranslocated ERAD substrates. At least a subset of ERAD substrates require unfolding for dislocation/retrotranslocation (Bhamidipati et al., 2005; Okuda-Shimizu and Hendershot, 2007; Soetandyo et al., 2010) and the exposed hydrophobic domains and unpaired residues need to be maintained in a soluble state in the cytosol. Recently, the Bag6 complex has been identified as an interaction partner of Hrd1 and gp78 and as a chaperoning complex for TCRα, MHC class I heavy chains in US11 expressing cells, CD4 and luciferase (Wang et al., 2011c). Recently, it was shown that a disordered Pro-rich region in Bag6 is necessary for its chaperone-like function (Xu et al., 2013). Dependency of chaperone-substrate interactions on disordered domains has been demonstrated as well for the yeast E3 San1 (Rosenbaum et al., 2011) and small heat shock proteins (sHSPs) (Haslbeck et al., 2004; Jaya et al., 2009; Stromer et al., 2004). The disordered region in the N-terminus of FAM8A1 is flexible, with a high proportion of Pro residues that could facilitate interaction with a broad range of clients. Further experiments will need to be conducted to determine whether FAM8A1 serves in such a capacity.

As FAM8A1 binds exclusively to Hrd1, a second hypothesis is that FAM8A1 regulates Hrd1 activity. In yeast, it has recently been demonstrated that N-

terminal acetylation of Der1p is necessary for targeting of a lumenal ERAD substrate to the Hrd1 complex, but is dispensable for ERAD-M (Zattas et al., 2013). Unacetylated Der1p occurs upon deletion of the N-acetyltransferase NatB, rendering Der1p an ERAD substrate and consequently perturbing Hrd1 activity towards a class of ERAD substrates (Zattas et al., 2013). FAM8A1 contains a putative N-acetylation site (NetAcet server 1.0) and it may be that acetylation of FAM8A1 is required for Hrd1-mediated degradation of lumenal substrates, comparable to Der1p.

Another factor important for Hrd1p ligase activity in yeast is Usa1p. The C-terminus of Usa1p links Hrd1p with Der1p, enabling degradation of lumenal ERAD substrates (Carvalho et al., 2006; Horn et al., 2009). Furthermore, the N-terminus of Usa1p interacts with the C-terminus of Hrd1p, which promotes oligomerisation of Hrd1 and facilitates degradation of ERAD-M substrates, but is less important for clearance of ERAD-L substrates (Horn et al., 2009). Hrd1 oligomerisation is pivotal for autoubiquitination of the ligase *in trans*, which is mediated by the N-terminal UBL domain of Usa1p (Carroll and Hampton, 2010). While the UBL domain of Usa1p is necessary for Hrd1p autoubiquitination, it is dispensable for ERAD substrate degradation, indicating that these two independent processes are mediated by the function of the same protein.

The mammalian homologue of Usa1p is believed to be Herp (Homocysteine-responsive endoplasmic reticulum-resident protein), a short-lived protein whose degradation is mediated by its N-terminal UBL-domain (Sai et al., 2003). Herp is one of the more highly up-regulated genes induced by the UPR in response to ER stress (Hori et al., 2004; Kokame et al., 2000; Sai et al., 2003). Herp is an integral component of the Hrd1 complex by direct interaction with Hrd1,

independent of its UBL-domain (Okuda-Shimizu and Hendershot, 2007; Schulze et al., 2005). An N-terminal region in close proximity to the UBL domain interacts with ubiquilins, proteins bridging E3s with the proteasome, which is required for degradation of CD3δ (Kim et al., 2008), indicating that the role of Herp may be connecting the Hrd1 complex with the proteasome. Furthermore, it was found that Herp is required for ERAD of unglycosylated substrates such as the $Ig\kappa_{LC}$ (Okuda-Shimizu and Hendershot, 2007) and that its silencing impaired ERAD of lumenal substrates (Christianson et al., 2012). In contrast to the yeast system, the UBL-domain of Herp is required for ERAD substrate degradation, at least in the case of NHK (Kny et al., 2011), indicating that Hrd1 regulation by Herp/Usa1p is different in yeast and mammals.

No experimental data to date is available that deciphers the role of Herp in Hrd1 oligomerisation, but previous studies have found Hrd1-homooligomers in mammals (Huang et al., 2013; Kny et al., 2011; Schulze et al., 2005). Like yeast, if mammals only required Hrd1 oligomers to form for ERAD of membrane proteins, FAM8A1 may prevent Hrd1 oligomerisation and therefore promote ERAD-L (Fig. 6.3). This would explain the observed accelerated degradation of membrane substrates and impaired degradation of lumenal substrates upon FAM8A1 silencing (Christianson et al., 2012). Furthermore, loss of FAM8A1 would not destabilise Hrd1, which is consistent with our results.

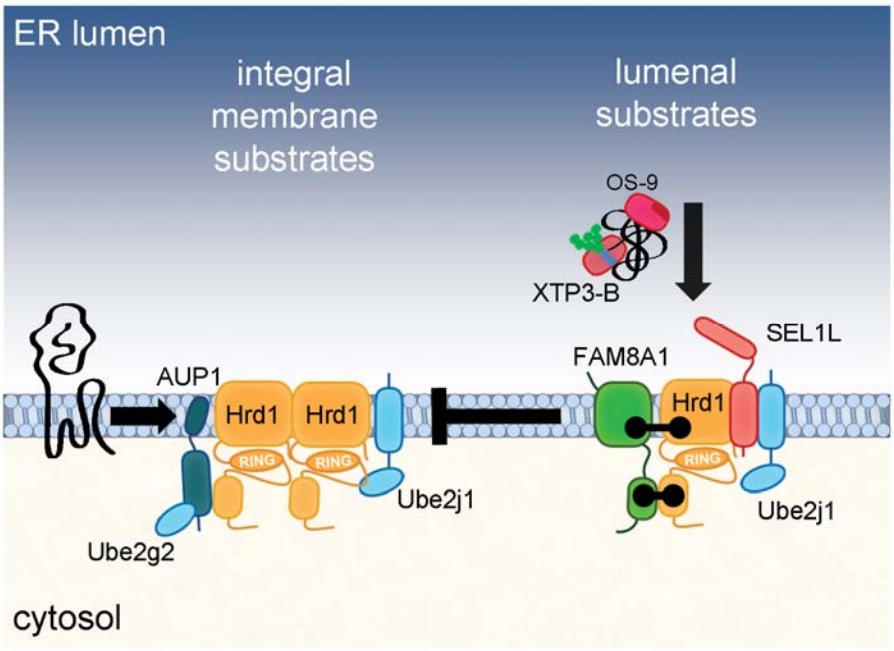


Fig. 6.3: Model of FAM8A1 function in ERAD. Incorporation of FAM8A1 into the Hrd1 complex facilitates degradation of lumenal substrates, while FAM8A1 has an inhibitory effect on turnover of membrane substrates, potentially by maintaining a monomeric state of Hrd1.

6.5 Conclusion

The work presented in this thesis provides insight into the organisation of the ERAD network. The interactions between Hrd1 and its accessory factors SEL1L, AUP1 and FAM8A1 are vital for ERAD to function efficiently. Moreover, this work highlights the utility of forming specific sub-complexes for ERAD of different substrate classes. Promiscuous ERAD factors, like AUP1, that are able to interact with more than one ubiquitin ligase, may increase the robustness of the ERAD machinery and protect cells against failure, loss or overload of a particular E3. Future studies are needed to establish whether redundancy is a more common feature in ERAD than is currently appreciated, where it may represent an undervalued adaptation within this degradation pathway. Relative abundance in the ER and stoichiometry within the Hrd1 complex are also important considerations for associated factors such as

SEL1L and FAM8A1. It will be important in the future to definitively determine the assembly and constituencies of Hrd1 complexes under both unchallenged and ER-stressed conditions, as it is their make-up and abundance ultimately governing the ERAD capacity within cells. With a more detailed understanding of the interactions within the ERAD network, a means by which to manipulate this pathway in order to treat diseases associated with protein misfolding, will hopefully be within reach of future research.

Bibliography

Aarvak, T., and Natvig, J.B. (2001). Cell-cell interactions in synovitis: antigen presenting cells and T cell interaction in rheumatoid arthritis. Arthritis research *3*, 13-17.

Adhikari, A., and Chen, Z.J. (2009). Diversity of polyubiquitin chains. Dev Cell *16*, 485-486.

Aikawa, J., Matsuo, I., and Ito, Y. (2012). In vitro mannose trimming property of human ER alpha-1,2 mannosidase I. Glycoconjugate journal *29*, 35-45.

Aiken, C., Konner, J., Landau, N.R., Lenburg, M.E., and Trono, D. (1994). Nef induces CD4 endocytosis: requirement for a critical dileucine motif in the membrane-proximal CD4 cytoplasmic domain. Cell *76*, 853-864.

Allen, J.R., Nguyen, L.X., Sargent, K.E., Lipson, K.L., Hackett, A., and Urano, F. (2004). High ER stress in beta-cells stimulates intracellular degradation of misfolded insulin. Biochem Biophys Res Commun *324*, 166-170.

Amano, T., Yamasaki, S., Yagishita, N., Tsuchimochi, K., Shin, H., Kawahara, K., Aratani, S., Fujita, H., Zhang, L., Ikeda, R.*, et al.* (2003). Synoviolin/Hrd1, an E3 ubiquitin ligase, as a novel pathogenic factor for arthropathy. Genes Dev *17*, 2436-2449.

Anfinsen, C.B. (1973). Principles that govern the folding of protein chains. Science *181*, 223-230.

Araki, E., Oyadomari, S., and Mori, M. (2003). Impact of endoplasmic reticulum stress pathway on pancreatic beta-cells and diabetes mellitus. Exp Biol Med (Maywood) *228*, 1213-1217.

Arnold, L.W., Grdina, T.A., Whitmore, A.C., and Haughton, G. (1988). Ig isotype switching in B lymphocytes. Isolation and characterization of clonal variants of the murine Ly-1+ B cell lymphoma, CH12, expressing isotypes other than IgM. J Immunol *140*, 4355-4363.

Arteaga, M.F., Wang, L., Ravid, T., Hochstrasser, M., and Canessa, C.M. (2006). An amphipathic helix targets serum and glucocorticoid-induced kinase 1 to the endoplasmic reticulum-associated ubiquitin-conjugation machinery. Proc Natl Acad Sci U S A *103*, 11178-11183.

Avezov, E., Frenkel, Z., Ehrlich, M., Herscovics, A., and Lederkremer, G.Z. (2008). Endoplasmic reticulum (ER) mannosidase I is compartmentalized and required for N-glycan trimming to Man5-6GlcNAc2 in glycoprotein ER-associated degradation. Mol Biol Cell *19*, 216-225.

Awe, K., Lambert, C., and Prange, R. (2008). Mammalian BiP controls posttranslational ER translocation of the hepatitis B virus large envelope protein. FEBS Lett *582*, 3179-3184.

Bagola, K., von Delbruck, M., Dittmar, G., Scheffner, M., Ziv, I., Glickman, M.H., Ciechanover, A., and Sommer, T. (2013). Ubiquitin binding by a CUE domain regulates ubiquitin chain formation by ERAD E3 ligases. Mol Cell *50*, 528-539.

Bailly, V., Lauder, S., Prakash, S., and Prakash, L. (1997). Yeast DNA repair proteins Rad6 and Rad18 form a heterodimer that has ubiquitin conjugating, DNA binding, and ATP hydrolytic activities. J Biol Chem *272*, 23360-23365.

Ballar, P., Ors, A.U., Yang, H., and Fang, S. (2010). Differential regulation of CFTRDeltaF508 degradation by ubiquitin ligases gp78 and Hrd1. Int J Biochem Cell Biol *42*, 167-173.

Bause, E. (1983). Structural requirements of N-glycosylation of proteins. Studies with proline peptides as conformational probes. Biochem J *209*, 331-336.

Bays, N.W., Gardner, R.G., Seelig, L.P., Joazeiro, C.A., and Hampton, R.Y. (2001a). Hrd1p/Der3p is a membrane-anchored ubiquitin ligase required for ER-associated degradation. Nat Cell Biol *3*, 24-29.

Bays, N.W., Wilhovsky, S.K., Goradia, A., Hodgkiss-Harlow, K., and Hampton, R.Y. (2001b). HRD4/NPL4 is required for the proteasomal processing of ubiquitinated ER proteins. Mol Biol Cell *12*, 4114-4128.

Bazirgan, O.A., and Hampton, R.Y. (2008). Cue1p is an activator of Ubc7p E2 activity in vitro and in vivo. J Biol Chem *283*, 12797-12810.

Beilharz, T., Egan, B., Silver, P.A., Hofmann, K., and Lithgow, T. (2003). Bipartite signals mediate subcellular targeting of tail-anchored membrane proteins in Saccharomyces cerevisiae. J Biol Chem *278*, 8219-8223.

Benlimame, N., Le, P.U., and Nabi, I.R. (1998). Localization of autocrine motility factor receptor to caveolae and clathrin-independent internalization of its ligand to smooth endoplasmic reticulum. Mol Biol Cell *9*, 1773-1786.

Benlimame, N., Simard, D., and Nabi, I.R. (1995). Autocrine motility factor receptor is a marker for a distinct membranous tubular organelle. J Cell Biol *129*, 459-471.

Benoist, F., and Grand-Perret, T. (1997). Co-translational degradation of apolipoprotein B100 by the proteasome is prevented by microsomal triglyceride transfer protein. Synchronized translation studies on HepG2 cells treated with an inhibitor of microsomal triglyceride transfer protein. J Biol Chem *272*, 20435-20442.

Bernardi, K.M., Williams, J.M., Kikkert, M., van Voorden, S., Wiertz, E.J., Ye, Y., and Tsai, B. (2010). The E3 ubiquitin ligases Hrd1 and gp78 bind to and promote cholera toxin retro-translocation. Mol Biol Cell *21*, 140-151.

Bernasconi, R., Galli, C., Calanca, V., Nakajima, T., and Molinari, M. (2010). Stringent requirement for HRD1, SEL1L, and OS-9/XTP3-B for disposal of ERAD-LS substrates. J Cell Biol *188*, 223-235.

Bernasconi, R., Galli, C., Noack, J., Bianchi, S., de Haan, C.A., Reggiori, F., and Molinari, M. (2012). Role of the SEL1L:LC3-I complex as an ERAD tuning receptor in the mammalian ER. Mol Cell *46*, 809-819.

Bernasconi, R., and Molinari, M. (2010). ERAD and ERAD tuning: disposal of cargo and of ERAD regulators from the mammalian ER. Curr Opin Cell Biol.

Bernasconi, R., Pertel, T., Luban, J., and Molinari, M. (2008). A dual task for the Xbp1-responsive OS-9 variants in the mammalian endoplasmic reticulum: inhibiting secretion of misfolded protein conformers and enhancing their disposal. J Biol Chem *283*, 16446-16454.

Bhamidipati, A., Denic, V., Quan, E.M., and Weissman, J.S. (2005). Exploration of the topological requirements of ERAD identifies Yos9p as a lectin sensor of misfolded glycoproteins in the ER lumen. Mol Cell *19*, 741-751.

Biederer, T., Volkwein, C., and Sommer, T. (1996). Degradation of subunits of the Sec61p complex, an integral component of the ER membrane, by the ubiquitin-proteasome pathway. EMBO J *15*, 2069-2076.

Biederer, T., Volkwein, C., and Sommer, T. (1997). Role of Cue1p in ubiquitination and degradation at the ER surface. Science *278*, 1806-1809.

Binette, J., Dube, M., Mercier, J., Halawani, D., Latterich, M., and Cohen, E.A. (2007). Requirements for the selective degradation of CD4 receptor molecules by the human immunodeficiency virus type 1 Vpu protein in the endoplasmic reticulum. Retrovirology *4*, 75.

Blond-Elguindi, S., Cwirla, S.E., Dower, W.J., Lipshutz, R.J., Sprang, S.R., Sambrook, J.F., and Gething, M.J. (1993). Affinity panning of a library of peptides displayed on bacteriophages reveals the binding specificity of BiP. Cell *75*, 717-728.

Boeddrich, A., Gaumer, S., Haacke, A., Tzvetkov, N., Albrecht, M., Evert, B.O., Muller, E.C., Lurz, R., Breuer, P., Schugardt, N.*, et al.* (2006). An arginine/lysine-rich motif is crucial for VCP/p97-mediated modulation of ataxin-3 fibrillogenesis. Embo Journal *25*, 1547-1558.

Bogan, A.A., and Thorn, K.S. (1998). Anatomy of hot spots in protein interfaces. J Mol Biol *280*, 1-9.

Bonifacino, J.S., Cosson, P., Shah, N., and Klausner, R.D. (1991). Role of potentially charged transmembrane residues in targeting proteins for retention and degradation within the endoplasmic reticulum. EMBO J *10*, 2783-2793.

Bonifacino, J.S., Suzuki, C.K., and Klausner, R.D. (1990). A peptide sequence confers retention and rapid degradation in the endoplasmic reticulum. Science *247*, 79-82.

Bonifacino, J.S., Suzuki, C.K., Lippincott-Schwartz, J., Weissman, A.M., and Klausner, R.D. (1989). Pre-Golgi degradation of newly synthesized T-cell antigen receptor chains: intrinsic sensitivity and the role of subunit assembly. J Cell Biol *109*, 73-83.

Bordallo, J., Plemper, R.K., Finger, A., and Wolf, D.H. (1998). Der3p/Hrd1p is required for endoplasmic reticulum-associated degradation of misfolded lumenal and integral membrane proteins. Mol Biol Cell *9*, 209-222.

Bose, S., Mucke, M., and Freedman, R.B. (1994). The characterization of a cyclophilin-type peptidyl prolyl cis-trans-isomerase from the endoplasmic-reticulum lumen. Biochem J *300 (Pt 3)*, 871-875.

Bour, S., Schubert, U., and Strebel, K. (1995). The human immunodeficiency virus type 1 Vpu protein specifically binds to the cytoplasmic domain of CD4: implications for the mechanism of degradation. Journal of virology *69*, 1510-1520.

Bozkurt, G., Stjepanovic, G., Vilardi, F., Amlacher, S., Wild, K., Bange, G., Favaloro, V., Rippe, K., Hurt, E., Dobberstein, B.*, et al.* (2009). Structural insights into tail-anchored protein binding and membrane insertion by Get3. Proc Natl Acad Sci U S A *106*, 21131-21136.

Brada, D., and Dubach, U.C. (1984). Isolation of a homogeneous glucosidase II from pig kidney microsomes. European journal of biochemistry / FEBS *141*, 149-156.

Brasaemle, D.L., Rubin, B., Harten, I.A., Gruia-Gray, J., Kimmel, A.R., and Londos, C. (2000). Perilipin A increases triacylglycerol storage by decreasing the rate of triacylglycerol hydrolysis. J Biol Chem *275*, 38486-38493.

Breitschopf, K., Bengal, E., Ziv, T., Admon, A., and Ciechanover, A. (1998). A novel site for ubiquitination: the N-terminal residue, and not internal lysines of MyoD, is essential for conjugation and degradation of the protein. EMBO J *17*, 5964-5973.

Bresnahan, P.A., Yonemoto, W., and Greene, W.C. (1999). Cutting edge: SIV Nef protein utilizes both leucine- and tyrosine-based protein sorting pathways for down-regulation of CD4. J Immunol *163*, 2977-2981.

Brodsky, J.L., and McCracken, A.A. (1999). ER protein quality control and proteasome-mediated protein degradation. Semin Cell Dev Biol *10*, 507-513.

Brown, M.S., and Goldstein, J.L. (1980). Multivalent feedback regulation of HMG CoA reductase, a control mechanism coordinating isoprenoid synthesis and cell growth. J Lipid Res *21*, 505-517.

Brzovic, P.S., Rajagopal, P., Hoyt, D.W., King, M.C., and Klevit, R.E. (2001). Structure of a BRCA1-BARD1 heterodimeric RING-RING complex. Nat Struct Biol *8*, 833-837.

Buchwald, G., van der Stoop, P., Weichenrieder, O., Perrakis, A., van Lohuizen, M., and Sixma, T.K. (2006). Structure and E3-ligase activity of the Ring-Ring complex of polycomb proteins Bmi1 and Ring1b. EMBO J *25*, 2465-2474.

Burns, D.M., and Touster, O. (1982). Purification and characterization of glucosidase II, an endoplasmic reticulum hydrolase involved in glycoprotein biosynthesis. J Biol Chem *257*, 9990-10000.

Burr, M.L., Cano, F., Svobodova, S., Boyle, L.H., Boname, J.M., and Lehner, P.J. (2011). HRD1 and UBE2J1 target misfolded MHC class I heavy chains for endoplasmic reticulum-associated degradation. Proc Natl Acad Sci U S A *108*, 2034-2039.

Burtey, A., Rappoport, J.Z., Bouchet, J., Basmaciogullari, S., Guatelli, J., Simon, S.M., Benichou, S., and Benmerah, A. (2007). Dynamic interaction of HIV-1 Nef with the clathrin-mediated endocytic pathway at the plasma membrane. Traffic *8*, 61-76.

Butler, A.E., Janson, J., Bonner-Weir, S., Ritzel, R., Rizza, R.A., and Butler, P.C. (2003). Beta-cell deficit and increased beta-cell apoptosis in humans with type 2 diabetes. Diabetes *52*, 102-110.

Butticaz, C., Michielin, O., Wyniger, J., Telenti, A., and Rothenberger, S. (2007). Silencing of both beta-TrCP1 and HOS (beta-TrCP2) is required to suppress human immunodeficiency virus type 1 Vpu-mediated CD4 down-modulation. Journal of virology *81*, 1502-1505.

Cabibbo, A., Pagani, M., Fabbri, M., Rocchi, M., Farmery, M.R., Bulleid, N.J., and Sitia, R. (2000). ERO1-L, a human protein that favors disulfide bond formation in the endoplasmic reticulum. J Biol Chem *275*, 4827-4833.

Cali, T., Galli, C., Olivari, S., and Molinari, M. (2008). Segregation and rapid turnover of EDEM1 by an autophagy-like mechanism modulates standard ERAD and folding activities. Biochem Biophys Res Commun *371*, 405-410.

Cao, Z., Tavender, T.J., Roszak, A.W., Cogdell, R.J., and Bulleid, N.J. (2011). Crystal structure of reduced and of oxidized peroxiredoxin IV enzyme reveals a stable oxidized decamer and a non-disulfide-bonded intermediate in the catalytic cycle. J Biol Chem *286*, 42257-42266.

Caramelo, J.J., Castro, O.A., Alonso, L.G., De Prat-Gay, G., and Parodi, A.J. (2003). UDP-Glc:glycoprotein glucosyltransferase recognizes structured and solvent accessible hydrophobic patches in molten globule-like folding intermediates. Proc Natl Acad Sci U S A *100*, 86-91.

Caramelo, J.J., Castro, O.A., de Prat-Gay, G., and Parodi, A.J. (2004). The endoplasmic reticulum glucosyltransferase recognizes nearly native glycoprotein folding intermediates. J Biol Chem *279*, 46280-46285.

Caramelo, J.J., and Parodi, A.J. (2008). Getting in and out from calnexin/calreticulin cycles. J Biol Chem *283*, 10221-10225.

Carroll, S.M., and Hampton, R.Y. (2010). Usa1p is required for optimal function and regulation of the Hrd1p endoplasmic reticulum-associated degradation ubiquitin ligase. J Biol Chem *285*, 5146-5156.

Carvalho, P., Goder, V., and Rapoport, T.A. (2006). Distinct ubiquitin-ligase complexes define convergent pathways for the degradation of ER proteins. Cell *126*, 361-373.

Carvalho, P., Stanley, A.M., and Rapoport, T.A. (2010). Retrotranslocation of a misfolded luminal ER protein by the ubiquitin-ligase Hrd1p. Cell *143*, 579-591.

Chartron, J.W., Suloway, C.J., Zaslaver, M., and Clemons, W.M., Jr. (2010). Structural characterization of the Get4/Get5 complex and its interaction with Get3. Proc Natl Acad Sci U S A *107*, 12127-12132.

Chau, V., Tobias, J.W., Bachmair, A., Marriott, D., Ecker, D.J., Gonda, D.K., and Varshavsky, A. (1989). A multiubiquitin chain is confined to specific lysine in a targeted short-lived protein. Science *243*, 1576-1583.

Chaudhuri, R., Lindwasser, O.W., Smith, W.J., Hurley, J.H., and Bonifacino, J.S. (2007). Downregulation of CD4 by human immunodeficiency virus type 1 Nef is dependent on clathrin and involves direct interaction of Nef with the AP2 clathrin adaptor. Journal of virology *81*, 3877-3890.

Chaudhuri, R., Mattera, R., Lindwasser, O.W., Robinson, M.S., and Bonifacino, J.S. (2009). A basic patch on alpha-adaptin is required for binding of human immunodeficiency virus type 1 Nef and cooperative assembly of a CD4-Nef-AP-2 complex. Journal of virology *83*, 2518-2530.

Chavan, M., Yan, A., and Lennarz, W.J. (2005). Subunits of the translocon interact with components of the oligosaccharyl transferase complex. J Biol Chem *280*, 22917-22924.

Chen, B., Mariano, J., Tsai, Y.C., Chan, A.H., Cohen, M., and Weissman, A.M. (2006). The activity of a human endoplasmic reticulum-associated degradation E3, gp78, requires its Cue domain, RING finger, and an E2-binding site. Proc Natl Acad Sci U S A *103*, 341-346.

Chen, M.M., Glover, K.J., and Imperiali, B. (2007). From peptide to protein: comparative analysis of the substrate specificity of N-linked glycosylation in C. jejuni. Biochemistry *46*, 5579-5585.

Chen, P., Johnson, P., Sommer, T., Jentsch, S., and Hochstrasser, M. (1993). Multiple ubiquitin-conjugating enzymes participate in the in vivo degradation of the yeast MAT alpha 2 repressor. Cell *74*, 357-369.

Chen, X., Tukachinsky, H., Huang, C.H., Jao, C., Chu, Y.R., Tang, H.Y., Mueller, B., Schulman, S., Rapoport, T.A., and Salic, A. (2011). Processing and turnover of the Hedgehog protein in the endoplasmic reticulum. J Cell Biol *192*, 825-838.

Cheng, S.H., Gregory, R.J., Marshall, J., Paul, S., Souza, D.W., White, G.A., O'Riordan, C.R., and Smith, A.E. (1990). Defective intracellular transport and processing of CFTR is the molecular basis of most cystic fibrosis. Cell *63*, 827-834.

Christianson, J.C., and Green, W.N. (2004). Regulation of nicotinic receptor expression by the ubiquitin-proteasome system. EMBO J *23*, 4156-4165.

Christianson, J.C., Olzmann, J.A., Shaler, T.A., Sowa, M.E., Bennett, E.J., Richter, C.M., Tyler, R.E., Greenblatt, E.J., Harper, J.W., and Kopito, R.R. (2012). Defining human ERAD networks through an integrative mapping strategy. Nat Cell Biol *14*, 93-105.

Christianson, J.C., Shaler, T.A., Tyler, R.E., and Kopito, R.R. (2008). OS-9 and GRP94 deliver mutant alpha1-antitrypsin to the Hrd1-SEL1L ubiquitin ligase complex for ERAD. Nat Cell Biol *10*, 272-282.

Chung, K.T., Shen, Y., and Hendershot, L.M. (2002). BAP, a mammalian BiP-associated protein, is a nucleotide exchange factor that regulates the ATPase activity of BiP. J Biol Chem *277*, 47557-47563.

Claessen, J.H., Mueller, B., Spooner, E., Pivorunas, V.L., and Ploegh, H.L. (2010). The transmembrane segment of a tail-anchored protein determines its degradative fate through dislocation from the endoplasmic reticulum. J Biol Chem *285*, 20732-20739.

Clerc, S., Hirsch, C., Oggier, D.M., Deprez, P., Jakob, C., Sommer, T., and Aebi, M. (2009). Htm1 protein generates the N-glycan signal for glycoprotein degradation in the endoplasmic reticulum. J Cell Biol *184*, 159-172.

Connolly, T., and Gilmore, R. (1986). Formation of a functional ribosome-membrane junction during translocation requires the participation of a GTP-binding protein. J Cell Biol *103*, 2253-2261.

Connolly, T., and Gilmore, R. (1989). The signal recognition particle receptor mediates the GTP-dependent displacement of SRP from the signal sequence of the nascent polypeptide. Cell *57*, 599-610.

Connolly, T., Rapiejko, P.J., and Gilmore, R. (1991). Requirement of GTP hydrolysis for dissociation of the signal recognition particle from its receptor. Science *252*, 1171-1173.

Copic, A., Dorrington, M., Pagant, S., Barry, J., Lee, M.C., Singh, I., Hartman, J.L.t., and Miller, E.A. (2009). Genomewide analysis reveals novel pathways affecting endoplasmic reticulum homeostasis, protein modification and quality control. Genetics *182*, 757-769.

Cormier, J.H., Tamura, T., Sunryd, J.C., and Hebert, D.N. (2009). EDEM1 recognition and delivery of misfolded proteins to the SEL1L-containing ERAD complex. Mol Cell *34*, 627-633.

Costanzo, M., Baryshnikova, A., Bellay, J., Kim, Y., Spear, E.D., Sevier, C.S., Ding, H., Koh, J.L., Toufighi, K., Mostafavi, S.*, et al.* (2010). The genetic landscape of a cell. Science *327*, 425-431.

Craig, H.M., Reddy, T.R., Riggs, N.L., Dao, P.P., and Guatelli, J.C. (2000). Interactions of HIV-1 nef with the mu subunits of adaptor protein complexes 1, 2, and 3: role of the dileucine-based sorting motif. Virology *271*, 9-17.

Cunnea, P.M., Miranda-Vizuete, A., Bertoli, G., Simmen, T., Damdimopoulos, A.E., Hermann, S., Leinonen, S., Huikko, M.P., Gustafsson, J.A., Sitia, R.*, et al.* (2003). ERdj5, an endoplasmic reticulum (ER)-resident protein containing DnaJ and thioredoxin domains, is expressed in secretory cells or following ER stress. J Biol Chem *278*, 1059-1066.

Dalemans, W., Barbry, P., Champigny, G., Jallat, S., Dott, K., Dreyer, D., Crystal, R.G., Pavirani, A., Lecocq, J.P., and Lazdunski, M. (1991). Altered chloride ion channel kinetics associated with the delta F508 cystic fibrosis mutation. Nature *354*, 526-528.

Dames, S.A., Martinez-Yamout, M., De Guzman, R.N., Dyson, H.J., and Wright, P.E. (2002). Structural basis for Hif-1 alpha /CBP recognition in the cellular hypoxic response. Proc Natl Acad Sci U S A *99*, 5271-5276.

Das, R., Liang, Y.H., Mariano, J., Li, J., Huang, T., King, A., Tarasov, S.G., Weissman, A.M., Ji, X., and Byrd, R.A. (2013). Allosteric regulation of E2:E3 interactions promote a processive ubiquitination machine. EMBO J *32*, 2504-2516.

Das, R., Mariano, J., Tsai, Y.C., Kalathur, R.C., Kostova, Z., Li, J., Tarasov, S.G., McFeeters, R.L., Altieri, A.S., Ji, X.*, et al.* (2009). Allosteric activation of E2-RING finger-mediated ubiquitylation by a structurally defined specific E2-binding region of gp78. Mol Cell *34*, 674-685.

daSilva, L.L., Sougrat, R., Burgos, P.V., Janvier, K., Mattera, R., and Bonifacino, J.S. (2009). Human immunodeficiency virus type 1 Nef protein targets CD4 to the multivesicular body pathway. Journal of virology *83*, 6578-6590.

Davis, D.P., Gallo, G., Vogen, S.M., Dul, J.L., Sciarretta, K.L., Kumar, A., Raffen, R., Stevens, F.J., and Argon, Y. (2001). Both the environment and somatic mutations govern the aggregation pathway of pathogenic immunoglobulin light chain. J Mol Biol *313*, 1021-1034.

DeMeo, D.L., and Silverman, E.K. (2004). Alpha1-antitrypsin deficiency. 2: genetic aspects of alpha(1)-antitrypsin deficiency: phenotypes and genetic modifiers of emphysema risk. Thorax *59*, 259-264.

Deshaies, R.J., Sanders, S.L., Feldheim, D.A., and Schekman, R. (1991). Assembly of yeast Sec proteins involved in translocation into the endoplasmic reticulum into a membrane-bound multisubunit complex. Nature *349*, 806-808.

Deshaies, R.J., and Schekman, R. (1987). A yeast mutant defective at an early stage in import of secretory protein precursors into the endoplasmic reticulum. J Cell Biol *105*, 633-645.

Deshaies, R.J., and Schekman, R. (1989). SEC62 encodes a putative membrane protein required for protein translocation into the yeast endoplasmic reticulum. J Cell Biol *109*, 2653-2664.

Dever, T.E. (2002). Gene-specific regulation by general translation factors. Cell *108*, 545-556.

Deveraux, Q., Ustrell, V., Pickart, C., and Rechsteiner, M. (1994). A 26 S protease subunit that binds ubiquitin conjugates. J Biol Chem *269*, 7059-7061.

Dickson, D.W. (1997). The pathogenesis of senile plaques. Journal of neuropathology and experimental neurology *56*, 321-339.

Dominguez, C., Bonvin, A.M., Winkler, G.S., van Schaik, F.M., Timmers, H.T., and Boelens, R. (2004). Structural model of the UbcH5B/CNOT4 complex revealed by combining NMR, mutagenesis, and docking approaches. Structure *12*, 633-644.

Doss-Pepe, E.W., Stenroos, E.S., Johnson, W.G., and Madura, K. (2003). Ataxin-3 interactions with Rad23 and valosin-containing protein and its associations with ubiquitin chains and the proteasome are consistent with a role in ubiquitin-mediated proteolysis. Molecular and Cellular Biology *23*, 6469-6483.

Dudek, J., Greiner, M., Muller, A., Hendershot, L.M., Kopsch, K., Nastainczyk, W., and Zimmermann, R. (2005). ERj1p has a basic role in protein biogenesis at the endoplasmic reticulum. Nature structural & molecular biology *12*, 1008-1014.

Dul, J.L., Burrone, O.R., and Argon, Y. (1992). A conditional secretory mutant in an Ig L chain is caused by replacement of tyrosine/phenylalanine 87 with histidine. J Immunol *149*, 1927-1933.

Dumax-Vorzet, A., Roboti, P., and High, S. (2013). OST4 is a subunit of the mammalian oligosaccharyltransferase required for efficient N-glycosylation. J Cell Sci *126 Pt 12*, 2595-2606.

Duncan, C.D., and Mata, J. (2011). Widespread cotranslational formation of protein complexes. PLoS genetics *7*, e1002398.

Edwards, P.A., Lan, S.F., and Fogelman, A.M. (1983). Alterations in the rates of synthesis and degradation of rat liver 3-hydroxy-3-methylglutaryl coenzyme A reductase produced by cholestyramine and mevinolin. J Biol Chem *258*, 10219-10222.

Edwards, T.A., and Wilson, A.J. (2011). Helix-mediated protein--protein interactions as targets for intervention using foldamers. Amino acids *41*, 743-754.

Elliott, P.R., Lomas, D.A., Carrell, R.W., and Abrahams, J.P. (1996). Inhibitory conformation of the reactive loop of alpha 1-antitrypsin. Nat Struct Biol *3*, 676-681.

Elouil, H., Bensellam, M., Guiot, Y., Vander Mierde, D., Pascal, S.M., Schuit, F.C., and Jonas, J.C. (2007). Acute nutrient regulation of the unfolded protein response and integrated stress response in cultured rat pancreatic islets. Diabetologia *50*, 1442-1452.

Ernst, R., Claessen, J.H., Mueller, B., Sanyal, S., Spooner, E., van der Veen, A.G., Kirak, O., Schlieker, C.D., Weihofen, W.A., and Ploegh, H.L. (2011). Enzymatic blockade of the ubiquitin-proteasome pathway. PLoS biology *8*, e1000605.

Ernst, R., Mueller, B., Ploegh, H.L., and Schlieker, C. (2009). The otubain YOD1 is a deubiquitinating enzyme that associates with p97 to facilitate protein dislocation from the ER. Mol Cell *36*, 28-38.

Esnault, Y., Feldheim, D., Blondel, M.O., Schekman, R., and Kepes, F. (1994). SSS1 encodes a stabilizing component of the Sec61 subcomplex of the yeast protein translocation apparatus. J Biol Chem *269*, 27478-27485.

Fairbank, M., Huang, K., El-Husseini, A., and Nabi, I.R. (2012). RING finger palmitoylation of the endoplasmic reticulum Gp78 E3 ubiquitin ligase. FEBS Lett *586*, 2488-2493.

Fang, S., Ferrone, M., Yang, C., Jensen, J.P., Tiwari, S., and Weissman, A.M. (2001). The tumor autocrine motility factor receptor, gp78, is a ubiquitin protein ligase implicated in degradation from the endoplasmic reticulum. Proc Natl Acad Sci U S A *98*, 14422-14427.

Faust, J.R., Luskey, K.L., Chin, D.J., Goldstein, J.L., and Brown, M.S. (1982). Regulation of synthesis and degradation of 3-hydroxy-3-methylglutaryl-coenzyme A reductase by low density lipoprotein and 25-hydroxycholesterol in UT-1 cells. Proc Natl Acad Sci U S A *79*, 5205-5209.

Fawcett, T.W., Martindale, J.L., Guyton, K.Z., Hai, T., and Holbrook, N.J. (1999). Complexes containing activating transcription factor (ATF)/cAMP-responsive-element-binding protein (CREB) interact with the CCAAT/enhancer-binding protein (C/EBP)-ATF composite site to regulate Gadd153 expression during the stress response. Biochem J *339 (Pt 1)*, 135-141.

Fayadat, L., and Kopito, R.R. (2003). Recognition of a single transmembrane degron by sequential quality control checkpoints. Mol Biol Cell *14*, 1268-1278.

Feige, M.J., Groscurth, S., Marcinowski, M., Shimizu, Y., Kessler, H., Hendershot, L.M., and Buchner, J. (2009). An unfolded CH1 domain controls the assembly and secretion of IgG antibodies. Mol Cell *34*, 569-579.

Feldheim, D., Rothblatt, J., and Schekman, R. (1992). Topology and functional domains of Sec63p, an endoplasmic reticulum membrane protein required for secretory protein translocation. Mol Cell Biol *12*, 3288-3296.

Feltham, R., Bettjeman, B., Budhidarmo, R., Mace, P.D., Shirley, S., Condon, S.M., Chunduru, S.K., McKinlay, M.A., Vaux, D.L., Silke, J*., et al.* (2011). Smac mimetics activate the E3 ligase activity of cIAP1 protein by promoting RING domain dimerization. J Biol Chem *286*, 17015-17028.

Feng, M., Gu, C., Ma, S., Wang, Y., Liu, H., Han, R., Gao, J., Long, Y., and Mi, H. (2011). Mouse FKBP23 mediates conformer-specific functions of BiP by catalyzing Pro117 cis/trans isomerization. Biochem Biophys Res Commun *408*, 537-540.

Fiebiger, E., Story, C., Ploegh, H.L., and Tortorella, D. (2002). Visualization of the ER-to-cytosol dislocation reaction of a type I membrane protein. Embo Journal *21*, 1041-1053.

Fisher, E.A., and Ginsberg, H.N. (2002). Complexity in the secretory pathway: the assembly and secretion of apolipoprotein B-containing lipoproteins. J Biol Chem *277*, 17377-17380.

Fisher, E.A., Khanna, N.A., and McLeod, R.S. (2011). Ubiquitination regulates the assembly of VLDL in HepG2 cells and is the committing step of the apoB-100 ERAD pathway. J Lipid Res *52*, 1170-1180.

Fisher, E.A., Zhou, M., Mitchell, D.M., Wu, X., Omura, S., Wang, H., Goldberg, A.L., and Ginsberg, H.N. (1997). The degradation of apolipoprotein B100 is mediated by the ubiquitin-proteasome pathway and involves heat shock protein 70. J Biol Chem *272*, 20427-20434.

Fleig, L., Bergbold, N., Sahasrabudhe, P., Geiger, B., Kaltak, L., and Lemberg, M.K. (2012). Ubiquitin-Dependent Intramembrane Rhomboid Protease Promotes ERAD of Membrane Proteins. Molecular Cell *47*, 558-569.

Flierman, D., Ye, Y.H., Dai, M., Chau, V., and Rapoport, T.A. (2003). Polyubiquitin serves as a recognition signal, rather than a ratcheting molecule, during retrotranslocation of proteins across the endoplasmic reticulum membrane. Journal of Biological Chemistry *278*, 34774-34782.

Fonseca, S.G., Urano, F., Burcin, M., and Gromada, J. (2010). Stress hypERactivation in the beta-cell. Islets *2*, 1-9.

Francisco, A.B., Singh, R., Li, S., Vani, A.K., Yang, L., Munroe, R.J., Diaferia, G., Cardano, M., Biunno, I., Qi, L.*, et al.* (2010). Deficiency of suppressor enhancer Lin12 1 like (SEL1L) in mice leads to systemic endoplasmic reticulum stress and embryonic lethality. J Biol Chem *285*, 13694-13703.

Frand, A.R., and Kaiser, C.A. (1998). The ERO1 gene of yeast is required for oxidation of protein dithiols in the endoplasmic reticulum. Mol Cell *1*, 161-170.

Freemont, P.S., Hanson, I.M., and Trowsdale, J. (1991). A novel cysteine-rich sequence motif. Cell *64*, 483-484.

Frenkel, Z., Gregory, W., Kornfeld, S., and Lederkremer, G.Z. (2003). Endoplasmic reticulum-associated degradation of mammalian glycoproteins involves sugar chain trimming to Man6-5GlcNAc2. J Biol Chem *278*, 34119-34124.

Friedlander, M., and Blobel, G. (1985). Bovine opsin has more than one signal sequence. Nature *318*, 338-343.

Fuest, M., Willim, K., MacNelly, S., Fellner, N., Resch, G.P., Blum, H.E., and Hasselblatt, P. (2012). The transcription factor c-Jun protects against sustained hepatic endoplasmic reticulum stress thereby promoting hepatocyte survival. Hepatology *55*, 408-418.

Fujimori, T., Kamiya, Y., Nagata, K., Kato, K., and Hosokawa, N. (2013). Endoplasmic reticulum lectin XTP3-B inhibits endoplasmic reticulum-associated degradation of a misfolded alpha1-antitrypsin variant. FEBS J *280*, 1563-1575.

Fujimoto, T., and Ohsaki, Y. (2006). Cytoplasmic lipid droplets: rediscovery of an old structure as a unique platform. Ann N Y Acad Sci *1086*, 104-115.

Gardner, A.M., Aviel, S., and Argon, Y. (1993). Rapid degradation of an unassembled immunoglobulin light chain is mediated by a serine protease and occurs in a pre-Golgi compartment. J Biol Chem *268*, 25940-25947.

Gardner, R.G., Shearer, A.G., and Hampton, R.Y. (2001). In vivo action of the HRD ubiquitin ligase complex: mechanisms of endoplasmic reticulum quality control and sterol regulation. Mol Cell Biol *21*, 4276-4291.

Gardner, R.G., Swarbrick, G.M., Bays, N.W., Cronin, S.R., Wilhovsky, S., Seelig, L., Kim, C., and Hampton, R.Y. (2000). Endoplasmic reticulum degradation requires lumen to cytosol signaling. Transmembrane control of Hrd1p by Hrd3p. J Cell Biol *151*, 69-82.

Garza, R.M., Sato, B.K., and Hampton, R.Y. (2009). In Vitro Analysis of Hrd1p-mediated Retrotranslocation of Its Multispanning Membrane Substrate 3-Hydroxy-3-methylglutaryl (HMG)-CoA Reductase. Journal of Biological Chemistry *284*, 14710-14722.

Gauss, R., Sommer, T., and Jarosch, E. (2006). The Hrd1p ligase complex forms a linchpin between ER-lumenal substrate selection and Cdc48p recruitment. EMBO J *25*, 1827-1835.

Gavel, Y., and von Heijne, G. (1990). Sequence differences between glycosylated and non-glycosylated Asn-X-Thr/Ser acceptor sites: implications for protein engineering. Protein engineering *3*, 433-442.

Geiger, R., Andritschke, D., Friebe, S., Herzog, F., Luisoni, S., Heger, T., and Helenius, A. (2011). BAP31 and BiP are essential for dislocation of SV40 from the endoplasmic reticulum to the cytosol. Nat Cell Biol *13*, 1305-1314.

Ghaemmaghami, S., Huh, W.K., Bower, K., Howson, R.W., Belle, A., Dephoure, N., O'Shea, E.K., and Weissman, J.S. (2003). Global analysis of protein expression in yeast. Nature *425*, 737-741.

Gillece, P., Pilon, M., and Romisch, K. (2000). The protein translocation channel mediates glycopeptide export across the endoplasmic reticulum membrane. Proc Natl Acad Sci U S A *97*, 4609-4614.

Gilmore, R., Blobel, G., and Walter, P. (1982a). Protein translocation across the endoplasmic reticulum. I. Detection in the microsomal membrane of a receptor for the signal recognition particle. J Cell Biol *95*, 463-469.

Gilmore, R., Walter, P., and Blobel, G. (1982b). Protein translocation across the endoplasmic reticulum. II. Isolation and characterization of the signal recognition particle receptor. J Cell Biol *95*, 470-477.

Glenner, G.G., and Wong, C.W. (1984). Alzheimer's disease: initial report of the purification and characterization of a novel cerebrovascular amyloid protein. Biochem Biophys Res Commun *120*, 885-890.

Gonzalez, D.S., Karaveg, K., Vandersall-Nairn, A.S., Lal, A., and Moremen, K.W. (1999). Identification, expression, and characterization of a cDNA encoding human endoplasmic reticulum mannosidase I, the enzyme that catalyzes the first mannose trimming step in mammalian Asn-linked oligosaccharide biosynthesis. J Biol Chem *274*, 21375-21386.

Gopalan, G., He, Z., Battaile, K.P., Luan, S., and Swaminathan, K. (2006). Structural comparison of oxidized and reduced FKBP13 from Arabidopsis thaliana. Proteins *65*, 789-795.

Gorlich, D., Prehn, S., Hartmann, E., Kalies, K.U., and Rapoport, T.A. (1992). A mammalian homolog of SEC61p and SECYp is associated with ribosomes and nascent polypeptides during translocation. Cell *71*, 489-503.

Gorlich, D., and Rapoport, T.A. (1993). Protein translocation into proteoliposomes reconstituted from purified components of the endoplasmic reticulum membrane. Cell *75*, 615-630.

Grabbe, C., and Dikic, I. (2009). Functional roles of ubiquitin-like domain (ULD) and ubiquitin-binding domain (UBD) containing proteins. Chemical reviews *109*, 1481-1494.

Greenberg, M.E., Bronson, S., Lock, M., Neumann, M., Pavlakis, G.N., and Skowronski, J. (1997). Co-localization of HIV-1 Nef with the AP-2 adaptor protein complex correlates with Nef-induced CD4 down-regulation. EMBO J *16*, 6964-6976.

Greenblatt, E.J., Olzmann, J.A., and Kopito, R.R. (2011). Derlin-1 is a rhomboid pseudoprotease required for the dislocation of mutant alpha-1 antitrypsin from the endoplasmic reticulum. Nature structural & molecular biology *18*, 1147-U1115.

Guerriero, C.J., and Brodsky, J.L. (2012). The delicate balance between secreted protein folding and endoplasmic reticulum-associated degradation in human physiology. Physiological reviews *92*, 537-576.

Guharoy, M., and Chakrabarti, P. (2007). Secondary structure based analysis and classification of biological interfaces: identification of binding motifs in protein-protein interactions. Bioinformatics *23*, 1909-1918.

Haass, C., Lemere, C.A., Capell, A., Citron, M., Seubert, P., Schenk, D., Lannfelt, L., and Selkoe, D.J. (1995). The Swedish mutation causes early-onset Alzheimer's disease by beta-secretase cleavage within the secretory pathway. Nat Med *1*, 1291-1296.

Halic, M., Becker, T., Pool, M.R., Spahn, C.M., Grassucci, R.A., Frank, J., and Beckmann, R. (2004). Structure of the signal recognition particle interacting with the elongation-arrested ribosome. Nature *427*, 808-814.

Hammarstrom, P., Jiang, X., Hurshman, A.R., Powers, E.T., and Kelly, J.W. (2002). Sequence-dependent denaturation energetics: A major determinant in amyloid disease diversity. Proc Natl Acad Sci U S A *99 Suppl 4*, 16427-16432.

Hammarstrom, P., Sekijima, Y., White, J.T., Wiseman, R.L., Lim, A., Costello, C.E., Altland, K., Garzuly, F., Budka, H., and Kelly, J.W. (2003). D18G transthyretin is monomeric, aggregation prone, and not detectable in plasma and cerebrospinal fluid: a prescription for central nervous system amyloidosis? Biochemistry *42*, 6656-6663.

Hampton, R.Y., Gardner, R.G., and Rine, J. (1996). Role of 26S proteasome and HRD genes in the degradation of 3-hydroxy-3-methylglutaryl-CoA reductase, an integral endoplasmic reticulum membrane protein. Mol Biol Cell *7*, 2029-2044.

Harada, Y., Li, H., and Lennarz, W.J. (2009). Oligosaccharyltransferase directly binds to ribosome at a location near the translocon-binding site. Proc Natl Acad Sci U S A *106*, 6945-6949.

Harding, H.P., Novoa, I., Zhang, Y., Zeng, H., Wek, R., Schapira, M., and Ron, D. (2000). Regulated translation initiation controls stress-induced gene expression in mammalian cells. Mol Cell *6*, 1099-1108.

Harding, H.P., Zeng, H., Zhang, Y., Jungries, R., Chung, P., Plesken, H., Sabatini, D.D., and Ron, D. (2001). Diabetes mellitus and exocrine pancreatic dysfunction in perk-/- mice reveals a role for translational control in secretory cell survival. Mol Cell *7*, 1153-1163.

Hartley, T., Siva, M., Lai, E., Teodoro, T., Zhang, L., and Volchuk, A. (2010). Endoplasmic reticulum stress response in an INS-1 pancreatic beta-cell line with inducible expression of a folding-deficient proinsulin. BMC cell biology *11*, 59.

Hartman, I.Z., Liu, P., Zehmer, J.K., Luby-Phelps, K., Jo, Y., Anderson, R.G., and DeBose-Boyd, R.A. (2010a). Sterol-induced dislocation of 3-hydroxy-3-methylglutaryl coenzyme A reductase from endoplasmic reticulum membranes into the cytosol through a subcellular compartment resembling lipid droplets. J Biol Chem *285*, 19288-19298.

Hartman, I.Z., Liu, P.S., Zehmer, J.K., Luby-Phelps, K., Jo, Y., Anderson, R.G.W., and Debose-Boyd, R.A. (2010b). Sterol-induced Dislocation of 3-Hydroxy-3-methylglutaryl Coenzyme A Reductase from Endoplasmic Reticulum Membranes into the Cytosol through a Subcellular Compartment Resembling Lipid Droplets. Journal of Biological Chemistry *285*, 19288-19298.

Haslbeck, M., Ignatiou, A., Saibil, H., Helmich, S., Frenzl, E., Stromer, T., and Buchner, J. (2004). A domain in the N-terminal part of Hsp26 is essential for chaperone function and oligomerization. J Mol Biol *343*, 445-455.

Hassink, G.C., Zhao, B., Sompallae, R., Altun, M., Gastaldello, S., Zinin, N.V., Masucci, M.G., and Lindsten, K. (2009). The ER-resident ubiquitin-specific protease 19 participates in the UPR and rescues ERAD substrates. EMBO reports *10*, 755-761.

Hatahet, F., and Ruddock, L.W. (2007). Substrate recognition by the protein disulfide isomerases. FEBS J *274*, 5223-5234.

Haws, C.M., Nepomuceno, I.B., Krouse, M.E., Wakelee, H., Law, T., Xia, Y., Nguyen, H., and Wine, J.J. (1996). Delta F508-CFTR channels: kinetics, activation by forskolin, and potentiation by xanthines. The American journal of physiology *270*, C1544-1555.

Haze, K., Yoshida, H., Yanagi, H., Yura, T., and Mori, K. (1999). Mammalian transcription factor ATF6 is synthesized as a transmembrane protein and activated by proteolysis in response to endoplasmic reticulum stress. Mol Biol Cell *10*, 3787-3799.

Hebert, D.N., Bernasconi, R., and Molinari, M. (2010). ERAD substrates: which way out? Semin Cell Dev Biol *21*, 526-532.

Hebert, D.N., Foellmer, B., and Helenius, A. (1995). Glucose trimming and reglucosylation determine glycoprotein association with calnexin in the endoplasmic reticulum. Cell *81*, 425-433.

Hebert, D.N., Zhang, J.X., Chen, W., Foellmer, B., and Helenius, A. (1997). The number and location of glycans on influenza hemagglutinin determine folding and association with calnexin and calreticulin. J Cell Biol *139*, 613-623.

Helenius, J., Ng, D.T., Marolda, C.L., Walter, P., Valvano, M.A., and Aebi, M. (2002). Translocation of lipid-linked oligosaccharides across the ER membrane requires Rft1 protein. Nature *415*, 447-450.

Herscovics, A., Romero, P.A., and Tremblay, L.O. (2002). The specificity of the yeast and human class I ER alpha 1,2-mannosidases involved in ER quality control is not as strict previously reported. Glycobiology *12*, 14G-15G.

Hettkamp, H., Legler, G., and Bause, E. (1984). Purification by affinity chromatography of glucosidase I, an endoplasmic reticulum hydrolase involved in the processing of asparagine-linked oligosaccharides. European journal of biochemistry / FEBS *142*, 85-90.

Hicke, L. (1999). Gettin' down with ubiquitin: turning off cell-surface receptors, transporters and channels. Trends Cell Biol *9*, 107-112.

Hicke, L. (2001). Protein regulation by monoubiquitin. Nat Rev Mol Cell Biol *2*, 195-201.

Hicke, L., Schubert, H.L., and Hill, C.P. (2005). Ubiquitin-binding domains. Nat Rev Mol Cell Biol *6*, 610-621.

Hirano, N., Shibasaki, F., Sakai, R., Tanaka, T., Nishida, J., Yazaki, Y., Takenawa, T., and Hirai, H. (1995). Molecular-Cloning of the Human Glucose-Regulated Protein Erp57/Grp58, a Thiol-Dependent Reductase - Identification of Its Secretory Form and Inducible Expression by the Oncogenic Transformation. European Journal of Biochemistry *234*, 336-342.

Hirao, K., Natsuka, Y., Tamura, T., Wada, I., Morito, D., Natsuka, S., Romero, P., Sleno, B., Tremblay, L.O., Herscovics, A.*, et al.* (2006). EDEM3, a soluble EDEM homolog, enhances glycoprotein endoplasmic reticulum-associated degradation and mannose trimming. J Biol Chem *281*, 9650-9658.

Honma, K., Iwao-Koizumi, K., Takeshita, F., Yamamoto, Y., Yoshida, T., Nishio, K., Nagahara, S., Kato, K., and Ochiya, T. (2008). RPN2 gene confers docetaxel resistance in breast cancer. Nat Med *14*, 939-948.

Hori, O., Ichinoda, F., Yamaguchi, A., Tamatani, T., Taniguchi, M., Koyama, Y., Katayama, T., Tohyama, M., Stern, D.M., Ozawa, K.*, et al.* (2004). Role of Herp in the endoplasmic reticulum stress response. Genes to cells : devoted to molecular & cellular mechanisms *9*, 457-469.

Horimoto, S., Ninagawa, S., Okada, T., Koba, H., Sugimoto, T., Kamiya, Y., Kato, K., Takeda, S., and Mori, K. (2013). The unfolded protein response transducer ATF6 represents a novel transmembrane-type endoplasmic reticulum-associated degradation substrate requiring both mannose trimming and SEL1L. J Biol Chem.

Horn, S.C., Hanna, J., Hirsch, C., Volkwein, C., Schutz, A., Heinemann, U., Sommer, T., and Jarosch, E. (2009). Usa1 Functions as a Scaffold of the HRD-Ubiquitin Ligase. Molecular Cell *36*, 782-793.

Hosoda, A., Kimata, Y., Tsuru, A., and Kohno, K. (2003). JPDI, a novel endoplasmic reticulum-resident protein containing both a BiP-interacting J-domain and thioredoxin-like motifs. J Biol Chem *278*, 2669-2676.

Hosokawa, N., Kamiya, Y., Kamiya, D., Kato, K., and Nagata, K. (2009a). Human OS-9, a lectin required for glycoprotein endoplasmic reticulum-associated degradation, recognizes mannose-trimmed N-glycans. J Biol Chem *284*, 17061-17068.

Hosokawa, N., Kamiya, Y., Kamiya, D., Kato, K., and Nagata, K. (2009b). Human OS-9, a Lectin Required for Glycoprotein Endoplasmic Reticulum-associated Degradation, Recognizes Mannose-trimmed N-Glycans. Journal of Biological Chemistry *284*, 17061-17068.

Hosokawa, N., Tremblay, L.O., Sleno, B., Kamiya, Y., Wada, I., Nagata, K., Kato, K., and Herscovics, A. (2010). EDEM1 accelerates the trimming of alpha1,2-linked mannose on the C branch of N-glycans. Glycobiology *20*, 567-575.

Hosokawa, N., Tremblay, L.O., You, Z., Herscovics, A., Wada, I., and Nagata, K. (2003). Enhancement of endoplasmic reticulum (ER) degradation of misfolded Null Hong Kong alpha1-antitrypsin by human ER mannosidase I. J Biol Chem *278*, 26287-26294.

Hosokawa, N., Wada, I., Hasegawa, K., Yorihuzi, T., Tremblay, L.O., Herscovics, A., and Nagata, K. (2001). A novel ER alpha-mannosidase-like protein accelerates ER-associated degradation. EMBO reports *2*, 415-422.

Hosokawa, N., Wada, I., Nagasawa, K., Moriyama, T., Okawa, K., and Nagata, K. (2008). Human XTP3-B forms an endoplasmic reticulum quality control scaffold with the HRD1-SEL1L ubiquitin ligase complex and BiP. J Biol Chem *283*, 20914-20924.

Hu, J., Li, J., Qian, X., Denic, V., and Sha, B. (2009). The crystal structures of yeast Get3 suggest a mechanism for tail-anchored protein membrane insertion. PLoS One *4*, e8061.

Hua, Z., and Vierstra, R.D. (2011). The cullin-RING ubiquitin-protein ligases. Annual review of plant biology *62*, 299-334.

Huang, C.H., Hsiao, H.T., Chu, Y.R., Ye, Y., and Chen, X. (2013). Derlin2 facilitates HRD1-mediated retro-translocation of sonic hedgehog at the endoplasmic reticulum. J Biol Chem.

Hubener, J., Vauti, F., Funke, C., Wolburg, H., Ye, Y.H., Schmidt, T., Wolburg-Buchholz, K., Schmitt, I., Gardyan, A., Driessen, S*., et al.* (2011). N-terminal ataxin-3 causes neurological symptoms with inclusions, endoplasmic reticulum stress and ribosomal dislocation. Brain *134*, 1925-1942.

Huntington, J.A., Read, R.J., and Carrell, R.W. (2000). Structure of a serpin-protease complex shows inhibition by deformation. Nature *407*, 923-926.

Husnjak, K., Elsasser, S., Zhang, N., Chen, X., Randles, L., Shi, Y., Hofmann, K., Walters, K.J., Finley, D., and Dikic, I. (2008). Proteasome subunit Rpn13 is a novel ubiquitin receptor. Nature *453*, 481-488.

Hussain, M.M., Shi, J., and Dreizen, P. (2003). Microsomal triglyceride transfer protein and its role in apoB-lipoprotein assembly. J Lipid Res *44*, 22-32.

Hwang, C., Sinskey, A.J., and Lodish, H.F. (1992). Oxidized redox state of glutathione in the endoplasmic reticulum. Science *257*, 1496-1502.

Iida, Y., Fujimori, T., Okawa, K., Nagata, K., Wada, I., and Hosokawa, N. (2011). SEL1L Protein Critically Determines the Stability of the HRD1-SEL1L Endoplasmic Reticulum-associated Degradation (ERAD) Complex to Optimize the Degradation Kinetics of ERAD Substrates. J Biol Chem *286*, 16929-16939.

Imai, Y., Soda, M., Inoue, H., Hattori, N., Mizuno, Y., and Takahashi, R. (2001). An unfolded putative transmembrane polypeptide, which can lead to endoplasmic reticulum stress, is a substrate of Parkin. Cell *105*, 891-902.

Inaba, K., Masui, S., Iida, H., Vavassori, S., Sitia, R., and Suzuki, M. (2010). Crystal structures of human Ero1alpha reveal the mechanisms of regulated and targeted oxidation of PDI. EMBO J *29*, 3330-3343.

Ishikura, S., Weissman, A.M., and Bonifacino, J.S. (2010). Serine residues in the cytosolic tail of the T-cell antigen receptor alpha-chain mediate ubiquitination and endoplasmic reticulum-associated degradation of the unassembled protein. J Biol Chem *285*, 23916-23924.

Iwawaki, T., Hosoda, A., Okuda, T., Kamigori, Y., Nomura-Furuwatari, C., Kimata, Y., Tsuru, A., and Kohno, K. (2001). Translational control by the ER transmembrane kinase/ribonuclease IRE1 under ER stress. Nat Cell Biol *3*, 158-164.

Jager, M., and Pluckthun, A. (1997). The rate-limiting steps for the folding of an antibody scFv fragment. FEBS Lett *418*, 106-110.

Jamain, S., Girondot, M., Leroy, P., Clergue, M., Quach, H., Fellous, M., and Bourgeron, T. (2001). Transduction of the human gene FAM8A1 by endogenous retrovirus during primate evolution. Genomics *78*, 38-45.

Jambunathan, S., Yin, J., Khan, W., Tamori, Y., and Puri, V. (2011). FSP27 promotes lipid droplet clustering and then fusion to regulate triglyceride accumulation. PLoS One *6*, e28614.

Jang, W., Weber, J.S., Bashir, R., Bushby, K., and Meisler, M.H. (1996). Aup1, a novel gene on mouse chromosome 6 and human chromosome 2p13. Genomics *36*, 366-368.

Jarosch, E., Taxis, C., Volkwein, C., Bordallo, J., Finley, D., Wolf, D.H., and Sommer, T. (2002). Protein dislocation from the ER requires polyubiquitination and the AAA-ATPase Cdc48. Nat Cell Biol *4*, 134-139.

Jaya, N., Garcia, V., and Vierling, E. (2009). Substrate binding site flexibility of the small heat shock protein molecular chaperones. Proc Natl Acad Sci U S A *106*, 15604-15609.

Jessop, C.E., Chakravarthi, S., Garbi, N., Hammerling, G.J., Lovell, S., and Bulleid, N.J. (2007). ERp57 is essential for efficient folding of glycoproteins sharing common structural domains. EMBO J *26*, 28-40.

Jessop, C.E., Watkins, R.H., Simmons, J.J., Tasab, M., and Bulleid, N.J. (2009). Protein disulphide isomerase family members show distinct substrate specificity: P5 is targeted to BiP client proteins. J Cell Sci *122*, 4287-4295.

Jin, Y.J., Cai, C.Y., Zhang, X., Zhang, H.T., Hirst, J.A., and Burakoff, S.J. (2005). HIV Nef-mediated CD4 down-regulation is adaptor protein complex 2 dependent. J Immunol *175*, 3157-3164.

Jo, Y., Hartman, I.Z., and DeBose-Boyd, R.A. (2013). Ancient ubiquitous protein-1 mediates sterol-induced ubiquitination of 3-hydroxy-3-methylglutaryl CoA reductase in lipid droplet-associated endoplasmic reticulum membranes. Mol Biol Cell *24*, 169-183.

Jo, Y., Lee, P.C., Sguigna, P.V., and DeBose-Boyd, R.A. (2011). Sterol-induced degradation of HMG CoA reductase depends on interplay of two Insigs and two ubiquitin ligases, gp78 and Trc8. Proc Natl Acad Sci U S A *108*, 20503-20508.

Joazeiro, C.A., Wing, S.S., Huang, H., Leverson, J.D., Hunter, T., and Liu, Y.C. (1999). The tyrosine kinase negative regulator c-Cbl as a RING-type, E2-dependent ubiquitin-protein ligase. Science *286*, 309-312.

Jones, S., and Thornton, J.M. (1995). Protein-protein interactions: a review of protein dimer structures. Progress in biophysics and molecular biology *63*, 31-65.

Jonikas, M.C., Collins, S.R., Denic, V., Oh, E., Quan, E.M., Schmid, V., Weibezahn, J., Schwappach, B., Walter, P., Weissman, J.S*., et al.* (2009). Comprehensive characterization of genes required for protein folding in the endoplasmic reticulum. Science *323*, 1693-1697.

Kabashima, K., Haynes, N.M., Xu, Y., Nutt, S.L., Allende, M.L., Proia, R.L., and Cyster, J.G. (2006). Plasma cell S1P1 expression determines secondary lymphoid organ retention versus bone marrow tropism. J Exp Med *203*, 2683-2690.

Kaether, C., Schmitt, S., Willem, M., and Haass, C. (2006). Amyloid precursor protein and Notch intracellular domains are generated after transport of their precursors to the cell surface. Traffic *7*, 408-415.

Kalbfleisch, T., Cambon, A., and Wattenberg, B.W. (2007). A bioinformatics approach to identifying tail-anchored proteins in the human genome. Traffic *8*, 1687-1694.

Kalz-Fuller, B., Bieberich, E., and Bause, E. (1995). Cloning and expression of glucosidase I from human hippocampus. European journal of biochemistry / FEBS *231*, 344-351.

Kamura, T., Koepp, D.M., Conrad, M.N., Skowyra, D., Moreland, R.J., Iliopoulos, O., Lane, W.S., Kaelin, W.G., Jr., Elledge, S.J., Conaway, R.C*., et al.* (1999). Rbx1, a component of the VHL tumor suppressor complex and SCF ubiquitin ligase. Science *284*, 657-661.

Kanapin, A., Batalov, S., Davis, M.J., Gough, J., Grimmond, S., Kawaji, H., Magrane, M., Matsuda, H., Schonbach, C., Teasdale, R.D*., et al.* (2003). Mouse proteome analysis. Genome research *13*, 1335-1344.

Kaneko, M., Koike, H., Saito, R., Kitamura, Y., Okuma, Y., and Nomura, Y. (2010). Loss of HRD1-mediated protein degradation causes amyloid precursor protein accumulation and amyloid-beta generation. J Neurosci *30*, 3924-3932.

Kaneko, M., Niinuma, Y., and Nomura, Y. (2003). Activation signal of nuclear factor-kappa B in response to endoplasmic reticulum stress is transduced via IRE1 and tumor necrosis factor receptor-associated factor 2. Biological & pharmaceutical bulletin *26*, 931-935.

Kaneko, M., Takahashi, T., Niinuma, Y., and Nomura, Y. (2004). Manganese superoxide dismutase is induced by endoplasmic reticulum stress through IRE1-mediated nuclear factor (NF)-kappaB and AP-1 activation. Biological & pharmaceutical bulletin *27*, 1202-1206.

Kaneko, M., Yasui, S., Niinuma, Y., Arai, K., Omura, T., Okuma, Y., and Nomura, Y. (2007). A different pathway in the endoplasmic reticulum stress-induced expression of human HRD1 and SEL1 genes. FEBS Lett *581*, 5355-5360.

Kang, R.S., Daniels, C.M., Francis, S.A., Shih, S.C., Salerno, W.J., Hicke, L., and Radhakrishnan, I. (2003). Solution structure of a CUE-ubiquitin complex reveals a conserved mode of ubiquitin binding. Cell *113*, 621-630.

Kapoor, M., Ellgaard, L., Gopalakrishnapai, J., Schirra, C., Gemma, E., Oscarson, S., Helenius, A., and Surolia, A. (2004). Mutational analysis provides molecular insight into the carbohydrate-binding region of calreticulin: pivotal roles of tyrosine-109 and aspartate-135 in carbohydrate recognition. Biochemistry *43*, 97-106.

Kass, I., Knaupp, A.S., Bottomley, S.P., and Buckle, A.M. (2012). Conformational properties of the disease-causing Z variant of alpha1-antitrypsin revealed by theory and experiment. Biophysical journal *102*, 2856-2865.

Katiyar, S., Joshi, S., and Lennarz, W.J. (2005). The retrotranslocation protein Derlin-1 binds peptide:N-glycanase to the endoplasmic reticulum. Mol Biol Cell *16*, 4584-4594.

Kato, A., Kawamata, N., Tamayose, K., Egashira, M., Miura, R., Fujimura, T., Murayama, K., and Oshimi, K. (2002). Ancient ubiquitous protein 1 binds to the conserved membrane-proximal sequence of the cytoplasmic tail of the integrin alpha subunits that plays a crucial role in the inside-out signaling of alpha IIbbeta 3. J Biol Chem *277*, 28934-28941.

Kato, A., and Oshimi, K. (2009). Ancient ubiquitous protein 1 and Syk link cytoplasmic tails of the integrin alpha(IIb)beta(3). Platelets *20*, 105-110.

Kelleher, D.J., Karaoglu, D., Mandon, E.C., and Gilmore, R. (2003). Oligosaccharyltransferase isoforms that contain different catalytic STT3 subunits have distinct enzymatic properties. Mol Cell *12*, 101-111.

Kemmink, J., Darby, N.J., Dijkstra, K., Nilges, M., and Creighton, T.E. (1996). Structure determination of the N-terminal thioredoxin-like domain of protein disulfide isomerase using multidimensional heteronuclear 13C/15N NMR spectroscopy. Biochemistry *35*, 7684-7691.

Kemmink, J., Darby, N.J., Dijkstra, K., Nilges, M., and Creighton, T.E. (1997). The folding catalyst protein disulfide isomerase is constructed of active and inactive thioredoxin modules. Curr Biol *7*, 239-245.

Kikkert, M., Doolman, R., Dai, M., Avner, R., Hassink, G., van Voorden, S., Thanedar, S., Roitelman, J., Chau, V., and Wiertz, E. (2004). Human HRD1 is an E3 ubiquitin ligase involved in degradation of proteins from the endoplasmic reticulum. J Biol Chem *279*, 3525-3534.

Kim, B.W., Zavacki, A.M., Curcio-Morelli, C., Dentice, M., Harney, J.W., Larsen, P.R., and Bianco, A.C. (2003). Endoplasmic reticulum-associated degradation of the human type 2 iodothyronine deiodinase (D2) is mediated via an association between mammalian UBC7 and the carboxyl region of D2. Mol Endocrinol *17*, 2603-2612.

Kim, S.M., Acharya, P., Engel, J.C., and Correia, M.A. (2010). Liver cytochrome P450 3A ubiquitination in vivo by gp78/autocrine motility factor receptor and C terminus of Hsp70-interacting protein (CHIP) E3 ubiquitin ligases: physiological and pharmacological relevance. J Biol Chem *285*, 35866-35877.

Kim, T.Y., Kim, E., Yoon, S.K., and Yoon, J.B. (2008). Herp enhances ER-associated protein degradation by recruiting ubiquilins. Biochem Biophys Res Commun *369*, 741-746.

Kim, W., Bennett, E.J., Huttlin, E.L., Guo, A., Li, J., Possemato, A., Sowa, M.E., Rad, R., Rush, J., Comb, M.J*., et al.* (2011). Systematic and quantitative assessment of the ubiquitin-modified proteome. Mol Cell *44*, 325-340.

Kinoshita, A., Fukumoto, H., Shah, T., Whelan, C.M., Irizarry, M.C., and Hyman, B.T. (2003). Demonstration by FRET of BACE interaction with the amyloid precursor protein at the cell surface and in early endosomes. J Cell Sci *116*, 3339-3346.

Kislinger, T., Cox, B., Kannan, A., Chung, C., Hu, P., Ignatchenko, A., Scott, M.S., Gramolini, A.O., Morris, Q., Hallett, M.T.*, et al.* (2006). Global survey of organ and organelle protein expression in mouse: combined proteomic and transcriptomic profiling. Cell *125*, 173-186.

Klappa, P., Ruddock, L.W., Darby, N.J., and Freedman, R.B. (1998). The b' domain provides the principal peptide-binding site of protein disulfide isomerase but all domains contribute to binding of misfolded proteins. EMBO J *17*, 927-935.

Klatzmann, D., Champagne, E., Chamaret, S., Gruest, J., Guetard, D., Hercend, T., Gluckman, J.C., and Montagnier, L. (1984). T-lymphocyte T4 molecule behaves as the receptor for human retrovirus LAV. Nature *312*, 767-768.

Klausner, R.D., Lippincott-Schwartz, J., and Bonifacino, J.S. (1990). The T cell antigen receptor: insights into organelle biology. Annual review of cell biology *6*, 403-431.

Klemm, E.J., Spooner, E., and Ploegh, H.L. (2011). Dual role of ancient ubiquitous protein 1 (AUP1) in lipid droplet accumulation and endoplasmic reticulum (ER) protein quality control. J Biol Chem *286*, 37602-37614.

Knop, M., Finger, A., Braun, T., Hellmuth, K., and Wolf, D.H. (1996). Der1, a novel protein specifically required for endoplasmic reticulum degradation in yeast. EMBO J *15*, 753-763.

Kny, M., Standera, S., Hartmann-Petersen, R., Kloetzel, P.M., and Seeger, M. (2011). Herp regulates Hrd1-mediated ubiquitylation in a ubiquitin-like domain-dependent manner. J Biol Chem *286*, 5151-5156.

Koegl, M., Hoppe, T., Schlenker, S., Ulrich, H.D., Mayer, T.U., and Jentsch, S. (1999). A novel ubiquitination factor, E4, is involved in multiubiquitin chain assembly. Cell *96*, 635-644.

Kokame, K., Agarwala, K.L., Kato, H., and Miyata, T. (2000). Herp, a new ubiquitin-like membrane protein induced by endoplasmic reticulum stress. J Biol Chem *275*, 32846-32853.

Kokame, K., Kato, H., and Miyata, T. (2001). Identification of ERSE-II, a new cis-acting element responsible for the ATF6-dependent mammalian unfolded protein response. J Biol Chem *276*, 9199-9205.

Kornfeld, S., and Mellman, I. (1989). The biogenesis of lysosomes. Annual review of cell biology *5*, 483-525.

Kostova, Z., Mariano, J., Scholz, S., Koenig, C., and Weissman, A.M. (2009). A Ubc7p-binding domain in Cue1p activates ER-associated protein degradation. J Cell Sci *122*, 1374-1381.

Kriechbaumer, V., Shaw, R., Mukherjee, J., Bowsher, C.G., Harrison, A.M., and Abell, B.M. (2009). Subcellular distribution of tail-anchored proteins in Arabidopsis. Traffic *10*, 1753-1764.

Lauffer, L., Garcia, P.D., Harkins, R.N., Coussens, L., Ullrich, A., and Walter, P. (1985). Topology of signal recognition particle receptor in endoplasmic reticulum membrane. Nature *318*, 334-338.

Lazar, C., Macovei, A., Petrescu, S., and Branza-Nichita, N. (2012). Activation of ERAD pathway by human hepatitis B virus modulates viral and subviral particle production. PLoS One *7*, e34169.

Le Fourn, V., Gaplovska-Kysela, K., Guhl, B., Santimaria, R., Zuber, C., and Roth, J. (2009). Basal autophagy is involved in the degradation of the ERAD component EDEM1. Cell Mol Life Sci *66*, 1434-1445.

Lee, J.N., Song, B., DeBose-Boyd, R.A., and Ye, J. (2006). Sterol-regulated degradation of Insig-1 mediated by the membrane-bound ubiquitin ligase gp78. J Biol Chem *281*, 39308-39315.

Lee, K.A., Hammerle, L.P., Andrews, P.S., Stokes, M.P., Mustelin, T., Silva, J.C., Black, R.A., and Doedens, J.R. (2011). Ubiquitin ligase substrate identification through quantitative proteomics at both the protein and peptide levels. J Biol Chem *286*, 41530-41538.

Lenk, U., Yu, H., Walter, J., Gelman, M.S., Hartmann, E., Kopito, R.R., and Sommer, T. (2002). A role for mammalian Ubc6 homologues in ER-associated protein degradation. J Cell Sci *115*, 3007-3014.

Levesque, K., Zhao, Y.S., and Cohen, E.A. (2003). Vpu exerts a positive effect on HIV-1 infectivity by down-modulating CD4 receptor molecules at the surface of HIV-1-producing cells. J Biol Chem *278*, 28346-28353.

Levkowitz, G., Waterman, H., Ettenberg, S.A., Katz, M., Tsygankov, A.Y., Alroy, I., Lavi, S., Iwai, K., Reiss, Y., Ciechanover, A*., et al.* (1999). Ubiquitin ligase activity and tyrosine phosphorylation underlie suppression of growth factor signaling by c-Cbl/Sli-1. Mol Cell *4*, 1029-1040.

Leznicki, P., Clancy, A., Schwappach, B., and High, S. (2010). Bat3 promotes the membrane integration of tail-anchored proteins. J Cell Sci *123*, 2170-2178.

Li, G., Zhao, G., Zhou, X., Schindelin, H., and Lennarz, W.J. (2006). The AAA ATPase p97 links peptide N-glycanase to the endoplasmic reticulum-associated E3 ligase autocrine motility factor receptor. Proc Natl Acad Sci U S A *103*, 8348-8353.

Li, H., Korennykh, A.V., Behrman, S.L., and Walter, P. (2010). Mammalian endoplasmic reticulum stress sensor IRE1 signals by dynamic clustering. Proc Natl Acad Sci U S A *107*, 16113-16118.

Li, W., Bengtson, M.H., Ulbrich, A., Matsuda, A., Reddy, V.A., Orth, A., Chanda, S.K., Batalov, S., and Joazeiro, C.A. (2008). Genome-wide and functional annotation of human E3 ubiquitin ligases identifies MULAN, a mitochondrial E3 that regulates the organelle's dynamics and signaling. PLoS One *3*, e1487.

Li, W., Tu, D., Brunger, A.T., and Ye, Y. (2007). A ubiquitin ligase transfers preformed polyubiquitin chains from a conjugating enzyme to a substrate. Nature *446*, 333-337.

Liang, J., Yin, C., Doong, H., Fang, S., Peterhoff, C., Nixon, R.A., and Monteiro, M.J. (2006). Characterization of erasin (UBXD2): a new ER protein that promotes ER-associated protein degradation. J Cell Sci *119*, 4011-4024.

Liberek, K., Marszalek, J., Ang, D., Georgopoulos, C., and Zylicz, M. (1991). Escherichia coli DnaJ and GrpE heat shock proteins jointly stimulate ATPase activity of DnaK. Proc Natl Acad Sci U S A *88*, 2874-2878.

Liew, C.W., Sun, H., Hunter, T., and Day, C.L. (2010). RING domain dimerization is essential for RNF4 function. Biochem J *431*, 23-29.

Lilley, B.N., Gilbert, J.M., Ploegh, H.L., and Benjamin, T.L. (2006). Murine polyomavirus requires the endoplasmic reticulum protein Derlin-2 to initiate infection. Journal of virology *80*, 8739-8744.

Lilley, B.N., and Ploegh, H.L. (2004). A membrane protein required for dislocation of misfolded proteins from the ER. Nature *429*, 834-840.

Lilley, B.N., and Ploegh, H.L. (2005). Multiprotein complexes that link dislocation, ubiquitination, and extraction of misfolded proteins from the endoplasmic reticulum membrane. Proc Natl Acad Sci U S A *102*, 14296-14301.

Lindwasser, O.W., Smith, W.J., Chaudhuri, R., Yang, P., Hurley, J.H., and Bonifacino, J.S. (2008). A diacidic motif in human immunodeficiency virus type 1 Nef is a novel determinant of binding to AP-2. Journal of virology *82*, 1166-1174.

Linke, K., Mace, P.D., Smith, C.A., Vaux, D.L., Silke, J., and Day, C.L. (2008). Structure of the MDM2/MDMX RING domain heterodimer reveals dimerization is required for their ubiquitylation in trans. Cell Death Differ *15*, 841-848.

Lippincott-Schwartz, J., Bonifacino, J.S., Yuan, L.C., and Klausner, R.D. (1988). Degradation from the endoplasmic reticulum: disposing of newly synthesized proteins. Cell *54*, 209-220.

Lohmann, D., Spandl, J., Stevanovic, A., Schoene, M., Philippou-Massier, J., and Thiele, C. (2013). Monoubiquitination of ancient ubiquitous protein 1 promotes lipid droplet clustering. PLoS One *8*, e72453.

Lok, G.T., Sy, S.M., Dong, S.S., Ching, Y.P., Tsao, S.W., Thomson, T.M., and Huen, M.S. (2012). Differential regulation of RNF8-mediated Lys48- and Lys63-based poly-ubiquitylation. Nucleic acids research *40*, 196-205.

Lorick, K.L., Jensen, J.P., Fang, S., Ong, A.M., Hatakeyama, S., and Weissman, A.M. (1999). RING fingers mediate ubiquitin-conjugating enzyme (E2)-dependent ubiquitination. Proc Natl Acad Sci U S A *96*, 11364-11369.

Loureiro, J., Lilley, B.N., Spooner, E., Noriega, V., Tortorella, D., and Ploegh, H.L. (2006). Signal peptide peptidase is required for dislocation from the endoplasmic reticulum. Nature *441*, 894-897.

Lovering, R., Hanson, I.M., Borden, K.L., Martin, S., O'Reilly, N.J., Evan, G.I., Rahman, D., Pappin, D.J., Trowsdale, J., and Freemont, P.S. (1993). Identification and preliminary characterization of a protein motif related to the zinc finger. Proc Natl Acad Sci U S A *90*, 2112-2116.

Luo, D., He, Y., Zhang, H., Yu, L., Chen, H., Xu, Z., Tang, S., Urano, F., and Min, W. (2008). AIP1 is critical in transducing IRE1-mediated endoplasmic reticulum stress response. J Biol Chem *283*, 11905-11912.

Ma, Y., Brewer, J.W., Diehl, J.A., and Hendershot, L.M. (2002). Two distinct stress signaling pathways converge upon the CHOP promoter during the mammalian unfolded protein response. J Mol Biol *318*, 1351-1365.

Mace, P.D., Linke, K., Feltham, R., Schumacher, F.R., Smith, C.A., Vaux, D.L., Silke, J., and Day, C.L. (2008). Structures of the cIAP2 RING domain reveal conformational changes associated with ubiquitin-conjugating enzyme (E2) recruitment. J Biol Chem *283*, 31633-31640.

Magadan, J.G., and Bonifacino, J.S. (2012). Transmembrane domain determinants of CD4 Downregulation by HIV-1 Vpu. Journal of virology *86*, 757-772.

Magadan, J.G., Perez-Victoria, F.J., Sougrat, R., Ye, Y., Strebel, K., and Bonifacino, J.S. (2010). Multilayered mechanism of CD4 downregulation by HIV-1 Vpu involving distinct ER retention and ERAD targeting steps. PLoS pathogens *6*, e1000869.

Marcinkiewicz, A., Gauthier, D., Garcia, A., and Brasaemle, D.L. (2006). The phosphorylation of serine 492 of perilipin a directs lipid droplet fragmentation and dispersion. J Biol Chem *281*, 11901-11909.

Margottin, F., Benichou, S., Durand, H., Richard, V., Liu, L.X., Gomas, E., and Benarous, R. (1996). Interaction between the cytoplasmic domains of HIV-1 Vpu and CD4: role of Vpu residues involved in CD4 interaction and in vitro CD4 degradation. Virology *223*, 381-386.

Mariappan, M., Li, X., Stefanovic, S., Sharma, A., Mateja, A., Keenan, R.J., and Hegde, R.S. (2010). A ribosome-associating factor chaperones tail-anchored membrane proteins. Nature *466*, 1120-1124.

Mariappan, M., Mateja, A., Dobosz, M., Bove, E., Hegde, R.S., and Keenan, R.J. (2011). The mechanism of membrane-associated steps in tail-anchored protein insertion. Nature *477*, 61-66.

Marin, M.B., Ghenea, S., Spiridon, L.N., Chiritoiu, G.N., Petrescu, A.J., and Petrescu, S.M. (2012). Tyrosinase degradation is prevented when EDEM1 lacks the intrinsically disordered region. PLoS One *7*, e42998.

Marzella, L., and Glaumann, H. (1983). Biogenesis, translocation, and function of lysosomal enzymes. International review of experimental pathology *25*, 239-278.

Mast, S.W., Diekman, K., Karaveg, K., Davis, A., Sifers, R.N., and Moremen, K.W. (2005). Human EDEM2, a novel homolog of family 47 glycosidases, is involved in ER-associated degradation of glycoproteins. Glycobiology *15*, 421-436.

Masters, C.L., Simms, G., Weinman, N.A., Multhaup, G., McDonald, B.L., and Beyreuther, K. (1985). Amyloid plaque core protein in Alzheimer disease and Down syndrome. Proc Natl Acad Sci U S A *82*, 4245-4249.

Mateja, A., Szlachcic, A., Downing, M.E., Dobosz, M., Mariappan, M., Hegde, R.S., and Keenan, R.J. (2009). The structural basis of tail-anchored membrane protein recognition by Get3. Nature *461*, 361-366.

Matlack, K.E., Misselwitz, B., Plath, K., and Rapoport, T.A. (1999). BiP acts as a molecular ratchet during posttranslational transport of prepro-alpha factor across the ER membrane. Cell *97*, 553-564.

Merlie, J.P., and Lindstrom, J. (1983). Assembly in vivo of mouse muscle acetylcholine receptor: identification of an alpha subunit species that may be an assembly intermediate. Cell *34*, 747-757.

Metzger, M.B., Liang, Y.H., Das, R., Mariano, J., Li, S., Li, J., Kostova, Z., Byrd, R.A., Ji, X., and Weissman, A.M. (2013). A structurally unique E2-binding domain activates ubiquitination by the ERAD E2, Ubc7p, through multiple mechanisms. Mol Cell *50*, 516-527.

Meunier, L., Usherwood, Y.K., Chung, K.T., and Hendershot, L.M. (2002). A subset of chaperones and folding enzymes form multiprotein complexes in endoplasmic reticulum to bind nascent proteins. Mol Biol Cell *13*, 4456-4469.

Meyer, H.H., Shorter, J.G., Seemann, J., Pappin, D., and Warren, G. (2000). A complex of mammalian ufd1 and npl4 links the AAA-ATPase, p97, to ubiquitin and nuclear transport pathways. EMBO J *19*, 2181-2192.

Mikami, K., Yamaguchi, D., Tateno, H., Hu, D., Qin, S.Y., Kawasaki, N., Yamada, M., Matsumoto, N., Hirabayashi, J., Ito, Y.*, et al.* (2010). The sugar-binding ability of human OS-9 and its involvement in ER-associated degradation. Glycobiology *20*, 310-321.

Miller, J.D., Wilhelm, H., Gierasch, L., Gilmore, R., and Walter, P. (1993). GTP binding and hydrolysis by the signal recognition particle during initiation of protein translocation. Nature *366*, 351-354.

Minami, Y., Samelson, L.E., and Klausner, R.D. (1987). Internalization and cycling of the T cell antigen receptor. Role of protein kinase C. J Biol Chem *262*, 13342-13347.

Mitra, N., Sinha, S., Ramya, T.N., and Surolia, A. (2006). N-linked oligosaccharides as outfitters for glycoprotein folding, form and function. Trends Biochem Sci *31*, 156-163.

Mize, N.K., Andrews, D.W., and Lingappa, V.R. (1986). A stop transfer sequence recognizes receptors for nascent chain translocation across the endoplasmic reticulum membrane. Cell *47*, 711-719.

Molinari, M., Calanca, V., Galli, C., Lucca, P., and Paganetti, P. (2003). Role of EDEM in the release of misfolded glycoproteins from the calnexin cycle. Science *299*, 1397-1400.

Molinari, M., Eriksson, K.K., Calanca, V., Galli, C., Cresswell, P., Michalak, M., and Helenius, A. (2004). Contrasting functions of calreticulin and calnexin in glycoprotein folding and ER quality control. Mol Cell *13*, 125-135.

Molinari, M., and Helenius, A. (2000). Chaperone selection during glycoprotein translocation into the endoplasmic reticulum. Science *288*, 331-333.

Mueller, B., Klemm, E.J., Spooner, E., Claessen, J.H., and Ploegh, H.L. (2008). SEL1L nucleates a protein complex required for dislocation of misfolded glycoproteins. Proc Natl Acad Sci U S A *105*, 12325-12330.

Mueller, B., Lilley, B.N., and Ploegh, H.L. (2006). SEL1L, the homologue of yeast Hrd3p, is involved in protein dislocation from the mammalian ER. J Cell Biol *175*, 261-270.

Murphy, L.A., Ramirez, E.A., Trinh, V.T., Herman, A.M., Anderson, V.C., and Brewster, J.L. (2011). Endoplasmic reticulum stress or mutation of an EF-hand Ca(2+)-binding domain directs the FKBP65 rotamase to an ERAD-based proteolysis. Cell stress & chaperones *16*, 607-619.

Nadav, E., Shmueli, A., Barr, H., Gonen, H., Ciechanover, A., and Reiss, Y. (2003). A novel mammalian endoplasmic reticulum ubiquitin ligase homologous to the yeast Hrd1. Biochem Biophys Res Commun *303*, 91-97.

Nakanishi, M., Goldstein, J.L., and Brown, M.S. (1988). Multivalent control of 3-hydroxy-3-methylglutaryl coenzyme A reductase. Mevalonate-derived product inhibits translation of mRNA and accelerates degradation of enzyme. J Biol Chem *263*, 8929-8937.

Neutzner, A., Neutzner, M., Benischke, A.S., Ryu, S.W., Frank, S., Youle, R.J., and Karbowski, M. (2011). A systematic search for endoplasmic reticulum (ER) membrane-associated RING finger proteins identifies Nixin/ZNRF4 as a regulator of calnexin stability and ER homeostasis. J Biol Chem *286*, 8633-8643.

Ng, W., Sergeyenko, T., Zeng, N., Brown, J.D., and Romisch, K. (2007). Characterization of the proteasome interaction with the Sec61 channel in the endoplasmic reticulum. J Cell Sci *120*, 682-691.

Nilsson, I., Kelleher, D.J., Miao, Y., Shao, Y., Kreibich, G., Gilmore, R., von Heijne, G., and Johnson, A.E. (2003). Photocross-linking of nascent chains to the STT3 subunit of the oligosaccharyltransferase complex. J Cell Biol *161*, 715-725.

Nilsson, I.M., and von Heijne, G. (1993). Determination of the distance between the oligosaccharyltransferase active site and the endoplasmic reticulum membrane. J Biol Chem *268*, 5798-5801.

Nishitoh, H., Matsuzawa, A., Tobiume, K., Saegusa, K., Takeda, K., Inoue, K., Hori, S., Kakizuka, A., and Ichijo, H. (2002). ASK1 is essential for endoplasmic reticulum stress-induced neuronal cell death triggered by expanded polyglutamine repeats. Genes Dev *16*, 1345-1355.

Novoa, I., Zeng, H., Harding, H.P., and Ron, D. (2001). Feedback inhibition of the unfolded protein response by GADD34-mediated dephosphorylation of eIF2alpha. J Cell Biol *153*, 1011-1022.

Oda, Y., Hosokawa, N., Wada, I., and Nagata, K. (2003). EDEM as an acceptor of terminally misfolded glycoproteins released from calnexin. Science *299*, 1394-1397.

Oda, Y., Okada, T., Yoshida, H., Kaufman, R.J., Nagata, K., and Mori, K. (2006). Derlin-2 and Derlin-3 are regulated by the mammalian unfolded protein response and are required for ER-associated degradation. J Cell Biol *172*, 383-393.

Ohsaki, Y., Cheng, J., Fujita, A., Tokumoto, T., and Fujimoto, T. (2006). Cytoplasmic lipid droplets are sites of convergence of proteasomal and autophagic degradation of apolipoprotein B. Mol Biol Cell *17*, 2674-2683.

Ohta, T., Michel, J.J., Schottelius, A.J., and Xiong, Y. (1999). ROC1, a homolog of APC11, represents a family of cullin partners with an associated ubiquitin ligase activity. Mol Cell *3*, 535-541.

Okuda-Shimizu, Y., and Hendershot, L.M. (2007). Characterization of an ERAD pathway for nonglycosylated BiP substrates, which require Herp. Mol Cell *28*, 544-554.

Olivari, S., Cali, T., Salo, K.E., Paganetti, P., Ruddock, L.W., and Molinari, M. (2006). EDEM1 regulates ER-associated degradation by accelerating de-mannosylation of folding-defective polypeptides and by inhibiting their covalent aggregation. Biochem Biophys Res Commun *349*, 1278-1284.

Olivari, S., Galli, C., Alanen, H., Ruddock, L., and Molinari, M. (2005). A novel stress-induced EDEM variant regulating endoplasmic reticulum-associated glycoprotein degradation. J Biol Chem *280*, 2424-2428.

Oliver, J.D., van der Wal, F.J., Bulleid, N.J., and High, S. (1997). Interaction of the thiol-dependent reductase ERp57 with nascent glycoproteins. Science *275*, 86-88.

Olofsson, S.O., Asp, L., and Boren, J. (1999). The assembly and secretion of apolipoprotein B-containing lipoproteins. Current opinion in lipidology *10*, 341-346.

Olzmann, J.A., and Kopito, R.R. (2011). Lipid Droplet Formation Is Dispensable for Endoplasmic Reticulum-associated Degradation. J Biol Chem *286*, 27872-27874.

Omura, F., Otsu, M., Yoshimori, T., Tashiro, Y., and Kikuchi, M. (1992). Non-lysosomal degradation of misfolded human lysozymes with and without an asparagine-linked glycosylation site. European journal of biochemistry / FEBS *210*, 591-599.

Omura, T., Kaneko, M., Okuma, Y., Orba, Y., Nagashima, K., Takahashi, R., Fujitani, N., Matsumura, S., Hata, A., Kubota, K*., et al.* (2006). A ubiquitin ligase HRD1 promotes the degradation of Pael receptor, a substrate of Parkin. J Neurochem *99*, 1456-1469.

Otsu, M., Urade, R., Kito, M., Omura, F., and Kikuchi, M. (1995). A possible role of ER-60 protease in the degradation of misfolded proteins in the endoplasmic reticulum. J Biol Chem *270*, 14958-14961.

Pabarcus, M.K., Hoe, N., Sadeghi, S., Patterson, C., Wiertz, E., and Correia, M.A. (2009). CYP3A4 ubiquitination by gp78 (the tumor autocrine motility factor receptor, AMFR) and CHIP E3 ligases. Arch Biochem Biophys *483*, 66-74.

Paetzel, M., Dalbey, R.E., and Strynadka, N.C. (1998). Crystal structure of a bacterial signal peptidase in complex with a beta-lactam inhibitor. Nature *396*, 186-190.

Pagani, M., Fabbri, M., Benedetti, C., Fassio, A., Pilati, S., Bulleid, N.J., Cabibbo, A., and Sitia, R. (2000). Endoplasmic reticulum oxidoreductin 1-lbeta (ERO1-Lbeta), a human gene induced in the course of the unfolded protein response. J Biol Chem *275*, 23685-23692.

Pal, D., and Chakrabarti, P. (1999). Cis peptide bonds in proteins: residues involved, their conformations, interactions and locations. J Mol Biol *294*, 271-288.

Park, S., Isaacson, R., Kim, H.T., Silver, P.A., and Wagner, G. (2005). Ufd1 exhibits the AAA-ATPase fold with two distinct ubiquitin interaction sites. Structure *13*, 995-1005.

Park, Y.C., Burkitt, V., Villa, A.R., Tong, L., and Wu, H. (1999). Structural basis for self-association and receptor recognition of human TRAF2. Nature *398*, 533-538.

Patil, A.R., Thomas, C.J., and Surolia, A. (2000). Kinetics and the mechanism of interaction of the endoplasmic reticulum chaperone, calreticulin, with monoglucosylated (Glc1Man9GlcNAc2) substrate. J Biol Chem *275*, 24348-24356.

Peer, C.J., Sissung, T.M., and Figg, W.D. (2011). CHIP and gp78-mediated ubiquitination of CYP3A4: Implications for the pharmacology of anticancer agents. Cancer biology & therapy *11*, 549-551.

Petroski, M.D., and Deshaies, R.J. (2005a). Function and regulation of cullin-RING ubiquitin ligases. Nat Rev Mol Cell Biol *6*, 9-20.

Petroski, M.D., and Deshaies, R.J. (2005b). Mechanism of lysine 48-linked ubiquitin-chain synthesis by the cullin-RING ubiquitin-ligase complex SCF-Cdc34. Cell *123*, 1107-1120.

Petrova, K., Oyadomari, S., Hendershot, L.M., and Ron, D. (2008). Regulated association of misfolded endoplasmic reticulum lumenal proteins with P58/DNAJc3. EMBO J *27*, 2862-2872.

Pickart, C.M. (2001). Mechanisms underlying ubiquitination. Annu Rev Biochem *70*, 503-533.

Pieren, M., Galli, C., Denzel, A., and Molinari, M. (2005). The use of calnexin and calreticulin by cellular and viral glycoproteins. J Biol Chem *280*, 28265-28271.

Plechanovova, A., Jaffray, E.G., McMahon, S.A., Johnson, K.A., Navratilova, I., Naismith, J.H., and Hay, R.T. (2011). Mechanism of ubiquitylation by dimeric RING ligase RNF4. Nature structural & molecular biology *18*, 1052-1059.

Plemper, R.K., Bohmler, S., Bordallo, J., Sommer, T., and Wolf, D.H. (1997). Mutant analysis links the translocon and BiP to retrograde protein transport for ER degradation. Nature *388*, 891-895.

Plemper, R.K., Bordallo, J., Deak, P.M., Taxis, C., Hitt, R., and Wolf, D.H. (1999). Genetic interactions of Hrd3p and Der3p/Hrd1p with Sec61p suggest a retro-translocation complex mediating protein transport for ER degradation. J Cell Sci *112 (Pt 22)*, 4123-4134.

Ploegh, H.L. (2007). A lipid-based model for the creation of an escape hatch from the endoplasmic reticulum. Nature *448*, 435-438.

Plutner, H., Davidson, H.W., Saraste, J., and Balch, W.E. (1992). Morphological analysis of protein transport from the ER to Golgi membranes in digitonin-permeabilized cells: role of the P58 containing compartment. J Cell Biol *119*, 1097-1116.

Polekhina, G., House, C.M., Traficante, N., Mackay, J.P., Relaix, F., Sassoon, D.A., Parker, M.W., and Bowtell, D.D. (2002). Siah ubiquitin ligase is structurally related to TRAF and modulates TNF-alpha signaling. Nat Struct Biol *9*, 68-75.

Pollard, M.G., Travers, K.J., and Weissman, J.S. (1998). Ero1p: a novel and ubiquitous protein with an essential role in oxidative protein folding in the endoplasmic reticulum. Mol Cell *1*, 171-182.

Ponting, C.P. (2000). Proteins of the endoplasmic-reticulum-associated degradation pathway: domain detection and function prediction. Biochem J *351 Pt 2*, 527-535.

Prag, G., Misra, S., Jones, E.A., Ghirlando, R., Davies, B.A., Horazdovsky, B.F., and Hurley, J.H. (2003). Mechanism of ubiquitin recognition by the CUE domain of Vps9p. Cell *113*, 609-620.

Quan, E.M., Kamiya, Y., Kamiya, D., Denic, V., Weibezahn, J., Kato, K., and Weissman, J.S. (2008). Defining the glycan destruction signal for endoplasmic reticulum-associated degradation. Mol Cell *32*, 870-877.

Rabinovich, E., Kerem, A., Frohlich, K.U., Diamant, N., and Bar-Nun, S. (2002). AAA-ATPase p97/Cdc48p, a cytosolic chaperone required for endoplasmic reticulum-associated protein degradation. Mol Cell Biol *22*, 626-634.

Rapoport, T.A. (2007). Protein translocation across the eukaryotic endoplasmic reticulum and bacterial plasma membranes. Nature *450*, 663-669.

Ravid, T., Doolman, R., Avner, R., Harats, D., and Roitelman, J. (2000). The ubiquitin-proteasome pathway mediates the regulated degradation of mammalian 3-hydroxy-3-methylglutaryl-coenzyme A reductase. J Biol Chem *275*, 35840-35847.

Ravid, T., and Hochstrasser, M. (2007). Autoregulation of an E2 enzyme by ubiquitin-chain assembly on its catalytic residue. Nat Cell Biol *9*, 422-427.

Ray-Sinha, A., Cross, B.C., Mironov, A., Wiertz, E., and High, S. (2009). Endoplasmic reticulum-associated degradation of a degron-containing polytopic membrane protein. Molecular membrane biology *26*, 448-464.

Reggiori, F., Monastyrska, I., Verheije, M.H., Cali, T., Ulasli, M., Bianchi, S., Bernasconi, R., de Haan, C.A., and Molinari, M. (2010). Coronaviruses Hijack the LC3-I-positive EDEMosomes, ER-derived vesicles exporting short-lived ERAD regulators, for replication. Cell host & microbe *7*, 500-508.

Rhee, S.S., and Marsh, J.W. (1994). Human immunodeficiency virus type 1 Nef-induced down-modulation of CD4 is due to rapid internalization and degradation of surface CD4. Journal of virology *68*, 5156-5163.

Richard, M., Boulin, T., Robert, V.J., Richmond, J.E., and Bessereau, J.L. (2013). Biosynthesis of ionotropic acetylcholine receptors requires the evolutionarily conserved ER membrane complex. Proc Natl Acad Sci U S A *110*, E1055-1063.

Riemer, J., Appenzeller-Herzog, C., Johansson, L., Bodenmiller, B., Hartmann-Petersen, R., and Ellgaard, L. (2009). A luminal flavoprotein in endoplasmic reticulum-associated degradation. Proc Natl Acad Sci U S A *106*, 14831-14836.

Riordan, J.R., Rommens, J.M., Kerem, B., Alon, N., Rozmahel, R., Grzelczak, Z., Zielenski, J., Lok, S., Plavsic, N., Chou, J.L*., et al.* (1989). Identification of the cystic fibrosis gene: cloning and characterization of complementary DNA. Science *245*, 1066-1073.

Ritter, C., Quirin, K., Kowarik, M., and Helenius, A. (2005). Minor folding defects trigger local modification of glycoproteins by the ER folding sensor GT. EMBO J *24*, 1730-1738.

Roboti, P., and High, S. (2012a). Keratinocyte-associated protein 2 is a bona fide subunit of the mammalian oligosaccharyltransferase. J Cell Sci *125*, 220-232.

Roboti, P., and High, S. (2012b). The oligosaccharyltransferase subunits OST48, DAD1 and KCP2 function as ubiquitous and selective modulators of mammalian N-glycosylation. J Cell Sci *125*, 3474-3484.

Rodrigues, A.J., Neves-Carvalho, A., Teixeira-Castro, A., Rokka, A., Corthals, G., Logarinho, E., and Maciel, P. (2011). Absence of Ataxin-3 Leads to Enhanced Stress Response in C. elegans. PLoS One *6*.

Rosenbaum, J.C., Fredrickson, E.K., Oeser, M.L., Garrett-Engele, C.M., Locke, M.N., Richardson, L.A., Nelson, Z.W., Hetrick, E.D., Milac, T.I., Gottschling, D.E.*, et al.* (2011). Disorder targets misorder in nuclear quality control degradation: a disordered ubiquitin ligase directly recognizes its misfolded substrates. Mol Cell *41*, 93-106.

Rothblatt, J.A., Deshaies, R.J., Sanders, S.L., Daum, G., and Schekman, R. (1989). Multiple genes are required for proper insertion of secretory proteins into the endoplasmic reticulum in yeast. J Cell Biol *109*, 2641-2652.

Rotin, D., Staub, O., and Haguenauer-Tsapis, R. (2000). Ubiquitination and endocytosis of plasma membrane proteins: role of Nedd4/Rsp5p family of ubiquitin-protein ligases. J Membr Biol *176*, 1-17.

Rouiller, I., DeLaBarre, B., May, A.P., Weis, W.I., Brunger, A.T., Milligan, R.A., and Wilson-Kubalek, E.M. (2002). Conformational changes of the multifunction p97 AAA ATPase during its ATPase cycle. Nat Struct Biol *9*, 950-957.

Rubenstein, E.M., Kreft, S.G., Greenblatt, W., Swanson, R., and Hochstrasser, M. (2012). Aberrant substrate engagement of the ER translocon triggers degradation by the Hrd1 ubiquitin ligase. Journal of Cell Biology *197*, 761-773.

Ruiz-Canada, C., Kelleher, D.J., and Gilmore, R. (2009). Cotranslational and posttranslational N-glycosylation of polypeptides by distinct mammalian OST isoforms. Cell *136*, 272-283.

Rutkowski, D.T., Kang, S.W., Goodman, A.G., Garrison, J.L., Taunton, J., Katze, M.G., Kaufman, R.J., and Hegde, R.S. (2007). The role of p58IPK in protecting the stressed endoplasmic reticulum. Mol Biol Cell *18*, 3681-3691.

Saeed, M., Suzuki, R., Watanabe, N., Masaki, T., Tomonaga, M., Muhammad, A., Kato, T., Matsuura, Y., Watanabe, H., Wakita, T*., et al.* (2011). Role of the endoplasmic reticulum-associated degradation (ERAD) pathway in degradation of hepatitis C virus envelope proteins and production of virus particles. J Biol Chem *286*, 37264-37273.

Saha, A., and Deshaies, R.J. (2008). Multimodal activation of the ubiquitin ligase SCF by Nedd8 conjugation. Mol Cell *32*, 21-31.

Sai, X., Kokame, K., Shiraishi, H., Kawamura, Y., Miyata, T., Yanagisawa, K., and Komano, H. (2003). The ubiquitin-like domain of Herp is involved in Herp degradation, but not necessary for its enhancement of amyloid beta-protein generation. FEBS Lett *553*, 151-156.

Samelson, L.E., Harford, J.B., and Klausner, R.D. (1985). Identification of the components of the murine T cell antigen receptor complex. Cell *43*, 223-231.

Satijn, D.P., and Otte, A.P. (1999). RING1 interacts with multiple Polycomb-group proteins and displays tumorigenic activity. Mol Cell Biol *19*, 57-68.

Sato, B.K., and Hampton, R.Y. (2006). Yeast Derlin Dfm1 interacts with Cdc48 and functions in ER homeostasis. Yeast *23*, 1053-1064.

Sato, B.K., Schulz, D., Do, P.H., and Hampton, R.Y. (2009). Misfolded membrane proteins are specifically recognized by the transmembrane domain of the Hrd1p ubiquitin ligase. Mol Cell *34*, 212-222.

Sato, T., Sako, Y., Sho, M., Momohara, M., Suico, M.A., Shuto, T., Nishitoh, H., Okiyoneda, T., Kokame, K., Kaneko, M.*, et al.* (2012). STT3B-dependent posttranslational N-glycosylation as a surveillance system for secretory protein. Mol Cell *47*, 99-110.

Satoh, T., Chen, Y., Hu, D., Hanashima, S., Yamamoto, K., and Yamaguchi, Y. (2010). Structural basis for oligosaccharide recognition of misfolded glycoproteins by OS-9 in ER-associated degradation. Mol Cell *40*, 905-916.

Schafer, A., and Wolf, D.H. (2009). Sec61p is part of the endoplasmic reticulum-associated degradation machinery. Embo Journal *28*, 2874-2884.

Schett, G., Tohidast-Akrad, M., Steiner, G., and Smolen, J. (2001). The stressed synovium. Arthritis research *3*, 80-86.

Schmid, F.X., and Baldwin, R.L. (1978). Acid catalysis of the formation of the slow-folding species of RNase A: evidence that the reaction is proline isomerization. Proc Natl Acad Sci U S A *75*, 4764-4768.

Schrag, J.D., Bergeron, J.J., Li, Y., Borisova, S., Hahn, M., Thomas, D.Y., and Cygler, M. (2001). The Structure of calnexin, an ER chaperone involved in quality control of protein folding. Mol Cell *8*, 633-644.

Schubert, U., Anton, L.C., Bacik, I., Cox, J.H., Bour, S., Bennink, J.R., Orlowski, M., Strebel, K., and Yewdell, J.W. (1998). CD4 glycoprotein degradation induced by human immunodeficiency virus type 1 Vpu protein requires the function of proteasomes and the ubiquitin-conjugating pathway. Journal of virology *72*, 2280-2288.

Schubert, U., Bour, S., Ferrer-Montiel, A.V., Montal, M., Maldarell, F., and Strebel, K. (1996). The two biological activities of human immunodeficiency virus type 1 Vpu protein involve two separable structural domains. Journal of virology *70*, 809-819.

Schuit, F.C., In't Veld, P.A., and Pipeleers, D.G. (1988). Glucose stimulates proinsulin biosynthesis by a dose-dependent recruitment of pancreatic beta cells. Proc Natl Acad Sci U S A *85*, 3865-3869.

Schuldiner, M., Metz, J., Schmid, V., Denic, V., Rakwalska, M., Schmitt, H.D., Schwappach, B., and Weissman, J.S. (2008). The GET complex mediates insertion of tail-anchored proteins into the ER membrane. Cell *134*, 634-645.

Schulman, S., Wang, B., Li, W., and Rapoport, T.A. (2010). Vitamin K epoxide reductase prefers ER membrane-anchored thioredoxin-like redox partners. Proc Natl Acad Sci U S A *107*, 15027-15032.

Schulze, A., Standera, S., Buerger, E., Kikkert, M., van Voorden, S., Wiertz, E., Koning, F., Kloetzel, P.M., and Seeger, M. (2005). The ubiquitin-domain protein HERP forms a complex

with components of the endoplasmic reticulum associated degradation pathway. J Mol Biol *354*, 1021-1027.

Scott, D.C., and Schekman, R. (2008). Role of Sec61p in the ER-associated degradation of short-lived transmembrane proteins. J Cell Biol *181*, 1095-1105.

Seol, J.H., Feldman, R.M., Zachariae, W., Shevchenko, A., Correll, C.C., Lyapina, S., Chi, Y., Galova, M., Claypool, J., Sandmeyer, S*., et al.* (1999). Cdc53/cullin and the essential Hrt1 RING-H2 subunit of SCF define a ubiquitin ligase module that activates the E2 enzyme Cdc34. Genes Dev *13*, 1614-1626.

Serohijos, A.W., Hegedus, T., Aleksandrov, A.A., He, L., Cui, L., Dokholyan, N.V., and Riordan, J.R. (2008). Phenylalanine-508 mediates a cytoplasmic-membrane domain contact in the CFTR 3D structure crucial to assembly and channel function. Proc Natl Acad Sci U S A *105*, 3256-3261.

Serrano-Pozo, A., Frosch, M.P., Masliah, E., and Hyman, B.T. (2011). Neuropathological alterations in Alzheimer disease. Cold Spring Harbor perspectives in medicine *1*, a006189.

Sever, N., Song, B.L., Yabe, D., Goldstein, J.L., Brown, M.S., and DeBose-Boyd, R.A. (2003a). Insig-dependent ubiquitination and degradation of mammalian 3-hydroxy-3-methylglutaryl-CoA reductase stimulated by sterols and geranylgeraniol. J Biol Chem *278*, 52479-52490.

Sever, N., Yang, T., Brown, M.S., Goldstein, J.L., and DeBose-Boyd, R.A. (2003b). Accelerated degradation of HMG CoA reductase mediated by binding of insig-1 to its sterol-sensing domain. Mol Cell *11*, 25-33.

Shabek, N., Herman-Bachinsky, Y., Buchsbaum, S., Lewinson, O., Haj-Yahya, M., Hejjaoui, M., Lashuel, H.A., Sommer, T., Brik, A., and Ciechanover, A. (2012). The size of the proteasomal substrate determines whether its degradation will be mediated by mono- or polyubiquitylation. Mol Cell *48*, 87-97.

Sharp, D.A., Kratowicz, S.A., Sank, M.J., and George, D.L. (1999). Stabilization of the MDM2 oncoprotein by interaction with the structurally related MDMX protein. J Biol Chem *274*, 38189-38196.

Shen, Y., Ballar, P., and Fang, S. (2006). Ubiquitin ligase gp78 increases solubility and facilitates degradation of the Z variant of alpha-1-antitrypsin. Biochem Biophys Res Commun *349*, 1285-1293.

Shen, Y., and Hendershot, L.M. (2005). ERdj3, a stress-inducible endoplasmic reticulum DnaJ homologue, serves as a cofactor for BiP's interactions with unfolded substrates. Mol Biol Cell *16*, 40-50.

Shenkman, M., Groisman, B., Ron, E., Avezov, E., Hendershot, L.M., and Lederkremer, G.Z. (2013). A shared endoplasmic reticulum-associated degradation pathway involving the EDEM1 protein for glycosylated and nonglycosylated proteins. J Biol Chem *288*, 2167-2178.

Shi, Y., Vattem, K.M., Sood, R., An, J., Liang, J., Stramm, L., and Wek, R.C. (1998). Identification and characterization of pancreatic eukaryotic initiation factor 2 alpha-subunit kinase, PEK, involved in translational control. Mol Cell Biol *18*, 7499-7509.

Shibatani, T., David, L.L., McCormack, A.L., Frueh, K., and Skach, W.R. (2005). Proteomic analysis of mammalian oligosaccharyltransferase reveals multiple subcomplexes that contain Sec61, TRAP, and two potential new subunits. Biochemistry *44*, 5982-5992.

Shih, S.C., Prag, G., Francis, S.A., Sutanto, M.A., Hurley, J.H., and Hicke, L. (2003). A ubiquitin-binding motif required for intramolecular monoubiquitylation, the CUE domain. EMBO J *22*, 1273-1281.

Shimizu, Y., Okuda-Shimizu, Y., and Hendershot, L.M. (2010). Ubiquitylation of an ERAD substrate occurs on multiple types of amino acids. Mol Cell *40*, 917-926.

Shinkai, Y., Yamamoto, C., and Kaji, T. (2010). Lead induces the expression of endoplasmic reticulum chaperones GRP78 and GRP94 in vascular endothelial cells via the JNK-AP-1 pathway. Toxicological sciences : an official journal of the Society of Toxicology *114*, 378-386.

Shloush, J., Vlassov, J.E., Engson, I., Duan, S., Saridakis, V., Dhe-Paganon, S., Raught, B., Sheng, Y., and Arrowsmith, C.H. (2011). Structural and functional comparison of the RING domains of two p53 E3 ligases, Mdm2 and Pirh2. J Biol Chem *286*, 4796-4808.

Shmueli, A., Tsai, Y.C., Yang, M., Braun, M.A., and Weissman, A.M. (2009). Targeting of gp78 for ubiquitin-mediated proteasomal degradation by Hrd1: cross-talk between E3s in the endoplasmic reticulum. Biochem Biophys Res Commun *390*, 758-762.

Sifers, R.N., Brashears-Macatee, S., Kidd, V.J., Muensch, H., and Woo, S.L. (1988). A frameshift mutation results in a truncated alpha 1-antitrypsin that is retained within the rough endoplasmic reticulum. J Biol Chem *263*, 7330-7335.

Simons, A.M., Horwitz, A.A., Starita, L.M., Griffin, K., Williams, R.S., Glover, J.N., and Parvin, J.D. (2006). BRCA1 DNA-binding activity is stimulated by BARD1. Cancer research *66*, 2012-2018.

Skowyra, D., Koepp, D.M., Kamura, T., Conrad, M.N., Conaway, R.C., Conaway, J.W., Elledge, S.J., and Harper, J.W. (1999). Reconstitution of G1 cyclin ubiquitination with complexes containing SCFGrr1 and Rbx1. Science *284*, 662-665.

Soetandyo, N., Wang, Q., Ye, Y., and Li, L. (2010). Role of intramembrane charged residues in the quality control of unassembled T-cell receptor alpha-chains at the endoplasmic reticulum. J Cell Sci *123*, 1031-1038.

Sommer, T., and Jentsch, S. (1993). A protein translocation defect linked to ubiquitin conjugation at the endoplasmic reticulum. Nature *365*, 176-179.

Song, B.L., Javitt, N.B., and DeBose-Boyd, R.A. (2005a). Insig-mediated degradation of HMG CoA reductase stimulated by lanosterol, an intermediate in the synthesis of cholesterol. Cell Metab *1*, 179-189.

Song, B.L., Sever, N., and DeBose-Boyd, R.A. (2005b). Gp78, a membrane-anchored ubiquitin ligase, associates with Insig-1 and couples sterol-regulated ubiquitination to degradation of HMG CoA reductase. Mol Cell *19*, 829-840.

Sorgjerd, K., Ghafouri, B., Jonsson, B.H., Kelly, J.W., Blond, S.Y., and Hammarstrom, P. (2006). Retention of misfolded mutant transthyretin by the chaperone BiP/GRP78 mitigates amyloidogenesis. J Mol Biol *356*, 469-482.

Sousa, M., and Parodi, A.J. (1995). The molecular basis for the recognition of misfolded glycoproteins by the UDP-Glc:glycoprotein glucosyltransferase. EMBO J *14*, 4196-4203.

Sousa, M.C., Ferrero-Garcia, M.A., and Parodi, A.J. (1992). Recognition of the oligosaccharide and protein moieties of glycoproteins by the UDP-Glc:glycoprotein glucosyltransferase. Biochemistry *31*, 97-105.

Sowa, M.E., Bennett, E.J., Gygi, S.P., and Harper, J.W. (2009). Defining the Human Deubiquitinating Enzyme Interaction Landscape. Cell *138*, 389-403.

Spandl, J., Lohmann, D., Kuerschner, L., Moessinger, C., and Thiele, C. (2010). Ancient ubiquitous protein 1 (AUP1) localizes to lipid droplets and binds the E2 ubiquitin conjugase G2 (UBE2G2) via its G2 binding region. J Biol Chem.

Spandl, J., White, D.J., Peychl, J., and Thiele, C. (2009). Live cell multicolor imaging of lipid droplets with a new dye, LD540. Traffic *10*, 1579-1584.

St-Pierre, P., Dang, T., Joshi, B., and Nabi, I.R. (2012). Peripheral endoplasmic reticulum localization of the Gp78 ubiquitin ligase activity. J Cell Sci *125*, 1727-1737.

Stagg, H.R., Thomas, M., van den Boomen, D., Wiertz, E.J., Drabkin, H.A., Gemmill, R.M., and Lehner, P.J. (2009). The TRC8 E3 ligase ubiquitinates MHC class I molecules before dislocation from the ER. J Cell Biol *186*, 685-692.

Stefanovic, S., and Hegde, R.S. (2007). Identification of a targeting factor for posttranslational membrane protein insertion into the ER. Cell *128*, 1147-1159.

Stefer, S., Reitz, S., Wang, F., Wild, K., Pang, Y.Y., Schwarz, D., Bomke, J., Hein, C., Lohr, F., Bernhard, F*., et al.* (2011). Structural basis for tail-anchored membrane protein biogenesis by the Get3-receptor complex. Science *333*, 758-762.

Stevanovic, A., and Thiele, C. (2013). Monotopic topology is required for lipid droplet targeting of ancient ubiquitous protein 1. J Lipid Res *54*, 503-513.

Stevens, R.H., and Williamson, A.R. (1974). mRNA for H and L chains of immunoglobulin: specific control of H-chain production. Contemporary topics in molecular immunology *3*, 85-110.

Stewart, D.E., Sarkar, A., and Wampler, J.E. (1990). Occurrence and role of cis peptide bonds in protein structures. J Mol Biol *214*, 253-260.

Stirling, C.J., Rothblatt, J., Hosobuchi, M., Deshaies, R., and Schekman, R. (1992). Protein translocation mutants defective in the insertion of integral membrane proteins into the endoplasmic reticulum. Mol Biol Cell *3*, 129-142.

Stromer, T., Fischer, E., Richter, K., Haslbeck, M., and Buchner, J. (2004). Analysis of the regulation of the molecular chaperone Hsp26 by temperature-induced dissociation: the N-terminal domail is important for oligomer assembly and the binding of unfolding proteins. J Biol Chem *279*, 11222-11228.

Suloway, C.J., Chartron, J.W., Zaslaver, M., and Clemons, W.M., Jr. (2009). Model for eukaryotic tail-anchored protein binding based on the structure of Get3. Proc Natl Acad Sci U S A *106*, 14849-14854.

Sussman, J.J., Bonifacino, J.S., Lippincott-Schwartz, J., Weissman, A.M., Saito, T., Klausner, R.D., and Ashwell, J.D. (1988). Failure to synthesize the T cell CD3-zeta chain: structure and function of a partial T cell receptor complex. Cell *52*, 85-95.

Suzuki, T. (2007). Cytoplasmic peptide: N-glycanase and catabolic pathway for free N-glycans in the cytosol. Seminars in Cell & Developmental Biology *18*, 762-769.

Tan, P., Fuchs, S.Y., Chen, A., Wu, K., Gomez, C., Ronai, Z., and Pan, Z.Q. (1999). Recruitment of a ROC1-CUL1 ubiquitin ligase by Skp1 and HOS to catalyze the ubiquitination of I kappa B alpha. Mol Cell *3*, 527-533.

Tavender, T.J., Sheppard, A.M., and Bulleid, N.J. (2008). Peroxiredoxin IV is an endoplasmic reticulum-localized enzyme forming oligomeric complexes in human cells. Biochem J *411*, 191-199.

Tavender, T.J., Springate, J.J., and Bulleid, N.J. (2010). Recycling of peroxiredoxin IV provides a novel pathway for disulphide formation in the endoplasmic reticulum. EMBO J *29*, 4185-4197.

Tcherpakov, M., Delaunay, A., Toth, J., Kadoya, T., Petroski, M.D., and Ronai, Z.A. (2009). Regulation of endoplasmic reticulum-associated degradation by RNF5-dependent ubiquitination of JNK-associated membrane protein (JAMP). J Biol Chem *284*, 12099-12109.

Thrower, J.S., Hoffman, L., Rechsteiner, M., and Pickart, C.M. (2000). Recognition of the polyubiquitin proteolytic signal. EMBO J *19*, 94-102.

Thuerauf, D.J., Marcinko, M., Belmont, P.J., and Glembotski, C.C. (2007). Effects of the isoform-specific characteristics of ATF6 alpha and ATF6 beta on endoplasmic reticulum stress response gene expression and cell viability. J Biol Chem *282*, 22865-22878.

Thuerauf, D.J., Morrison, L., and Glembotski, C.C. (2004). Opposing roles for ATF6alpha and ATF6beta in endoplasmic reticulum stress response gene induction. J Biol Chem *279*, 21078-21084.

Tirasophon, W., Lee, K., Callaghan, B., Welihinda, A., and Kaufman, R.J. (2000). The endoribonuclease activity of mammalian IRE1 autoregulates its mRNA and is required for the unfolded protein response. Genes Dev *14*, 2725-2736.

Tirasophon, W., Welihinda, A.A., and Kaufman, R.J. (1998). A stress response pathway from the endoplasmic reticulum to the nucleus requires a novel bifunctional protein kinase/endoribonuclease (Ire1p) in mammalian cells. Genes Dev *12*, 1812-1824.

Tirosh, B., Furman, M.H., Tortorella, D., and Ploegh, H.L. (2003). Protein unfolding is not a prerequisite for endoplasmic reticulum-to-cytosol dislocation. J Biol Chem *278*, 6664-6672.

Tiwari, S., and Weissman, A.M. (2001). Endoplasmic reticulum (ER)-associated degradation of T cell receptor subunits. Involvement of ER-associated ubiquitin-conjugating enzymes (E2s). J Biol Chem *276*, 16193-16200.

Totani, K., Ihara, Y., Tsujimoto, T., Matsuo, I., and Ito, Y. (2009). The recognition motif of the glycoprotein-folding sensor enzyme UDP-Glc:glycoprotein glucosyltransferase. Biochemistry *48*, 2933-2940.

Tremblay, L.O., and Herscovics, A. (1999). Cloning and expression of a specific human alpha 1,2-mannosidase that trims Man9GlcNAc2 to Man8GlcNAc2 isomer B during N-glycan biosynthesis. Glycobiology *9*, 1073-1078.

Trombetta, E.S., and Helenius, A. (2000). Conformational requirements for glycoprotein reglucosylation in the endoplasmic reticulum. J Cell Biol *148*, 1123-1129.

Tsai, Y.C., Mendoza, A., Mariano, J.M., Zhou, M., Kostova, Z., Chen, B., Veenstra, T., Hewitt, S.M., Helman, L.J., Khanna, C*., et al.* (2007). The ubiquitin ligase gp78 promotes sarcoma metastasis by targeting KAI1 for degradation. Nat Med *13*, 1504-1509.

Tsuchiya, Y., Morita, T., Kim, M., Iemura, S., Natsume, T., Yamamoto, M., and Kobayashi, A. (2011). Dual regulation of the transcriptional activity of Nrf1 by beta-TrCP- and Hrd1-dependent degradation mechanisms. Mol Cell Biol *31*, 4500-4512.

Tu, B.P., Ho-Schleyer, S.C., Travers, K.J., and Weissman, J.S. (2000). Biochemical basis of oxidative protein folding in the endoplasmic reticulum. Science *290*, 1571-1574.

Tu, B.P., and Weissman, J.S. (2002). The FAD- and O(2)-dependent reaction cycle of Ero1-mediated oxidative protein folding in the endoplasmic reticulum. Mol Cell *10*, 983-994.

Tyler, R.E., Pearce, M.M., Shaler, T.A., Olzmann, J.A., Greenblatt, E.J., and Kopito, R.R. (2012). Unassembled CD147 is an endogenous endoplasmic reticulum-associated degradation substrate. Mol Biol Cell *23*, 4668-4678.

Urade, R., Nasu, M., Moriyama, T., Wada, K., and Kito, M. (1992). Protein degradation by the phosphoinositide-specific phospholipase C-alpha family from rat liver endoplasmic reticulum. J Biol Chem *267*, 15152-15159.

Urano, F., Wang, X., Bertolotti, A., Zhang, Y., Chung, P., Harding, H.P., and Ron, D. (2000). Coupling of stress in the ER to activation of JNK protein kinases by transmembrane protein kinase IRE1. Science *287*, 664-666.

Urban, S., and Dickey, S.W. (2011). The rhomboid protease family: a decade of progress on function and mechanism. Genome biology *12*, 231.

Ushioda, R., Hoseki, J., Araki, K., Jansen, G., Thomas, D.Y., and Nagata, K. (2008). ERdj5 is required as a disulfide reductase for degradation of misfolded proteins in the ER. Science *321*, 569-572.

Van den Berg, B., Clemons, W.M., Jr., Collinson, I., Modis, Y., Hartmann, E., Harrison, S.C., and Rapoport, T.A. (2004). X-ray structure of a protein-conducting channel. Nature *427*, 36-44.

van Huizen, R., Martindale, J.L., Gorospe, M., and Holbrook, N.J. (2003). P58IPK, a novel endoplasmic reticulum stress-inducible protein and potential negative regulator of eIF2alpha signaling. J Biol Chem *278*, 15558-15564.

Vander Kooi, C.W., Ohi, M.D., Rosenberg, J.A., Oldham, M.L., Newcomer, M.E., Gould, K.L., and Chazin, W.J. (2006). The Prp19 U-box crystal structure suggests a common dimeric architecture for a class of oligomeric E3 ubiquitin ligases. Biochemistry *45*, 121-130.

Vecchi, L., Petris, G., Bestagno, M., and Burrone, O.R. (2012). Selective targeting of proteins within secretory pathway for endoplasmic reticulum-associated degradation. J Biol Chem *287*, 20007-20015.

Vembar, S.S., and Brodsky, J.L. (2008). One step at a time: endoplasmic reticulum-associated degradation. Nat Rev Mol Cell Biol *9*, 944-957.

Vilardi, F., Lorenz, H., and Dobberstein, B. (2011). WRB is the receptor for TRC40/Asna1-mediated insertion of tail-anchored proteins into the ER membrane. J Cell Sci *124*, 1301-1307.

Voigt, S., Jungnickel, B., Hartmann, E., and Rapoport, T.A. (1996). Signal sequence-dependent function of the TRAM protein during early phases of protein transport across the endoplasmic reticulum membrane. J Cell Biol *134*, 25-35.

von Heijne, G. (1983). Patterns of amino acids near signal-sequence cleavage sites. European journal of biochemistry / FEBS *133*, 17-21.

Wahlman, J., DeMartino, G.N., Skach, W.R., Bulleid, N.J., Brodsky, J.L., and Johnson, A.E. (2007). Real-time fluorescence detection of ERAD substrate retrotranslocation in a mammalian in vitro system. Cell *129*, 943-955.

Walter, P., and Blobel, G. (1980). Purification of a membrane-associated protein complex required for protein translocation across the endoplasmic reticulum. Proc Natl Acad Sci U S A *77*, 7112-7116.

Walter, P., and Blobel, G. (1981a). Translocation of proteins across the endoplasmic reticulum III. Signal recognition protein (SRP) causes signal sequence-dependent and site-specific arrest of chain elongation that is released by microsomal membranes. J Cell Biol *91*, 557-561.

Walter, P., and Blobel, G. (1981b). Translocation of proteins across the endoplasmic reticulum. II. Signal recognition protein (SRP) mediates the selective binding to microsomal membranes of in-vitro-assembled polysomes synthesizing secretory protein. J Cell Biol *91*, 551-556.

Walter, P., and Blobel, G. (1982). Signal recognition particle contains a 7S RNA essential for protein translocation across the endoplasmic reticulum. Nature *299*, 691-698.

Walter, P., Ibrahimi, I., and Blobel, G. (1981). Translocation of proteins across the endoplasmic reticulum. I. Signal recognition protein (SRP) binds to in-vitro-assembled polysomes synthesizing secretory protein. J Cell Biol *91*, 545-550.

Walter, P., and Ron, D. (2011). The unfolded protein response: from stress pathway to homeostatic regulation. Science *334*, 1081-1086.

Walther, T.C., and Farese, R.V., Jr. (2012). Lipid droplets and cellular lipid metabolism. Annu Rev Biochem *81*, 687-714.

Wang, F., Brown, E.C., Mak, G., Zhuang, J., and Denic, V. (2010a). A chaperone cascade sorts proteins for posttranslational membrane insertion into the endoplasmic reticulum. Mol Cell *40*, 159-171.

Wang, F., Whynot, A., Tung, M., and Denic, V. (2011a). The mechanism of tail-anchored protein insertion into the ER membrane. Mol Cell *43*, 738-750.

Wang, G.H., Sawai, N., Kotliarova, S., Kanazawa, I., and Nukina, N. (2000). Ataxin-3, the MJD1 gene product, interacts with the two human homologs of yeast DNA repair protein RAD23, HHR23A and HHR23B. Human Molecular Genetics *9*, 1795-1803.

Wang, H., Li, Q., Shen, Y., Sun, A., Zhu, X., and Fang, S. (2011b). The ubiquitin ligase Hrd1 promotes degradation of the Z variant alpha 1-antitrypsin and increases its solubility. Molecular and cellular biochemistry *346*, 137-145.

Wang, H.J., Benlimame, N., and Nabi, I. (1997). The AMF-R tubule is a smooth ilimaquinone-sensitive subdomain of the endoplasmic reticulum. J Cell Sci *110 (Pt 24)*, 3043-3053.

Wang, J., and Schulman, B.A. (2009). (G2)BRinging an E2 to E3. Structure *17*, 916-917.

Wang, M., and Pickart, C.M. (2005). Different HECT domain ubiquitin ligases employ distinct mechanisms of polyubiquitin chain synthesis. EMBO J *24*, 4324-4333.

Wang, Q., Song, C.C., and Li, C.C.H. (2004). Molecular perspectives on p97-VCP: progress in understanding its structure and diverse biological functions. J Struct Biol *146*, 44-57.

Wang, Q.Y., Li, L.Y., and Ye, Y.H. (2006). Regulation of retrotranslocation by p97-associated deubiquitinating enzyme ataxin-3. Journal of Cell Biology *174*, 963-971.

Wang, Q.Y., Li, L.Y., and Ye, Y.H. (2008). Inhibition of p97-dependent protein degradation by Eeyarestatin I. Journal of Biological Chemistry *283*, 7445-7454.

Wang, Q.Y., Liu, Y.F., Soetandyo, N., Baek, K., Hegde, R., and Ye, Y.H. (2011c). A Ubiquitin Ligase-Associated Chaperone Holdase Maintains Polypeptides in Soluble States for Proteasome Degradation. Molecular Cell *42*, 758-770.

Wang, Q.Y., Shinkre, B.A., Lee, J.G., Weniger, M.A., Liu, Y.F., Chen, W.P., Wiestner, A., Trenkle, W.C., and Ye, Y.H. (2010b). The ERAD Inhibitor Eeyarestatin I Is a Bifunctional Compound with a Membrane-Binding Domain and a p97/VCP Inhibitory Group. PLoS One *5*.

Wang, X., Wang, L., Sun, F., and Wang, C.C. (2012a). Structural insights into the peroxidase activity and inactivation of human peroxiredoxin 4. Biochem J *441*, 113-118.

Wang, Y., Guan, S., Acharya, P., Liu, Y., Thirumaran, R.K., Brandman, R., Schuetz, E.G., Burlingame, A.L., and Correia, M.A. (2012b). Multisite phosphorylation of human liver cytochrome P450 3A4 enhances Its gp78- and CHIP-mediated ubiquitination: a pivotal role of its Ser-478 residue in the gp78-catalyzed reaction. Molecular & cellular proteomics : MCP *11*, M111 010132.

Wiertz, E.J., Jones, T.R., Sun, L., Bogyo, M., Geuze, H.J., and Ploegh, H.L. (1996a). The human cytomegalovirus US11 gene product dislocates MHC class I heavy chains from the endoplasmic reticulum to the cytosol. Cell *84*, 769-779.

Wiertz, E.J., Tortorella, D., Bogyo, M., Yu, J., Mothes, W., Jones, T.R., Rapoport, T.A., and Ploegh, H.L. (1996b). Sec61-mediated transfer of a membrane protein from the endoplasmic reticulum to the proteasome for destruction. Nature *384*, 432-438.

Wild, S., Roglic, G., Green, A., Sicree, R., and King, H. (2004). Global prevalence of diabetes: estimates for the year 2000 and projections for 2030. Diabetes care *27*, 1047-1053.

Willer, M., Forte, G.M., and Stirling, C.J. (2008). Sec61p is required for ERAD-L: genetic dissection of the translocation and ERAD-L functions of Sec61P using novel derivatives of CPY. J Biol Chem *283*, 33883-33888.

Willey, R.L., Maldarelli, F., Martin, M.A., and Strebel, K. (1992). Human immunodeficiency virus type 1 Vpu protein induces rapid degradation of CD4. Journal of virology *66*, 7193-7200.

Wilson, C.M., and High, S. (2007). Ribophorin I acts as a substrate-specific facilitator of N-glycosylation. J Cell Sci *120*, 648-657.

Wilson, C.M., Kraft, C., Duggan, C., Ismail, N., Crawshaw, S.G., and High, S. (2005). Ribophorin I associates with a subset of membrane proteins after their integration at the sec61 translocon. J Biol Chem *280*, 4195-4206.

Wilson, C.M., Roebuck, Q., and High, S. (2008). Ribophorin I regulates substrate delivery to the oligosaccharyltransferase core. Proc Natl Acad Sci U S A *105*, 9534-9539.

Winnefeld, M., Grewenig, A., Schnolzer, M., Spring, H., Knoch, T.A., Gan, E.C., Rommelaere, J., and Cziepluch, C. (2006). Human SGT interacts with Bag-6/Bat-3/Scythe and cells with reduced levels of either protein display persistence of few misaligned chromosomes and mitotic arrest. Experimental cell research *312*, 2500-2514.

Wu, L.C., Wang, Z.W., Tsan, J.T., Spillman, M.A., Phung, A., Xu, X.L., Yang, M.C., Hwang, L.Y., Bowcock, A.M., and Baer, R. (1996). Identification of a RING protein that can interact in vivo with the BRCA1 gene product. Nat Genet *14*, 430-440.

Wu, Y., Swulius, M.T., Moremen, K.W., and Sifers, R.N. (2003). Elucidation of the molecular logic by which misfolded alpha 1-antitrypsin is preferentially selected for degradation. Proc Natl Acad Sci U S A *100*, 8229-8234.

Xu, P., Duong, D.M., Seyfried, N.T., Cheng, D., Xie, Y., Robert, J., Rush, J., Hochstrasser, M., Finley, D., and Peng, J. (2009). Quantitative proteomics reveals the function of unconventional ubiquitin chains in proteasomal degradation. Cell *137*, 133-145.

Xu, Y., Liu, Y., Lee, J.G., and Ye, Y. (2013). A ubiquitin-like domain recruits an oligomeric chaperone to a retrotranslocation complex in endoplasmic reticulum-associated degradation. J Biol Chem *288*, 18068-18076.

Yamagata, A., Mimura, H., Sato, Y., Yamashita, M., Yoshikawa, A., and Fukai, S. (2010). Structural insight into the membrane insertion of tail-anchored proteins by Get3. Genes to cells : devoted to molecular & cellular mechanisms *15*, 29-41.

Yamaguchi, D., Hu, D., Matsumoto, N., and Yamamoto, K. (2010). Human XTP3-B binds to alpha1-antitrypsin variant null(Hong Kong) via the C-terminal MRH domain in a glycan-dependent manner. Glycobiology *20*, 348-355.

Yamamoto, K., Sato, T., Matsui, T., Sato, M., Okada, T., Yoshida, H., Harada, A., and Mori, K. (2007). Transcriptional induction of mammalian ER quality control proteins is mediated by single or combined action of ATF6alpha and XBP1. Dev Cell *13*, 365-376.

Yamamoto, K., Yoshida, H., Kokame, K., Kaufman, R.J., and Mori, K. (2004). Differential contributions of ATF6 and XBP1 to the activation of endoplasmic reticulum stress-responsive cis-acting elements ERSE, UPRE and ERSE-II. J Biochem *136*, 343-350.

Yamamoto, Y., and Sakisaka, T. (2012). Molecular machinery for insertion of tail-anchored membrane proteins into the endoplasmic reticulum membrane in mammalian cells. Mol Cell *48*, 387-397.

Yamasaki, S., Yagishita, N., Sasaki, T., Nakazawa, M., Kato, Y., Yamadera, T., Bae, E., Toriyama, S., Ikeda, R., Zhang, L*., et al.* (2007). Cytoplasmic destruction of p53 by the endoplasmic reticulum-resident ubiquitin ligase 'Synoviolin'. EMBO J *26*, 113-122.

Yamasaki, S., Yagishita, N., Tsuchimochi, K., Kato, Y., Sasaki, T., Amano, T., Beppu, M., Aoki, H., Nakamura, H., Nishioka, K*., et al.* (2006). Resistance to endoplasmic reticulum stress is an acquired cellular characteristic of rheumatoid synovial cells. International journal of molecular medicine *18*, 113-117.

Yan, W., Frank, C.L., Korth, M.J., Sopher, B.L., Novoa, I., Ron, D., and Katze, M.G. (2002). Control of PERK eIF2alpha kinase activity by the endoplasmic reticulum stress-induced molecular chaperone P58IPK. Proc Natl Acad Sci U S A *99*, 15920-15925.

Yanagitani, K., Imagawa, Y., Iwawaki, T., Hosoda, A., Saito, M., Kimata, Y., and Kohno, K. (2009). Cotranslational targeting of XBP1 protein to the membrane promotes cytoplasmic splicing of its own mRNA. Mol Cell *34*, 191-200.

Yang, H., Zhong, X., Ballar, P., Luo, S., Shen, Y., Rubinsztein, D.C., Monteiro, M.J., and Fang, S. (2007). Ubiquitin ligase Hrd1 enhances the degradation and suppresses the toxicity of polyglutamine-expanded huntingtin. Experimental cell research *313*, 538-550.

Yang, L., Ding, Y.F., Chen, Y., Zhang, S.Y., Huo, C.X., Wang, Y., Yu, J.H., Zhang, P., Na, H.M., Zhang, H.N*., et al.* (2012). The proteomics of lipid droplets: structure, dynamics, and functions of the organelle conserved from bacteria to humans. Journal of Lipid Research *53*, 1245-1253.

Yang, M., Omura, S., Bonifacino, J.S., and Weissman, A.M. (1998). Novel aspects of degradation of T cell receptor subunits from the endoplasmic reticulum (ER) in T cells: importance of oligosaccharide processing, ubiquitination, and proteasome-dependent removal from ER membranes. J Exp Med *187*, 835-846.

Ye, J., Rawson, R.B., Komuro, R., Chen, X., Dave, U.P., Prywes, R., Brown, M.S., and Goldstein, J.L. (2000). ER stress induces cleavage of membrane-bound ATF6 by the same proteases that process SREBPs. Mol Cell *6*, 1355-1364.

Ye, Y., Meyer, H.H., and Rapoport, T.A. (2001). The AAA ATPase Cdc48/p97 and its partners transport proteins from the ER into the cytosol. Nature *414*, 652-656.

Ye, Y., Shibata, Y., Kikkert, M., van Voorden, S., Wiertz, E., and Rapoport, T.A. (2005). Recruitment of the p97 ATPase and ubiquitin ligases to the site of retrotranslocation at the endoplasmic reticulum membrane. Proc Natl Acad Sci U S A *102*, 14132-14138.

Ye, Y., Shibata, Y., Yun, C., Ron, D., and Rapoport, T.A. (2004). A membrane protein complex mediates retro-translocation from the ER lumen into the cytosol. Nature *429*, 841-847.

Ye, Y.H., Meyer, H.H., and Rapoport, T.A. (2003). Function of the p97-Ufd1-Npl4 complex in retrotranslocation from the ER to the cytosol: dual recognition of nonubiquitinated polypeptide segments and polyubiquitin chains. Journal of Cell Biology *162*, 71-84.

Yeung, S.J., Chen, S.H., and Chan, L. (1996). Ubiquitin-proteasome pathway mediates intracellular degradation of apolipoprotein B. Biochemistry *35*, 13843-13848.

Yin, Q., Lin, S.C., Lamothe, B., Lu, M., Lo, Y.C., Hura, G., Zheng, L., Rich, R.L., Campos, A.D., Myszka, D.G.*, et al.* (2009). E2 interaction and dimerization in the crystal structure of TRAF6. Nature structural & molecular biology *16*, 658-666.

Ying, Z., Wang, H., Fan, H., Zhu, X., Zhou, J., Fei, E., and Wang, G. (2009). Gp78, an ER associated E3, promotes SOD1 and ataxin-3 degradation. Hum Mol Genet *18*, 4268-4281.

Yokouchi, M., Kondo, T., Houghton, A., Bartkiewicz, M., Horne, W.C., Zhang, H., Yoshimura, A., and Baron, R. (1999). Ligand-induced ubiquitination of the epidermal growth factor receptor involves the interaction of the c-Cbl RING finger and UbcH7. J Biol Chem *274*, 31707-31712.

Yoneda, T., Imaizumi, K., Oono, K., Yui, D., Gomi, F., Katayama, T., and Tohyama, M. (2001). Activation of caspase-12, an endoplastic reticulum (ER) resident caspase, through tumor necrosis factor receptor-associated factor 2-dependent mechanism in response to the ER stress. J Biol Chem *276*, 13935-13940.

Yoshida, H., Matsui, T., Yamamoto, A., Okada, T., and Mori, K. (2001). XBP1 mRNA is induced by ATF6 and spliced by IRE1 in response to ER stress to produce a highly active transcription factor. Cell *107*, 881-891.

Yoshida, Y., Adachi, E., Fukiya, K., Iwai, K., and Tanaka, K. (2005). Glycoprotein-specific ubiquitin ligases recognize N-glycans in unfolded substrates. EMBO reports *6*, 239-244.

Yoshida, Y., Tokunaga, F., Chiba, T., Iwai, K., Tanaka, K., and Tai, T. (2003). Fbs2 is a new member of the E3 ubiquitin ligase family that recognizes sugar chains. J Biol Chem *278*, 43877-43884.

Younger, J.M., Chen, L., Ren, H.Y., Rosser, M.F., Turnbull, E.L., Fan, C.Y., Patterson, C., and Cyr, D.M. (2006). Sequential quality-control checkpoints triage misfolded cystic fibrosis transmembrane conductance regulator. Cell *126*, 571-582.

Zapun, A., Darby, N.J., Tessier, D.C., Michalak, M., Bergeron, J.J., and Thomas, D.Y. (1998). Enhanced catalysis of ribonuclease B folding by the interaction of calnexin or calreticulin with ERp57. J Biol Chem *273*, 6009-6012.

Zattas, D., Adle, D.J., Rubenstein, E.M., and Hochstrasser, M. (2013). N-terminal acetylation of the yeast Derlin Der1 is essential for Hrd1 ubiquitin-ligase activity toward luminal ER substrates. Mol Biol Cell *24*, 890-900.

Zhang, X., Shaw, A., Bates, P.A., Newman, R.H., Gowen, B., Orlova, E., Gorman, M.A., Kondo, H., Dokurno, P., Lally, J.*, et al.* (2000). Structure of the AAA ATPase p97. Mol Cell *6*, 1473-1484.

Zhang, Z.R., Bonifacino, J.S., and Hegde, R.S. (2013). Deubiquitinases Sharpen Substrate Discrimination during Membrane Protein Degradation from the ER. Cell.

Zhao, G., Zhou, X., Wang, L., Li, G., Schindelin, H., and Lennarz, W.J. (2007). Studies on peptide:N-glycanase-p97 interaction suggest that p97 phosphorylation modulates endoplasmic reticulum-associated degradation. Proc Natl Acad Sci U S A *104*, 8785-8790.

Zhao, P., Xiao, X., Kim, A.S., Leite, M.F., Xu, J., Zhu, X., Ren, J., and Li, J. (2008). c-Jun inhibits thapsigargin-induced ER stress through up-regulation of DSCR1/Adapt78. Exp Biol Med (Maywood) *233*, 1289-1300.

Zhong, X., Shen, Y., Ballar, P., Apostolou, A., Agami, R., and Fang, S. (2004). AAA ATPase p97/valosin-containing protein interacts with gp78, a ubiquitin ligase for endoplasmic reticulum-associated degradation. J Biol Chem *279*, 45676-45684.

Zhong, X.Y., and Pittman, R.N. (2006). Ataxin-3 binds VCP/p97 and regulates retrotranslocation of ERAD substrates. Human Molecular Genetics *15*, 2409-2420.

Zimmerman, S.B., and Trach, S.O. (1991). Estimation of macromolecule concentrations and excluded volume effects for the cytoplasm of Escherichia coli. J Mol Biol *222*, 599-620.

Zito, E., Melo, E.P., Yang, Y., Wahlander, A., Neubert, T.A., and Ron, D. (2010). Oxidative protein folding by an endoplasmic reticulum-localized peroxiredoxin. Mol Cell *40*, 787-797.

Zopf, D., Bernstein, H.D., Johnson, A.E., and Walter, P. (1990). The methionine-rich domain of the 54 kd protein subunit of the signal recognition particle contains an RNA binding site and can be crosslinked to a signal sequence. EMBO J *9*, 4511-4517.

Zuber, C., Cormier, J.H., Guhl, B., Santimaria, R., Hebert, D.N., and Roth, J. (2007). EDEM1 reveals a quality control vesicular transport pathway out of the endoplasmic reticulum not involving the COPII exit sites. Proc Natl Acad Sci U S A *104*, 4407-4412.